

RMA

**RESOURCE MANAGEMENT ASSOCIATES, INC.
FAIRFIELD, CALIFORNIA**

**Upper Newport Bay
Water Quality Model Development**

**Prepared for
State Water Resources Control Board**

November 2008

EXECUTIVE SUMMARY

Newport Bay has been listed as an impaired water body due to eutrophication. A TMDL program has resulted in reduced nutrient inflows in the Bay, but macroalgal blooms continue to impair beneficial uses. The TMDL implementation plan requires determination of new numeric nutrient water quality objectives for freshwater tributaries to Newport Bay.

The Regional Board has funded Resource Management Associates (RMA) to develop water quality model of Newport Bay that includes macroalgae. The new model is an expansion of a previous version of the model that successfully simulated the occurrence of macroalgal blooms, but could not precisely predict yearly variations in the blooms. An interesting study by Southern California Coastal Water Research Project (SCCWRP) suggests that sediment fluxes play an important role as an internal loading of nutrients in Newport Bay. It was hypothesized that the magnitude of the macroalgal bloom in any given year is strongly dependent on the amount of sediment entering the Bay during the previous wet season. Based on the SCCWRP study and a thorough review of literature on the subjects of macroalgae, sediment processes and Newport Bay in general, the water quality model has been updated to include sediment nutrient fluxes. The updated model has been calibrated and validated using new data sets from an annual monitoring program performed by the Regional Board from 2004 through 2006 so that it can be run in a predictive mode to evaluate the impacts of alternative nutrient load levels entering the Bay. These simulations will be the main tool for selecting appropriate numeric water quality objectives.

Conceptual models for Newport Bay describe a linkage between macroalgal blooms and nutrient cycles. The main constituents of the water quality model include macroalgae, nitrate, ammonia, phosphate, dissolved oxygen, and deposited particulate organic matter (POM). DO, POM, NH₃, NO₃ and PO₄ are considered in the sediment flux model. Concentrations of DO, NO₃, NH₃ and PO₄ in the sediments affect water column concentrations. A separate sediment transport simulation is run to provide mass and distribution of deposited sediment to the sediment flux model.

The model is calibrated for January through December 2004. The validation period is from January 2005 through December 2006. These periods include a year with a dryer winter and smaller blooms later in the year (2004), and a year with large winter flows and subsequent larger macroalgal blooms later in the year (2004 – 2005). The validation is extended into 2006 to cover another dryer year.

Model simulations were run with nutrients simulated as conservative constituents to help determine the relative importance of the tidal and creek inflow boundary contributions to total nutrient concentrations in the Bay. Similarly, simulations were run with biological and chemical reactions but no sediment flux and compared with the calibrated model. Each of these simulations helped discern the importance of the different processes and sources.

Residence time simulations were run for a two-month summer period to determine the range of residence times that occur in the Bay over the spring-neap tidal cycle. Peak residence time is around 12 days, occurring in Rhine Channel.

The calibrated model was run in a predictive mode to evaluate the impacts of alternative total nitrogen load levels entering the Bay. Six alternative nitrogen loading levels were analyzed with different total nitrogen limits during storm and low flow periods. The fraction of particulate nitrogen in the suspended sediment was set to reduced levels corresponding to the storm flow nitrogen limits. Alternative simulation results indicate that reductions in total nitrogen in storm flows and fraction of particulate nitrogen in the sediment have a greater impact on reducing macroalgae blooms than reduction in total nitrogen inputs during low flow periods. Sediment flux appears to be one of the most important sources of nutrients for macroalgae growth.

Table of Contents

1. Introduction.....	1
1.1 Background	1
1.2 Objectives.....	2
2. Literature review.....	3
2.1 Characteristics of macroalgal blooms	3
2.2 Characteristics of macroalgae modeling	4
3. Conceptual models for macroalgal blooms in Newport Bay	7
3.1 Macroalgae.....	9
3.1.1 Growth	10
3.1.2 Respiration	13
3.1.3 Sloughing	13
3.1.4 Mortality	14
3.2 Nitrogen.....	14
3.3 Phosphorus	17
3.4 Dissolved oxygen (DO).....	18
3.5 Sediment fluxes	21
4. Description of hydrodynamic model (RMA2) and sediment transport and water quality model (RMA11).....	33
4.1 Model Configuration.....	33
4.1.1 Bathymetry.....	34
4.1.2 Boundary conditions	34
4.2 Previous Model Calibration	35
5. Water quality model calibration and validation.....	39
5.1 Calibration and validation periods	40
5.2 Boundary conditions	40
5.2.1 Development and application of deposited sediment boundary condition	60
5.3 Initial conditions.....	69
5.4 Calibration and validation results.....	71
5.4.1 Calibration results in 2004.....	77
5.4.2 Validation results in 2005	78
5.4.3 Validation results in 2006.....	80

5.5	Comparison of Nutrient concentrations in the sediments	133
5.6	Limiting factors for macroalgae growth.....	141
5.6.1	Limiting factors in 2004.....	141
5.6.2	Limiting factors in 2005.....	141
5.6.3	Limiting factors in 2006.....	142
5.7	Nutrient cycles in Newport Bay: Discussion of nutrient budgets	147
5.7.1	Nitrogen	147
5.7.2	Phosphorus.....	149
5.7.3	Nitrate loading during a storm period.....	163
6.	Additional model simulations, results and discussion	165
6.1	Scenarios with conservative constituents.....	165
6.2	Scenarios with biological and chemical reactions.....	179
6.3	Residence time simulations.....	186
7.	Reduced nutrient load simulations.....	189
8.	Summary and conclusions	211
9.	References.....	213

Table of Figures

Figure 2-1. Three common species of macroalgae appeared in Newport Bay.	4
Figure 3-1. Schematic of the ecological model (with major nutrient interactions) of Newport Bay. Boxes indicate the constituents and arrows indicate biological, chemical and physical processes.	8
Figure 3-2. Conceptual model for macroalgae in Newport Bay.	9
Figure 3-3. Conceptual model for nitrogen in Newport Bay.	17
Figure 3-4. Conceptual model for phosphorus in Newport Bay.	18
Figure 3-5. Conceptual model for dissolved oxygen in Newport Bay.	19
Figure 3-6 Conceptual sediment model for Newport Bay.	22
Figure 4-1 Finite element model configuration of Newport Bay, with monthly water quality monitoring stations of the Orange County where UNBJAM is Upper Newport Bay – Unit 1 Basin; UNBSDC is Upper Newport Bay – Unit 2 Basin; UNBNSB is Upper Newport Bay – North Star Beach; UNBCHB is Upper Newport Bay – Coast Highway Bridge.	36
Figure 4-2 Color contours of the Newport Bay model bathymetry.	37
Figure 5-1 Map of Newport Bay water quality monitoring stations (from nutrient TMDL report, County of Orange et. al, 2004).	45
Figure 5-2 San Diego Creek and Santa Ana Delhi Channel inflows for December 2003 - December 2006.	46
Figure 5-3 San Diego Creek and Santa Ana Delhi Channel inflows for December 2003 - December 2006, shown in log scale.	47
Figure 5-4 Santa Ana Delhi temperature: measured data (red dots), estimated (blue line) and model boundary condition (light blue line) from 2004 through 2006.	48
Figure 5-5 San Diego Creek temperature: measured data (red dots), estimated (blue line) and model boundary condition (light blue line) 2004 through 2006.	48
Figure 5-6 Santa Ana Delhi DO: measured data (red dots), estimated (blue line) and model boundary condition (light blue line) from 2004 through 2006.	49
Figure 5-7 San Diego Creek DO: measured data (red dots), estimated (blue line) and model boundary condition (light blue line) from 2004 through 2006.	49
Figure 5-8 Santa Ana Delhi NO ₃ : measured data (red dots), estimated (blue line) and model boundary condition (light blue line) from 2004 through 2006.	50
Figure 5-9 San Diego Creek NO ₃ : measured data (red dots), estimated (blue line) and model boundary condition (light blue line) from 2004 through 2006.	50
Figure 5-10 Santa Ana Delhi NH ₃ : measured data (red dots), estimated (blue line) and model boundary condition (light blue line) from 2004 through 2006.	51
Figure 5-11 San Diego Creek NH ₃ : measured data (red dots), estimated (blue line) and model boundary condition (light blue line) from 2004 through 2006.	51

Figure 5-12 Santa Ana Delhi PO4: measured data (red dots), estimated (blue line) and model boundary condition (light blue line) from 2004 through 2006.	52
Figure 5-13 San Diego Creek PO4: measured data (red dots), estimated (blue line) and model boundary condition (light blue line) from 2004 through 2006.	52
Figure 5-14 Santa Ana Delhi EC: measured data (red dots), estimated (blue line) and EC used to compute salinity model boundary condition (light blue line) 2004 through 2006.	53
Figure 5-15 San Diego Creek EC: measured data (red dots), estimated (blue line) and EC used to compute salinity model boundary condition (light blue line) 2004 through 2006.	53
Figure 5-16 Santa Ana Delhi estimated Salinity using a regression between EC and salinity from 2004 through 2006.	54
Figure 5-17 San Diego Creek estimated Salinity using a regression between EC and salinity from 2004 through 2006.	54
Figure 5-18 Regression of both water temperature and air temperature multiplied by flow rate of San Diego Creek from 2004 through 2006.	55
Figure 5-19 Regression of both water temperature and air temperature multiplied by flow rate of Santa Ana Delhi from 2004 through 2006.	55
Figure 5-20 Regression of both DO and air temperature multiplied by flow rate of Santa Ana Delhi from 2004 through 2006.	56
Figure 5-21 Regression of both DO and air temperature multiplied by flow rate of San Diego Creek from 2004 through 2006.	56
Figure 5-22 Regression of NO ₃ multiplied by air temperature and air temperature multiplied by flow rate of Santa Ana Delhi from 2004 through 2006.	57
Figure 5-23 Regression of both NO ₃ multiplied by air temperature and air temperature multiplied by flow rate of San Diego Creek from 2004 through 2006.	57
Figure 5-24 Regression of NH ₃ multiplied by air temperature and air temperature multiplied by flow rate of Santa Ana Delhi from 2004 through 2006.	58
Figure 5-25 Regression of both NH ₃ multiplied by air temperature and air temperature multiplied by flow rate of San Diego Creek from 2004 through 2006.	58
Figure 5-26 Regression of PO ₄ multiplied by air temperature and air temperature multiplied by flow rate of Santa Ana Delhi from 2004 through 2006.	59
Figure 5-27 Regression of both PO ₄ multiplied by air temperature and air temperature multiplied by flow rate of San Diego Creek from 2004 through 2006.	59
Figure 5-28. Santa Ana Delhi daily TSS data from 2004 through 2006.	63
Figure 5-29. San Diego Creek daily TSS data from 2004 through 2006.	63
Figure 5-30 Time series plot of simulated cumulative sediment deposition January 1 through December 31, 2004, at a location of peak deposition in Unit I basin.	64
Figure 5-31 Time series plot of simulated cumulative sediment deposition January 1 through December 31, 2005, at a location of peak deposition in Unit I basin.	64
Figure 5-32 Time series plot of simulated cumulative sediment deposition January 1 through July 1, 2006, at a location of peak deposition in Unit I basin.	65

Figure 5-33	Contours of simulated deposited sediment depth accumulated during the period of December 1, 2003 through June 1, 2004.	66
Figure 5-34	Contours of simulated deposited sediment depth accumulated during the period of January 1 through June 1, 2005.	67
Figure 5-35	Contours of simulated deposited sediment depth accumulated during the period of January 1 through June 1, 2006.	68
Figure 5-36	Contours of the initial condition of macroalgae on January 1, 2004.	70
Figure 5-37	Map of Newport Bay macroalgae sampling stations (from nutrient TMDL report, County of Orange et. al, 2004).....	72
Figure 5-38	Comparison of computed total macroalgae mass computed for 2004, 2005 and 2006.....	73
Figure 5-39	Spatial contours of computed macroalgae concentration (Kg/m ²) on July 1, 2004.	74
Figure 5-40	Spatial contours of computed macroalgae concentration (Kg/m ²) on July 1, 2005.	75
Figure 5-41	Spatial contours of computed macroalgae concentration (Kg/m ²) on July 1, 2006.	76
Figure 5-42	Comparison of computed macroalgae concentrations at sampling sites in 2004.....	82
Figure 5-43	Comparison of computed macroalgae concentrations with the measured data at ALG24 in 2004.	83
Figure 5-44	Comparison of computed macroalgae concentrations with the measured data at ALG19 in 2004.	83
Figure 5-45	Comparison of computed macroalgae concentrations with the measured data at ALG16 in 2004.	84
Figure 5-46	Comparison of computed macroalgae concentrations with the measured data at ALG9 in 2004.	84
Figure 5-47	Comparison of computed macroalgae concentrations with the measured data at ALG7 in 2004.	85
Figure 5-48	Comparison of computed macroalgae concentrations with the measured data at ALG4 in 2004.	85
Figure 5-49	Comparison of computed macroalgae concentrations with the measured data at ALG2 in 2004.	86
Figure 5-50	Comparison of computed temperature (°C) with the measured data at UNBJAM in 2004.....	87
Figure 5-51	Comparison of computed temperature (°C) with the measured data at UNBSDC in 2004.....	87
Figure 5-52	Comparison of computed temperature (°C) with the measured data at UNBNSB in 2004.....	88
Figure 5-53	Comparison of computed temperature (°C) with the measured data at UNBCHB in 2004.....	88
Figure 5-54	Comparison of computed DO concentrations with the measured data at UNBJAM in 2004.....	89

Figure 5-55 Comparison of computed DO concentrations with the measured data at UNBSDC in 2004.....	89
Figure 5-56 Comparison of computed DO concentrations with the measured data at UNBNSB in 2004.....	90
Figure 5-57 Comparison of computed DO concentrations with the measured data at UNBCHB in 2004.	90
Figure 5-58 Comparison of computed NO ₃ concentrations with the measured data at UNBJAM in 2004.	91
Figure 5-59 Comparison of computed NO ₃ concentrations with the measured data at UNBSDC in 2004.	91
Figure 5-60 Comparison of computed NO ₃ concentrations with the measured data at UNBNSB in 2004.	92
Figure 5-61 Comparison of computed NO ₃ concentrations with the measured data at UNBCHB in 2004.	92
Figure 5-62 Comparison of computed NH ₃ concentrations with the measured data at UNBJAM in 2004.	93
Figure 5-63 Comparison of computed NH ₃ concentrations with the measured data at UNBSDC in 2004.	93
Figure 5-64 Comparison of computed NH ₃ concentrations with the measured data at UNBNSB in 2004.	94
Figure 5-65 Comparison of computed NH ₃ concentrations with the measured data at UNBCHB in 2004.	94
Figure 5-66 Comparison of computed PO ₄ concentrations with the measured data at UNBJAM in 2004.	95
Figure 5-67 Comparison of computed PO ₄ concentrations with the measured data at UNBSDC in 2004.	95
Figure 5-68 Comparison of computed PO ₄ concentrations with the measured data at UNBNSB in 2004.	96
Figure 5-69 Comparison of computed PO ₄ concentrations with the measured data at UNBCHB in 2004.	96
Figure 5-70 Comparison of computed macroalgae concentrations at sampling sites in 2005.....	97
Figure 5-71 Comparison of computed macroalgae concentrations with the measured data at ALG24 in 2005.	98
Figure 5-72 Comparison of computed macroalgae concentrations with the measured data at ALG19 in 2005.	98
Figure 5-73 Comparison of computed macroalgae concentrations with the measured data at ALG16 in 2005.	99
Figure 5-74 Comparison of computed macroalgae concentrations with the measured data at ALG9 in 2005.	99

Figure 5-75 Comparison of computed macroalgae concentrations with the measured data at ALG7 in 2005.	100
Figure 5-76 Comparison of computed macroalgae concentrations with the measured data at ALG4 in 2005.	100
Figure 5-77 Comparison of computed macroalgae concentrations with the measured data at ALG2 in 2005.	101
Figure 5-78 Comparison of computed temperature (°C) with the measured data at UNBJAM in 2005.	102
Figure 5-79 Comparison of computed temperature (°C) with the measured data at UNBSDC in 2005.	102
Figure 5-80 Comparison of computed temperature (°C) with the measured data at UNBNSB in 2005.	103
Figure 5-81 Comparison of computed temperature (°C) with the measured data at UNBCHB in 2005.	103
Figure 5-82 Location of continuous water quality measurements in Upper Newport Bay during 2005. Surface and bottom measurements are available for each station: one 0.5 m from the surface and one 0.5 m off the bottom.	104
Figure 5-83 Comparison of computed temperature (°C) with the measured data at S3 in 2005.	105
Figure 5-84 Comparison of computed temperature (°C) with the measured data at S2 in 2005.	106
Figure 5-85 Comparison of computed temperature (°C) with the measured data at S1 in 2005.	107
Figure 5-86 Comparison of computed DO concentrations with the measured data at UNBJAM in 2005.	108
Figure 5-87 Comparison of computed DO concentrations with the measured data at UNBSDC in 2005.	108
Figure 5-88 Comparison of computed DO concentrations with the measured data at UNBNSB in 2005.	109
Figure 5-89 Comparison of computed DO concentrations with the measured data at UNBCHB in 2005.	109
Figure 5-90 Comparison of computed DO concentrations with the measured data at S3 in 2005.	110
Figure 5-91 Comparison of computed DO concentrations with the measured data at S2 in 2005.	111
Figure 5-92 Comparison of computed DO concentrations with the measured data at S1 in 2005.	112
Figure 5-93 Comparison of computed NO ₃ concentrations with the measured data at UNBJAM in 2005.	113

Figure 5-94 Comparison of computed NO ₃ concentrations with the measured data at UNBSDC in 2005.	113
Figure 5-95 Comparison of computed NO ₃ concentrations with the measured data at UNBNSB in 2005.	114
Figure 5-96 Comparison of computed NO ₃ concentrations with the measured data at UNBCHB in 2005.	114
Figure 5-97 Comparison of computed NH ₃ concentrations with the measured data at UNBJAM in 2005.	115
Figure 5-98 Comparison of computed NH ₃ concentrations with the measured data at UNBSDC in 2005.	115
Figure 5-99 Comparison of computed NH ₃ concentrations with the measured data at UNBNSB in 2005.	116
Figure 5-100 Comparison of computed NH ₃ concentrations with the measured data at UNBCHB in 2005.	116
Figure 5-101 Comparison of computed PO ₄ concentrations with the measured data at UNBJAM in 2005.	117
Figure 5-102 Comparison of computed PO ₄ concentrations with the measured data at UNBSDC in 2005.	117
Figure 5-103 Comparison of computed PO ₄ concentrations with the measured data at UNBNSB in 2005.	118
Figure 5-104 Comparison of computed PO ₄ concentrations with the measured data at UNBCHB in 2005.	118
Figure 5-105 Comparison of computed macroalgae concentrations at sampling sites in 2006.	119
Figure 5-106 Comparison of computed macroalgae concentrations with the measured data at ALG24 in 2006.	120
Figure 5-107 Comparison of computed macroalgae concentrations with the measured data at ALG19 in 2006.	120
Figure 5-108 Comparison of computed macroalgae concentrations with the measured data at ALG16 in 2006.	121
Figure 5-109 Comparison of computed macroalgae concentrations with the measured data at ALG7 in 2006.	121
Figure 5-110 Comparison of computed temperature (°C) with the measured data at UNBJAM in 2006.	122
Figure 5-111 Comparison of computed temperature (°C) with the measured data at UNBSDC in 2006.	122
Figure 5-112 Comparison of computed temperature (°C) with the measured data at UNBNSB in 2006.	123
Figure 5-113 Comparison of computed temperature (°C) with the measured data at UNBCHB in 2006.	123

Figure 5-114 Comparison of computed DO concentrations with the measured data at UNBJAM in 2006.	124
Figure 5-115 Comparison of computed DO concentrations with the measured data at UNBSDC in 2006.	124
Figure 5-116 Comparison of computed DO concentrations with the measured data at UNBNSB in 2006.	125
Figure 5-117 Comparison of computed DO concentrations with the measured data at UNBCHB in 2006.	125
Figure 5-118 Comparison of computed NO ₃ concentrations with the measured data at UNBJAM in 2006.	126
Figure 5-119 Comparison of computed NO ₃ concentrations with the measured data at UNBSDC in 2006.	126
Figure 5-120 Comparison of computed NO ₃ concentrations with the measured data at UNBNSB in 2006.	127
Figure 5-121 Comparison of computed NO ₃ concentrations with the measured data at UNBCHB in 2006.	127
Figure 5-122 Comparison of computed NH ₃ concentrations with the measured data at UNBJAM in 2006.	128
Figure 5-123 Comparison of computed NH ₃ concentrations with the measured data at UNBSDC in 2006.	128
Figure 5-124 Comparison of computed NH ₃ concentrations with the measured data at UNBNSB in 2006.	129
Figure 5-125 Comparison of computed NH ₃ concentrations with the measured data at UNBCHB in 2006.	129
Figure 5-126 Comparison of computed PO ₄ concentrations with the measured data at UNBJAM in 2006.	130
Figure 5-127 Comparison of computed PO ₄ concentrations with the measured data at UNBSDC in 2006.	130
Figure 5-128 Comparison of computed PO ₄ concentrations with the measured data at UNBNSB in 2006.	131
Figure 5-129 Comparison of computed PO ₄ concentrations with the measured data at UNBCHB in 2006.	131
Figure 5-130 Comparison of computed total dry mass of macroalgae for calibration years of 2004, 2005 and 2006.	132
Figure 5-131 Map of sediment porewater sampling sites in Upper Newport Bay (UNB) (Source: Sutula et al., 2006).	134
Figure 5-132 Comparison of surface sediment observed (0-1 cm) and computed (up to 10 cm) NH ₃ at the intertidal region of NB1 (Site 1 in Figure 5-131).	135
Figure 5-133 Comparison of surface sediment observed (0-1 cm) and computed (up to 10 cm) PO ₄ at the intertidal region of NB1 (Site 1 in Figure 5-131).	135

Figure 5-134 Comparison of surface sediment observed (0-1 cm) and computed (up to 10 cm) NH3 at the subtidal region of NB1 (Site 1 in Figure 5-131).	136
Figure 5-135 Comparison of surface sediment observed (0-1 cm) and computed (up to 10 cm) PO4 at the subtidal region of NB1 (Site 1 in Figure 5-131).	136
Figure 5-136 Comparison of surface sediment observed (0-1 cm) and computed (up to 10 cm) NH3 at the intertidal region of NB2 (Site 2 in Figure 5-131).	137
Figure 5-137 Comparison of surface sediment observed (0-1 cm) and computed (up to 10 cm) PO4 at the intertidal region of NB2 (Site 2 in Figure 5-131).	137
Figure 5-138 Comparison of surface sediment observed (0-1 cm) and computed (up to 10 cm) NH3 at the subtidal region of NB2 (Site 2 in Figure 5-131).	138
Figure 5-139 Comparison of surface sediment observed (0-1 cm) and computed (up to 10 cm) PO4 at the subtidal region of NB2 (Site 2 in Figure 5-131).	138
Figure 5-140 Comparison of surface sediment observed (0-1 cm) and computed (up to 10 cm) NH3 at the intertidal region of NB3 (Site 3 in Figure 5-131).	139
Figure 5-141 Comparison of surface sediment observed (0-1 cm) and computed (up to 10 cm) PO4 at the intertidal region of NB3 (Site 3 in Figure 5-131).	139
Figure 5-142 Comparison of surface sediment observed (0-1 cm) and computed (up to 10 cm) NH3 at the subtidal region of NB3 (Site 3 in Figure 5-131).	140
Figure 5-143 Comparison of surface sediment observed (0-1 cm) and computed (up to 10 cm) PO4 at the subtidal region of NB3 (Site 3 in Figure 5-131).	140
Figure 5-144 Limiting factors of macroalgae growth at each monitoring stations in 2004. The values of one, two, three and four indicate light limiting, internal nitrogen, phosphorus and freshwater stress, respectively. (a) Station ALG19; (b) Station ALG13; (c) Station ALG7.	143
Figure 5-145 Limiting factors of macroalgae growth at each monitoring stations in 2005. The values of one, two, three and four indicate light limiting, internal nitrogen, phosphorus and freshwater stress, respectively. (a) Station ALG19; (b) Station ALG13; (c) Station ALG7.	144
Figure 5-146 Time series plot of light, internal nitrogen, phosphorus, space and temperature limitation factors at Station ALG19 during summer 2005.	145
Figure 5-147 Limiting factors of macroalgae growth at each monitoring stations in 2006. The values of one, two, three and four indicate light limiting, internal nitrogen, phosphorus and freshwater stress, respectively. (a) Station ALG19; (b) Station ALG13; (c) Station ALG7.	146
Figure 5-152. Time series of accumulated nitrogen mass into Newport Bay from January, 2004 to December, 2004 as input to the model. Very dark blue indicates particulate nitrogen from two inflows, cyan and light blue indicate NH3 and NO3 of San Diego Creek, respectively, and dark blue and blue indicate NH3 and NO3 of Santa Ana Delhi.	151
Figure 5-151. Time series of distribution of nitrogen in Newport Bay as computed in the model from January, 2004 to December, 2004. Dark brown indicates buried sediments, light brown indicates active sediment layer including N-POM, dark green indicates sloughing and non-recycled dead macroalgae (NRM), light green indicates internal nitrogen, light blue indicates NH3 in the water column, cyan indicates NO3 in the water column, very dark blue indicates	

particulate nitrogen out to the ocean, dark blue indicates NH₃ out to the ocean, blue indicates NO₃ out to the ocean and pale blue indicates denitrification. 152

Figure 5-154. Time series of accumulated nitrogen mass into Newport Bay from January, 2005 to December, 2005 as input to the model. Very dark blue indicates nitrogen from two inflows, cyan and light blue indicate NH₃ and NO₃ of San Diego Creek, respectively, and dark blue and blue indicate NH₃ and NO₃ of Santa Ana Delhi. 153

Figure 5-153. Time series of distribution of nitrogen in Newport Bay as computed in the model from January, 2005 to December, 2005. Dark brown indicates buried sediments, light brown indicates active sediment layer including N-POM, dark green indicates sloughing and non-recycled dead macroalgae (NRM), light green indicates internal nitrogen, light blue indicates NH₃ in the water column, cyan indicates NO₃ in the water column, very dark blue indicates particulate nitrogen out to the ocean, dark blue indicates NH₃ out to the ocean, blue indicates NO₃ out to the ocean and pale blue indicates denitrification. 154

Figure 5-156. Time series of accumulated nitrogen mass into Newport Bay from January, 2006 to June, 2006 as input to the model. Very dark blue indicates nitrogen from two inflows, cyan and light blue indicate NH₃ and NO₃ of San Diego Creek, respectively, and dark blue and blue indicate NH₃ and NO₃ of Santa Ana Delhi. 155

Figure 5-155. Time series of distribution of nitrogen in Newport Bay as computed in the model from January, 2006 to June, 2006. Dark brown indicates buried sediments, light brown indicates active sediment layer including N-POM, dark green indicates sloughing and non-recycled dead macroalgae (NRM), light green indicates internal nitrogen, light blue indicates NH₃ in the water column, cyan indicates NO₃ in the water column, very dark blue indicates particulate nitrogen out to the ocean, dark blue indicates NH₃ out to the ocean, blue indicates NO₃ out to the ocean and pale blue indicates denitrification. 156

Figure 5-157. Time series of distribution of phosphorus in Newport Bay as computed in the model from January, 2004 to December, 2004. Dark brown indicates buried sediments, light brown indicates active sediment layer including P-POM, dark green indicates sloughing and non-recycled dead macroalgae (NRM), light green indicates phosphorus in macroalgae, cyan indicates PO₄ in the water column, very dark blue indicates particulate phosphorus out to the ocean, and blue indicates PO₄ out to the ocean. 157

Figure 5-158. Time series of accumulated phosphorus mass into Newport Bay from January, 2004 to December, 2004 as input to the model. Very dark blue indicates particulate phosphorus from two inflows, cyan and light blue indicate NH₃ and NO₃ of San Diego Creek, respectively, and dark blue and blue indicate NH₃ and NO₃ of Santa Ana Delhi. 158

Figure 5-160. Time series of accumulated phosphorus mass into Newport Bay from January, 2005 to December, 2005 as input to the model. Very dark blue indicates particulate phosphorus from two inflows, cyan and light blue indicate NH₃ and NO₃ of San Diego Creek, respectively, and dark blue and blue indicate NH₃ and NO₃ of Santa Ana Delhi. 159

Figure 5-159. Time series of distribution of phosphorus in Newport Bay as computed in the model from January, 2005 to December, 2005. Dark brown indicates buried sediments, light

brown indicates active sediment layer including P-POM, dark green indicates sloughing and non-recycled dead macroalgae (NRM), light green indicates phosphorus in macroalgae, cyan indicates PO₄ in the water column, very dark blue indicates particulate phosphorus out to the ocean, and blue indicates PO₄ out to the ocean..... 160

Figure 5-162. Time series of accumulated phosphorus mass into Newport Bay from January, 2006 to June, 2006 as input to the model. Very dark blue indicates particulate phosphorus from two inflows, cyan and light blue indicate NH₃ and NO₃ of San Diego Creek, respectively, and dark blue and blue indicate NH₃ and NO₃ of Santa Ana Delhi. 161

Figure 5-161. Time series of distribution of phosphorus in Newport Bay as computed in the model from January, 2006 to June, 2006. Dark brown indicates buried sediments, light brown indicates active sediment layer including P-POM, dark green indicates sloughing and non-recycled dead macroalgae (NRM), light green indicates phosphorus in macroalgae, cyan indicates PO₄ in the water column, very dark blue indicates particulate phosphorus out to the ocean, and blue indicates PO₄ out to the ocean..... 162

Figure 5-163 NO₃-N for storm events between February and March 2004..... 164

Figure 6-1 Observed and conservatively computed NO₃ at UNBJAM for years 2004 - 2006. Conservative simulations were performed both with tidal boundaries set using observed data, and set to zero. 167

Figure 6-2 Observed and conservatively computed NO₃ at UNBSDC for years 2004 - 2006. Conservative simulations were performed both with tidal boundaries set using observed data, and set to zero. 168

Figure 6-3 Observed and conservatively computed NO₃ at UNBNSB for years 2004 - 2006. Conservative simulations were performed both with tidal boundaries set using observed data, and set to zero. 169

Figure 6-4 Observed and conservatively computed NO₃ at UNBCHB for years 2004 - 2006. Conservative simulations were performed both with tidal boundaries set using observed data, and set to zero. 170

Figure 6-5 Observed and conservatively computed NH₃ at UNBJAM for years 2004 - 2006. Conservative simulations were performed both with tidal boundaries set using observed data, and set to zero. 171

Figure 6-6 Observed and conservatively computed NH₃ at UNBSDC for years 2004 - 2006. Conservative simulations were performed both with tidal boundaries set using observed data, and set to zero. 172

Figure 6-7 Observed and conservatively computed NH₃ at UNBNSB for years 2004 - 2006. Conservative simulations were performed both with tidal boundaries set using observed data, and set to zero. 173

Figure 6-8 Observed and conservatively computed NH₃ at UNBCHB for years 2004 - 2006. Conservative simulations were performed both with tidal boundaries set using observed data, and set to zero. 174

Figure 6-9 Observed and conservatively computed PO ₄ at UNBJAM for years 2004 - 2006. Conservative simulations were performed both with tidal boundaries set using observed data, and set to zero.	175
Figure 6-10 Observed and conservatively computed PO ₄ at UNBSDC for years 2004 - 2006. Conservative simulations were performed both with tidal boundaries set using observed data, and set to zero.	176
Figure 6-11 Observed and conservatively computed PO ₄ at UNBNSB for years 2004 - 2006. Conservative simulations were performed both with tidal boundaries set using observed data, and set to zero.	177
Figure 6-12 Observed and conservatively computed PO ₄ at UNBCHB for years 2004 - 2006. Conservative simulations were performed both with tidal boundaries set using observed data, and set to zero.	178
Figure 6-13 Comparison of total dry mass of macroalgae simulated with and without sediment fluxes in 2004.	180
Figure 6-14 Comparison of total dry mass of macroalgae simulated with and without sediment fluxes in 2005.	181
Figure 6-15 Comparison of total dry mass of macroalgae simulated with and without sediment fluxes in 2006.	182
Figure 6-16 Comparison of total dry mass of macroalgae simulated with and without NO ₃ inputs from inflows in 2004.	183
Figure 6-17 Comparison of total dry mass of macroalgae simulated with and without NO ₃ inputs from inflows in 2005.	184
Figure 6-18 Comparison of total dry mass of macroalgae simulated with and without NO ₃ inputs from inflows in 2006.	185
Figure 6-19 Color contour plots showing the range of residence times occurring during the 01 July – 31 August 2004 simulation period. Tidal phase and stage at the times of these plots can be seen in Figure 6-20.	187
Figure 6-20 Time series of stage applied at the downstream model boundary for the 01 July – 31 August 2004 residence time simulation. Red dots indicate times of contour plots in Figure 6-19.	188
Figure 7-1 Time series of total nitrogen entering the Bay from Santa Ana Delhi and San Diego Creek for Base case and Alternative 1 (3.0 mg/L-0.5 mg/L).	191
Figure 7-2 Time series of total nitrogen entering the Bay from Santa Ana Delhi and San Diego Creek for Base case and Alternative 2 (3.0 mg/L-1.0 mg/L).	191
Figure 7-3 Time series of total nitrogen entering the Bay from Santa Ana Delhi and San Diego Creek for Base case and Alternative 3 (3.0 mg/L-2.0 mg/L).	192
Figure 7-4 Time series of total nitrogen entering the Bay from Santa Ana Delhi and San Diego Creek for Base case and Alternative 4 (5.0 mg/L-0.5 mg/L).	192
Figure 7-5 Time series of total nitrogen entering the Bay from Santa Ana Delhi and San Diego Creek for Base case and Alternative 5 (5.0 mg/L-1.0 mg/L).	193

Figure 7-6 Time series of total nitrogen entering the Bay from Santa Ana Delhi and San Diego Creek for Base case and Alternative 6 (5.0 mg/L-2.0 mg/L).....	193
Figure 7-7 Annually averaged total nitrogen concentration of Santa Ana Delhi for Base case and alternatives.....	194
Figure 7-8 Annually averaged total nitrogen concentration of San Diego Creek for Base case and alternatives.....	194
Figure 7-9 Annual median of total nitrogen concentration of Santa Ana Delhi for Base case and alternatives. Note that the alternatives with the same dry season loading (e.g. 1 and 4) have nearly identical annual medians and thus plot on top of one another.....	195
Figure 7-10 Annual median of total nitrogen concentration of San Diego Creek for Base case and alternatives. Note that the alternatives with the same dry season loading (e.g. 1 and 4) have nearly identical annual medians and thus plot on top of one another.....	195
Figure 7-11 Comparison of total dry mass of macroalgae among alternatives with the Base case in 2004.....	196
Figure 7-12 Comparison of macroalgae concentrations among alternatives with the Base case at station ALG24 in 2004.....	197
Figure 7-13 Comparison of macroalgae concentrations among alternatives with the Base case at station ALG19 in 2004.....	197
Figure 7-14 Comparison of macroalgae concentrations among alternatives with the Base case at station ALG16 in 2004.....	198
Figure 7-15 Comparison of macroalgae concentrations among alternatives with the Base case at station ALG13 in 2004.....	198
Figure 7-16 Comparison of macroalgae concentrations among alternatives with the Base case at station ALG9 in 2004.....	199
Figure 7-17 Comparison of macroalgae concentrations among alternatives with the Base case at station ALG7 in 2004.....	199
Figure 7-18 Comparison of macroalgae concentrations among alternatives with the Base case at station ALG4 in 2004.....	200
Figure 7-19 Comparison of macroalgae concentrations among alternatives with the Base case at station ALG2 in 2004.....	200
Figure 7-20 Comparison of total dry mass of macroalgae among alternatives with the Base case in 2005.....	201
Figure 7-21 Comparison of macroalgae concentrations among alternatives with the Base case at station ALG24 in 2005.....	202
Figure 7-22 Comparison of macroalgae concentrations among alternatives with the Base case at station ALG19 in 2005.....	202
Figure 7-23 Comparison of macroalgae concentrations among alternatives with the Base case at station ALG16 in 2005.....	203
Figure 7-24 Comparison of macroalgae concentrations among alternatives with the Base case at station ALG13 in 2005.....	203

Figure 7-25 Comparison of macroalgae concentrations among alternatives with the Base case at station ALG9 in 2005..... 204

Figure 7-26 Comparison of macroalgae concentrations among alternatives with the Base case at station ALG7 in 2005..... 204

Figure 7-27 Comparison of macroalgae concentrations among alternatives with the Base case at station ALG4 in 2005..... 205

Figure 7-28 Comparison of macroalgae concentrations among alternatives with the Base case at station ALG2 in 2005..... 205

Figure 7-29 Comparison of total dry mass of macroalgae among alternatives with the Base case in 2006. 206

Figure 7-30 Comparison of macroalgae concentrations among alternatives with the Base case at station ALG24 in 2006..... 207

Figure 7-31 Comparison of macroalgae concentrations among alternatives with the Base case at station ALG19 in 2006..... 207

Figure 7-32 Comparison of macroalgae concentrations among alternatives with the Base case at station ALG16 in 2006..... 208

Figure 7-33 Comparison of macroalgae concentrations among alternatives with the Base case at station ALG13 in 2006..... 208

Figure 7-34 Comparison of macroalgae concentrations among alternatives with the Base case at station ALG9 in 2006..... 209

Figure 7-35 Comparison of macroalgae concentrations among alternatives with the Base case at station ALG7 in 2006..... 209

Figure 7-36 Comparison of macroalgae concentrations among alternatives with the Base case at station ALG4 in 2006..... 210

Figure 7-37 Comparison of macroalgae concentrations among alternatives with the Base case at station ALG2 in 2006..... 210

List of Tables

Table 3-1. Estimated sloughing thresholds and current speeds at which total sloughing is reached, calculated from linear regression between sloughed biomass and current speed for two species of macroalgae (source: Flindt et al., 2007).....	13
Table 3-2 List of symbols of the water quality model	24
Table 3-3. The coefficients and constants of the water quality model	27
Table 3-4. Summary of differential equations for the constituents of the water quality model ...	30
Table 4-1 Hydrodynamic and water quality constituents for boundary conditions.....	34
Table 5-1 Constants of non-linear regression for water quality constituents of inflows	42
Table 5-2 Summary of data sources and estimation methods for water quality model constituent boundary conditions.....	44
Table 5-3 Sediment model parameter values used in sediment transport simulations.	61
Table 5-4 Initial conditions of water quality constituents.	69
Table 5-5 Newport Bay nitrogen budget for calibration years.	150
Table 5-6 Newport Bay phosphorus budget for calibration years.	150
Table 7-1 Summary of concentration limits and particulate nitrogen to suspended sediment ratios for alternatives.....	190

UPPER NEWPORT BAY WATER QUALITY MODEL DEVELOPMENT
NOVEMBER 2008

Prepared by
Resource Management Associates, Inc.

1. Introduction

1.1 Background

Newport Bay has been listed as an impaired water body due to eutrophication, and a total maximum daily load (TMDL) for nutrients was adopted by the Santa Ana Regional Water Quality Control Board (Regional Board) in 1998. The TMDL program has resulted in reduced nutrient inflows in the Bay, but macroalgal blooms continue to impair beneficial uses. The TMDL implementation plan requires determination of new numeric nutrient water quality objectives for freshwater tributaries to Newport Bay. Calibration of these new objectives is a complex scientific problem; the U.S. EPA is still in the process of formulating methodologies for determining appropriate numeric objectives.

For a better understanding of the macroalgal blooms, the Regional Board has funded development of a water quality simulation model for macroalgae in the Newport Bay. Development of the Newport Bay model was originally funded by the U.S. Army Corps of Engineers for evaluation of alternative dredging options for Newport Bay (RMA, 19979; 1998a; 1998b; 1999). The Regional Board subsequently funded expansion of the model to simulate macroalgae and other water quality constituents (RMA, 2003).

Previous versions of the model have successfully simulated the occurrence of macroalgal blooms, however, the model could not precisely predict yearly variations in the blooms. A study by Southern California Coastal Water Research Project (SCCWRP) (Sutula et al., 2006) suggests that sediment fluxes play an important role as an internal loading of nutrients in Newport Bay. It was hypothesized that the magnitude of the macroalgal bloom in any given year is strongly dependent on the amount of sediment entering the Bay during the previous wet season. Based on SCCWRP study, a thorough literature review and monitoring data collected by the County of Orange from 2001 to 2007, the model has been updated with sediment nutrient fluxes, and calibrated and validated using the new data sets from the annual monitoring program from 2004 to 2006.

The water quality model has thus been updated to include sediment fluxes, re-calibrated using the new data sets and run in a predictive mode to evaluate the impacts of alternative nutrient load

levels entering the Bay. These simulations are intended to assist the Regional Board in selecting appropriate numeric water quality objectives for freshwater creeks that drain into the Bay.

1.2 Objectives

The objective of the current Upper Newport Bay Water Quality Model Development project is to update and calibrate the water quality model and perform simulations to evaluate alternative loading strategies in support the short term and long term management of Newport Bay. The project consists of the following:

- Modification of the water quality model, including the addition of a sediment flux model;
- Re-calibration and validation of the water quality model over the three-year period of 2004 through 2006; and
- Evaluation of reduced total nitrogen loading alternatives.

2. Literature review

2.1 Characteristics of macroalgal blooms

Cultural eutrophication of coastal ecosystems has increased largely due to augmented supplies of nutrients (i.e., nitrogen (N) and phosphorus (P)) from the watershed, of which land uses are dominated by agricultural activity and urbanization (Hauxwell and Valiela, 2004; Kamer et al., 2001).

Nitrogen tends to be the more limiting nutrient controlling eutrophication of coastal waters because:

- nitrogen fixation generally does not occur in estuaries with salinities > 10 to 12 even when they are strongly nitrogen limited;
- denitrification tends to be one of the major sinks (although this may be slightly less important in ecosystems with shorter water residence times, such as Newport Bay); and
- phosphorus availability in estuaries is greater relative to other water bodies due to desorption from suspended matters under high salinity conditions (Howarth and Marino, 2006).

Thus, as inputs of nitrogen to a coastal system such as Newport Bay increase, the growth limitation is reduced. The increases of nutrient inputs, especially nitrogen, have changed the composition and abundance of the primary producers present in coastal systems. Primary producers in coastal ecosystems are typically made up of various forms of microalgae (benthic, epiphytic and pelagic), and macroalgae (ephemeral and persistent) and rooted macrophytes (Sand-Jensen and Nielsen, 2004; Pedersen et al., 2004). In particular, periodic and massive macroalgal blooms, such as *Ulva*, *Cladophora*, *Enteromorpha* and *Chaetomorpha*, have become common phenomena in temperate, relatively nutrient-rich waters where the bottom is within the photic zone (Naldi and Viaroli, 2002; Valiela et al., 1997). The three most common species of macroalgae in Newport Bay are *Ulva*, *Enteromorpha* and *Ceramium* (see Figure 2-1).

Even though both macroalgal and microalgal blooms may have intensive consequences, macroalgal blooms differ from microalgal blooms in three major ways (Valiela et al., 1997). Macroalgal blooms:

- lack direct chemical toxicity;
- have a broader range of ecological effects (i.e., thoroughly altering function and structure of affected ecosystems); and
- have a longer life.

Macroalgal blooms show strong seasonal patterns which are often related to large inputs of nutrients (Kamer et al, 2001). In the case of green macroalgae, such as *Enteromorpha* and *Ulva*, they can store both nitrogen and phosphorus and their growth rates are considered to be dependent on internal nutrient concentrations, while their uptake rates depend on the difference between internal nutrient concentration in macroalgae cells and external nutrient concentration in the water (Martins et al., 2001). Some of macroalgal species (e.g., *Enteromorpha intestinalis*) have preference of ammonium to nitrate in the water column for nitrogen uptake (Cohen and Fong, 2004).

In the case of *Enteromorpha*, in spite of their ability to fix to substrata on the sediment, it cannot completely resist the water flow. Strong tidal currents erode the attachment of *Enteromorpha* or tear away their fronds once they reach a critical length. This detachment was found in Langstone Harbour (U.K.), where the maximum current velocity is about 1.22 m s^{-1} (Martins et al., 2001).



Figure 2-1. Three common species of macroalgae appeared in Newport Bay.

2.2 Characteristics of macroalgae modeling

The following controls on macroalgal blooms are considerations for the model formulation.

- Temperature (Martins and Marques, 2002; Valiela et al., 1997).
- Light (Martins and Marques, 2002; Valiela et al., 1997). The formation of layered biomass mats has the potential to affect photosynthesis and respiration via various light attenuations (Brush and Nixon, 2003).
- Limiting nutrients (nitrogen, phosphorus) (Kamer et al., 2001; Martins and Marques, 2002; Valiela et al., 1997). Increased nutrient supply increases nutrient uptake rates,

tissue nutrient contents, and growth rates of macroalgae (Valiela et al., 1997). Macroalgae in the Bay have a relatively low tissue N:P (molar) ratio (e.g., 16.4-28.1 for *Enteromorpha intestinalis*; 21.8-40.1 for *Ceramium* spp.; 19.8-30.0 for *Ulva expansa*) which may indicate nitrogen limitation (Kamer et al, 2001). Therefore, nitrogen is likely the most limiting nutrient in Newport Bay, and phosphorus is the secondary (Kamer and Schiff, 2002).

Aside from creek inflows, possible sources for nutrients in the Bay include the following.

- ➔ Upwelling: quite large amounts of nitrate (approximately 0.2 mg L^{-1}) can be present in ocean water since the west coast of the Pacific Ocean is an upwelling zone (AHA, 1997). The ocean current, carrying cold water from northern latitudes, flows along the shore from Washington-Oregon border to southern California. Seasonal winds, combined with the Coriolis effect, drive surface waters offshore beginning in the spring. The driven surface waters from the coast are replaced by denser, cold water below carrying dissolved nutrients (<http://ceres.ca.gov/ceres/calweb/coastal/waters.html>). This process, known as upwelling, generally continues until September.
 - ➔ Nutrients released by sediments: organic materials delivered from inflows are decomposed in the sediments and the remineralized nutrients are released from the sediments.
- Salinity (Martins and Marques, 2002; Martins et al., 1999). Martins et al., (1999) showed that the growth of *Enteromorpha intestinalis* varies along a bell-shaped curve with salinity and that the optimum salinity range for growth is 18-22 ppt. *E. intestinalis* is more affected by lower than by higher salinity.
 - Grazing rate (Valiela et al., 1997).
 - Respiration and mortality rate (Trancoso et al., 2005).
 - Detachment stress (Martins and Marques, 2002; Trancoso et al., 2005).

Although macroalgae and microalgae (e.g., phytoplankton) are subject to the same growth requirements (temperature, light and nutrients) and the same basic processes, major differences between the two (Trancoso et al., 2005) must be taken into account in the model.

- Macroalgae are associated with the bottom substrate and are expressed in terms of areal densities (kg m^{-2}) rather than volumetric densities or concentrations (mg L^{-1}).
- Macroalgae are not dominantly subject to hydrodynamic transport.
- Macroalgae have no settling losses, but instead they have additional losses by sloughing and scouring from the bottom substrate where bottom shear stress is high.
- Macroalgal growth varies areally due to bed elevation because of light limitation and tidal stage. Light limitation reduces growth at bed elevations below the optimal elevation, and prevents colonization altogether at the lowest bed elevations. At higher bed elevation,

macroalgae can become emerged at low tide. Emerged macroalgae are considered to be dormant, reducing the overall growth rate, and extended emergence results in mortality. The productivity yield after reimmersion is not affected unless emergence results in mortality.

3. Conceptual models for macroalgal blooms in Newport Bay

The conceptual model for Upper Newport Bay describes the linkages between nutrient inputs and other parameters (temperature, light, salinity, etc.) and macroalgal blooms. The major constituents of the conceptual model include macroalgae, nitrogen (nitrate, ammonia, and particulate organic nitrogen), phosphorus (phosphate), dissolved oxygen, salinity, temperature and particulate organic matter, as shown in Figure 3-1.

These constituents are inter-related through biological, chemical, and physical processes in the Bay. The conceptual model is used to build the water quality model, which consists of a set of governing equations.

Table 3-2 lists the variables and symbols used in the water quality model. The coefficients, constants, and forcing parameters of the water quality model are shown in Table 3-3 and the governing equations are shown in Table 3-4.

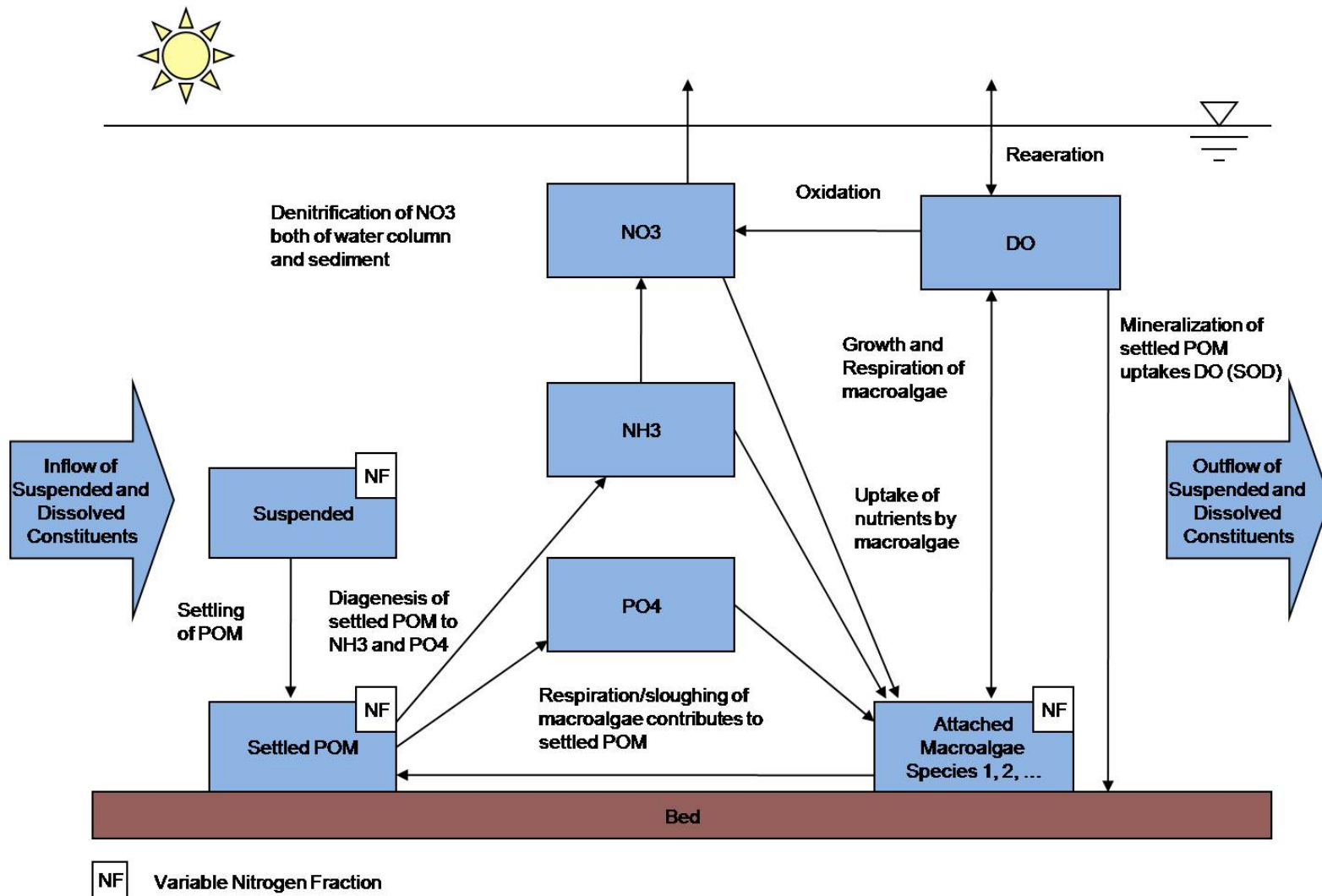


Figure 3-1. Schematic of the ecological model (with major nutrient interactions) of Newport Bay. Boxes indicate the constituents and arrows indicate biological, chemical and physical processes.

3.1 Macroalgae

The macroalgal community of Newport Bay is dominated by three main species including *Enteromorpha intestinalis*, *Ulva expansa* and filamentous red *Ceramium spp.* (Kamer et al., 2001). In the conceptual model, the three species are not modeled specifically, rather rates and coefficients are set to best characterize the overall macroalgae growth dynamics in the Bay. Macroalgal dynamics are governed in the model by the following processes: growth, respiration (and excretion), sloughing, and mortality, as shown in Figure 3-2. The concentration of macroalgae (M) changes as follows:

$$\frac{dM}{dt} = (\mu - r - s - m) \times M \quad (3.1)$$

where μ is growth, r is respiration, s denotes sloughing, and m is mortality.

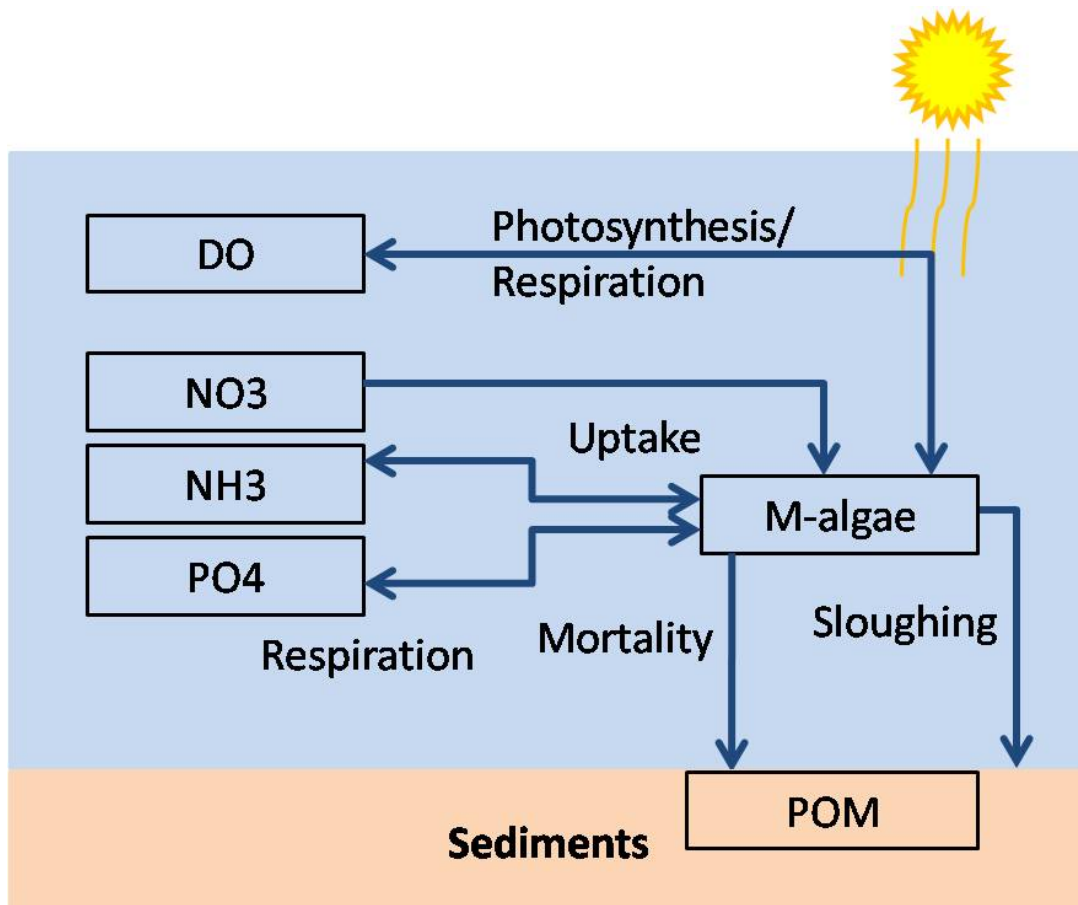


Figure 3-2. Conceptual model for macroalgae in Newport Bay.

3.1.1 Growth

The growth rate of macroalgae is described as a function of maximum growth rate at the optimum temperature (μ_{max}), temperature ($f(T)$), light ($f(I)$), salinity ($f(S)$), space ($f(SP)$), water depth ($f(D)$) and nutrients ($f(QN)$, and $f(P)$) where QN indicates internal nitrogen quota of macroalgae.

$$\mu = \mu_{max} \times f(T) \times f(I) \times f(S) \times f(SP) \times f(D) \times \min(f(QN), f(P)) \quad (3.2)$$

(1) Temperature function

The temperature function is computed as:

$$f(T) = \exp \left[-2.3 \times \left(\frac{T - T_{opt}}{T_x - T_{opt}} \right)^2 \right] \quad (3.3)$$

where T_{opt} is the optimum temperature at which growth rate is maximum

$$\begin{aligned} \text{If } T < T_{opt}, \quad T_x &= T_{min} \\ \text{If } T > T_{opt}, \quad T_x &= T_{max} \end{aligned}$$

where T_{min} is lower temperature limit below which growth ceases and T_{max} is upper temperature limit above which growth ceases (Martins et al., 2007; Martins and Marques, 2002).

(2) Salinity function

The salinity function is computed as:

$$\begin{aligned} f(S) &= 1 - \left(\frac{S - S_{opt}}{S_x - S_{opt}} \right)^m & \text{for } S \geq 5 \\ f(S) &= \left(\frac{S - S_{min}}{S_{opt} - S_{min}} \right)^m & \text{for } S < 5 \end{aligned} \quad (3.4)$$

where S_{opt} is the optimum salinity at which growth rate is maximum

$$\begin{aligned} \text{If } S < S_{opt}, \quad S_x &= S_{min} \text{ and } m = 2.5 \\ \text{If } S \geq S_{opt}, \quad S_x &= S_{max} \text{ and } m = 2 \end{aligned}$$

where S_{min} is lower salinity limit below which growth ceases and S_{max} is upper salinity limit above which growth ceases (Martins et al., 2007; Martins and Marques, 2002).

(3) Light function

There are three options for the light function is in the model:

1) Half Saturation

$$f(I) = \frac{I_z}{k_{LS} + I_z} \quad (3.5)$$

2) Smith function

$$f(I) = \frac{I_z}{\sqrt{k_{LS}^2 + I_z^2}} \quad (3.6)$$

3) Steele formula

$$f(I) = \frac{I_z}{I_0} \exp\left(1 - \frac{I_z}{I_0}\right) \quad (3.7)$$

where I_z is light intensity at depth z , k_{LS} is a half saturation constant for light; I_0 is optimal light level (Bowie et al., 1985). In this study, the Steele formula of the light function was used for the simulation of macroalgae. The Steele light function includes macroalgal self shading and was selected because it resulted in the best fit to the macroalgal data among three formulas. The attenuation of light in natural waters can be quantified by the Beer-Lambert law,

$$I_z = I_0 \exp(-\lambda z) \quad (3.8)$$

where λ is the light attenuation coefficient and I_0 is surface light intensity (energy). For the macroalgae modeling, the light intensity was calculated at the bottom of the water column. The light extinction coefficient is coupled to the macroalgal concentration using the non-linear Riley equation (Bowie et al., 1985):

$$\lambda = \lambda_0 + \lambda_1 M \quad (3.9)$$

where λ_0 is non-algal portion of the light extinction coefficient, (m^{-1}) and λ_1 is linear macroalgal self-shading coefficient, ($kg\ m^{-3}$).

(4) Space function

The macroalgal space limitation factor is defined as follows:

$$f(SF) = 1 - \frac{M}{k_{sp}} \quad (3.10)$$

where k_{sp} is the space limitation half-saturation constant for growth limitation (RMA, 2003).

(5) Depth function

The macroalgal depth limitation factor is expressed as:

$$\begin{aligned} f(D) &= 1 & \text{if } D > k_D \\ f(D) &= 0 & \text{if } D < k_D \end{aligned} \quad (3.11)$$

where D is the water depth and k_D is the critical water depth for growth limitation (RMA, 2003). The critical depth is defined as shallow water (e.g., water depth at low tide).

(6) Nutrients function

The internal nitrogen limitation factor of macroalgae is expressed as:

$$f(QN) = \frac{QN - QN_{min}}{k_q + QN - QN_{min}} \quad (3.12)$$

where $QN = \frac{IN}{M}$, where IN is internal nitrogen concentration of macroalgae; QN_{min} is the minimum internal nitrogen quota (i.e., minimum possible value for nitrogen concentration in macroalgae tissue) and k_q is the nitrogen half-saturation constant for growth limitation (Solidoro et al., 1997).

Chlorophyte macroalgae, like *Ulva* and *Enteromorpha*, have a lower internal phosphorus concentration than that of nitrogen. The range of internal phosphorus concentration is restricted only between 1 and 5 mg P (g dw)⁻¹ (Solidoro et al., 1997). In addition, the critical concentration level for internal phosphorus, where the growth reaches its maximum efficiency, is close to the minimum quota value (Solidoro et al., 1997). Therefore, the growth of macroalgae is assumed to use externally available phosphorus rather than to store phosphorus in the biomass. The growth rate of macroalgae of Newport Bay is conceptualized in the model to be related to the external phosphorus

concentration through the Monod kinetic. The phosphorus limitation factor of macroalgae is expressed as:

$$f(P) = \frac{PO_4}{k_{PO_4} + PO_4} \quad (3.13)$$

where k_{PO_4} is phosphate half-saturation constant for growth limitation (Solidoro et al., 1997).

3.1.2 Respiration

Respiration is a function of temperature (Bowie et al., 1985) and is expressed as:

$$r = r_{max} \times f(T) \quad (3.14)$$

where r_{max} is maximum respiration rate at the optimum temperature.

3.1.3 Sloughing

Macroalgae are sloughed by bottom currents, which transport them close to the bed (Flindt et al., 2007; Trancoso et al., 2005). Flindt et al. (2007) suggested a linear regression between sloughed biomass and current speed for four species of macroalgae. Their linear regressions for two kinds of macroalgae (i.e., *Ulva sp.* and *Enteromorpha sp.*) are presented in

Table 3-1.

Table 3-1. Estimated sloughing thresholds and current speeds at which total sloughing is reached, calculated from linear regression between sloughed biomass and current speed for two species of macroalgae (source: Flindt et al., 2007).

Species	Threshold (cm s ⁻¹)	Regression	r ²	Total sloughing (cm s ⁻¹)
<i>Ulva sp.</i>	12	y = 0.0143x-0.17	0.91	82

<i>Enteromorpha sp.</i>	21	$y = 0.0094x - 0.2$	0.86	128
-------------------------	----	---------------------	------	-----

y is a ratio of sloughing biomass to total biomass; x is a current speed (cm s⁻¹)

*No data is available for *Ceramium*.

In the model, when macroalgae are sloughed they are not transported; rather they are removed from the system at the time of sloughing (i.e., it is assumed that sloughed macroalgae exited the system to the ocean due to high water current speed, and did not settle and decay). The sloughing term in the model serves primarily to eliminate macroalgae in the deeper channels where the velocities are higher.

Sloughing rate for a time interval is expressed as follows:

$$s = \frac{U - U_{min}}{U_{max} - U_{min}} \quad \text{if } U \geq U_{min} \quad (3.15)$$

where U is current speed; U_{min} is minimum current speed at which sloughing occurs and U_{max} is maximum current speed at which sloughing of all the macroalgae occurs.

3.1.4 Mortality

In the conceptual model, mortality and algal decomposition are minimal when growth conditions are optimal, and maximum when conditions are severely limiting (Bowie et al., 1985). Macroalgal mortality is expressed as:

$$m = m_{max} \times \left[1 - \left(f(S) \times f(I) \times \min(f(QN), f(P)) \right) \right] \quad (3.16)$$

where m_{max} is maximum mortality rate at the optimum temperature.

In the model, a certain portion (70 – 80%) of the dead macroalgae is assumed to be recycled as deposited **POM** on the bed where it decays and returns nutrients to the system. The percentage of dead macroalgae that was recycled was a calibrated parameter in the model.

It is important to note that macroalgae is modeled as a fixed constituent and is never transported. Therefore, recycled macroalgae enters the bed at the location where it grew.

3.2 Nitrogen

The conceptual model of nitrogen consists of nitrate, ammonia, and internal nitrogen (see Figure 3-3).

- Nitrate

Nitrate (NO_3) is provided with nitrification of ammonia (NH_3), but consumed by the uptake by macroalgae and denitrification of NO_3 . Mass transfer of NO_3 between porewater and water column is in the model as well. The direction of mass transfer depends on the concentration gradient between the porewater and water column. Reaction rates of these processes are described as the first-order kinetics. The equation of nitrate dynamics is as follows:

$$\frac{dNO_3}{dt} = (k_{nitr} \times NH_3 \times f_{nitr} - k_{denit} \times NO_3) \times \theta^{T-20} - V_{NO} \times \frac{M}{D} - K_{aNO_3}(NO_3 - NO_{3s}) \quad (3.17)$$

$$V_{NO} = V_{m,NO} \times \frac{NO_3}{k_{NO_3} + NO_3} \times \frac{QN_{max} - QN}{QN_{max} - QN_{min}} \quad (3.18)$$

where k_{nitr} is the nitrification rate of NH_3 ; k_{denit} is the denitrification rate of NO_3 ; θ^{T-20} is the non-dimensional temperature multiplier of reaction; V_{NO} is nitrate uptake rate; K_{aNO_3} is the mass transfer rate of NO_3 ; NO_{3s} is the concentration of NO_3 in the sediment; $V_{m,NO}$ is maximum nitrate uptake rate; k_{NO_3} is half saturation constant for NO_3 ; and QN_{max} and QN_{min} are the maximum and minimum internal nitrogen quotas for macroalgae, respectively.

The nitrification reaction depends on ammonium concentration and sufficient oxygen levels (greater than 1 to 2 mg L⁻¹). The nitrification inhibition factor, f_{nitr} , is expressed by a function of the concentration of dissolved oxygen (DO) as follows (Chapra, 1997):

$$f_{nitr} = 1 - \exp(-k_{nitr} \times DO) \quad (3.19)$$

where k_{nitr} denotes first-order nitrification inhibition coefficient (≈ 0.6 L mg⁻¹). All other coefficients are previously defined.

- Ammonia

Ammonia (NH_3) is provided with respiration (or excretion) of macroalgae, and is consumed by nitrification and the uptake by macroalgae in the water column. NH_3 is also produced by mineralization of settled POM in the sediments. NH_3 in the sediments is

transferred to the water column corresponding difference of concentrations of two media. The mass transfer of NH_3 is included in the model. The equation of ammonia dynamics is as follows:

$$\frac{dNH_3}{dt} = r \times QN \times \frac{M}{D} - V_{NH} \times \frac{M}{D} - k_{nit} \times NH_3 \times f_{nit} \times \theta_{T-20}^{T-20} - K_{DNH_3} (NH_3 - NH_{3s}) \quad (3.20)$$

$$V_{NH} = V_{mNH} \times \frac{NH_3}{K_{NH_3} + NH_3} \times \frac{QN_{max} - QN}{QN_{max} - QN_{min}} \quad (3.21)$$

where V_{NH} is ammonia uptake rate; k_{nit} is the nitrification rate of NH_3 ; K_{DNH_3} is the mass transfer rate of NH_3 ; NH_{3s} is the concentration of NH_3 in the sediment; V_{mNH} is maximum ammonia uptake rate; and K_{NH_3} is half saturation constant for NH_3 . All other coefficients are previously defined.

- Internal nitrogen

IN is provided with the uptake of NO_3 and NH_3 , and consumed by respiration, sloughing and mortality of macroalgae.

$$\frac{dIN}{dt} = (V_{NO} + V_{NH}) \times M - (r + s + m) \times IN \quad (3.22)$$

where V_{NO} is the nitrate uptake rate by macroalgae and V_{NH} is the ammonia uptake rate. All other coefficients are previously defined.

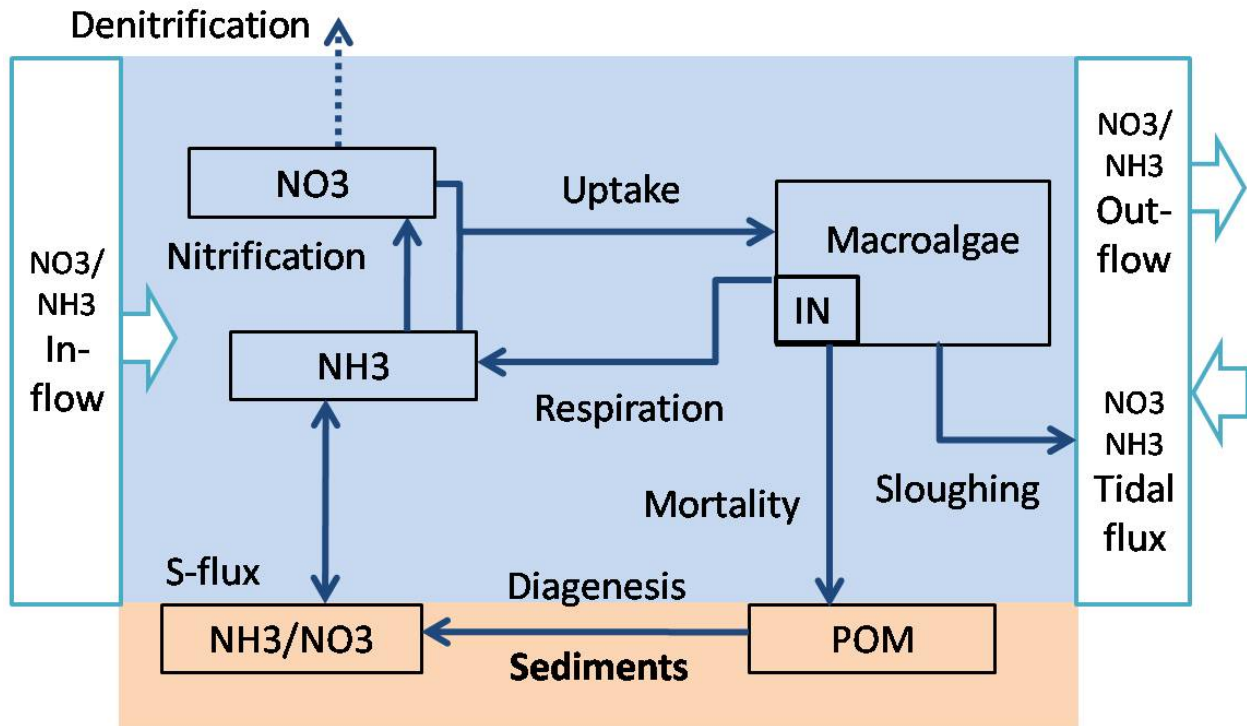


Figure 3-3. Conceptual model for nitrogen in Newport Bay.

3.3 Phosphorus

In the conceptual model, orthophosphate (PO_4) (see Figure 3-4) is provided by respiration of macroalgae, and consumed by biological uptake and adsorption of PO_4 to POM . In the model, adsorption is included to account for accumulation of PO_4 on the surface of suspended solids in the water column which will be flushed out of system (adsorbed PO_4 does not contribute to the sediments in the model). PO_4 is also produced from settled POM in the sediments which is included in the model as the mass transfer. There is no mineral phosphorus in the model. Rate constants of these processes are described as the first order kinetics. The equation describing orthophosphate dynamics is as follows:

$$\frac{dPO_4}{dt} = (r - \mu) \times a_p \times \frac{M}{D} - K_{SP_4}(PO_4 - PO_{4s}) - k_{ads} \times PO_4 \times \theta_{min}^{T-20} \quad (3.23)$$

where a_p is a fraction of macroalgae that is phosphorus; K_{SP_4} is the mass transfer rate of PO_4 ; PO_{4s} is concentration of PO_4 in the sediment; and k_{ads} is a rate of adsorption onto suspended solids (day^{-1}). All other coefficients are previously defined.

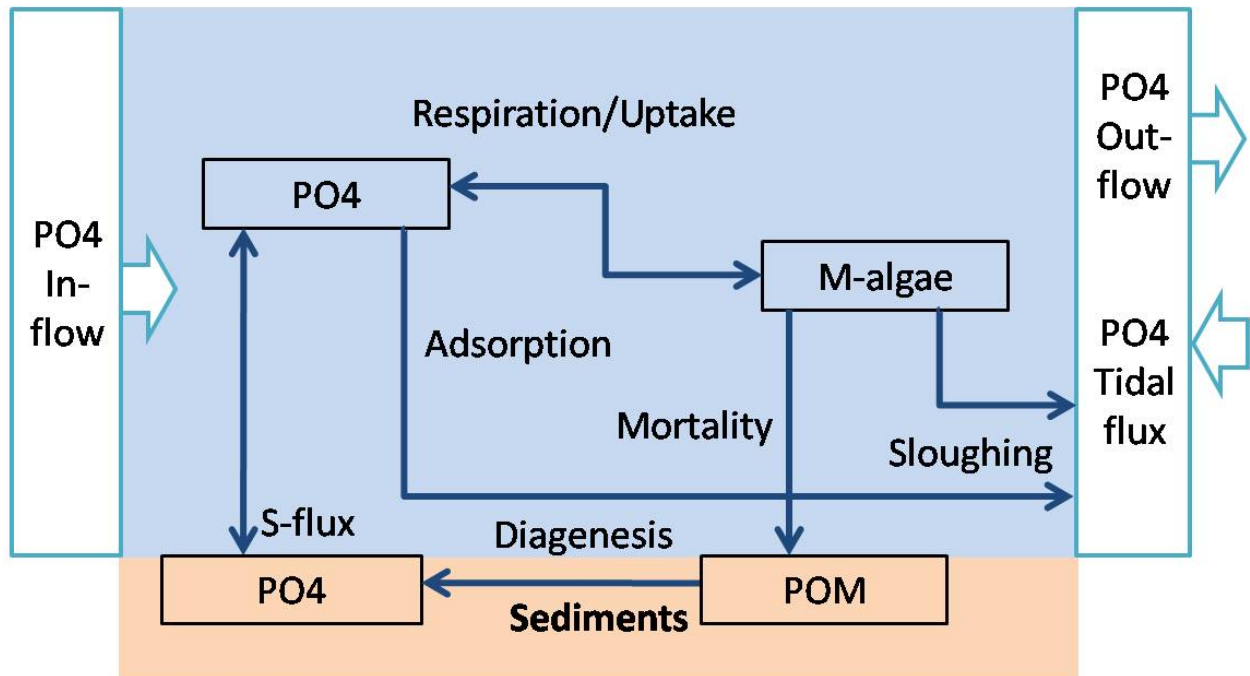


Figure 3-4. Conceptual model for phosphorus in Newport Bay.

3.4 Dissolved oxygen (DO)

Dissolved oxygen (**DO**) is affected by nutrient cycles that generally demand oxygen. The conceptual model of dissolved oxygen in Newport Bay includes the processes of reaeration of O₂ gas (gas transfer), photosynthesis, respiration of macroalgae, nitrogenous biochemical oxygen demand (NBOD) for nitrification and sediment oxygen demand (SOD) from nutrient-rich benthic sediment (see Figure 3-5). **DO** in the water column and sediments is exchanged via mass transfer. Reaction rates are described as first-order kinetics (Chapra, 1997).

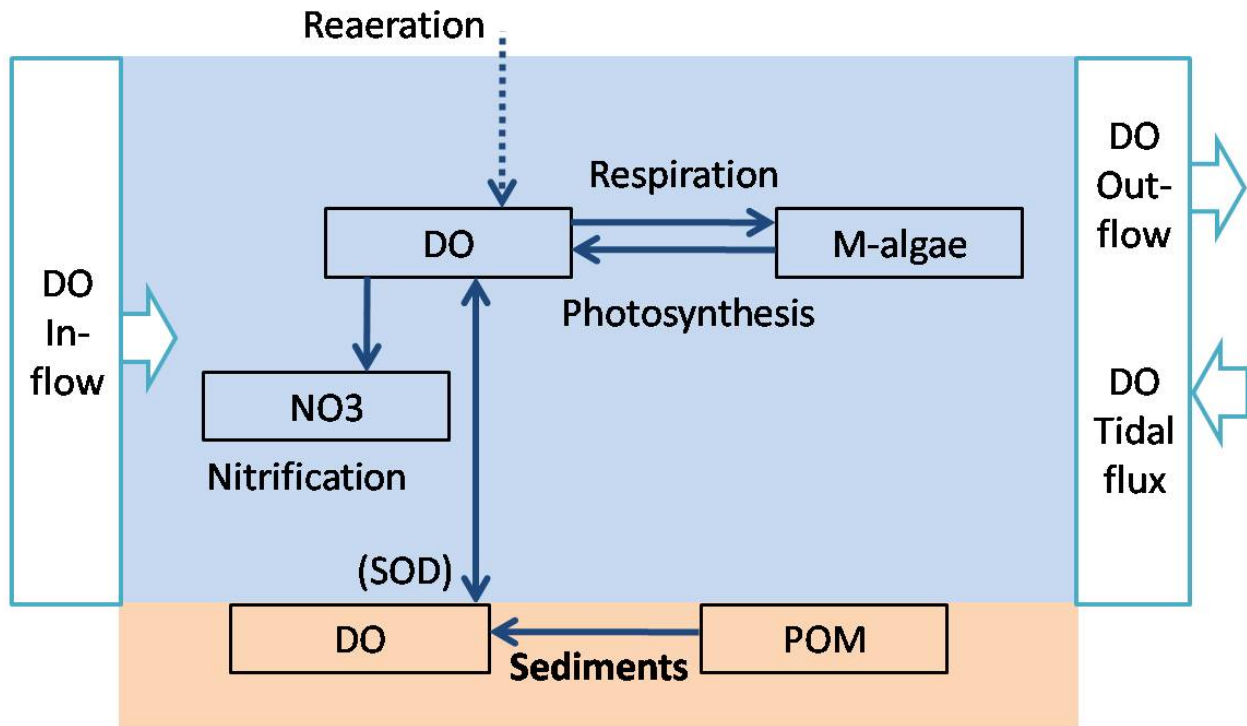


Figure 3-5. Conceptual model for dissolved oxygen in Newport Bay.

DO concentration in the water column is described by the following equation:

$$\frac{dDO}{dt} = k_a \times \theta_{DO}^{T-20} \times (O_s - DO) + (\mu - r) \times r_{OC} \times a_c \times \frac{M}{D} - K_{SDO} (DO - DO_s) \times \theta_{SOD}^{T-20} - k_{mtc} \times r_{ON} \times NH3 \times f_{mtc} \times \theta_{T-20}^{T-20}$$

where k_a is the reaeration rate; O_s is the saturation concentration of oxygen at non-standard pressure, r_{OC} is the ratio of mass of oxygen consumed per mass of carbon assimilated; a_c is a fraction of macroalgae that is carbon; K_{SDO} is the mass transfer rate of DO between sediment and water column; DO_s is concentration of DO in the sediment; r_{ON} is the ratio of mass of oxygen consumed per mass of nitrogen oxidized. All other terms have been previously defined.

- Reaeration rate

Estuary gas transfer, k_a , can be affected by both water and wind velocity. The water velocity effects are typically computed with the O'Connor-Bobbins formula (Chapra, 1997).

$$k_a = \frac{\sqrt{D_{L,O} U_0}}{H^{3/2}} \quad (3.25)$$

where U_0 is mean tidal velocity over a complete tidal cycle; $D_{L,O}$ is liquid diffusion coefficient. The diffusivity of oxygen in natural waters is approximately $2.09 \times 10^{-5} \text{ cm}^2 \text{ s}^{-1}$.

The wind effects can be computed with any of the formulas developed for standing waters (Chapra, 1997) as follows:

$$k_a = \frac{0.728U_w^{0.85} - 0.317U_w + 0.0372U_w^2}{H} \quad (3.26)$$

where U_w is wind speed measured 10 m and above the water surface (m s^{-1}). Combining the above two approaches for estuaries affected by both tidal velocities and wind gives the following:

$$k_a = 3.93 \frac{\sqrt{U_0}}{H^{3/2}} + \frac{0.728U_w^{0.85} - 0.317U_w + 0.0372U_w^2}{H} \quad (3.27)$$

The formula both with water and wind velocity was applied for Newport Bay.

- Saturation of dissolved oxygen (RMA, 2003)

Solubility of dissolved oxygen is dependent on temperature, salinity, and atmospheric pressure. The conceptual model limits the dependence to temperature, salinity and atmospheric pressure when temperature is a defined constituent.

The relationships take the following forms:

$$b_1 O_{m} = -13934410 + \frac{1.575701e5}{T_a} - \frac{6.642308e7}{T_a^2} + \frac{1.243800e10}{T_a^3} - \frac{8.621949e11}{T_a^4} - \frac{1}{1.80655} \times S_{at} \times \left[(3.1929e - 2) - \left(\frac{1.9428e1}{T_a} \right) + \left(\frac{3.8673e3}{T_a^2} \right) \right]$$

where O_m is equilibrium oxygen concentration at 1.00 atm (mg L^{-1}); T_a is water temperature ($^{\circ}\text{K}$), within the range 0.0 to 40.0 $^{\circ}\text{C}$; and S_{at} is salinity (if active in the simulation).

$$O_s = O_m P \frac{(1 - P_{WV}/P)(1 - \varphi P)}{(1 - P_{WV})(1 - \varphi)} \quad (3.29)$$

where O_s is equilibrium oxygen concentration at non-standard pressure (mg L^{-1}); P is atmospheric pressure (atm); P_{WV} is partial pressure of water vapor (atm), which may be computed from:

$$\ln P_{WV} = 11.8571 - \frac{3840.7}{T} - \frac{216961}{T^2}$$

$$\varphi = 0.000975 - 1.426e - 5 T + 6.436e - 8 T^2 \quad (3.30)$$

where T is temperature in $^{\circ}\text{C}$.

3.5 Sediment fluxes

A schematic of the conceptual sediment model is shown in Figure 3-6. The sediment conceptual model includes fluxes and transformations of dissolved oxygen (DO), POM , NH_3 , NO_3 and PO_4 . Sedimentary organic matter, which has been recently deposited, is transformed microbially and chemically into inorganic matter. This process is called diagenesis. DO , NO_3 , NH_3 and PO_4 in the sediments affect concentrations of these same constituents in the water column through mass transfer, as described in the equations above. This mass transfer is described in the equations as a diffusion process, but in reality includes other processes such as bioperturbation and tidal pumping. Coefficients were calibrated based on empirical experiments and field data, thus they do indirectly include bioperturbation and tidal pumping.

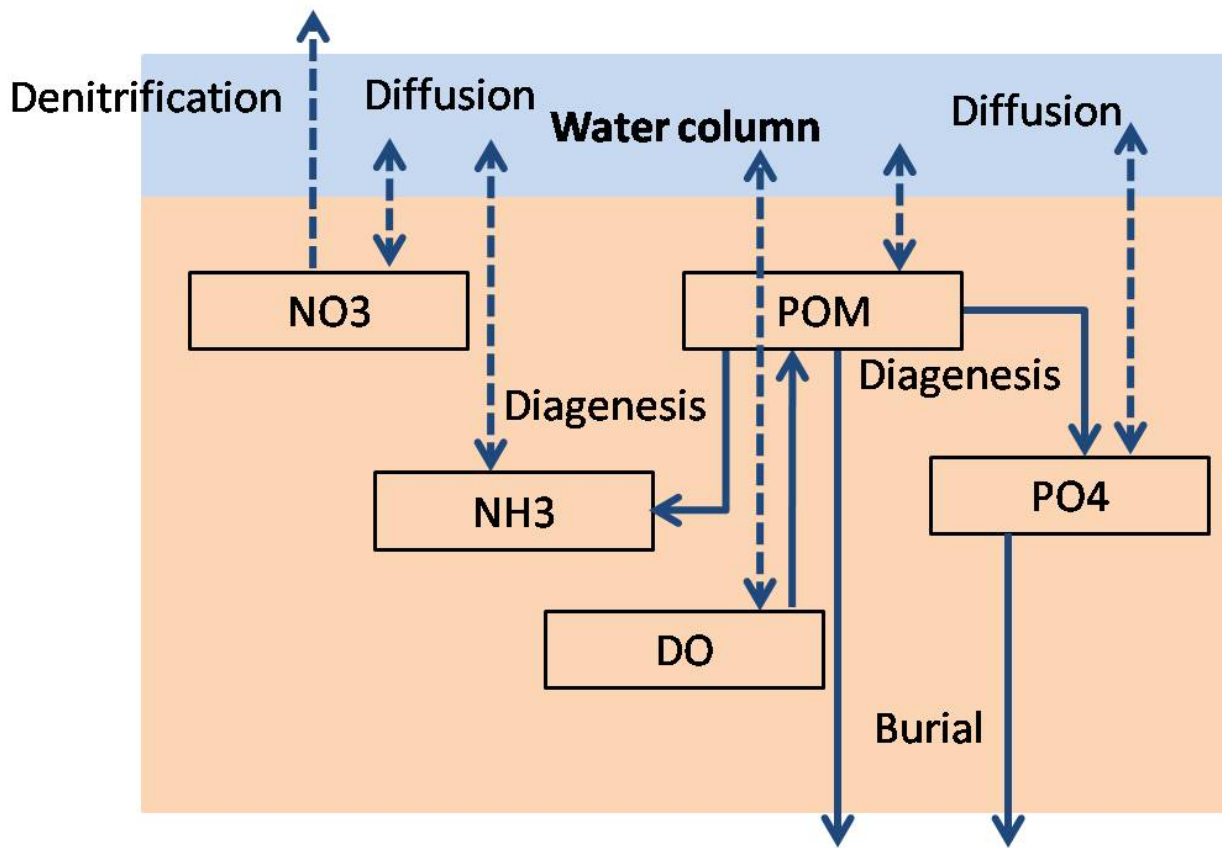


Figure 3-6 Conceptual sediment model for Newport Bay.

The following equations describe the sediment processes:

$$H_s \times \frac{dDO_s}{dt} = K_{sDO} \times (DO - DO_s) - k \times \theta_{\text{ran}}^{T-20} \times r_{\text{sc}} \times POM_s \times H_s \quad (3.31)$$

where H_s is the depth of the (active) sediment layer; K_{sDO} is the mass transfer rate of DO between sediment and water column; k is the decay rate of POM and r_{sc} is a carbon content of sediment POM_s .

$$H_s \times \frac{dNH3_s}{dt} = k \times \theta_{\text{ran}}^{T-20} \times r_{\text{sn}} \times POM_s \times H_s + K_{sNH3} \times (NH3 - NH3_s) - k_{\text{mtz}} \times \theta_{\text{ran}}^{T-20} \times NH3_s \times H_s$$

where r_{SN} is a nitrogen content of sediment *POM* and k_{nitr} is the nitrification rate of *NH₃* in the sediment.

$$H_s \times \frac{dNO_3_s}{dt} = k_{nitr} \times \theta_{r_{SN}}^{T-20} \times NH_3_s \times H_s + K_{denitr} \times (NO_3 - NO_3_s) - k_{denitr} \times \theta_{r_{SN}}^{T-20} \times NO_3_s \times H_s$$

where k_{denitr} is the denitrification rate in the sediment.

$$H_s \times \frac{dPO_4_s}{dt} = k \times \theta_{r_{SP}}^{T-20} \times r_{SP} \times POM_s \times H_s + K_{pp04} \times (PO_4 - PO_4_s) \quad (3.34)$$

where r_{SP} is a phosphorus content of sediment *POM*. All other coefficients have been previously defined.

Table 3-2 List of symbols of the water quality model

Symbols	Description
Biological symbols	
M	concentration of macroalgae (kg m^{-2})
μ	macroalgae growth rate (day^{-1});
r	macroalgae respiration (and excretion) rate (day^{-1})
s	macroalgae scouring rate (day^{-1})
m	macroalgae mortality (day^{-1})
$f(T)$	function of temperature on macroalgal growth rate
$f(S)$	function of salinity on macroalgal growth rate
$f(I)$	function of light on macroalgal growth rate
$f(QN)$	function of internal nitrogen on macroalgal growth rate
$f(P)$	function of phosphorus on macroalgal growth rate
$f(SP)$	function of space limitation on macroalgal growth rate
$f(D)$	function of water depth on macroalgal growth rate
T	water temperature ($^{\circ}\text{C}$)
T_{opt}	optimum water temperature ($^{\circ}\text{C}$)
T_{min}	lower temperature limit below which growth ceases ($^{\circ}\text{C}$)
T_{max}	upper temperature limit below which growth ceases ($^{\circ}\text{C}$)
S	salinity (ppt)
S_{opt}	optimum salinity (ppt)
S_{min}	lower salinity limit below which growth ceases (ppt)
S_{max}	upper salinity limit below which growth ceases (ppt)
I_0	light intensity at water surface (W m^{-2})
I_z	light intensity at depth z (W m^{-2})
k_{LS}	half saturation constant for light (W m^{-2})
I_5	optimal light level (W m^{-2})
λ	light attenuation coefficient (m^{-1})
λ_0	non-algal portion of the light extinction coefficient (m^{-1})
λ_1	linear macroalgal self-shading coefficient ($\text{m}^{-1} (\text{kg m}^{-2})^{-1}$)
z	water depth in the water column (vertical coordinate) (m)
k_{sp}	space limitation half-saturation constant for growth (kg m^{-2})
D	surface water depth (m)
k_D	critical water depth for growth limitation (m)
QN	internal nitrogen quota of macroalgae
QN_{min}	minimum internal nitrogen quota
QN_{max}	maximum internal nitrogen quotas for macroalgae
k_q	nitrogen half-saturation constant for growth limitation
k_{PO4}	phosphate half-saturation constant for growth limitation (mg m^{-3})
U	current speed (cm s^{-1})
U_{min}	minimum current speed at which sloughing occurs (cm s^{-1})
U_{max}	maximum current speed at which sloughing of all the macroalgae occurs (cm s^{-1})

M_{max}	maximum mortality rate at the optimum temperature (day^{-1})
Chemical symbols	
NO_3	concentration of nitrate (mg m^{-3})
k_{nit}	nitrification rate of NH_3 (day^{-1})
k_{denit}	denitrification rate of NO_3 (day^{-1})
$\theta_{T_{max}}^{T-20}$	non-dimensional temperature multiplier of reaction
K_{SNO_3}	mass transfer rate of NO_3 (m day^{-1})
V_{NO}	nitrate uptake rate ($\text{mg-N dwg}^{-1} \text{d}^{-1}$)
V_{maxNO}	maximum nitrate uptake rate ($\text{mg-N dwg}^{-1} \text{d}^{-1}$)
k_{NO_3}	half saturation constant for NO_3 (mg m^{-3})
f_{nit}	The nitrification inhibition factor
k_{nitv}	first-order nitrification inhibition coefficient
NH_3	concentration of ammonia (mg m^{-3})
V_{NH}	ammonia uptake rate ($\text{mg-N dwg}^{-1} \text{d}^{-1}$)
K_{SNH_3}	mass transfer rate of NH_3 ($\text{mg-N dwg}^{-1} \text{d}^{-1}$)
V_{maxNH}	maximum ammonia uptake rate ($\text{mg-N dwg}^{-1} \text{d}^{-1}$)
k_{NH_3}	half saturation constant for NH_3 (mg m^{-3})
IN	internal nitrogen (kg m^{-2})
PO_4	orthophosphate concentration (mg m^{-3})
a_p	fraction of macroalgae that is phosphorus
K_{SPO_4}	mass transfer rate of PO_4 (m day^{-1})
k_{ads}	rate of adsorption onto suspended solids (day^{-1})
POM	particulate organic matter (mg m^{-3})
DO	dissolved oxygen concentration (mg L^{-1})
θ_{DO}^{T-20}	non-dimensional temperature multiplier of DO
k_a	reaeration rate (day^{-1})
O_s	saturation concentration of oxygen at non-standard pressure (mg L^{-1})
r_{OC}	ratio of mass of oxygen consumed per mass of carbon assimilated
a_c	fraction of macroalgae that is carbon
K_{SDO}	mass transfer rate of DO between sediment and water column (m day^{-1})
r_{ON}	ratio of mass of oxygen consumed per mass of nitrogen oxidized
$K_{L,O}$	mass-transfer velocity in the water layer (m d^{-1})
U_0	mean tidal velocity over a complete tidal cycle (m day^{-1})
U_w	wind speed measured 10 m and above the water surface (m s^{-1})
O_{sm}	equilibrium oxygen concentration at 1 atm (mg L^{-1}) within the range 0.0 to 40.0 °C
T_a	water temperature (°K)
P	atmospheric pressure (atm)
P_{wv}	partial pressure of water vapor (atm)
Sediment symbols	
POM_s	settled POM in the sediments (mg m^{-2})
H_s	depth of biologically-active sediment layer (m)
K_{SDO}	mass transfer rate of DO between sediment and water column (m day^{-1})
k	decay rate of POM (day^{-1})

γ_{SC}	carbon content of sediment POM_s
γ_{SN}	nitrogen content of sediment POM_s
k_{nit}	nitrification rate of NH_3 in the sediment (day^{-1})
k_{denitr}	denitrification rate in the sediment (day^{-1})
γ_{SP}	phosphorus content of sediment POM_s
DO_s	concentration of dissolved oxygen in the sediment (mg m^{-3})
NH_3_s	concentration of ammonia in the sediment (mg m^{-3})
NO_3_s	concentration of nitrate in the sediment (mg m^{-3})
PO_4_s	concentration of phosphate in the sediment (mg m^{-3})

Table 3-3. The coefficients and constants of the water quality model

Symbols	Description	Lit. Range	Calibrated Value	Units	Source
Biological processes					
μ_{max}	maximum growth rate at the optimum temperature	0.15-1.5	1.2	day ⁻¹	Martins and Marques (2002); Oberg (2006); Solidoro et al. (1997)
T_{opt}	optimum temperature at which growth rate is maximum	15-30	24.5	°C	Martins and Marques (2002)
T_{min}	lower temperature limit below which growth ceases	10	10	°C	Martins and Marques (2002)
T_{max}	upper temperature limit above which growth ceases	35	35	°C	Martins and Marques (2002)
S_{opt}	optimum salinity at which growth rate is maximum	18-22	18	ppt	Martins and Marques (2002)
S_{min}	lower salinity limit at which growth rate ceases	0	0	ppt	Martins and Marques (2002)
S_{max}	upper salinity limit at which growth ceases	45	45	ppt	Martins and Marques (2002)
I_s	optimum (saturating) light intensity	48-192	160	W m ⁻²	Chapra (1997)
λ_0	non-algal portion of the light extinction coefficient	0.4	1.0*	m ⁻¹	Solidoro et al. (1997)
λ_1	linear macroalgae self-shading coefficient	-	1.0**	kg m ⁻³	Solidoro et al. (1997)
k_{sp}	space limitation half-saturation constant for growth limitation	-	4.5**	kg m ⁻²	Oberg (2006): max. areal density (0.5-3.0 kg dw m ⁻²)
k_D	critical water depth for growth limitation	-	0.05**	m	
k_q	half saturation constant for <i>IN</i>	5.6, 7.0, 8.0	35****	mg-N dwg ⁻¹	Martins and Marques (2002); Solidoro et al. (1997); Solidoro et al. (1997)
Q_{Nmin}	minimum internal nitrogen quota	7.0-24.0	10	mg-N dwg ⁻¹	Martins and Marques (2002); Solidoro et al. (1997)
Q_{Nmax}	maximum internal nitrogen quota	27.0-60.0	55	mg-N dwg ⁻¹	Martins and Marques (2002); Solidoro et al. (1997)
V_{NNO_3}	maximum nitrate uptake rate	0.35-28.8	21	mg-N dwg ⁻¹ d ⁻¹	Martins and Marques (2002); Oberg (2006); Solidoro et al. (1997)
k_{NNO_3}	half saturation constant for <i>NNO₃</i>	0.02-0.25	0.15	mg-N L ⁻¹	Martins and Marques (2002); Oberg (2006); Solidoro et al. (1997)
V_{NNH_4}	maximum ammonia uptake rate	16.8-124.8	120	mg-N dwg ⁻¹ d ⁻¹	Martins and Marques (2002); Solidoro et al. (1997)
k_{NHE}	half saturation constant for <i>NHE</i>	0.07-0.6	0.27	mg-N L ⁻¹	Martins and Marques (2002); Solidoro et al. (1997)
k_{PO_4}	phosphate half-saturation constant for growth limitation	0.01	0.04*	mg-P L ⁻¹	Solidoro et al. (1995)
r_{max}	maximum respiration rate at the optimum temperature	0.02-0.1	0.085	day ⁻¹	Martins and Marques (2002)
U_{min}	minimum current speed for sloughing	12-21	12	cm s ⁻¹	Flindt et al. (2007)

U_{max}	maximum current speed for total sloughing	82-128	88	cm s ⁻¹	Flindt et al. (2007)
M_{max}	maximum mortality rate at the optimum temperature	0.003-0.8	0.006	day ⁻¹	Coffaro and Sfriso (1997); Solidoro et al. (1995); Trancoso et al. (2005)
a_p	fraction of macroalgae that is phosphorus	0.0004-0.0086	0.002	-	Kamer et al.(2001); Sutula et al. (2006); Wheeler and Bjornsater (1992)
a_c	fraction of macroalgae that is carbon	0.27-0.36	0.3	-	Hernandez et al.(1997)
Chemical processes					
k_{nit}	nitrification rate of NH_3	0.001-1.3	0.150	day ⁻¹	Bowie et al. (1985)
k_{den}	denitrification rate of NOS	0.0-1.0	***0.01/0.15	day ⁻¹	Bowie et al. (1985)
$\theta_{T_{max}}^{Q-20}$	the non-dimensional temperature multipliers of reaction	1.045-1.08	1.08	-	Bowie et al. (1985)
k_{nitr}	first-order nitrification inhibition coefficient	0.6	0.6	L mg ⁻¹	Chapra (1997)
k_{ads}	rate of adsorption of phosphate onto suspended solids	-	0.001**	day ⁻¹	
θ_{DO}	temperature coefficient for oxygen transfer	1.024	1.065	-	Chapra (1997)
γ_{OC}	ratio of mass of oxygen consumed per mass of carbon assimilated	2.67	2.67	mg O mg C ⁻¹	Chapra (1997)
γ_{ON}	ratio of mass of oxygen consumed per mass of nitrogen oxidized	4.57	4.57	mg O mg N ⁻¹	Chapra (1997)
θ_{SOD}	temperature coefficient for SOD	1.04-1.13	1.065	-	Chapra (1997)
Sediment processes					
k	decay rate of POM	0.0018-0.035	***0.02/0.025	day ⁻¹	DiToro (2001)
H_2	depth of biologically-active sediment layer	-	0.1**	m	
k_{snit}	nitrification rate of ammonia in the sediment	-	0.15**	day ⁻¹	
k_{sden}	Denitrification rate in the sediment	-	***0.01/0.15**	day ⁻¹	
K_{sDO}	mass transfer rate of DO in the sediment	-	0.15**	m day ⁻¹	
K_{sNH_3}	mass transfer rate of NH_3 in the sediment	0.06-0.1464	0.15****	m day ⁻¹	Sanford and Crawford(2000)
K_{sNO_2}	mass transfer rate of NO_2 in the sediment	-	0.08**	m day ⁻¹	
K_{sPO_4}	mass transfer rate of PO_4 in the sediment	0.0816	0.08*	m day ⁻¹	Sanford and Crawford(2000)
γ_{SC}	carbon content of sediment POM	0.0096-0.012	0.01	-	Peng et al.(2007); Sutula et al.(2006)
γ_{SN}	nitrogen content of sediment POM	0.0008-0.0012	0.001	-	Peng et al.(2007); Sutula et al.(2006)
γ_{SP}	phosphorus content of sediment POM	0.00048-0.00054	0.0005	-	Sutula et al.(2006)

* k_{sed} : Since only one literature value is available, a calibrated value within reasonable range of the observed value was considered acceptable.

** Literature values are not available..

*** Considering spatial variation of the bay, two values were used in the simulation.

****Model results were improved by using a value outside the range of literature values.

Table 3-4. Summary of differential equations for the constituents of the water quality model

Macroalgae	
$\frac{dM}{dt} = (\mu - r - s - m) \times M$	(3.1)
$\mu = \mu_{max} \times f(T) \times f(S) \times f(I) \times f(SP) \times f(D) \times \min(f(QN), f(P))$	(3.2)
$f(T) = \exp\left[-2.3 \times \left(\frac{T - T_{opt}}{T_x - T_{opt}}\right)^2\right]$	(3.3)
$\text{if } T < T_{opt} \quad T_x = T_{min}$	
$\text{if } T > T_{opt} \quad T_x = T_{max}$	
$f(S) = 1 - \left(\frac{S - S_{opt}}{S_x - S_{opt}}\right)^m \quad \text{for } S \geq 5$	(3.4)
$f(S) = \left(\frac{S - S_{min}}{S_{opt} - S_{min}}\right)^m \quad \text{for } S < 5$	
$\text{if } S < S_{opt} \quad S_x = S_{min} \text{ and } m = 2.5$	
$\text{if } S \geq S_{opt} \quad S_x = S_{max} \text{ and } m = 2$	
$f(I) = \frac{I}{I_0} \exp\left(1 - \frac{I}{I_0}\right)$	(3.5)
$I_0 = I_0 \exp(-\lambda z)$	(3.8)
$\lambda = \lambda_0 + \lambda_1 M$	(3.9)
$f(SP) = 1 - \frac{M}{k_{sp}}$	(3.10)
$f(D) = 1 \quad \text{if } D > k_D \quad f(D) = 0 \quad \text{if } D \leq k_D;$	(3.11)
$f(QN) = \frac{QN - QN_{min}}{k_{QN} + QN - QN_{min}}$	(3.12)
$f(P) = \frac{PO_4}{k_{PO_4} + PO_4}$	(3.13)
$r = r_{max} \times f(T)$	(3.14)

$$s = \frac{U - U_{\min}}{U_{\max} - U_{\min}} \quad \text{if } U > U_{\min} \quad (3.15)$$

$$m = m_{\max} \times \left[1 - \left(f(S) \times f(I) \times \min(f(QN), f(P)) \right) \right] \quad (3.16)$$

Nitrogen

$$\frac{dNO_3}{dt} = (k_{nit} \times NH_3 \times f_{nit} - k_{dnt} \times NO_3) \times \theta_{T_{NO_3}}^{T-20} - V_{NO} \times \frac{M}{D} - K_{SNO_3}(NO_3 - NO_{3s}) \quad (3.17)$$

$$V_{NO} = V_{mNO} \times \frac{NO_3}{k_{NH_3} + NO_3} \times \frac{QN_{\max} - QN}{QN_{\max} - QN_{\min}} \quad (3.18)$$

$$f_{nit} = 1 - \exp(-k_{nit} \times DO) \quad (3.19)$$

$$\frac{dNH_3}{dt} = r \times QN \times \frac{M}{D} - V_{NH} \times \frac{M}{D} - k_{nit} \times NH_3 \times f_{nit} \times \theta_{T_{NH_3}}^{T-20} - K_{SNH_3}(NH_3 - NH_{3s}) \quad (3.20)$$

$$V_{NH} = V_{mNH} \times \frac{NH_3}{k_{NH_3} + NH_3} \times \frac{QN_{\max} - QN}{QN_{\max} - QN_{\min}} \quad (3.21)$$

$$\frac{dIN}{dt} = (V_{NO} + V_{NH}) \times M - (r + s + m) \times IN \quad (3.22)$$

Phosphorus

$$\frac{dPO_4}{dt} = (r - \mu) \times a_p \times \frac{M}{D} - K_{SPO_4}(PO_4 - PO_{4s}) - k_{ads} \times PO_4 \times \theta_{T_{PO_4}}^{T-20} \quad (3.23)$$

DO

$$\frac{dDO}{dt} = k_a \times \theta_{DO}^{T-20} \times (O_s - DO) + (\mu - r) \times r_{pC} \times a_c \times \frac{M}{D} - K_{SPO_2}(DO - DO_s) - k_{nit} \times r_{pN} \times NH_3 \times f_{nit} \times \theta_{T_{DO}}^{T-20} \quad (3.24)$$

$$k_a = 3.93 \frac{\sqrt{O_s}}{D^{3/4}} + \frac{0.7285O_s^2 - 0.3175O_s + 0.0872O_s^3}{D} \quad (3.27)$$

$$\ln O_{sm} = -139.34410 + \frac{1.575701e5}{T_a} - \frac{6.642308e7}{T_a^2} + \frac{1.243300e10}{T_a^3} - \frac{8.621949e11}{T_a^4} - \frac{1}{1.80655} \times S \times \left[(3.19298 - 2) - \left(\frac{1.9428e1}{T_a} \right) + \left(\frac{3.9673e3}{T_a^2} \right) \right] \quad (3.28)$$

$$O_s = O_{sm} P^{\frac{(1-P_{[P]})^2(1-\varphi)}{(1-P_{[P]})(1-\varphi)}} \quad (3.29)$$

$$\ln P_{WT} = 11.8571 - \frac{8940.7}{T} - \frac{216951}{T^2}; \quad (3.30)$$

$$\varphi = 0.000975 - 1.426e - 5 T + 6.436e - 6 T^2$$

Sediment

$$H_S \times \frac{dDO_S}{dt} = K_{SDO} \times (DO - DO_S) - k \times \theta_{rxn}^{T-20} r_{SC} \times POM_S \times H_S \quad (3.31)$$

$$H_S \times \frac{dNH3_S}{dt} = k \times \theta_{rxn}^{T-20} \times r_{3N} \times POM_S \times H_S + K_{SNH3} \times (NH3 - NH3_S) - k_{smtr} \times \theta_{rxn}^{T-20} \times NH3_S \times H_S \quad (3.32)$$

$$H_S \times \frac{dNO3_S}{dt} = k_{smtr} \times \theta_{rxn}^{T-20} \times NH3_S \times H_S + K_{SNO3} \times (NO3 - NO3_S) - k_{sdntr} \times \theta_{rxn}^{T-20} \times NO3_S \times H_S \quad (3.33)$$

$$H_S \times \frac{dPO4_S}{dt} = k \times \theta_{rxn}^{T-20} \times r_{3P} \times POM_S \times H_S + K_{SPC4} \times (PO4 - PO4_S) \quad (3.34)$$

4. Description of hydrodynamic model (RMA2) and sediment transport and water quality model (RMA11)

The RMA suite of finite element hydrodynamic, sediment transport and water quality models employed for this study have been used extensively since 1977 in engineering applications to examine flow and transport of constituents in surface water systems (RMA, 1997; 1998a; 1998b; 1999; 2001; 2003). One of the unique characteristics of the suite of models is the ability to represent a physical system using 1, 2, and/or 3 dimensional approximations within a single computational network. This allows construction of efficient computational networks where the level of spatial resolution varies according to the needs of the problem. Originally developed with the support of the U.S. Army Corps of Engineers Waterways Experiments Station, the models have undergone continued development and refinement by RMA. One of the most important additions has been the capability to accurately represent wetting and drying in shallow estuaries (RMA, 2001).

Hydrodynamics have been simulated for this study using RMA-2, a two-dimensional depth-averaged finite element model that solves the shallow water equations to provide temporal and spatial descriptions of velocities and water depths throughout the regions of interest. The model uses the Smagorinski formulation for modeling of turbulent momentum transfer (King et al., 1975). RMA-2, capable of simulating the de-watering of tidal flats, is uniquely suited for modeling of inter-tidal hydrodynamics in the marshes and mudflats that characterize boundaries of Upper Newport Bay.

Sediment transport and water quality are simulated using the finite element water quality model, RMA-11, which solves the mass transport equation in divergence or non-divergence form for multiple non-linearly coupled constituents. RMA-11 has been successfully applied in numerous previous projects to simulate the fate and transport of sediments and other conservative and non-conservative water quality constituents in surface water systems. Velocities and water depths obtained from hydrodynamic model results are used to solve the advection-dispersion equation for each constituent simulated. RMA-11 has been designed for compatibility with model results obtained from one-, two-, or three-dimensional hydrodynamic simulations (US Army Corps of Engineers, 1997; 1998).

4.1 Model Configuration

The RMA finite element model of Newport Bay, shown in Figure 4-1, extends from the tidal boundary at the entrance to the Lower Bay to San Diego Creek just upstream from Jamboree Bridge. Tributary inflows include San Diego Creek and Santa Ana Delhi Channel. The Bay is represented using a two-dimensional depth averaged approximation, with short one-dimensional

cross-sectionally averaged segments at the tidal boundary, San Diego Creek, and Santa Ana Delhi Channel. Even though 2-D model cannot simulate vertical variations in dissolved oxygen or other water quality parameters, modeling studies have focused on the shallow Upper Bay where stratification is not typically important, especially during storm seasons, and depth-average representation of flow and water quality constituent concentrations provides a good approximation for most of the year.

4.1.1 Bathymetry

The finite element mesh includes the area of the Bay up to approximately +1 m (3.3 ft) MSL. Because the bed elevations in the Bay change over time, several bathymetric data sets have been developed for the model. The grid used for this study was developed using the most recent bathymetric data, which is from the comprehensive bathymetry survey performed by the County of Orange and the Unit III dredging design plans (County of Orange Public Facilities and Resources Department, 1997; unpublished data from U.S. Army Corps of Engineering, 2004; 2006). The individual data sets do not cover the entire Bay, therefore, at any given location in the finite element mesh, the most recent available data were used to set the elevations. The 2006 data (collected prior to the most recent dredging project) were used to set elevations for all areas above PCH Bridge except for the Newport Dunes. The most recent data for the Newport Dunes was collected in 2004. The Lower Bay elevations were set using the 1997 data. A color contour plot of the model bathymetry is shown in Figure 4-2.

4.1.2 Boundary conditions

Boundary conditions for hydrodynamics that are required for dynamic simulations include tidal elevations at the ocean boundary and tributary inflows to the system. A steady or time-varying surface wind, with a specified direction, may be applied to examine the effects of wind stress on circulation in the system, however wind has not been applied in this study.

Table 4-1 Hydrodynamic and water quality constituents for boundary conditions

Boundary	Constituents for boundary conditions
Ocean	Tide elevation, temperature, salinity, DO, NO ₃ , NH ₃ , PO ₄
Tributaries	Flow rate, temperature, salinity, DO, NO ₃ , NH ₃ , PO ₄
Sediment	Deposited sediments (from sediment transport model result)
Atmosphere	Air temperature, air pressure, vapor pressure, solar radiation, cloudiness

Water quality simulations require specification of constant or time-varying concentrations at the San Diego Creek and Santa Ana Delhi inflow boundaries, and the tidal boundary for all water column constituents simulated. Meteorological data inputs are also required, including solar radiation, air temperature, wind speed and vapor pressure. These data can be applied over the entire model or varied by element type.

Table 4-1 shows hydrodynamic and water quality constituents used for each boundary condition for this study.

Sediment transport simulations require specification of sediment concentrations for the San Diego Creek and Santa Ana Delhi inflows. Tidal boundary sediment concentrations are set to zero.

Results from the sediment transport model serve as an additional boundary condition for the water quality model. The sediment depth and distribution are fed into the water quality model to calculate nutrients available for flux into the water column.

4.2 Previous Model Calibration

The model of Newport Bay was previously calibrated for hydrodynamics, salinity transport and sediment transport during the initial studies for U.S. Army Corp of Engineers (RMA, 1997, 1998a and 1998b). No additional calibration of hydrodynamics or transport is performed as part of this study as recent velocity data were not available and the minor bathymetry modifications would not affect stage or transport.

The hydrodynamic model was calibrated to observed stage time-series and spot velocity measurements from the 1992 – 1993 Reconnaissance Study (Coastal Frontiers Corporation, 1993).

The salinity model was calibrated separately for wet and dry weather periods using salinity observations in Newport Bay including time-series of near-surface salinity collected by IRWD and spot measurements of salinity profiles over the water column collected by IRWD and the County of Orange during November 1996 and August – September 1997.

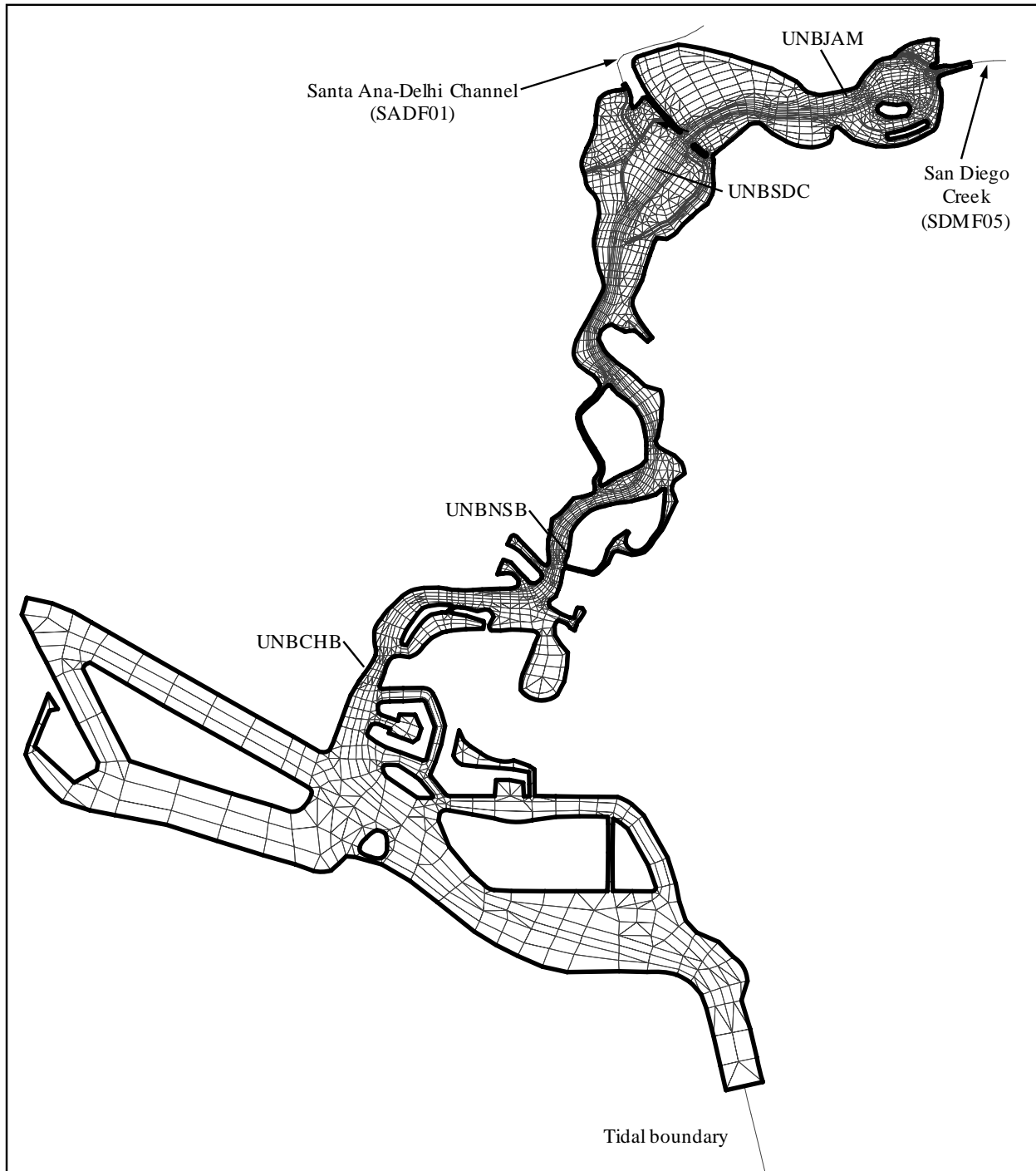


Figure 4-1 Finite element model configuration of Newport Bay, with monthly water quality monitoring stations of the Orange County where UNBJAM is Upper Newport Bay – Unit 1 Basin; UNBSDC is Upper Newport Bay – Unit 2 Basin; UNBNSB is Upper Newport Bay – North Star Beach; UNBCHB is Upper Newport Bay – Coast Highway Bridge.

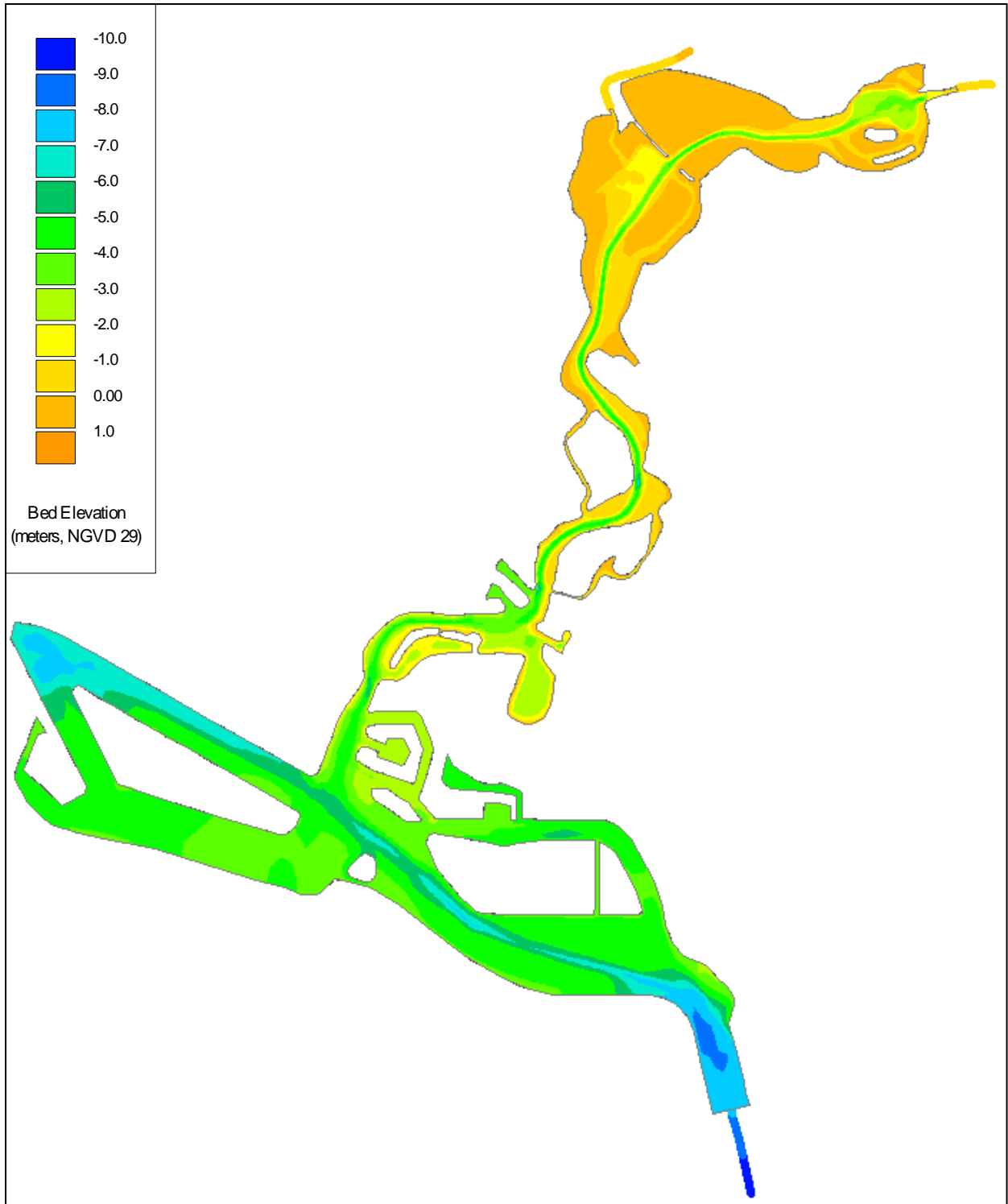


Figure 4-2 Color contours of the Newport Bay model bathymetry.

5. Water quality model calibration and validation

To calibrate the water quality model, variations in water quality throughout the Bay were computed using time varying water quality boundary conditions and daily averaged tributary inflows for San Diego Creek and Santa Ana Delhi Channel, the tide corresponding to the calibration period, and meteorological data from the California Irrigation Management System (CIMIS) station at Irvine and from the weather station at John Wayne Airport.

The objective of the water quality model calibration is to reproduce the depth average of observed temperature, dissolved oxygen, macroalgae and nutrient values in the Upper Newport Bay, and the seasonal macroalgal growth patterns. Calibration of the water quality model involves adjustment of model parameters to best represent temperature, DO, macroalgae and nutrient concentrations throughout the system. The following constituents are included in the water quality model.

- Salinity
- Temperature
- DO
- Ammonia (NH₃)
- Nitrate (NO₃)
- Phosphate (PO₄)
- Macroalgae
- Macroalgal internal nitrogen
- Deposited particulate organic matter (POM)

The constituents of the water quality model exclude dissolved organic nitrogen (DON) since the time series of DON is not available. Therefore, total nitrogen (TN) is assumed to consist mainly of dissolved inorganic nitrogen and particulate organic nitrogen in this study.

The primary goal of model validation is to assure that the simulated macroalgal growth patterns follow the observed variations from year to year that are presumed to result from variations in wet season inflows (and associated suspended sediment) to the Bay.

Calibration of the model was a complicated process involving adjustment of many interrelated parameters. Adjustment of one parameter could improve the macroalgae calibration result, but at the same worsen results for one of the nutrients in the water column. Improvement in DO calibration could result in worse macroalgae calibration, and so on. As such, model parameters were adjusted until a balance was achieved with good calibration results for all constituents.

Although there are many unknowns in the system, this balance gives good indication that all model parameters are reasonably well calibrated.

5.1 Calibration and validation periods

The model calibration period is from January through December 2004. The validation period is from January 2005 through December 2006. These periods were chosen because they include a year with a dryer winter and smaller blooms later in the year (2003-2004), and a year with large winter flows and subsequent larger macroalgal blooms later in the year (2004 – 2005). The validation is extended into 2006 to cover another dryer year. Sediment inflow data are only available through June 2006, however the full year was still simulated as for any given year, there is typically very little sediment deposited after June 1st until wet weather arrives again at the end of the year.

If model parameters calibrated for a dry year can also produce a good match with observed data during a wet year, this provides much better assurance of model validation than calibrating and validating for similar year types.

5.2 Boundary conditions

Model boundary conditions are set for the January 2004 through December 2006 calibration and validation period using the following data sets.

- San Diego Creek and Santa Ana Delhi daily inflows and two- to four-times monthly electrical conductivity (EC), NH₃, NO₃, PO₄, DO, and total suspended solids (TSS) concentrations: Nutrient TMDL reports (County of Orange et al., 2004; 2005; 2006, <http://www.ocwatersheds.com/watersheds/tmdls.asp>).
- San Diego Creek and Santa Ana Delhi daily TSS concentrations: estimated from regression equations in Sediment TMDL reports (The County of Orange et al., 2004; 2005; 2006, <http://www.ocwatersheds.com/watersheds/tmdls.asp>).
- Downstream tidal boundary: National Oceanic and Atmospheric Administration (NOAA) 6-minute predicted tide at Newport Harbor entrance (<http://tidesandcurrents.noaa.gov>).
- Tidal boundary temperature and salinity from Newport Pier in Newport Beach: shore station program at the University of California at San Diego (http://shorestation.ucsd.edu/active/index_active.html).
- Tidal boundary DO, NO₃, PO₄ and phytoplankton (chlorophyll-*a*): California Cooperative Oceanic Fisheries Investigations (<http://www.calcofi.org>). Boundary conditions for remaining constituents, for which no data were available, were estimated.
- Hourly solar radiation and vapor pressure: California Irrigation Management System (CIMIS) station at Irvine (<http://www.cimis.water.ca.gov>).

- Hourly air temperature and wind speed at John Wayne Airport: MesoWest (<http://www.met.utah.edu/mesowest/>).

TKN data from San Diego Creek and Santa Ana Delhi was not used for model boundary conditions because it provides no information on particulate vs. dissolved fractions. Instead the particulate fraction was estimated using TSS and assumptions about TOC and % nitrogen of TOC. The dissolved organic nitrogen component of TKN was assumed to be not significant since the TN concentrations from inflows matched the sum of observed data of NO₃, NH₄ and particulate organic nitrogen (% nitrogen of TSS).

Daily creek inflows are plotted in Figure 5-2 for the period of December 2003 through the end of 2006. To more clearly display the summertime flows, a log scale plot is also provided in Figure 5-3.

Many of the water quality data sets are limited and estimation of boundary conditions was required. Maps of the data collections stations are shown in Figure 5-1 (maps from TMDL report, Orange County et. al, 2004).

The daily concentrations of water quality constituents were estimated by non-linear regressions between available data for the constituents and daily flow rates multiplied by daily air temperatures. Regressions using daily flows and air temperatures are useful because these data sets are complete. Inclusion of air temperature in the regression equations brings seasonality into the estimated time series. Daily water temperatures were estimated by the following regression equation:

$$\log_{10}(\text{water temperature} \times \text{flow rate}) = a + b \times \log_{10}(\text{air temperature} \times \text{flow rate}) \quad (4.1)$$

where *a* and *b* are defined in Table 5-1.

Daily DO values were estimated using the following regression equation:

$$\log_{10}(\text{DO} \times \text{air temperature}) = a + b \times \log_{10}(\text{air temperature} \times \text{flow rate}) + c \times \log_{10}(\text{air temperature} \times \text{flow rate})^2$$

where *a* and *b* are defined in Table 5-1.

As with daily DO, daily nutrients were estimated using non-linear base-10 logarithmic regressions between nutrients X daily temperature and daily flow rates X air temperatures.

$$\log_{10}(\text{nutrients} \times \text{air temperature}) = a + b \times \log_{10}(\text{air temperature} \times \text{flow rate}) + c \times \log_{10}(\text{air temperature} \times \text{flow rate})^2 \quad (4.3)$$

where a and b are defined in

Table 5-1. For consistency of generating input files, the same strategy was used for estimating all nutrient model input time series.

Final boundary conditions were input to the model as daily averages and included the observed data points with estimated values filling in missing data. Plots of observed, estimated and model boundary condition water temperature, DO, NO₃, NH₃ and PO₄ for San Diego Creek and Santa Ana Delhi Channel are shown in Figure 5-4 through Figure 5-13 for the 2004 through 2006 calibration/validation period. Note that observed data values are affected by detection limits and significant figures in reported data, particularly for NH₃ and PO₄.

Table 5-1 Constants of non-linear regression for water quality constituents of inflows

	a		b		c	
	SAD	SDC	SAD	SDC	SAD	SDC
Water temperature	1.007626	0.993695	0.07879	0.091694		
EC	0.137876	-0.069	0.211749	1.09074	3.020371	2.319728
DO	-0.02843	-0.09291	0.002322	0.4763	2.362099	1.646

NH3	-0.097063	-0.111486	0.666649	0.643793	-0.650654	-0.637465
NO3	-0.120713	-0.191206	0.239155	0.90983	1.493929	0.722991
PO4	0.187453	0.093587	-0.558701	-0.002167	0.136198	-0.707945

SAD = Santa Ana Delhi channel; SDC = San Diego Creek

EC was not modeled, but used to compute boundary conditions for salinity. EC was estimated using the following regression equation:

$$\log_{10}(EC \times flow\ rate) = a + b \times \log_{10}(abr\ temperature \times flow\ rate) + c \times \log_{10}(abr\ temperature \times flow\ rate)^2$$

where *a* and *b* are defined in

Table 5-1.

Salinity was calculated from the combined observed and estimated EC, shown in Figure 5-14 and Figure 5-15, using a regression between EC and salinity as follows:

$$Salinity = a + b * EC \tag{4.5}$$

where *a* and *b* are constants set as values of 2.18 and 0.554062, respectively. The regression was obtained from one of the Sacramento – San Joaquin delta channels with a similar range of salinity (e.g., one of which EC minimum is 129 and EC maximum is 7100 μmhos/cm). Estimated salinity of the two inflows is presented in Figure 5-16 and Figure 5-17. The regressions of water quality constituents of Santa Ana Delhi and San Diego Creek are shown in from Figure 5-18 to Figure 5-27.

Daily temperature and salinity for the ocean boundary of Newport Bay were obtained from the shore station program at the University of California at San Diego (UCSD) (http://shorestation.ucsd.edu/active/index_active.html).

Water quality data for the ocean boundary are available at LA harbor with a sampling interval of four times a year from the California Cooperative Oceanic Fisheries Investigation (CalCOFI) (<http://www.calcofi.org/>). Available data include NO₃, PO₄, DO and chlorophyll - *a*. Averages of data for 2004 through 2006 were used. Ocean boundary conditions for the remaining constituents (NH₃ and VSS) were set as constants based on Southern California Coastal Water Research Project (SCCWRP) measurements (via personal communication).

Table 5-2 summarizes the data sources and missing data estimation methods for all model boundary conditions.

Table 5-2 Summary of data sources and estimation methods for water quality model constituent boundary conditions.

Constituent	Data Source			Estimation Method for Missing Data		
	San Diego Creek	Santa Ana Delhi	Tidal boundary	San Diego Creek	Santa Ana Delhi	Tidal boundary
Flow/stage	Nutrient TMDL	Nutrient TMDL	NOAA	No missing data	No missing data	Linear interpolation (few missing data points)
Temperature	Nutrient TMDL	Nutrient TMDL	UCSD	Air/water temperature, flow non-linear regression	Air/water temperature, flow non-linear regression	Linear interpolation (few missing data points)
Salinity	Nutrient TMDL	Nutrient TMDL	UCSD	EC linear regression	EC linear regression	Linear interpolation (few missing data points)
DO	Nutrient TMDL	Nutrient TMDL	CalCOFI	Air temperature, flow non-linear regression	Air temperature, flow non-linear regression	Set constant to average of available data
NH3	Nutrient TMDL	Nutrient TMDL	SCCWRP	Air temperature, flow non-linear regression	Air temperature, flow non-linear regression	Set constant to average of available data
NO3	Nutrient TMDL	Nutrient TMDL	CalCOFI	Air temperature, flow non-linear regression	Air temperature, flow non-linear regression	Set constant to average of available data
PO4	Nutrient TMDL	Nutrient TMDL	CalCOFI	Air temperature, flow non-linear regression	Air temperature, flow non-linear regression	Set constant to average of available data
Phytoplankton	Set to zero	Set to zero	CalCOFI	--	--	Set constant to average of available data
TSS*	Sediment TMDL	Sediment TMDL	Set to zero	Regression from Sediment TMDL reports	Regression from Sediment TMDL reports	--

NOAA = National Oceanic and Atmospheric Administration; UCSD = University of California, San Diego; CalCOFI = California Cooperative Oceanic Fisheries Investigation; SCCWRP = Southern California Coastal Water Research Project.

* TSS is a constituent in the sediment transport model, which is run separately from the water quality model as discussed below.

** Refer to abbreviations in Table 5-2 in page 37.

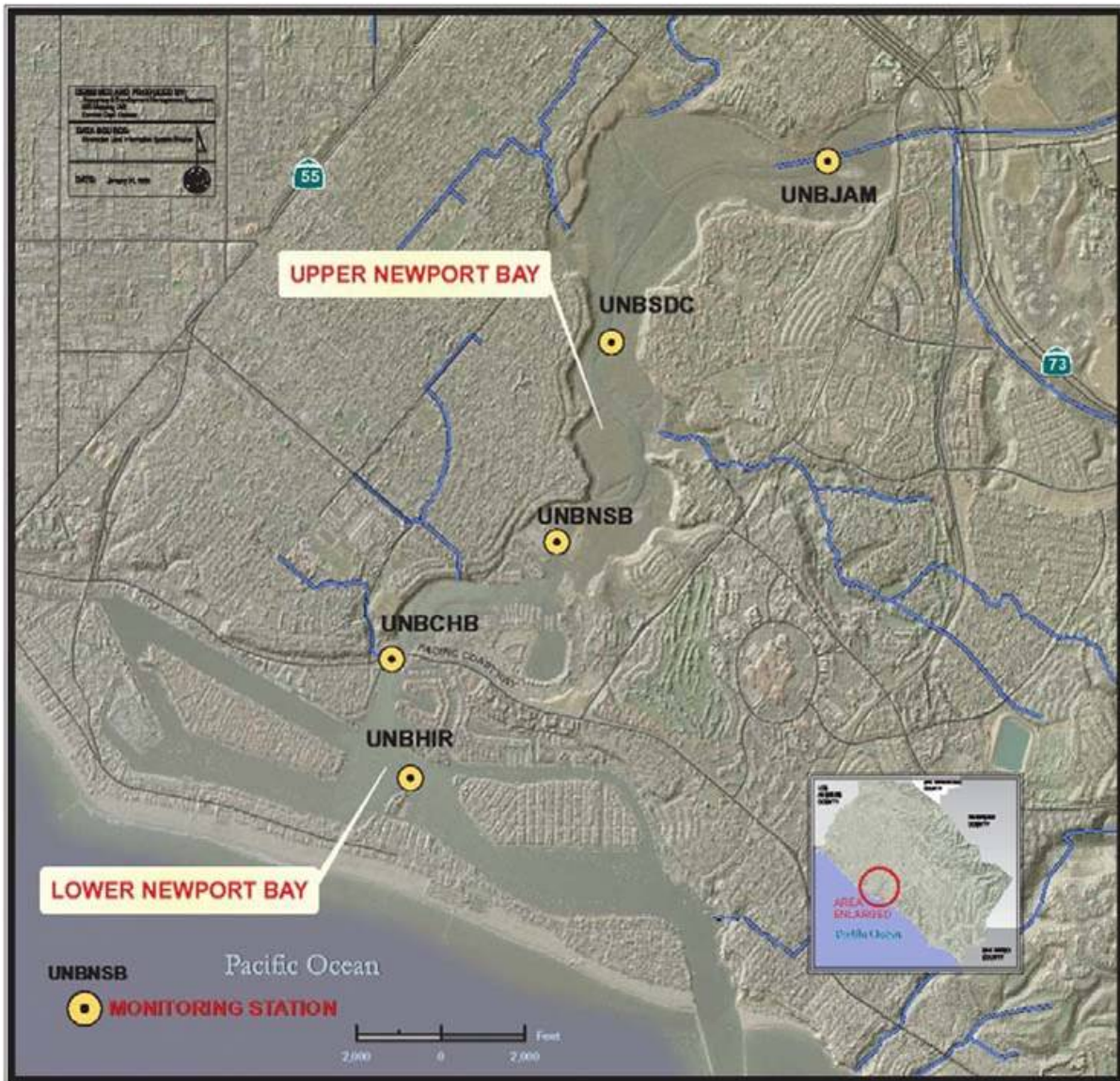


Figure 5-1 Map of Newport Bay water quality monitoring stations (from nutrient TMDL report, County of Orange et. al, 2004).

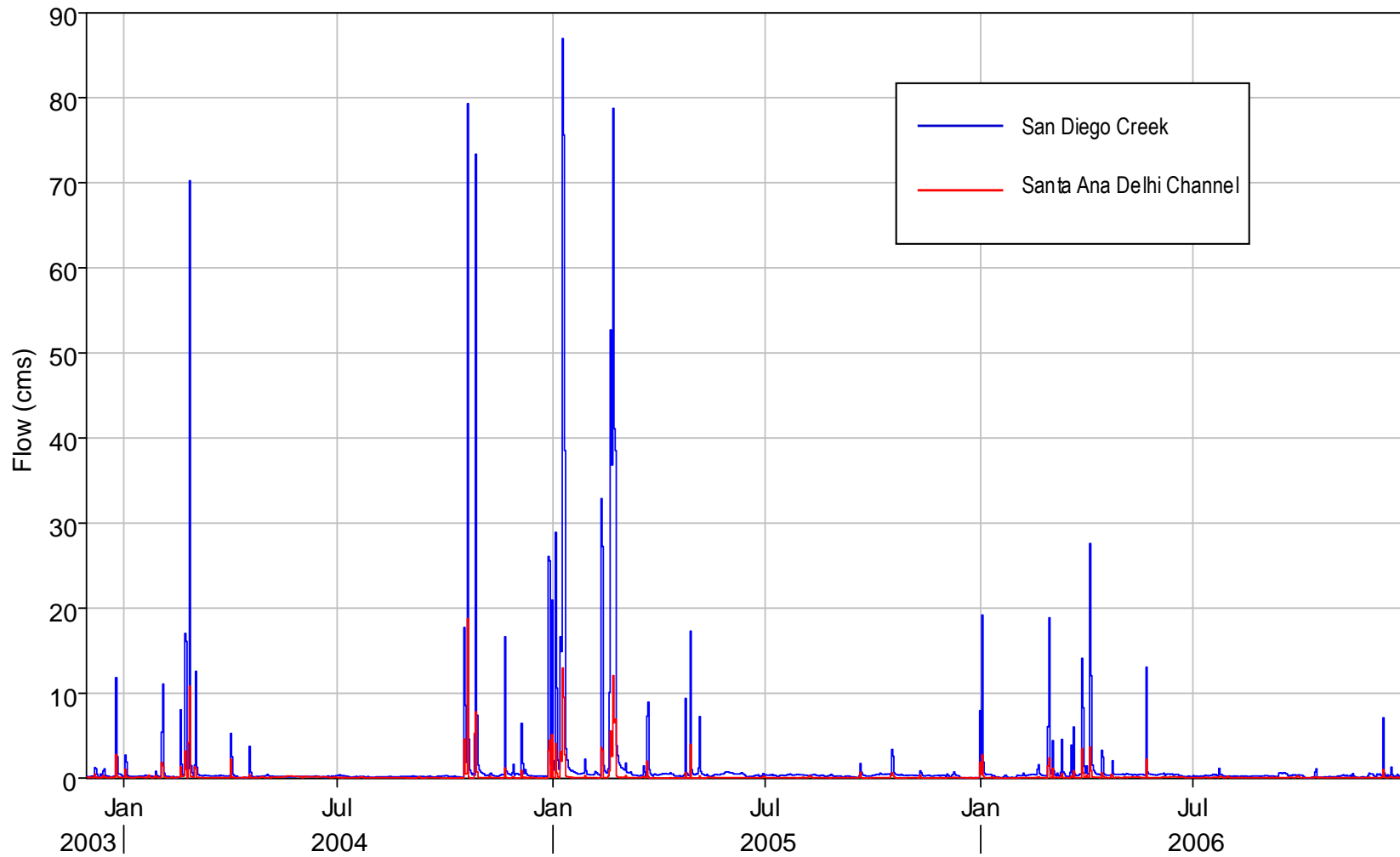


Figure 5-2 San Diego Creek and Santa Ana Delhi Channel inflows for December 2003 - December 2006.

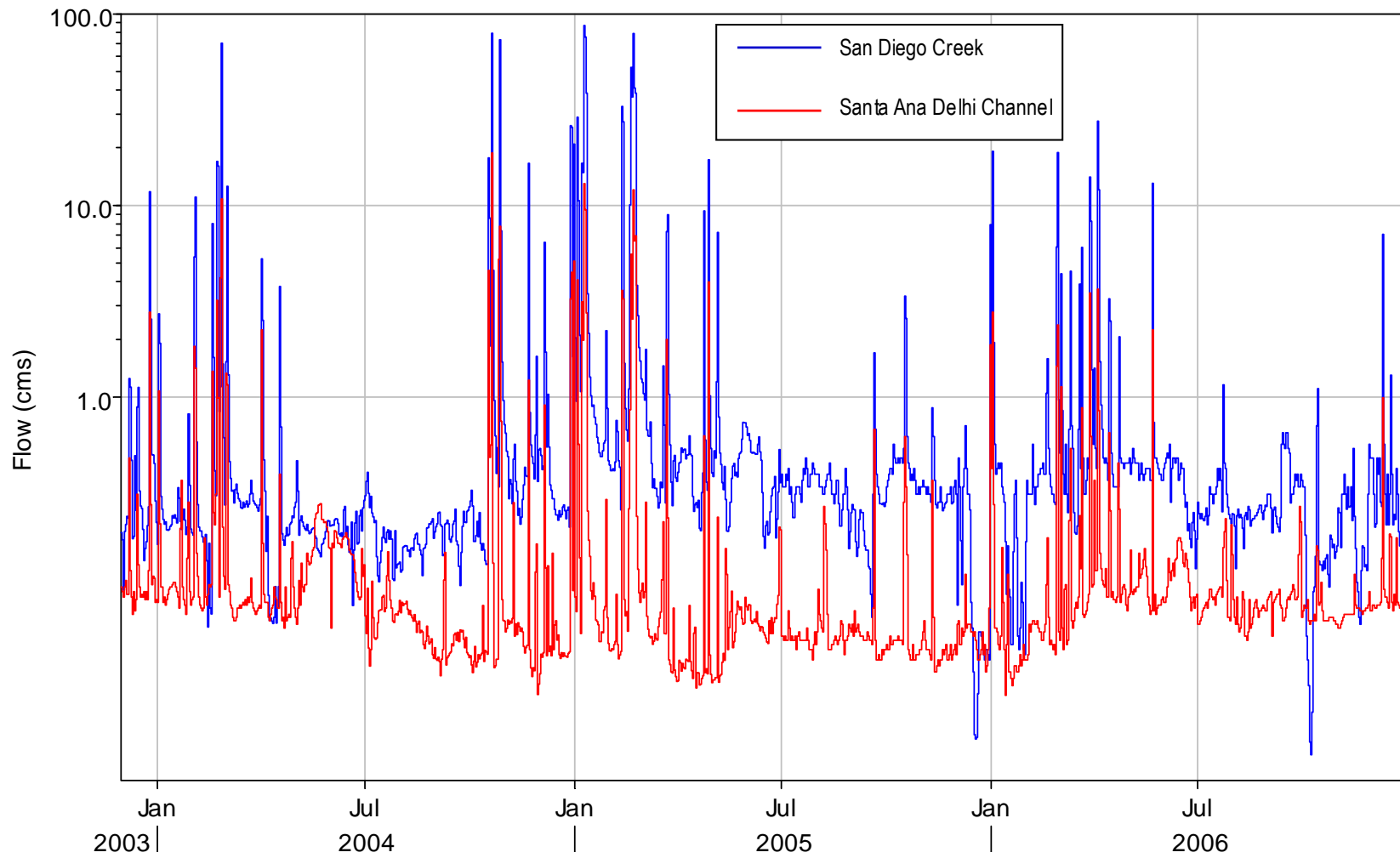


Figure 5-3 San Diego Creek and Santa Ana Delhi Channel inflows for December 2003 - December 2006, shown in log scale.

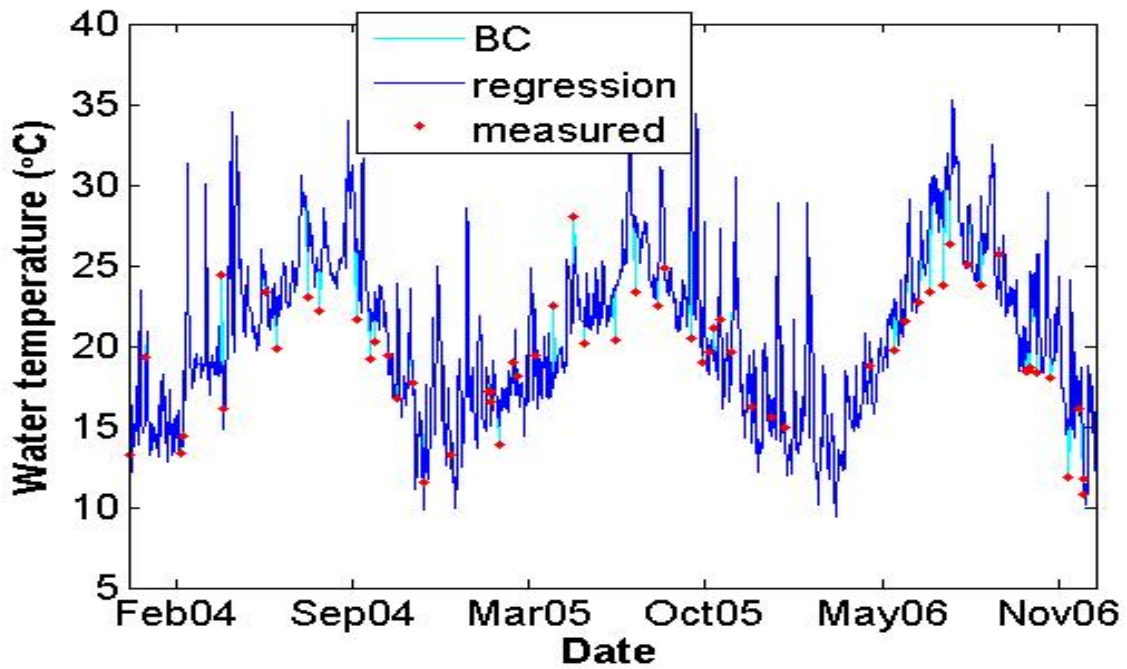


Figure 5-4 Santa Ana Delhi temperature: measured data (red dots), estimated (blue line) and model boundary condition (light blue line) from 2004 through 2006.

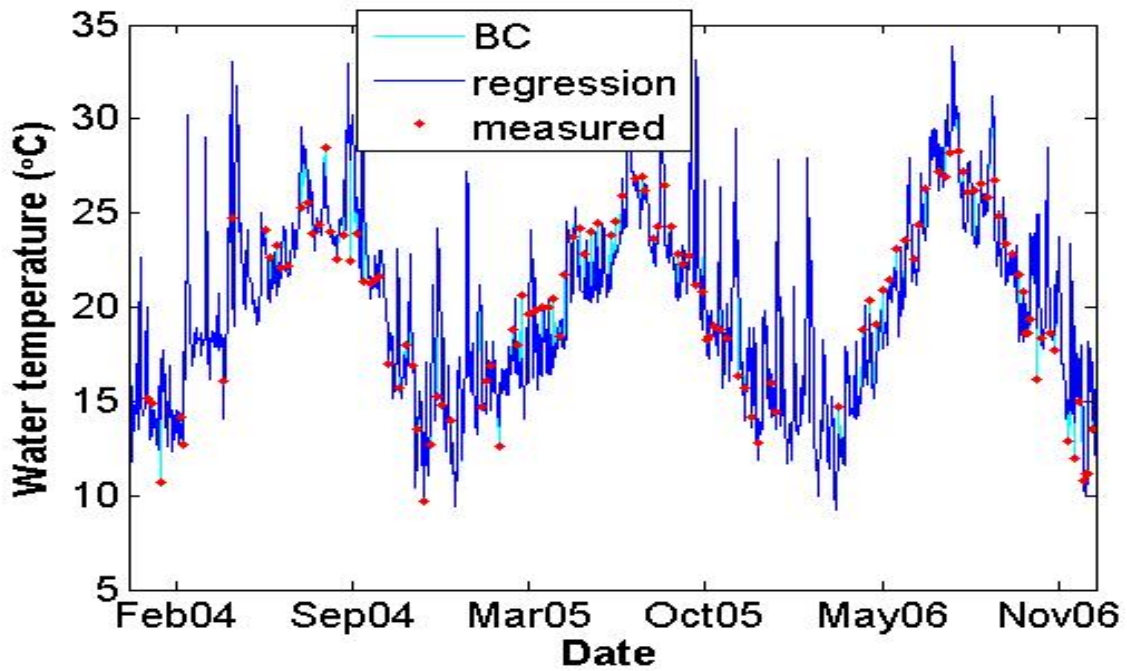


Figure 5-5 San Diego Creek temperature: measured data (red dots), estimated (blue line) and model boundary condition (light blue line) 2004 through 2006.

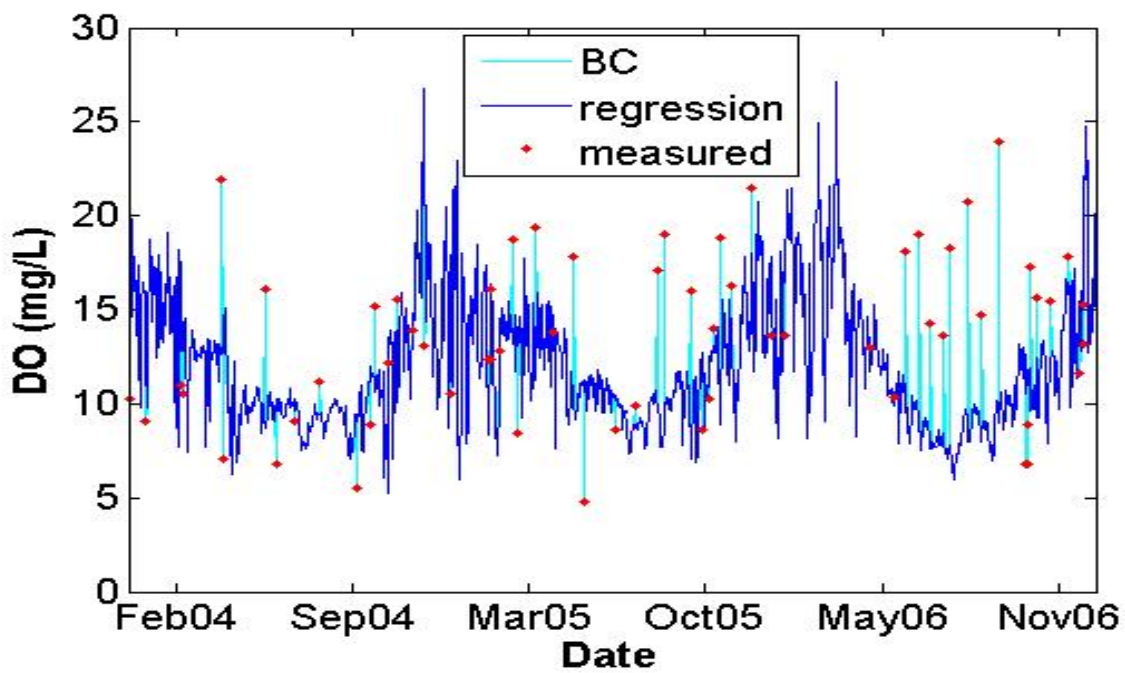


Figure 5-6 Santa Ana Delhi DO: measured data (red dots), estimated (blue line) and model boundary condition (light blue line) from 2004 through 2006.

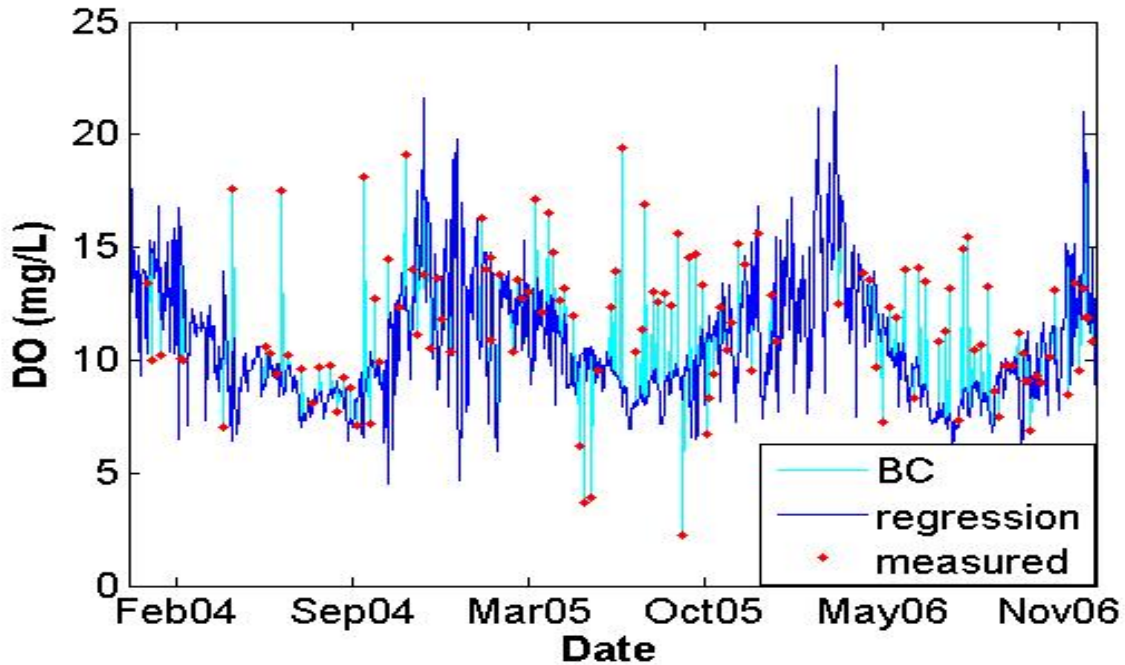


Figure 5-7 San Diego Creek DO: measured data (red dots), estimated (blue line) and model boundary condition (light blue line) from 2004 through 2006.

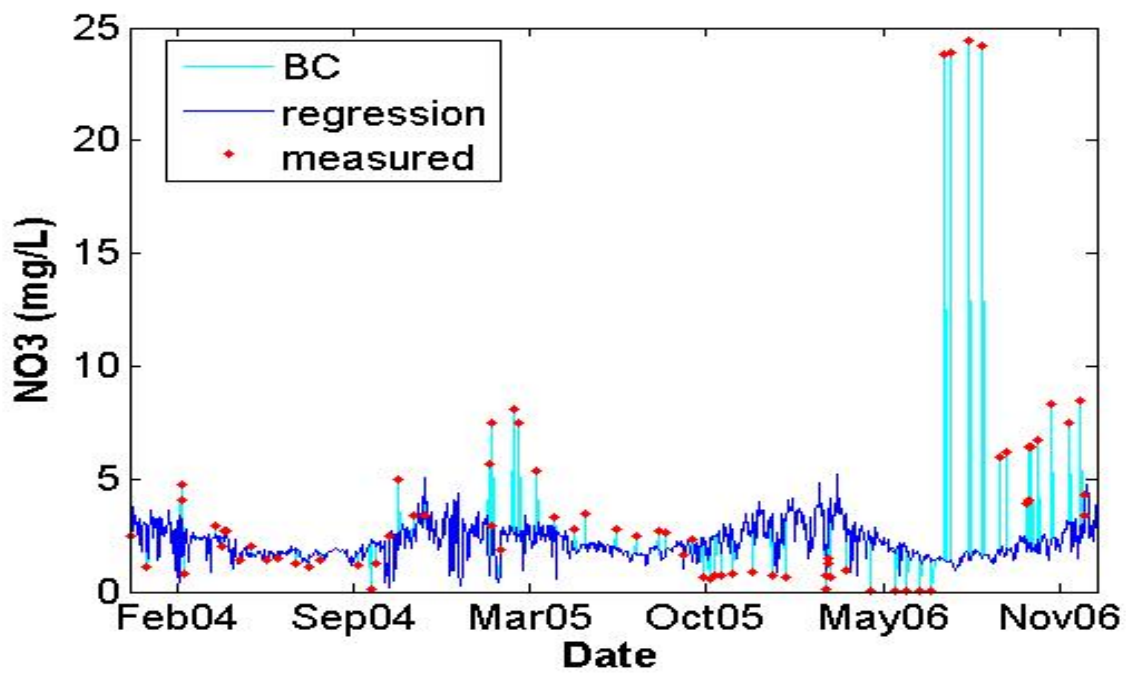


Figure 5-8 Santa Ana Delhi NO3: measured data (red dots), estimated (blue line) and model boundary condition (light blue line) from 2004 through 2006.

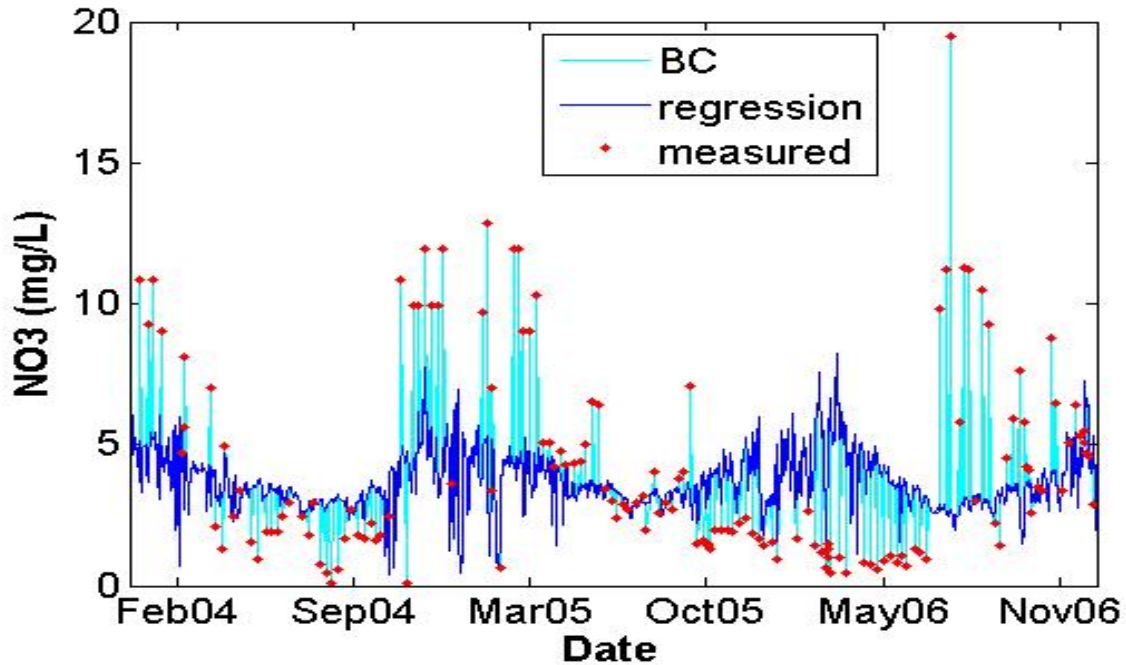


Figure 5-9 San Diego Creek NO3: measured data (red dots), estimated (blue line) and model boundary condition (light blue line) from 2004 through 2006.

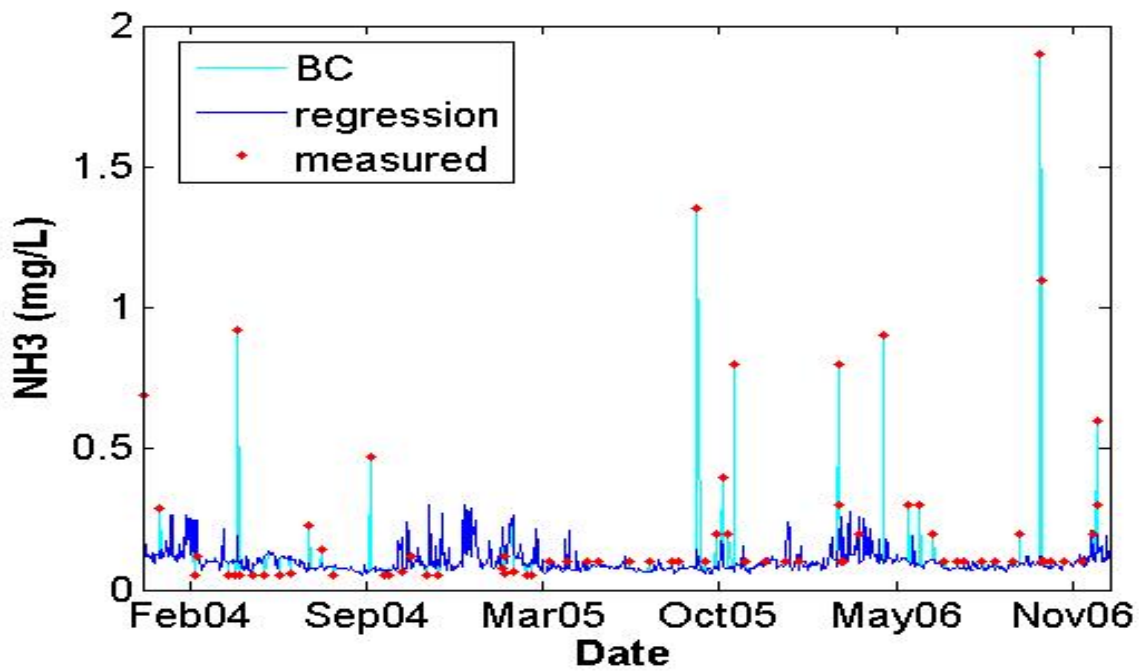


Figure 5-10 Santa Ana Delhi NH3: measured data (red dots), estimated (blue line) and model boundary condition (light blue line) from 2004 through 2006.

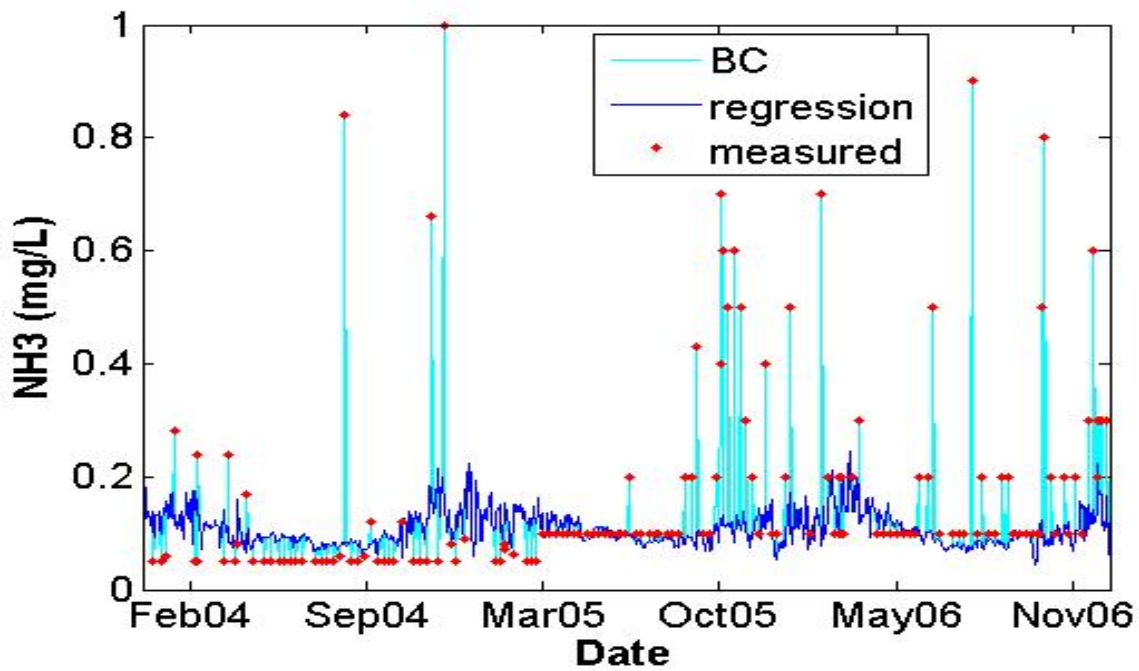


Figure 5-11 San Diego Creek NH3: measured data (red dots), estimated (blue line) and model boundary condition (light blue line) from 2004 through 2006.

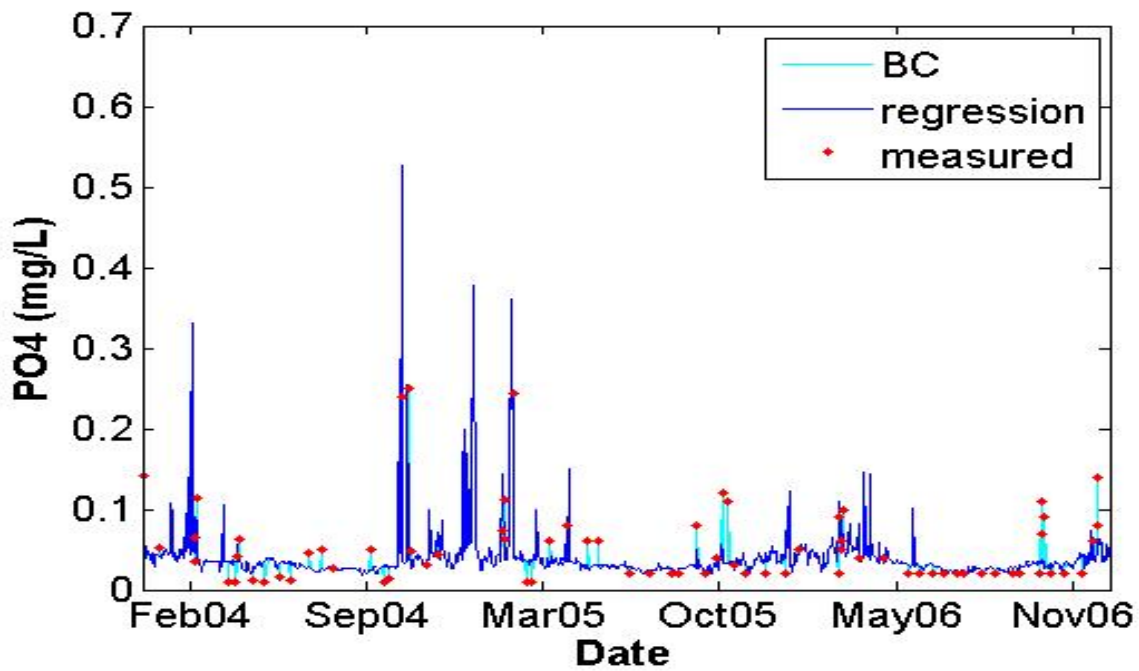


Figure 5-12 Santa Ana Delhi PO4: measured data (red dots), estimated (blue line) and model boundary condition (light blue line) from 2004 through 2006.

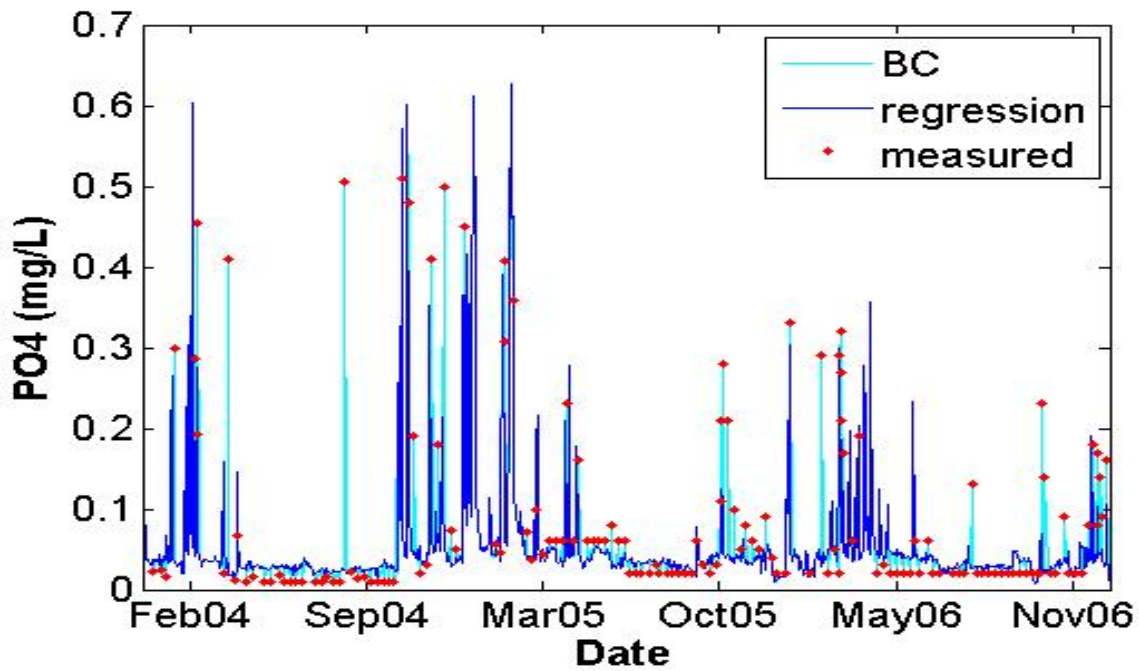


Figure 5-13 San Diego Creek PO4: measured data (red dots), estimated (blue line) and model boundary condition (light blue line) from 2004 through 2006.

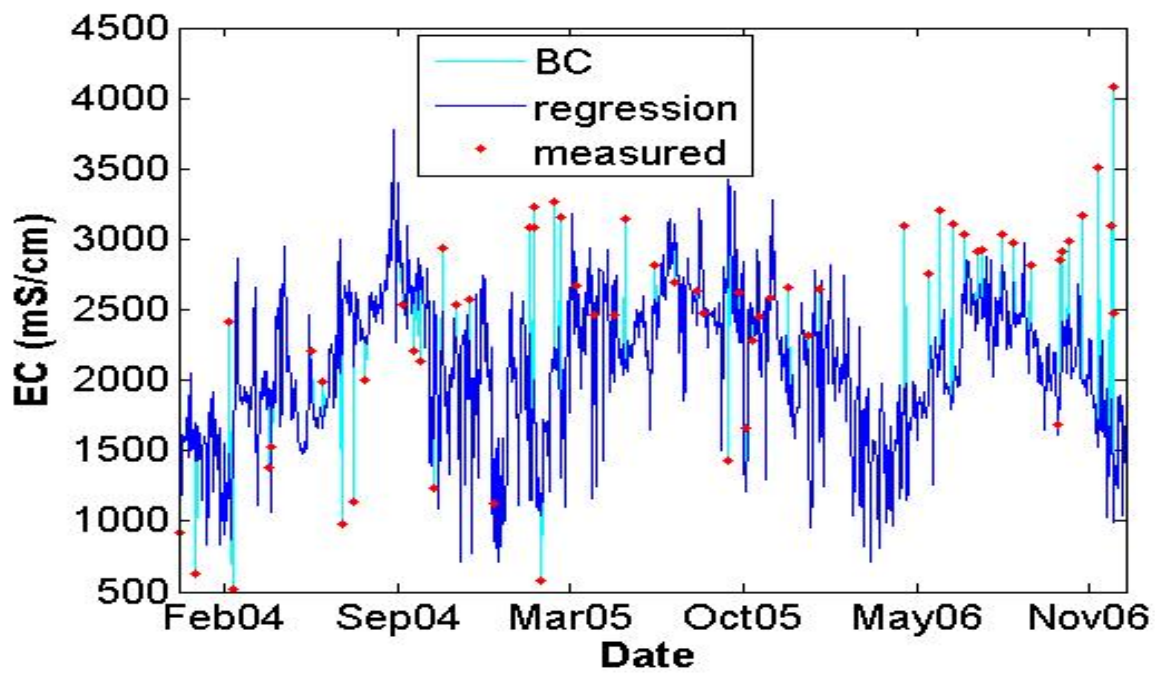


Figure 5-14 Santa Ana Delhi EC: measured data (red dots), estimated (blue line) and EC used to compute salinity model boundary condition (light blue line) 2004 through 2006.

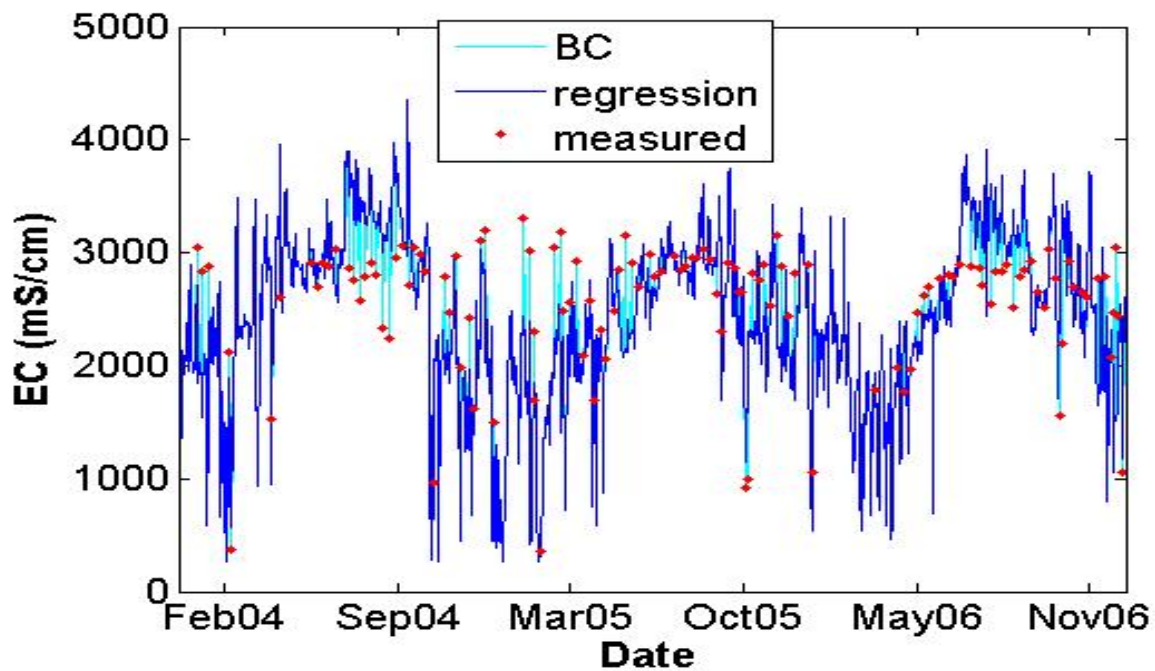


Figure 5-15 San Diego Creek EC: measured data (red dots), estimated (blue line) and EC used to compute salinity model boundary condition (light blue line) 2004 through 2006.

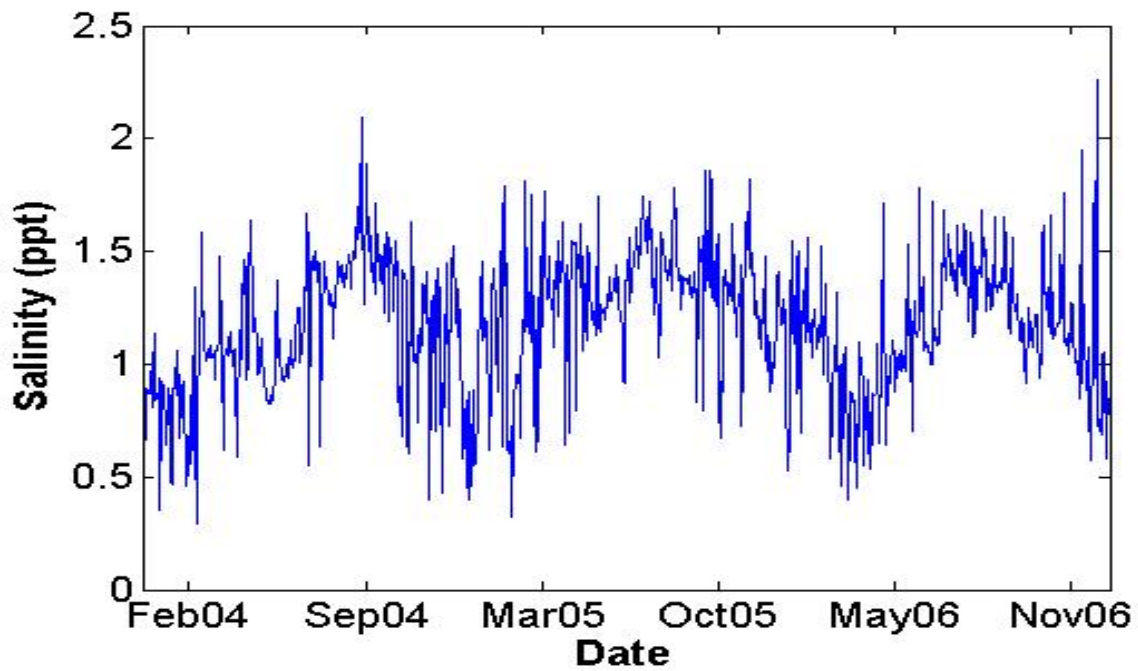


Figure 5-16 Santa Ana Delhi estimated Salinity using a regression between EC and salinity from 2004 through 2006.

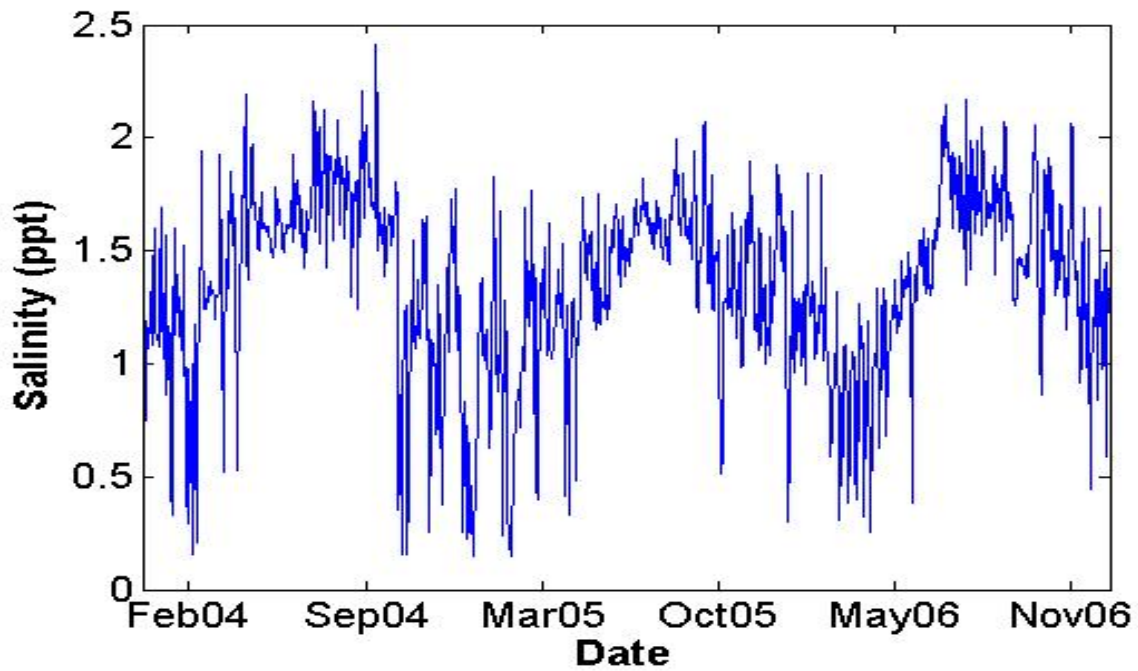


Figure 5-17 San Diego Creek estimated Salinity using a regression between EC and salinity from 2004 through 2006.

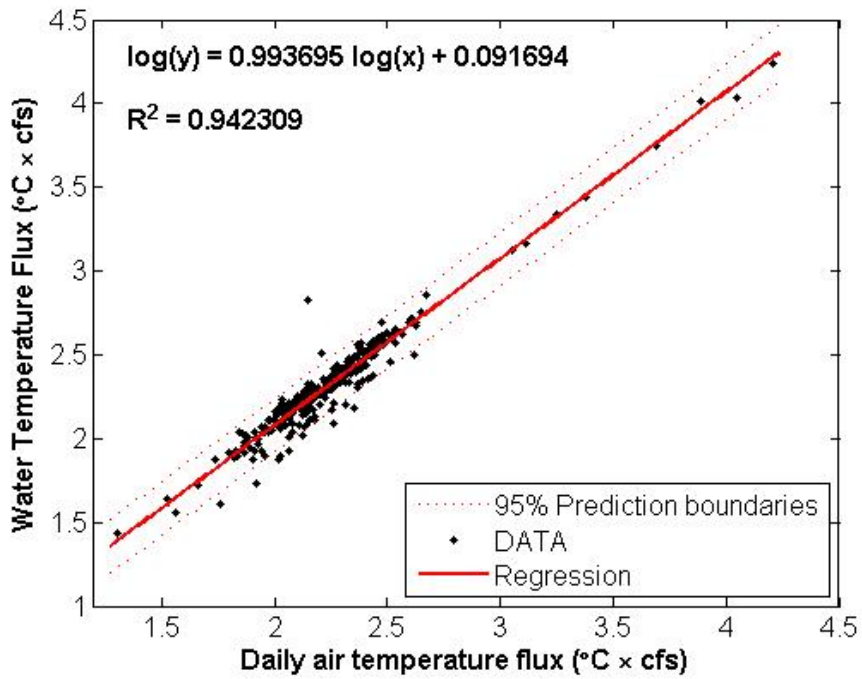


Figure 5-18 Regression of both water temperature and air temperature multiplied by flow rate of San Diego Creek from 2004 through 2006.

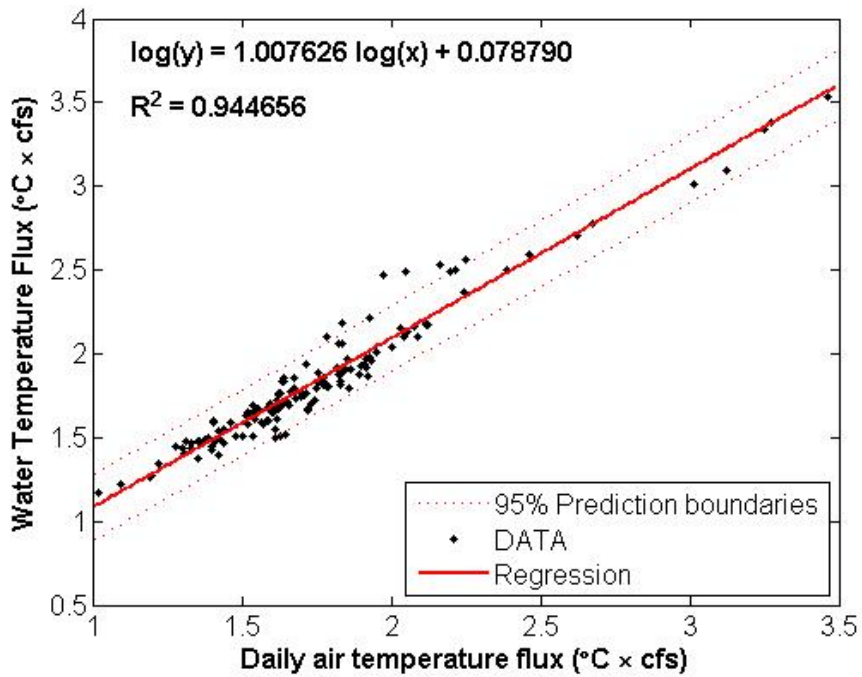


Figure 5-19 Regression of both water temperature and air temperature multiplied by flow rate of Santa Ana Delhi from 2004 through 2006.

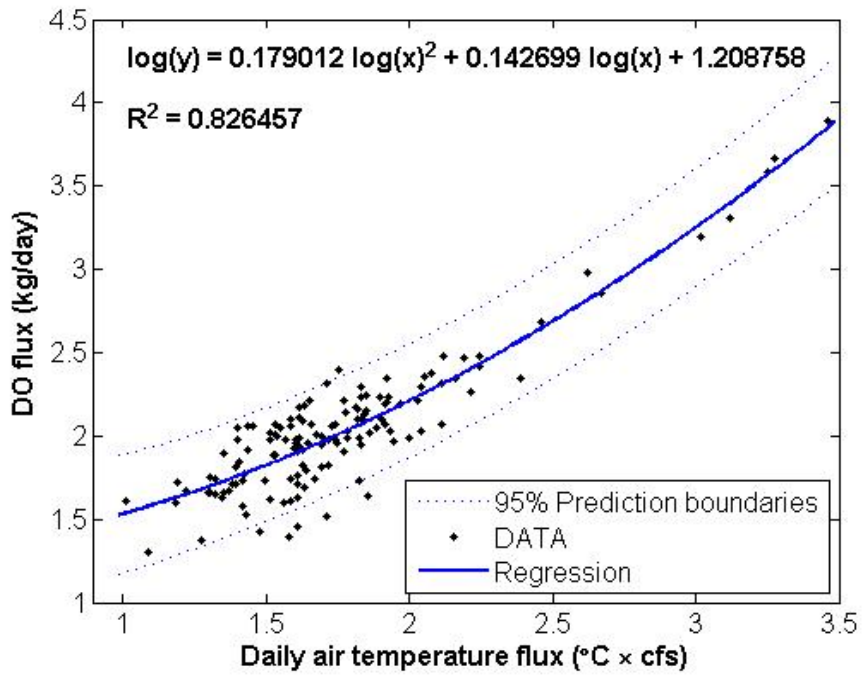


Figure 5-20 Regression of both DO and air temperature multiplied by flow rate of Santa Ana Delhi from 2004 through 2006.

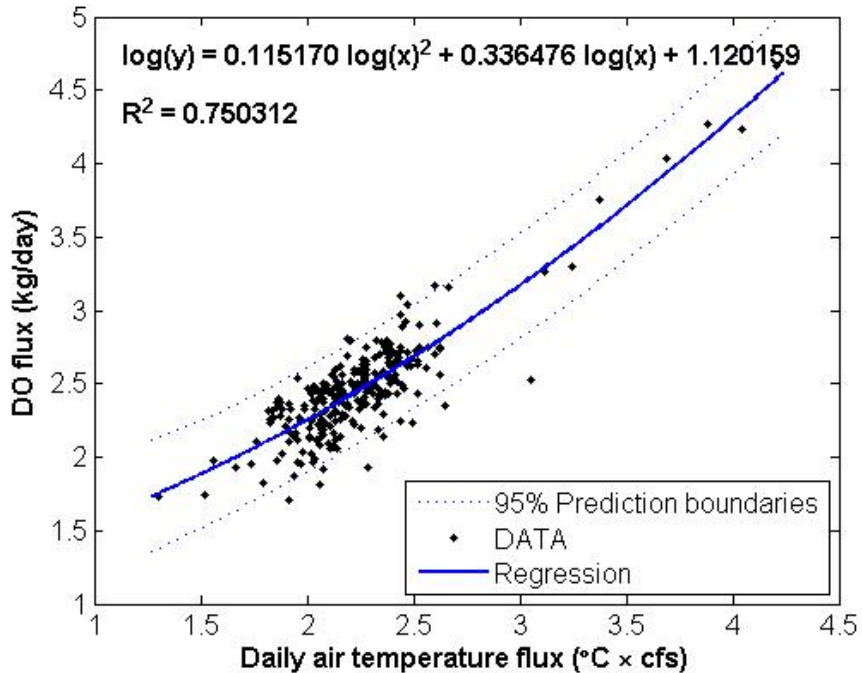


Figure 5-21 Regression of both DO and air temperature multiplied by flow rate of San Diego Creek from 2004 through 2006.

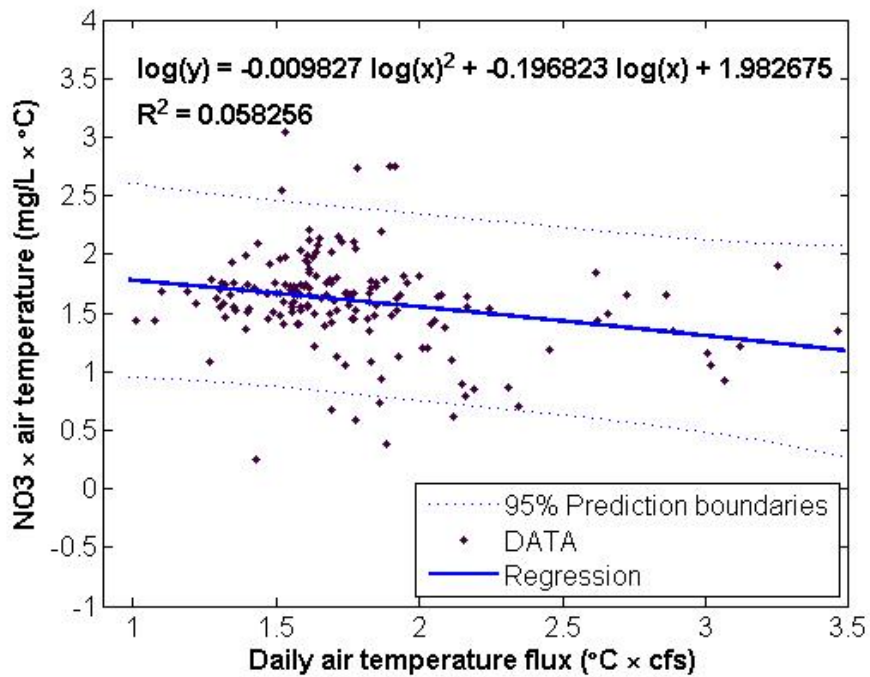


Figure 5-22 Regression of NO3 multiplied by air temperature and air temperature multiplied by flow rate of Santa Ana Delhi from 2004 through 2006.

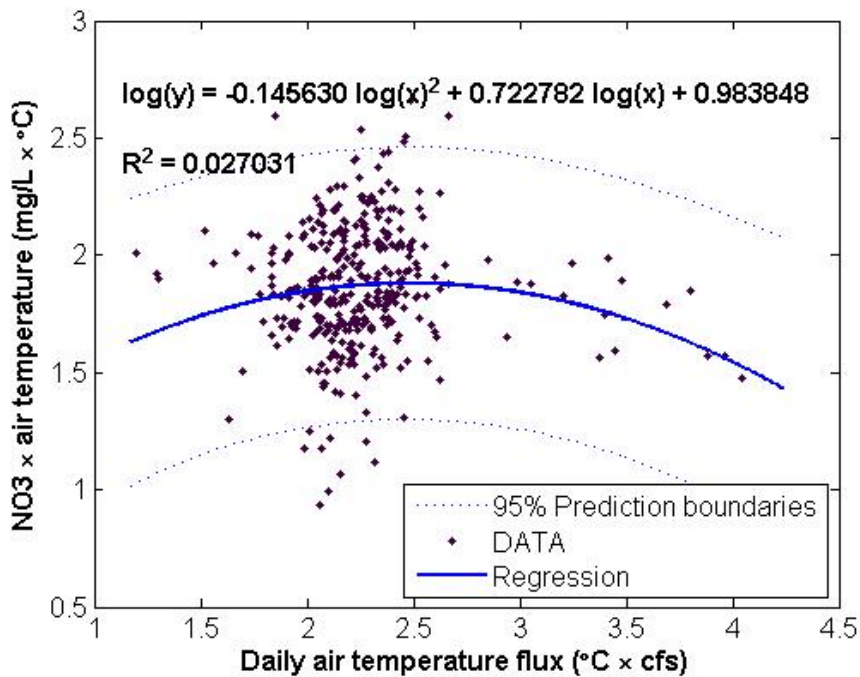


Figure 5-23 Regression of both NO3 multiplied by air temperature and air temperature multiplied by flow rate of San Diego Creek from 2004 through 2006.

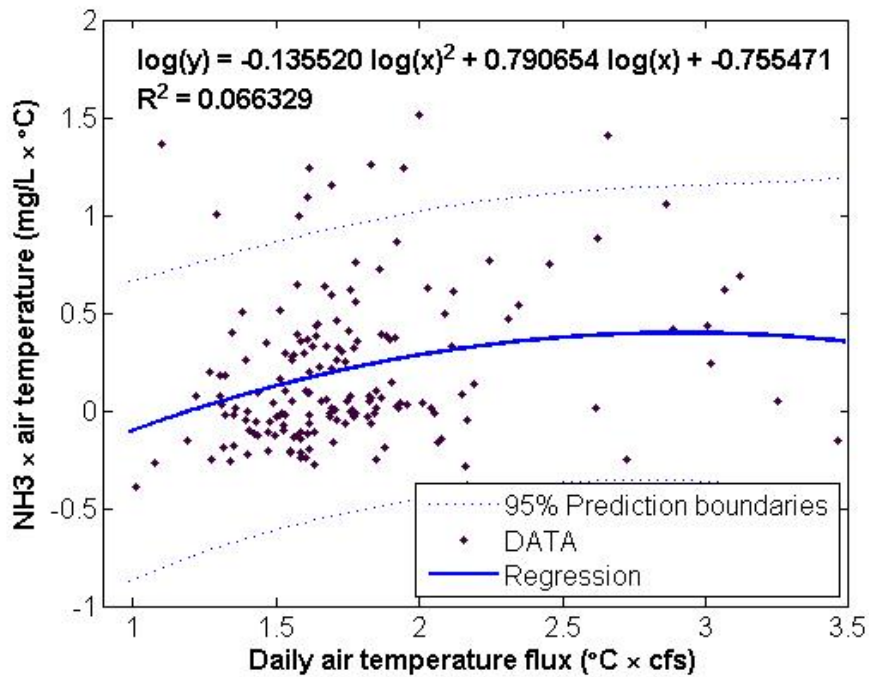


Figure 5-24 Regression of NH3 multiplied by air temperature and air temperature multiplied by flow rate of Santa Ana Delhi from 2004 through 2006.

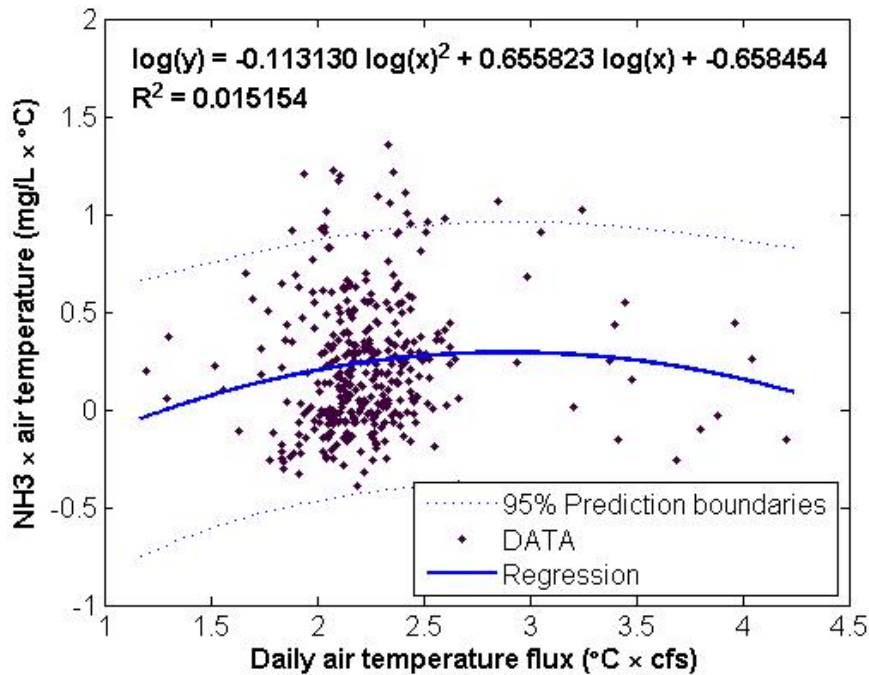


Figure 5-25 Regression of both NH3 multiplied by air temperature and air temperature multiplied by flow rate of San Diego Creek from 2004 through 2006.

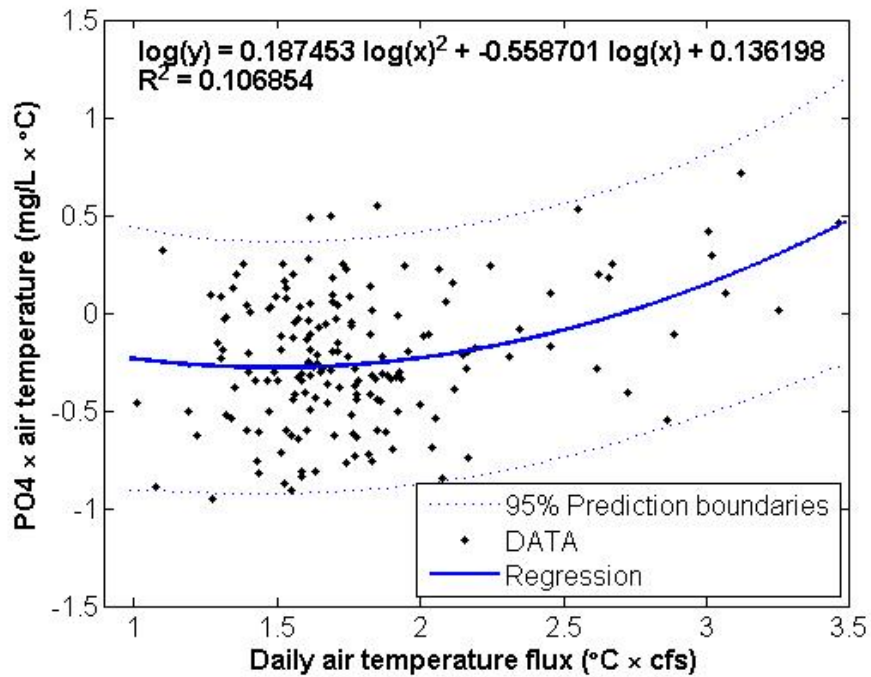


Figure 5-26 Regression of PO4 multiplied by air temperature and air temperature multiplied by flow rate of Santa Ana Delhi from 2004 through 2006.

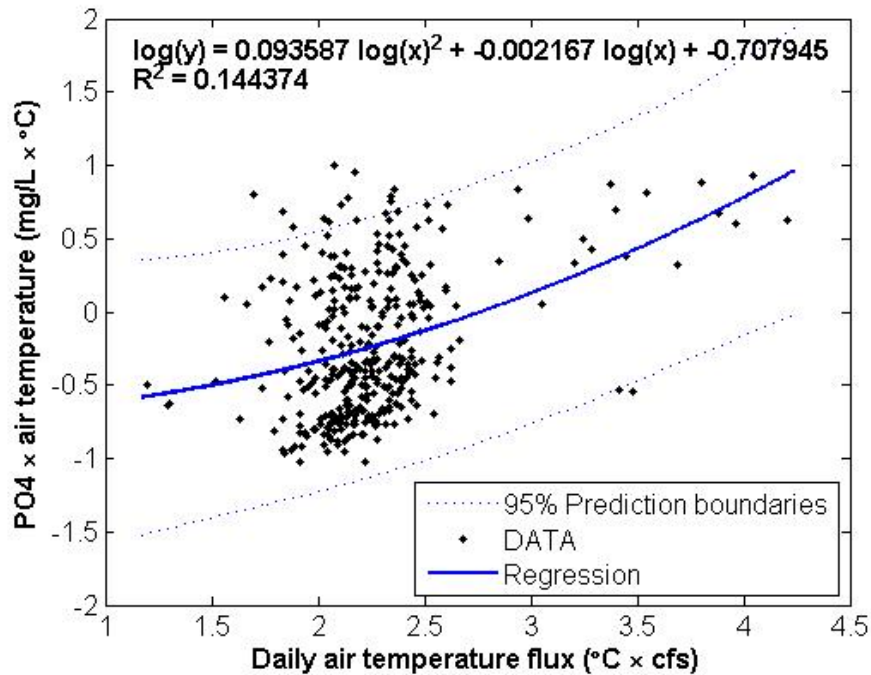


Figure 5-27 Regression of both PO4 multiplied by air temperature and air temperature multiplied by flow rate of San Diego Creek from 2004 through 2006.

5.2.1 Development and application of deposited sediment boundary condition

Mass and distribution of deposited sediment are supplied to the water quality model as a boundary condition for the 2004 – 2006 calibration and validation period. From the sediment deposition data, the water quality model generates particulate organic matter inputs in the sediment. POM is assumed to make up 1% of the total deposited sediment (Peng et al., 2007).

5.2.1.1 Sediment transport

To generate the sediment mass and distribution boundary condition, RMA11 sediment transport simulations were run. Although water quality simulations begin in January 2004, sediment transport simulations were begun in December 2003 to capture all significant storm events that contributed sediment to the Bay during that winter. Simulations are run for the three consecutive years. However, POM is run for a full year, and then restarted from zero deposition to simulate the following year. This allowed the three years to be simulated in parallel and was justifiable because the previous year's deposition would not have an important impact on the results. Large storms do occur near the end of 2004, however there is such a large sediment load to the Bay during early 2005 that much of the older sediment becomes buried and unavailable to the water column. Thus the impact of the load from the end of 2004 is small relative to the 2005 loads. Significant storms in the winter of 2005-2006 do not begin until around the beginning of January.

For the sediment transport simulations, hydrodynamic boundary conditions were as described in section 5.2. Daily TSS estimated data from daily flow using regressions (source: sediment TMDL reports) were used to set sediment boundary conditions for Santa Ana Delhi Channel and San Diego Creek, as shown in Figure 5-28 and Figure 5-29. Ocean boundary TSS was set to zero.

The parameters required by the sediment transport model include the number and thickness of sediment bed layers, critical shear stress for erosion for each layer, sediment density for each layer, critical shear stress for deposition, and sediment particle settling rate.

Sediment properties are a function of depth. Newly deposited sediment is generally less dense and more easily scoured than sediments which have been covered and have begun to consolidate. The variation in sediment properties is often significant over the first few centimeters of the bed. RMA11 represents the variation in bed properties as series of thin fixed layers over a variable thickness layer. Sediment is always deposited into the top layer. As the top layer fills, sediment is shifted down to the lower layers. The bottom layer can grow indefinitely. When scour occurs, the upper layers are removed first. A six-layer model was used for Newport Bay. The set of sediment properties for each layer is shown in Table 5-3. Parameters were calibrated during the Upper Newport Bay Feasibility Study for the U.S. Army Corps of Engineers (RMA, 1998).

Note that the bed layers applied in the sediment transport model are not used in the water quality model.

Deposition can only occur when the shear stress on the bed is less than the critical shear stress for deposition. The critical shear stress for deposition is only a function of the uppermost bed layer so only one value is required.

Sediment particle settling velocities are calculated in the model as the d50 (median) particle size settling velocity based on particle size distribution reported from sediment TMDL samples collected at Campus Drive (County of Orange, 2004).

Shown in Figure 5-30 through Figure 5-32 are time series plots of computed sediment deposition accumulating January 1 through December 1 of each simulation year at a location of maximum deposition in Unit I basin. These plots illustrate that virtually all of the deposition occurs during the wet season, with very little change through the dry season. The time series of sediment accumulation applied as boundary conditions in the water quality model start at zero deposition on January 1st of 2005 and 2006.

Color contour plots of deposited sediment depth on June 1 of each year are shown in Figure 5-33 through Figure 5-35. As shown in these plots and in the time series plot (Figure 5-30), sediment deposition during the winter of 2005 was far greater than during either of the other wet seasons. Sediment depth was computed assuming a density of 1000 kg/m³.

Table 5-3 Sediment model parameter values used in sediment transport simulations.

Layer	Layer Thickness (cm)	Critical Shear Stress for Erosion (N/m ²)	Bulk Density (kg/m ³)
1	1.0	0.090	1062
2	2.0	0.120	1125
3	2.0	0.200	1187
4	10.0	0.400	1249
5	10.0	1.017	1311
6	--	2.200	1374

Critical Shear Stress for Deposition (N/m²) 0.08
d50 Particle Size Settling Velocity (m/s) 7.9x10-5

5.2.1.2 Use of the sediment transport runs for sediment POM

The sediment runs for 2004 - 2006 were post-processed to get the daily sediment deposition or scour. Fractions of the deposited sediment are assumed for POM carbon, nitrogen and phosphorus as follows: (Peng et al., 2007; Sutula et al., 2006)

$$C = 1\%$$

$$N = 0.1\%$$

$$P = 0.05\%$$

The daily sediment deposition is used to compute the POM-C, nitrogen and phosphorus added daily to the bed according to the above percentages times the daily sediment deposition rate. The top 100 kg/m² dry weight of sediment (about 10 cm) is considered biologically active. Deposition >100 kg/m² is considered buried. Thus the max sediment related POM is as follows.

$$C = 1000 \text{ g/m}^2$$

$$N = 100 \text{ g/m}^2$$

$$P = 50 \text{ g/m}^2$$

Any previous material in excess of these values is buried.

POM-C, nitrogen and phosphorus are lost from the bed over time by decay. POM-C consumes oxygen in the bed pore water (the bed being about 10 cm with 50% porosity) and DO diffuses from the water column to the bed depending on the difference between water column and sediment concentrations, thus more sediment deposition results in reduced oxygen concentrations in the water column. POM-N and POM-P convert to NH₃ and PO₄ in the bed via diagenesis. NH₃ and PO₄ exchange with the overlying water column. With increased sediment load resulting in more NH₃ and PO₄ in the bed, flux will tend to be from the bed to the water column, increasing water column concentrations and promoting macroalgae growth.

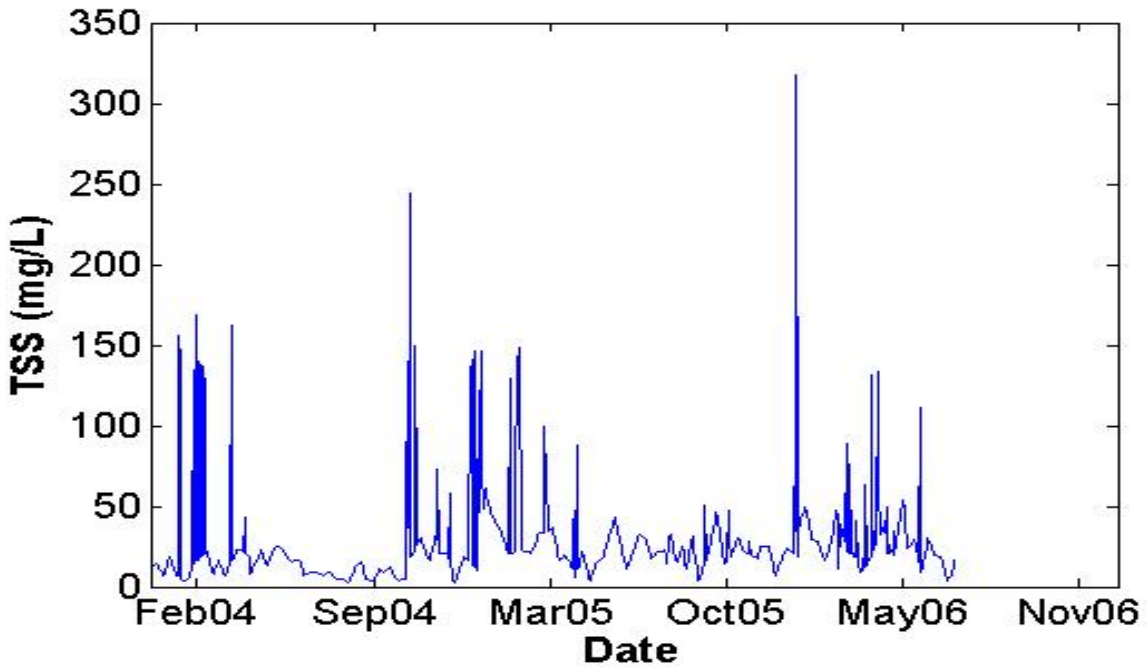


Figure 5-28. Santa Ana Delhi daily TSS data from 2004 through 2006.

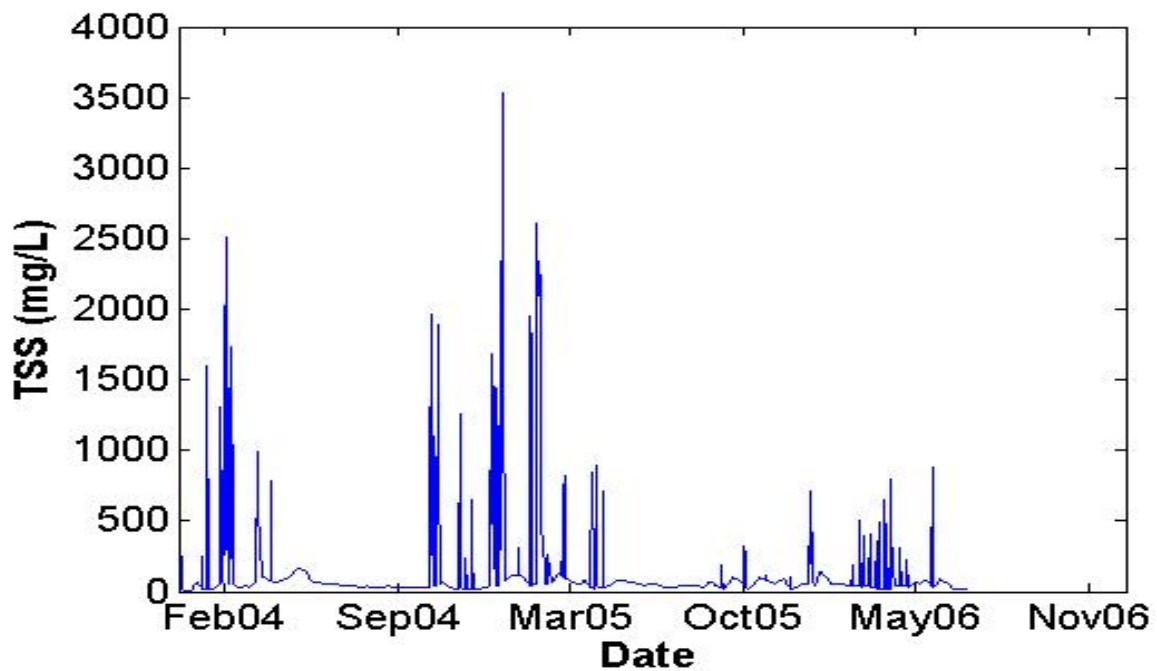


Figure 5-29. San Diego Creek daily TSS data from 2004 through 2006.

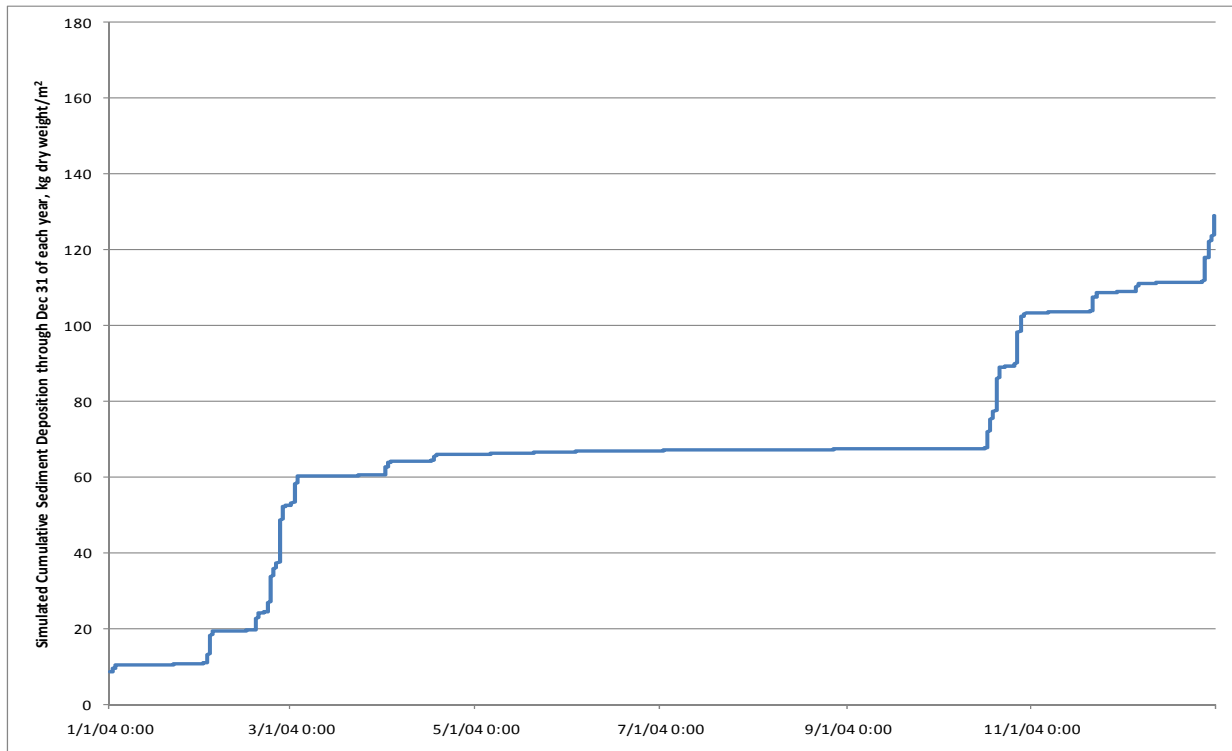


Figure 5-30 Time series plot of simulated cumulative sediment deposition January 1 through December 31, 2004, at a location of peak deposition in Unit I basin.

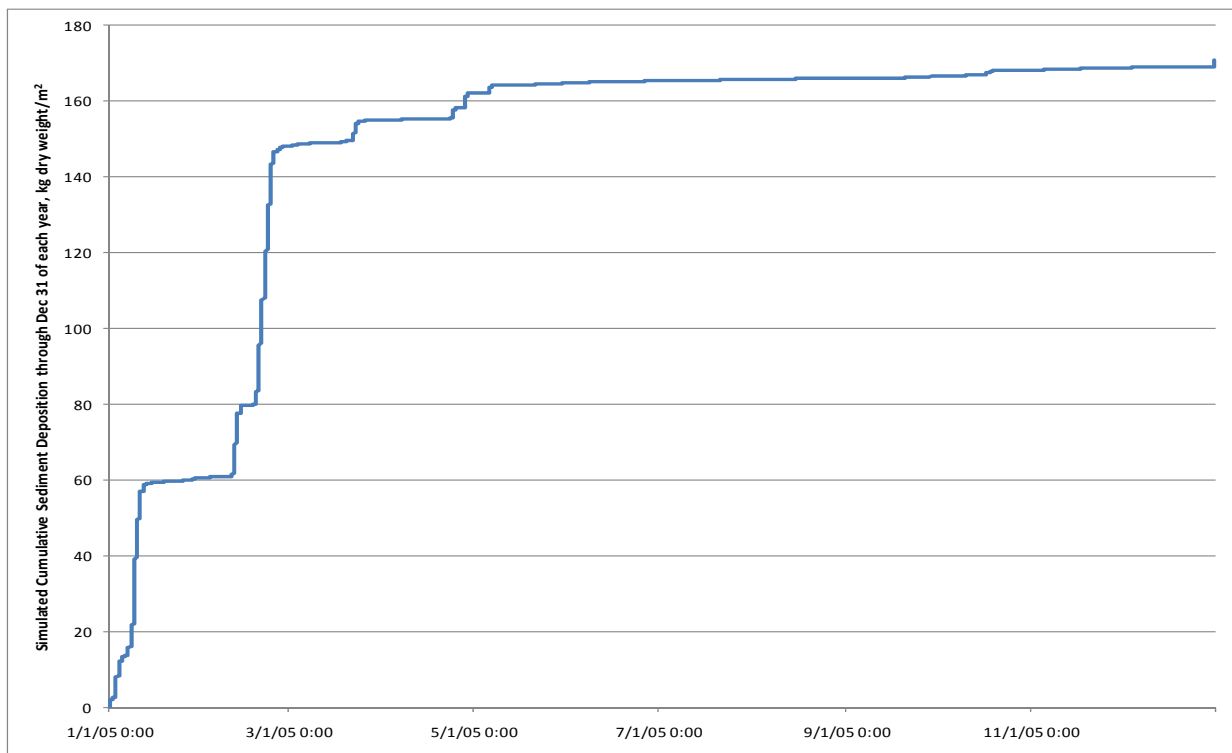


Figure 5-31 Time series plot of simulated cumulative sediment deposition January 1 through December 31, 2005, at a location of peak deposition in Unit I basin.

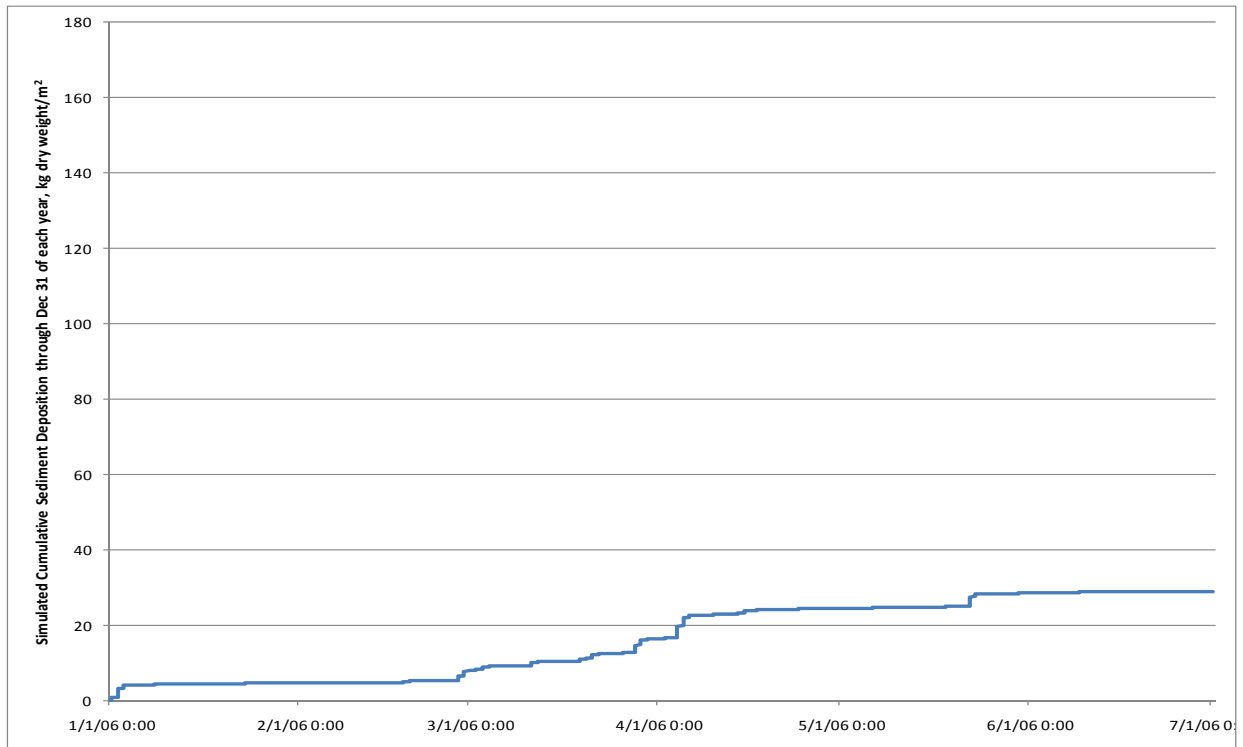


Figure 5-32 Time series plot of simulated cumulative sediment deposition January 1 through July 1, 2006, at a location of peak deposition in Unit I basin.

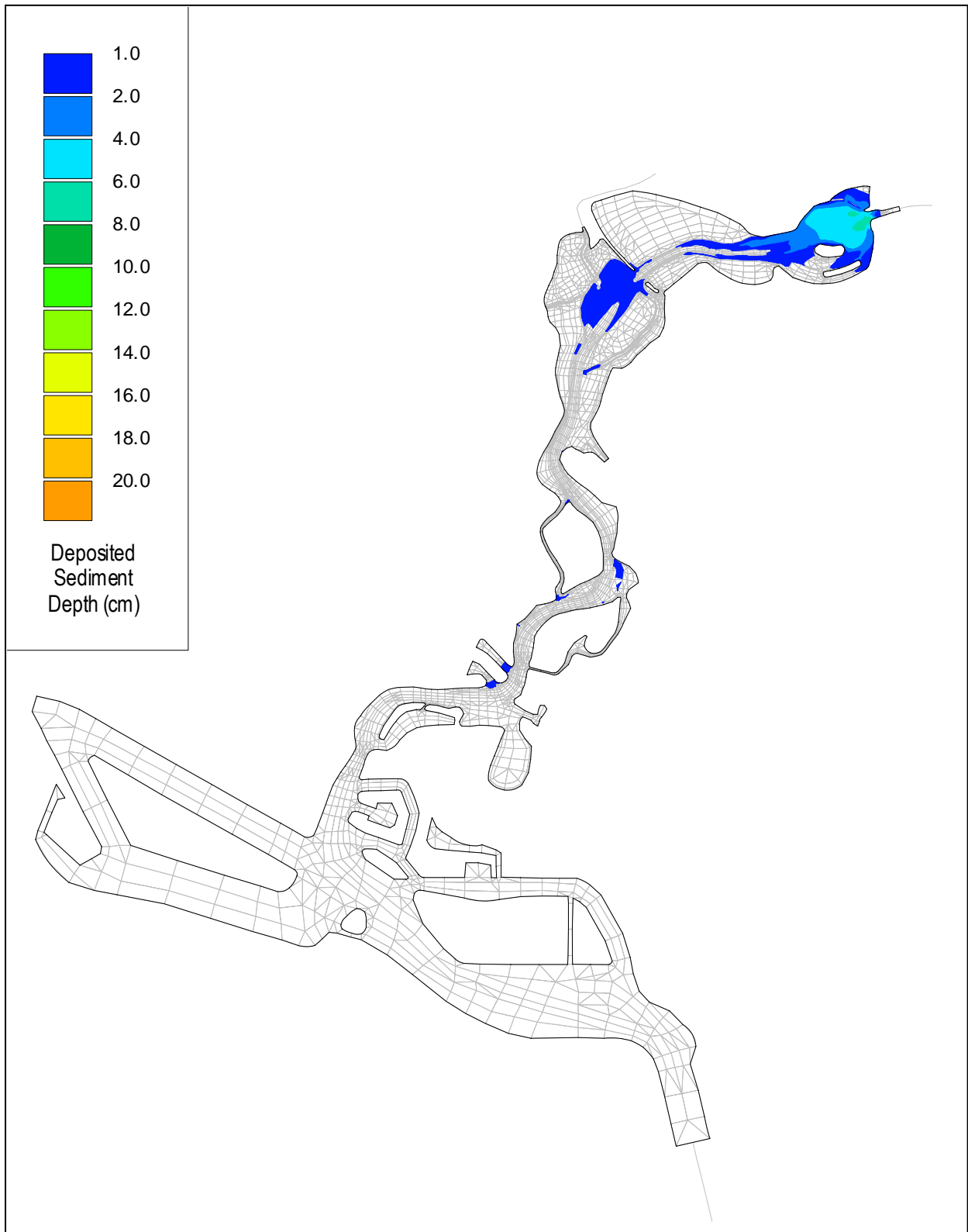


Figure 5-33 Contours of simulated deposited sediment depth accumulated during the period of December 1, 2003 through June 1, 2004.

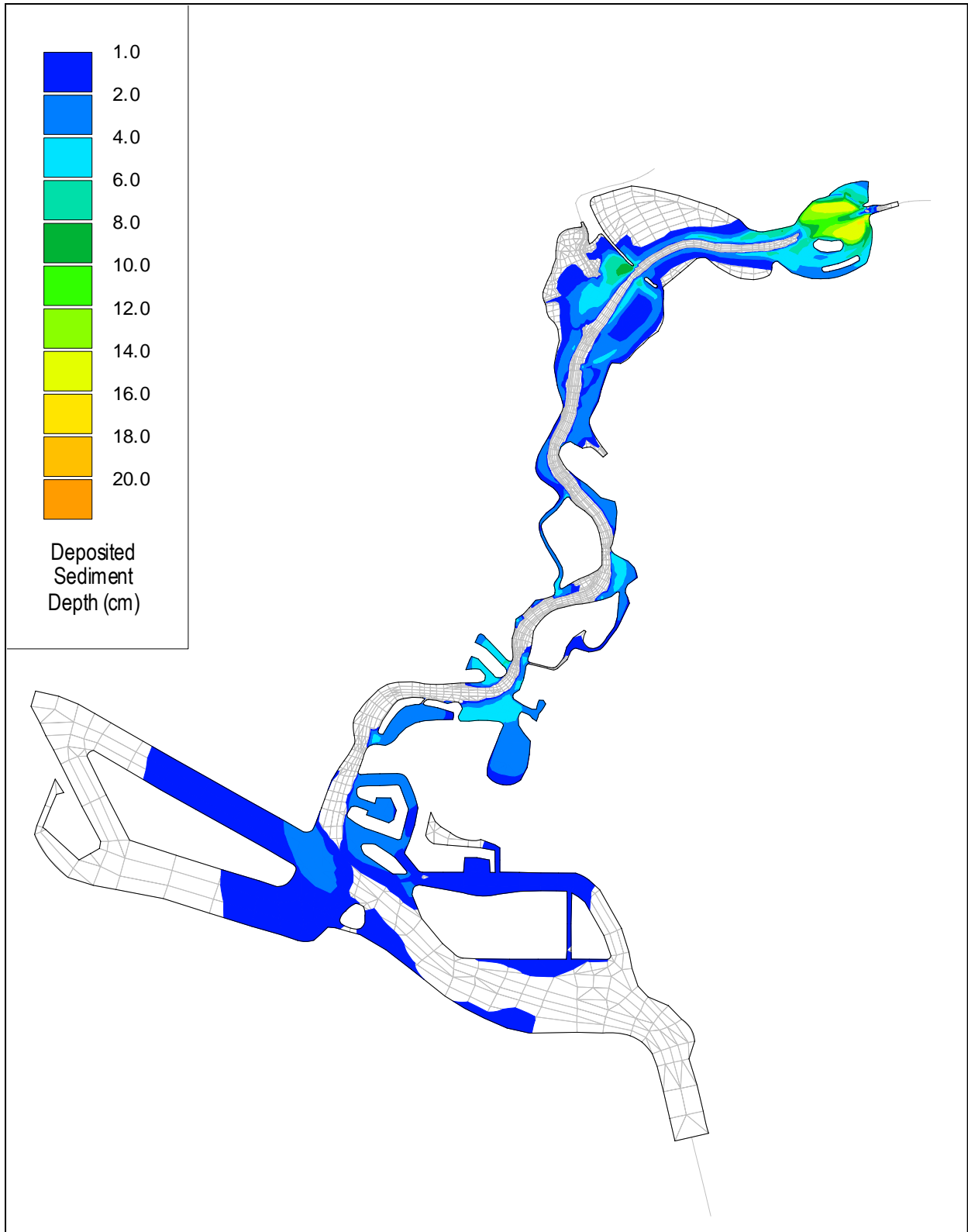


Figure 5-34 Contours of simulated deposited sediment depth accumulated during the period of January 1 through June 1, 2005.

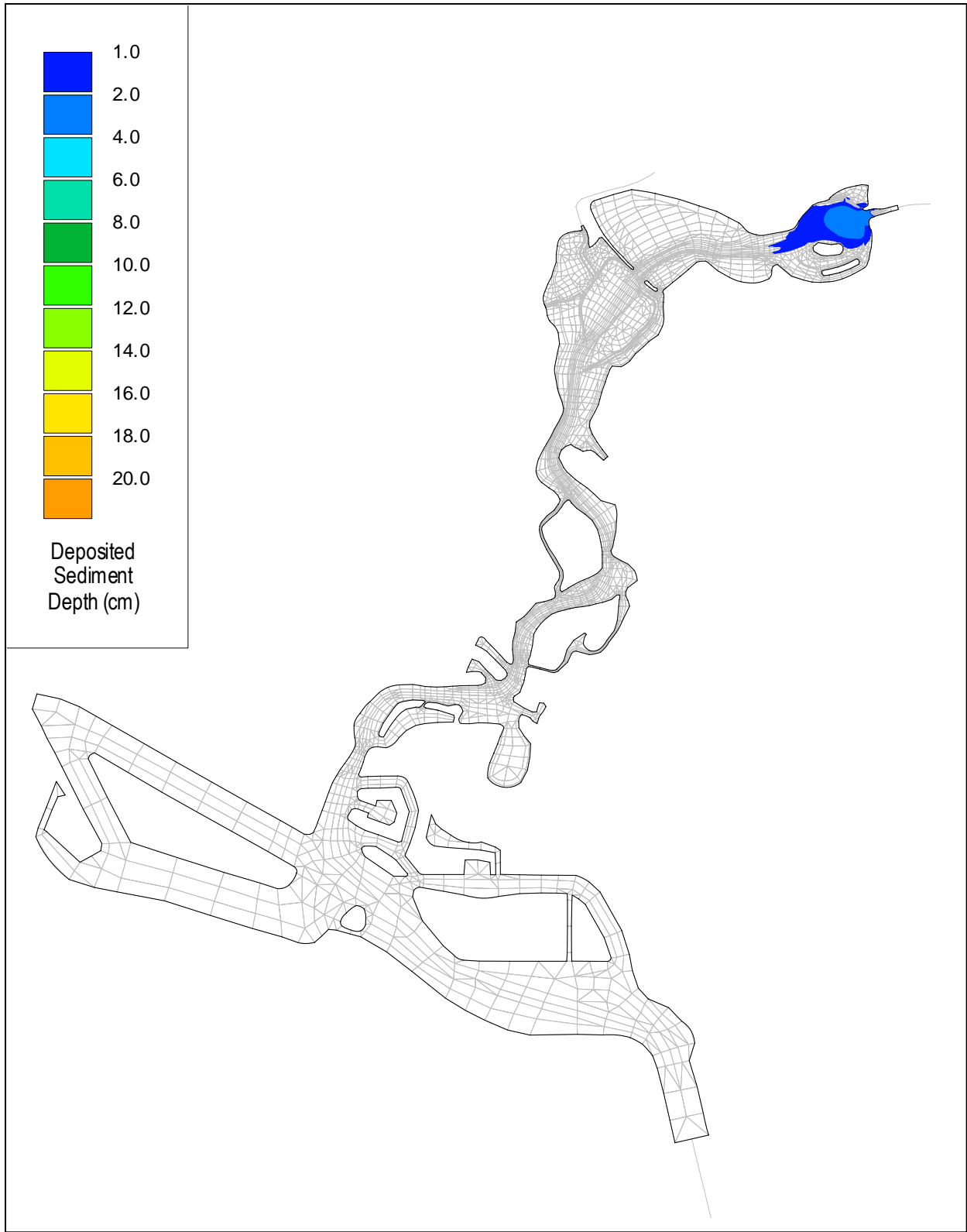


Figure 5-35 Contours of simulated deposited sediment depth accumulated during the period of January 1 through June 1, 2006.

5.3 Initial conditions

The initial conditions for water column constituents in the Newport Bay water quality model were based on nutrient TMDL values for January of each year and set to constant values throughout the Bay as listed in Table 5-4. These initial conditions were set to give reasonable starting values, but have little impact on the modeling results as they are quickly washed away under high flow conditions. Initial conditions were set for each year to allow the years to be computed in parallel and save time. The benefit of using the ending condition from one year as the initial condition for the next year was minimal and did not justify the time cost of running the three years of simulation in series.

The initial concentrations of macroalgae were sinusoidally distributed over depth, with a maximum value of 0.1 kg/m² only on the inter-tidal region. For example, while 0.1 kg/m² of macroalgae was assigned at intertidal elevations, such as 1.5 m, 0.01 kg/m² was applied at low elevations, such as -0.6 m, declining to zero in the deepest areas. Additionally, initial macroalgae concentrations declined to zero at the higher elevations with the longest exposure time at low tide. A color contour plot of the initial conditions of macroalgae is shown in Figure 5-36.

Table 5-4 Initial conditions of water quality constituents.

Constituents	DO (mg/L)	NH3 (mg/L)	NO3 (mg/L)	PO4 (mg/L)	Temperature (°C)	Salinity (ppt)
Values	8.7	0.089	0.205	0.029	13.1	32.3

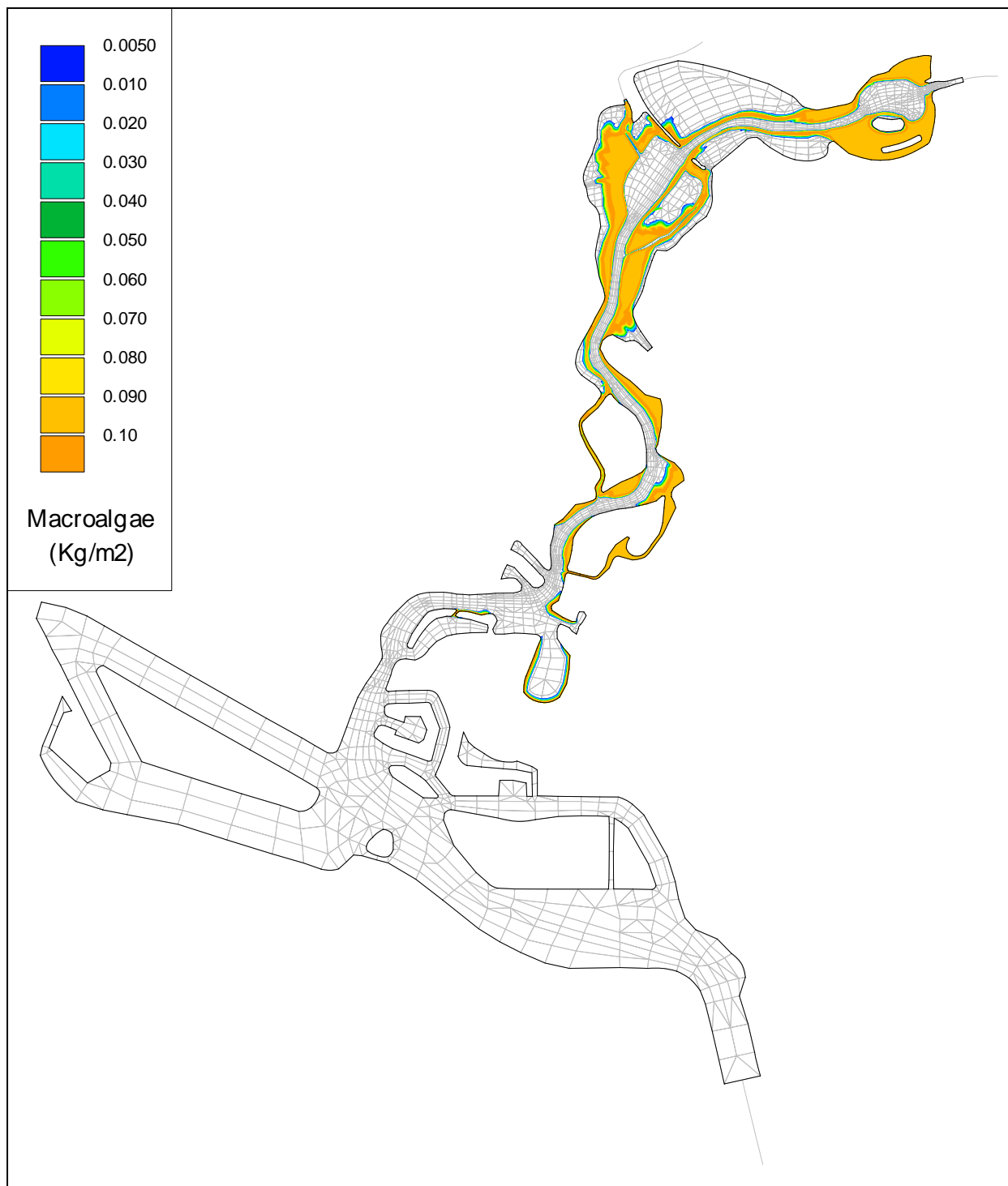


Figure 5-36 Contours of the initial condition of macroalgae on January 1, 2004.

5.4 Calibration and validation results

The measured water quality data used for the Newport Bay model calibration and validation were available from nutrient TMDL reports (County of Orange et al., 2004). Data were available for the 2004 through 2006 calibration and validation period. Eight macroalgae monitoring locations are shown in Figure 5-37 (The County of Orange et al., 2004; 2005; July-September 2005; October-December 2005; January-March 2006; April-Jun 2006; July-September 2006; October-December 2006).

The simulated daily macroalgae mass summed for the whole Upper Newport Bay region is shown in Figure 5-38. The model appropriately produced the largest macroalgae concentrations during 2005. Observed data show year 2005, the wettest year during the three-year simulations period, to have the greatest macroalgae concentrations. The computed peak total macroalgae mass for 2005 was more than twice that for 2004 as shown in Figure 5-38. Computed total mass for 2004 and 2006 were somewhat similar with 2006 slightly greater.

Color contour plots of macroalgae concentration for 2004, 2005 and 2006 are provided in Figure 5-39 through Figure 5-41. While observed data showed varying comparisons between 2004 and 2006, the peaks for 2004 were generally higher than those for 2006. Timing of the measurements was different among the years, so it is difficult to say if peak concentrations were captured in all cases.

Overall, the model does an excellent job of reproducing “depth-averaged” nutrient and DO concentrations in the Bay. This is an indication that the system is well balanced in consumption and production of nutrients and DO by macroalgae growth and respiration, and sediment processes.

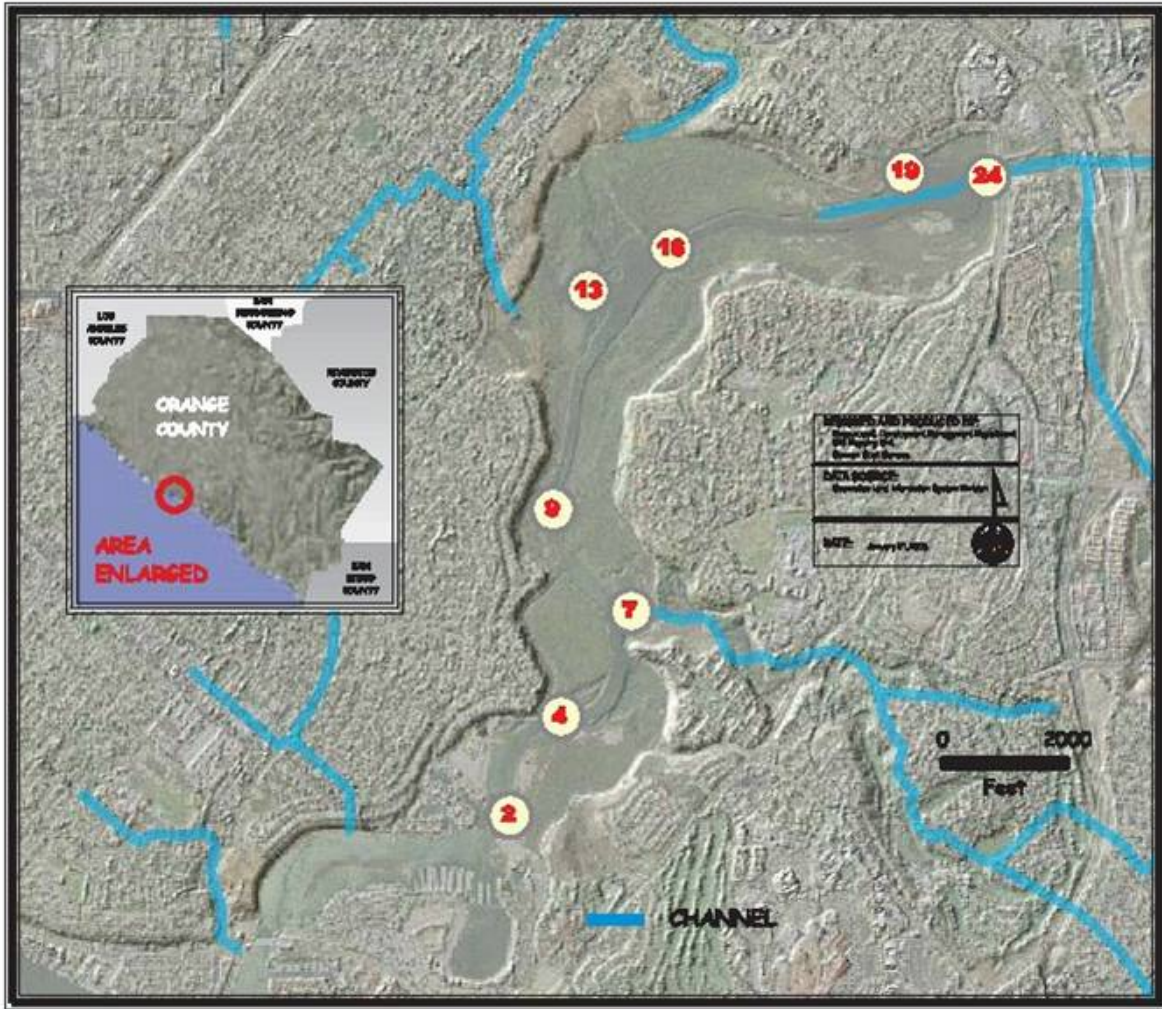


Figure 5-37 Map of Newport Bay macroalgae sampling stations (from nutrient TMDL report, County of Orange et. al, 2004).

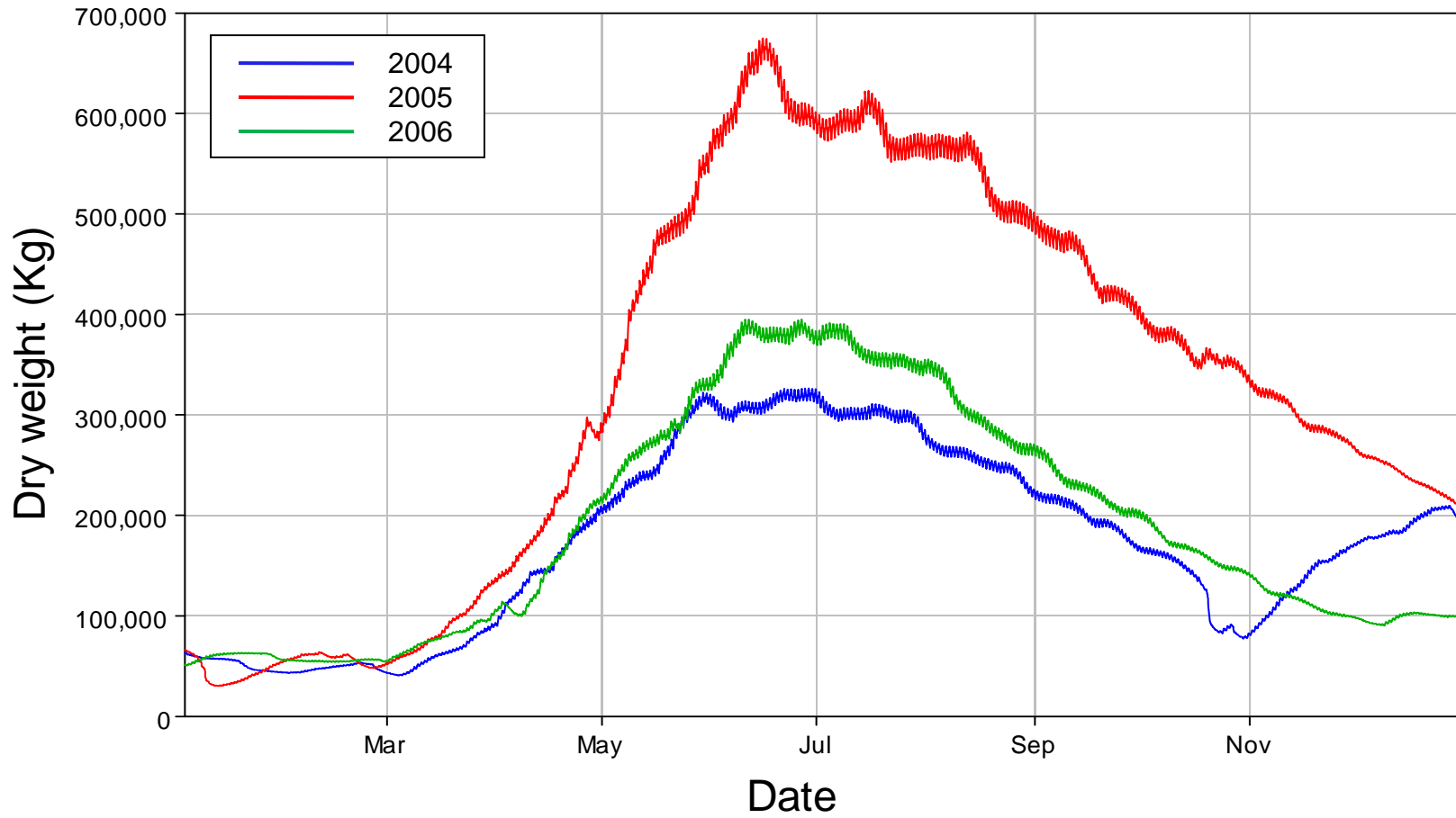


Figure 5-38 Comparison of computed total macroalgae mass computed for 2004, 2005 and 2006.

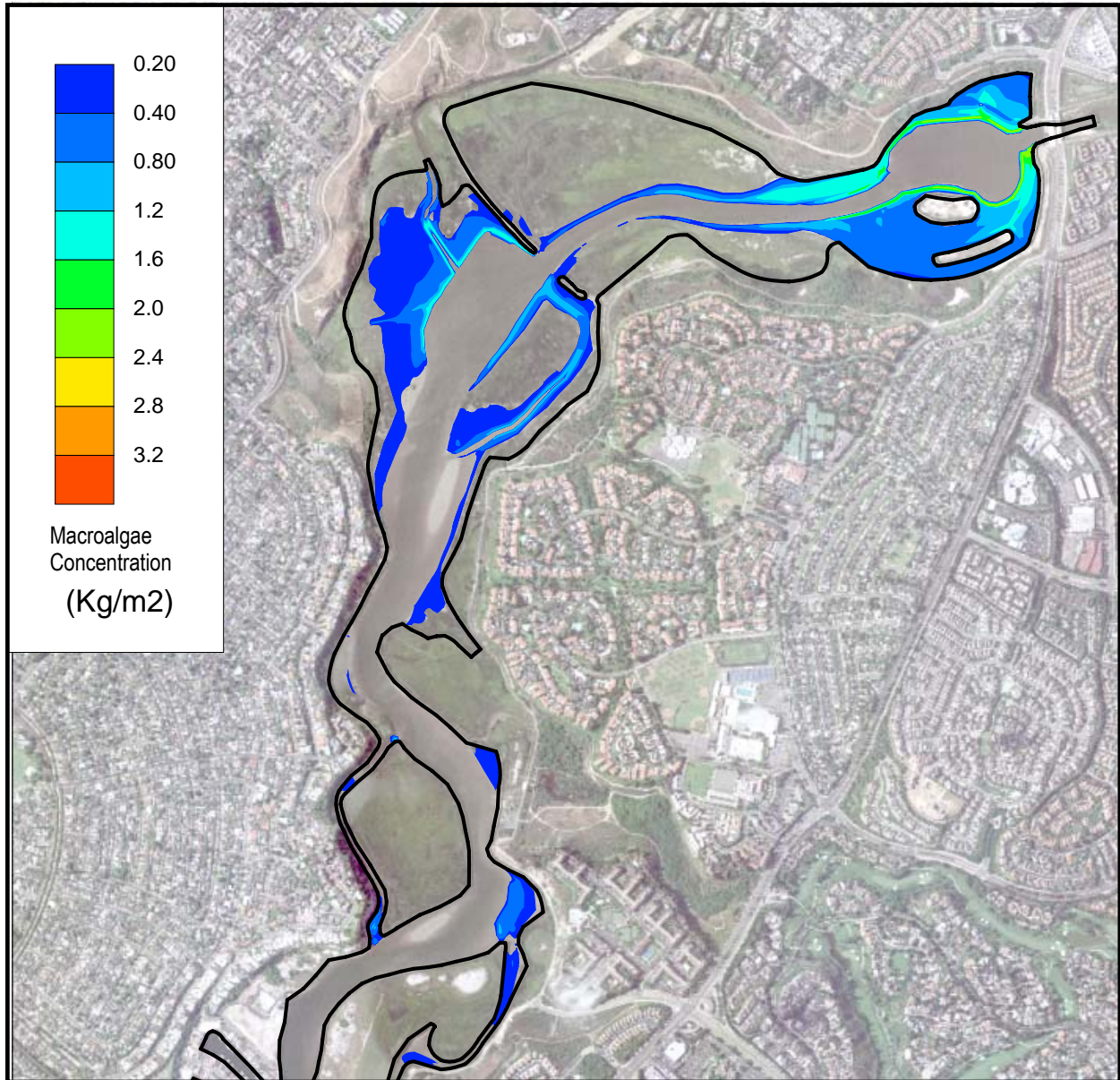


Figure 5-39 Spatial contours of computed macroalgae concentration (Kg/m²) on July 1, 2004.

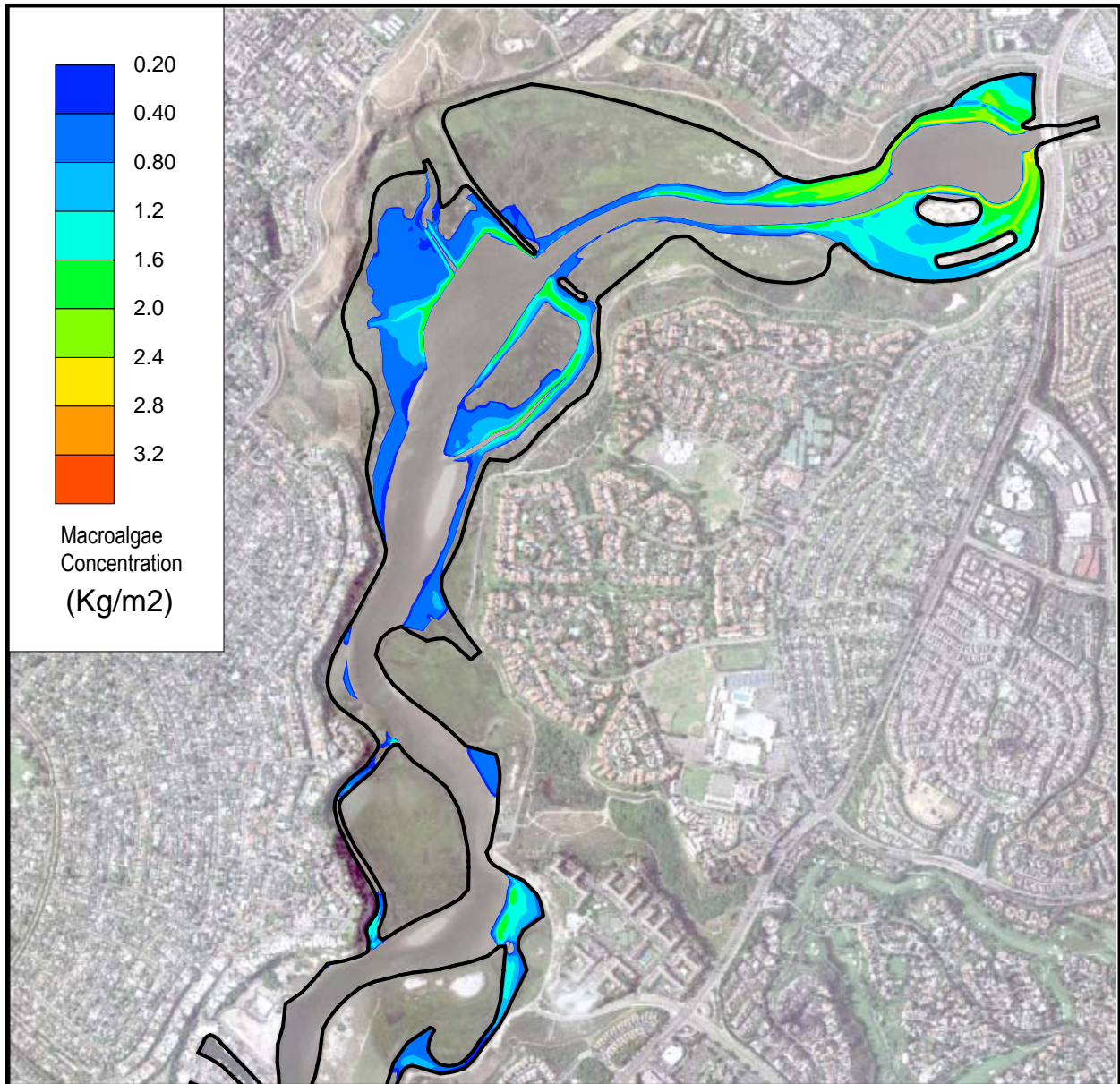


Figure 5-40 Spatial contours of computed macroalgae concentration (Kg/m²) on July 1, 2005.

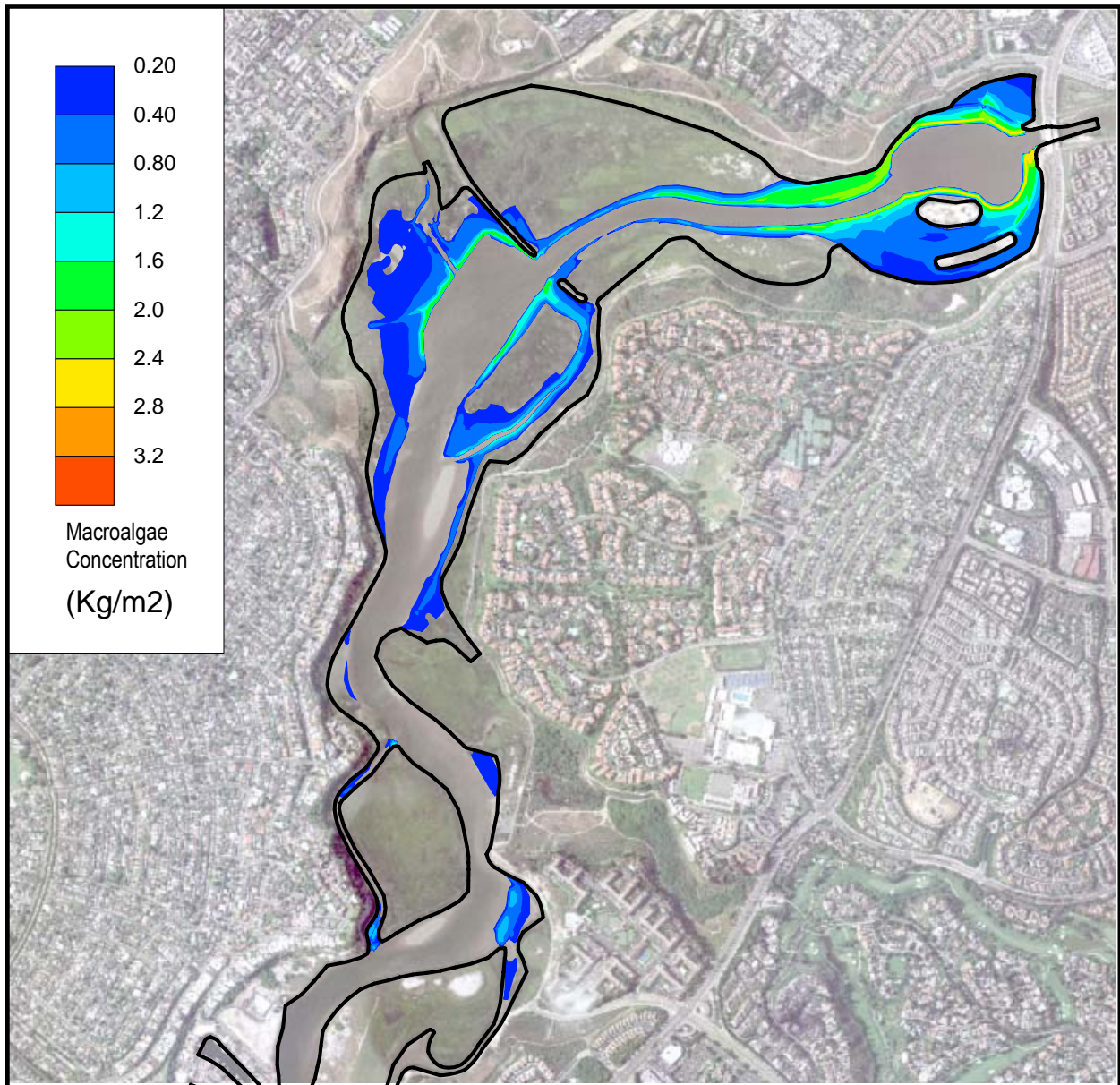


Figure 5-41 Spatial contours of computed macroalgae concentration (Kg/m²) on July 1, 2006.

5.4.1 Calibration results in 2004

The year 2004 was a relatively dry year with corresponding smaller macroalgae blooms in the summer. The model was able to reproduce the seasonal macroalgae growth characteristics with macroalgae concentrations increasing during the spring, peaking around July and declining again in the fall. The simulated macroalgae growth also tended resurge beginning in November due to nutrient loading (except at station ALG19 where there was sloughing). Even though the model captures the seasonal trends, there were some discrepancies between the simulated macroalgae and the observed data at each station. The model tended to underpredict the peak biomass at stations including ALG24, ALG16, ALG9 and ALG7. Moreover, the model produced a more gradual buildup in macroalgae biomass, while the observed data suggest low growth until June followed by a sharp increase in biomass production. However, the aerial photography conducted three times in 2005 and the land-based photographs tend to support the more gradual buildup produced by the model. In addition, the monthly macroalgae samples are subject to great variability introduced by the sampling method as well as the naturally patchy nature of macroalgal growth (Doug Shibberu, personal communication). The model also reproduced observed spatial variation in macroalgal concentrations in the Bay. For example the model reproduced high concentrations of macroalgae observed in the Unit I (near UNBJAM) and low concentrations observed nearer the ocean. A plot comparing computed macroalgae concentration at each sampling location is shown in Figure 5-42 and plots of computed and observed macroalgae concentrations during 2004 are shown in Figure 5-43 through Figure 5-49.

Computed temperatures are in good agreement with observed data during the summer as shown in Figure 5-50 through Figure 5-53. Based on the simulation results, the spatial variation of temperature was not as significant as the temporal variation. Computed temperatures are lower than observed during September through November at all stations, as much as 4° C lower at UNBJAM, although the cause is unclear.

Plots of computed and observed dissolved oxygen are shown in Figure 5-54 through Figure 5-57. The model produces DO concentrations in the range of observed data. At the furthest downstream stations, UNBNSB and UNBCHB, the observed data seem to indicate more variation than is computed. The simulated DO did not show any anoxia for the entire year 2004 probably due to depth averaging. Near the beginning of November, in response to macroalgae growth in the model, computed DO concentrations begin to increase above the observed values. Although there are no macroalgae measurements during this time, the lack of DO response in the observed data is a likely indicator that this late fall macroalgae growth did not actually occur.

Computed and observed nutrient concentrations for 2004 including nitrate, ammonia, and phosphate are shown in Figure 5-58 through Figure 5-69. Computed nitrate concentrations correspond well with observed data, reproducing the higher values during the periods of higher inflow to the Bay, and the lower values in the summer at all the stations. The model was able to

produce the spatial variation of NO₃ (i.e., high peak concentrations at UNBJAM were between 5 and 6 mg/L while those near ocean were between 2 and 3 mg/L) indicating that NO₃ was mainly coming from San Diego Creek and that there might be sinks in the bay. Note that while computed values at the stations lower in the Bay appear to be too low, the lowest observations are at the detection limit.

Ammonia concentrations are in good agreement with observed data at stations UNBJAM and UNBSDC, slightly lower than observed and UNBNSB and even lower at UNBCHB. The model did not capture the peaks in the early of December possibly due to sediment processes which were not used in our current model. Although observed data detection limits (i.e., 0.05 and 0.1 mg/L) may be a factor for deviations between computed and observed for the lowest summer values, the downstream boundary condition may be set too low in the model. Data available for the ocean boundary were very limited and thus constant boundary condition values were used for all water quality constituents.

Phosphate concentrations are plotted in Figure 5-66 through Figure 5-69. Computed concentrations are in good agreement with observed data at all locations. At the uppermost station, UNBJAM, observed data show some greater variation than computed. This may be due to uncertainty in the creek inflow concentrations.

5.4.2 Validation results in 2005

The year 2005 was a wet year with relatively large macroalgae blooms in the summer. The model was able to reproduce the larger bloom relative to the other simulation years, and reproduce the seasonal macroalgae growth characteristics with macroalgae concentrations increasing during the spring, peaking around July and declining again in the fall, although with a lower peak and less rapid decline than indicated by observed data. The model continued to show a more gradual build up in macroalgal biomass compared with observations. The model reproduced observed spatial variation in macroalgal concentrations in the Bay. For example, high concentrations of macroalgae observed in the Unit I (near UNBJAM) and low concentrations observed nearer the ocean were reproduced by the model. A plot comparing computed macroalgae concentration at each sampling location is shown in Figure 5-70 and plots of computed and observed macroalgae concentrations during 2005 are shown in Figure 5-71 through Figure 5-77.

Computed temperatures are in good agreement with observed data throughout the year as shown in Figure 5-78 through Figure 5-81. Based on the simulation results, the spatial variation of temperature was not as significant as the temporal variation. Additional time series data measured at the surface and the bottom at 30 minute intervals were compared with the simulated depth averaged data at stations S1, S2 and S3 (see Figure 5-82) during June through December, shown in Figure 5-83 through Figure 5-85. Weak thermal stratification appeared in the summer (i.e., from July to September in 2005) that was not able to be captured by the 2-D model. These

data confirm that temperature is well represented in the model, although with slightly less daily variation.

Plots of computed and observed dissolved oxygen are shown in Figure 5-86 through Figure 5-89. The model produces DO concentrations in the range of observed data at station UNBSDC and slightly higher than observed at the other stations. The simulated DO tended to be higher than the observed, especially in winter (e.g., November and December), which might be related to the high concentrations of macroalgae as well as the ocean boundary condition for DO. Additional time series data available during June through December (measured at the surface and the bottom at 30 minute intervals) generally show good agreement with observed data at stations S1, S2 and S3, as shown in Figure 5-92. Measured data showed some events of anoxia in the summer and in the fall, which were not reproduced by the model.

Computed and observed nutrient concentrations including nitrate, ammonia, and phosphate for 2005 are shown in Figure 5-93 through Figure 5-104. At station UNBJAM, observed seasonal trends of nitrate concentrations are well represented by the model. At the remaining stations, computed nitrate concentrations tend to be higher than observed during storm periods and lower than observed during the summer. Observed data do not reflect the higher nitrate concentrations in the winter as they did in 2004. It is unclear whether the peaks did not actually occur or whether they were simply missed due to infrequent sampling. Some of the summertime nitrate observations are at detection limit, however, it does still appear that computed summer values are too low. The model was also able to produce the spatial variation of NO₃ (i.e., peak concentrations at UNBJAM were between 6 and 7 mg/L while those near the ocean were between 2 and 3 mg/L) indicating that NO₃ was mainly coming from San Diego Creek and that there might be sinks in the Bay. DO concentrations indicate that the macroalgae concentrations and associated growth and respiration are appropriate and thus should not be over-consuming nutrients, but the low computed nitrate values could be due to boundary concentrations set too low.

Ammonia concentrations are also higher than observed during the storm periods (see Figure 5-97 through Figure 5-100). Otherwise, the seasonal trends of ammonia results are in good agreement with observed data at stations UNBJAM and UNBSDC, but slightly lower than observed at UNBNSB and even lower at UNBCHB. Although observed data detection limits may be a factor for deviations between computed and observed for the lowest summer values, the downstream boundary condition may be too low due to limited data availability.

Phosphate concentrations are plotted in Figure 5-101 through Figure 5-104. Compute concentrations in general show much more seasonal variation than observed. Model results are too high in the winter and spring come into agreement with observed data during the summer, and begin to fall below observed during the fall.

5.4.3 Validation results in 2006

The year 2006 was a relatively dry year with corresponding smaller macroalgae blooms in the summer. The model was able to reproduce the seasonal macroalgae growth characteristics with macroalgae concentrations increasing during the spring, peaking around July and declining again in the fall, although with a less rapid decline than indicated by observed data. Even though the model captures the seasonal trends, there were some discrepancies between the simulated results and the observed data at each station. The model again continued to show a more gradual build up in macroalgal biomass, than the observed. The model tended to overpredict the peak biomass at almost all stations. The model produced spatial variation in macroalgal concentrations in the Bay. For example, high concentrations of macroalgae observed in the Unit I (near UNBJAM) and lower concentrations observed nearer the ocean were reproduced by the model. A plot comparing computed macroalgae concentration at each sampling location is shown in Figure 5-105 and plots of computed and observed macroalgae concentrations during 2006 are shown in Figure 5-106 through Figure 5-109.

The temporal and spatial computed temperatures are generally in good agreement with observed data as shown in Figure 5-110 through Figure 5-113. Computed temperatures are as much as 3° C lower than observed at UNBJAM during September through November. This could again be due to problem with the input meteorological data, or could be a result of inflow temperatures set too low in the model.

Plots of computed and observed dissolved oxygen are shown in Figure 5-114 through Figure 5-117. The model produces DO concentrations in March that are higher than observed by as much as 5 mg/l. This could indicate that there was macroalgae growth during the spring that is not reflected in the model, however there are no macroalgae data to confirm this. During the summer and fall, model DO at stations UNBJAM, UNBNSB, and UNBCHB is in the range of observed data but tends to fluctuate to the high side. The larger computed fluctuations may indicate that there is too much macroalgae growth in the model, and this would be confirmed by the macroalgae calibration results. At these three stations during November and December, computed values are generally higher than observed by 1 to 4 mg/L. One macroalgae data point at station ALG19 indicates there may have been a small bloom in November that was not reproduced by the model. Respiration and decay of this macroalgae could explain the lower observed DO. At the furthest downstream station, UNBCHB, the model results are in good agreement with the remaining data points during the spring and summer.

Computed and observed nutrient concentrations including nitrate, ammonia, and phosphate for 2006 are shown in Figure 5-118 through Figure 5-129. Computed nitrate concentrations correspond well with observed data, reproducing the higher values during the periods of higher inflow to the Bay, and the lower values in the summer. Note that the lowest observations are at the detection limit. The model was also able to reproduce the observed spatial variation of NO₃

(i.e., peak concentrations at UNBJAM were between 5 and 6 mg/L while those near ocean were between 1 and 2 mg/L) indicating that NO₃ was mainly coming from San Diego Creek and that there probably were sinks in the Bay.

Computed ammonia concentrations at stations UNBJAM, UNBSDC and UNBNSB lower than observed during the spring, late fall and winter. The higher observed values during the fall and winter may have been due to dredging the bay in 2006 that might have disturbed the biochemical system of sediments (The County of Orange et al., 2006). At UNBNSB and UNBCHB, concentrations are low during spring through mid-summer. Simulated spatial variations (e.g., peaks ranging from 0.1 – 0.5 mg/L) were much larger than the temporal variations.

Phosphate concentrations are plotted in Figure 5-126 through Figure 5-129. Compute concentrations are generally in good agreement with observed data at all locations during spring and summer but fall below observed during fall and winter. The higher observed values during the fall and winter may have been a result of the dredging. As with PO₄, the simulated spatial variations (e.g., peaks ranging from 0.1 – 0.4 mg/L) were much larger than the temporal variations.

Finally, the total dry mass of macroalgae for each of the calibrated years was compared in Figure 5-130. The total dry mass in 2005 was larger than the mass in 2004 by almost two times in the summer (e.g., June, July, and August). The mass in 2004 was smaller than the mass in 2006 in the summer, which might be due to higher concentrations of nitrogen in 2006, although there were fewer storm events in 2006 than in 2004.

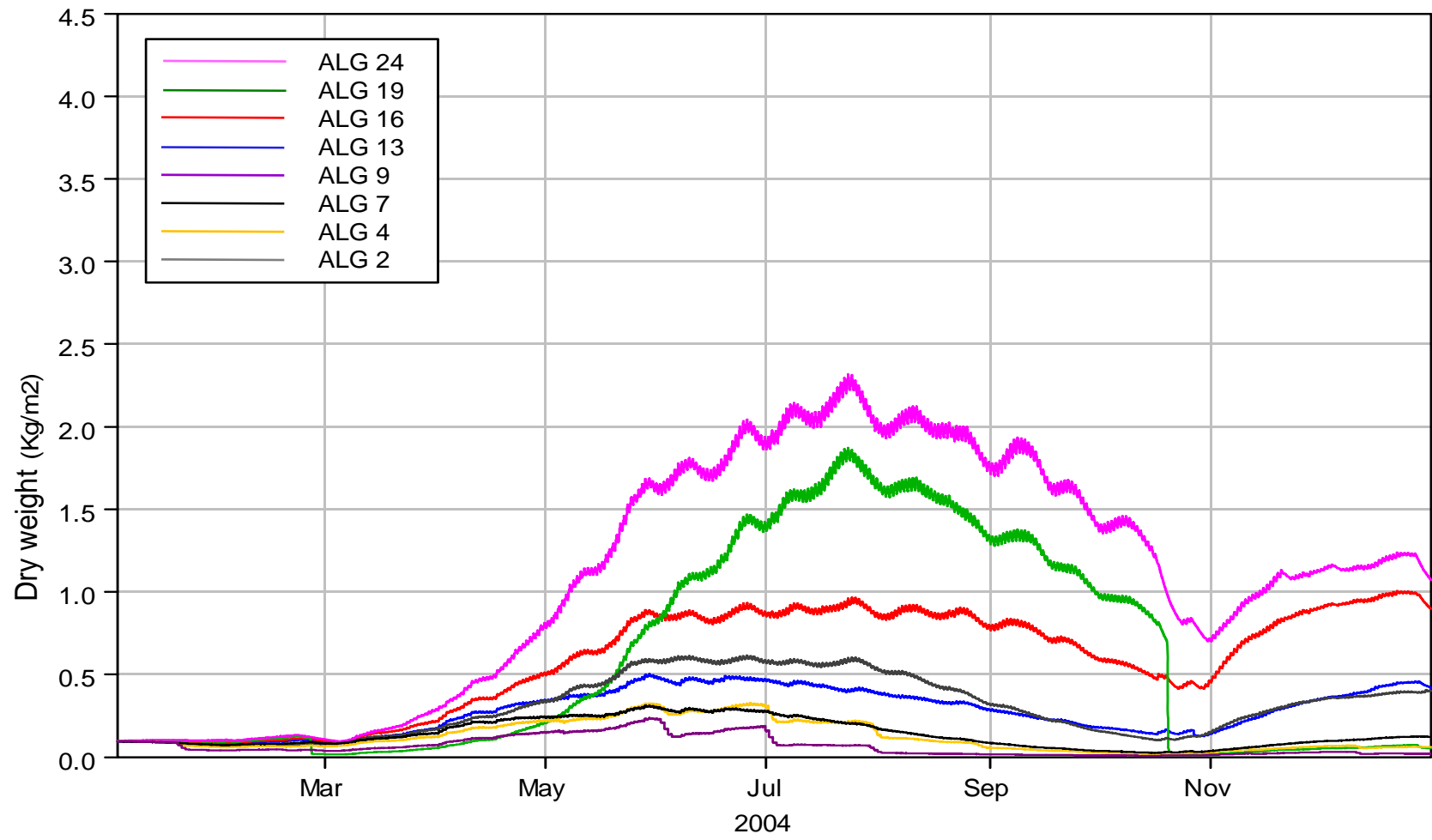


Figure 5-42 Comparison of computed macroalgae concentrations at sampling sites in 2004.

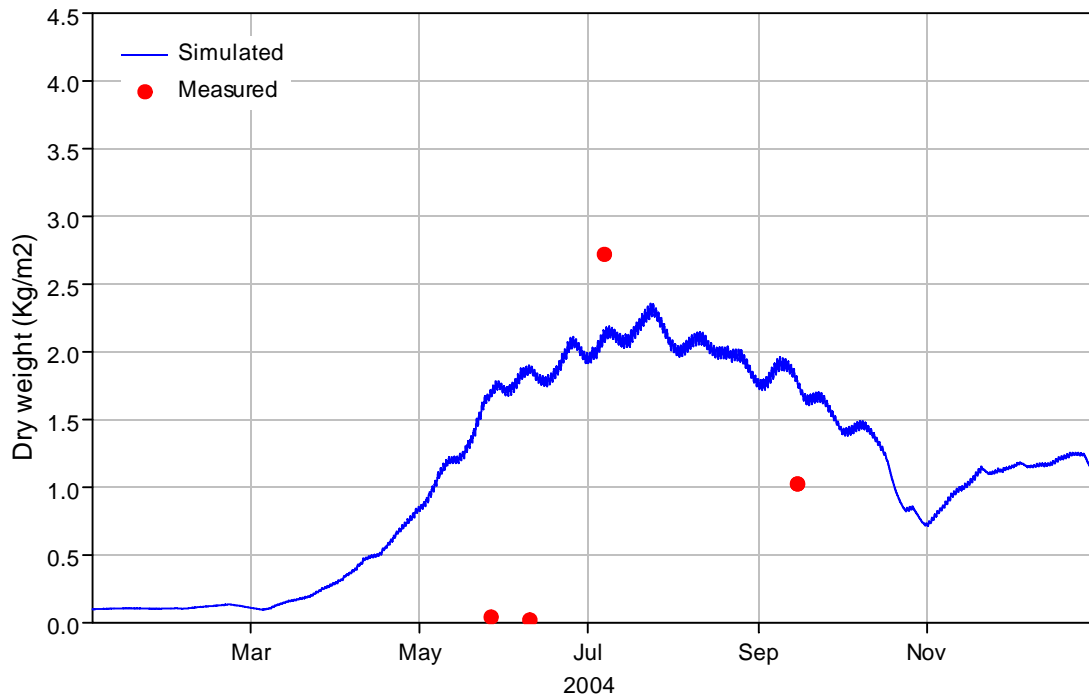


Figure 5-43 Comparison of computed macroalgae concentrations with the measured data at ALG24 in 2004.

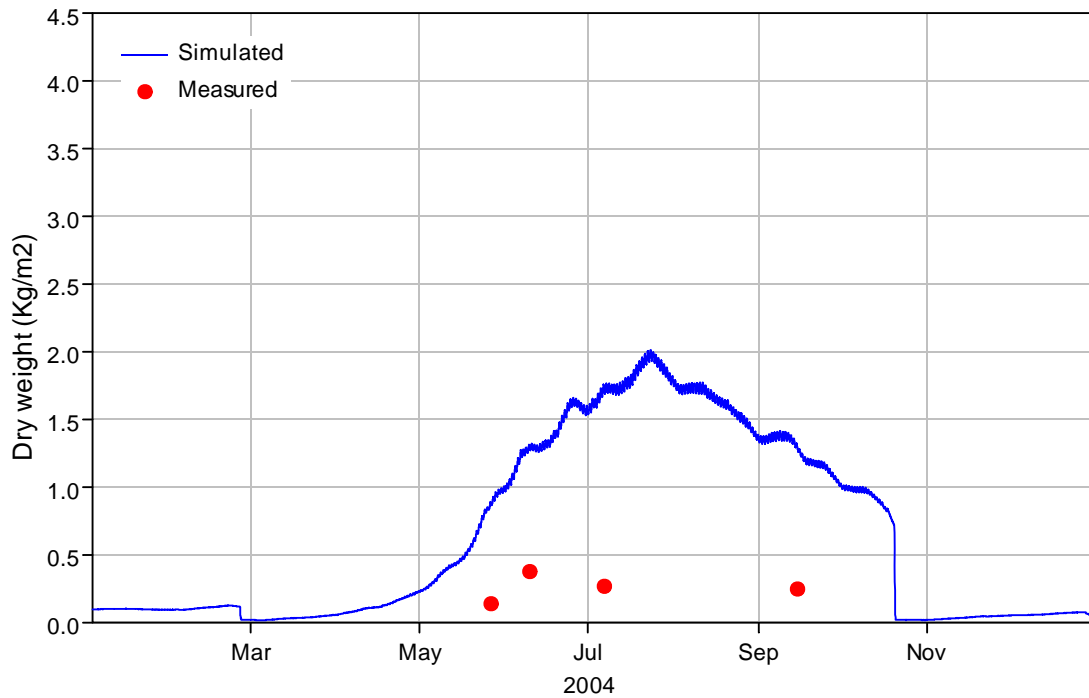


Figure 5-44 Comparison of computed macroalgae concentrations with the measured data at ALG19 in 2004.

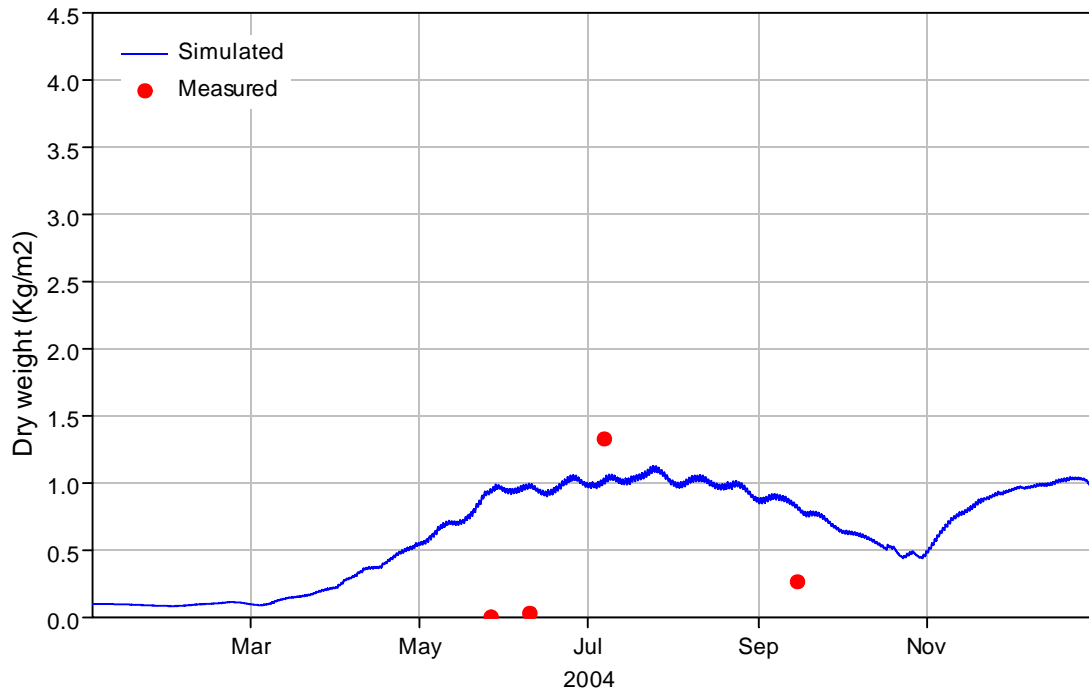


Figure 5-45 Comparison of computed macroalgae concentrations with the measured data at ALG16 in 2004.

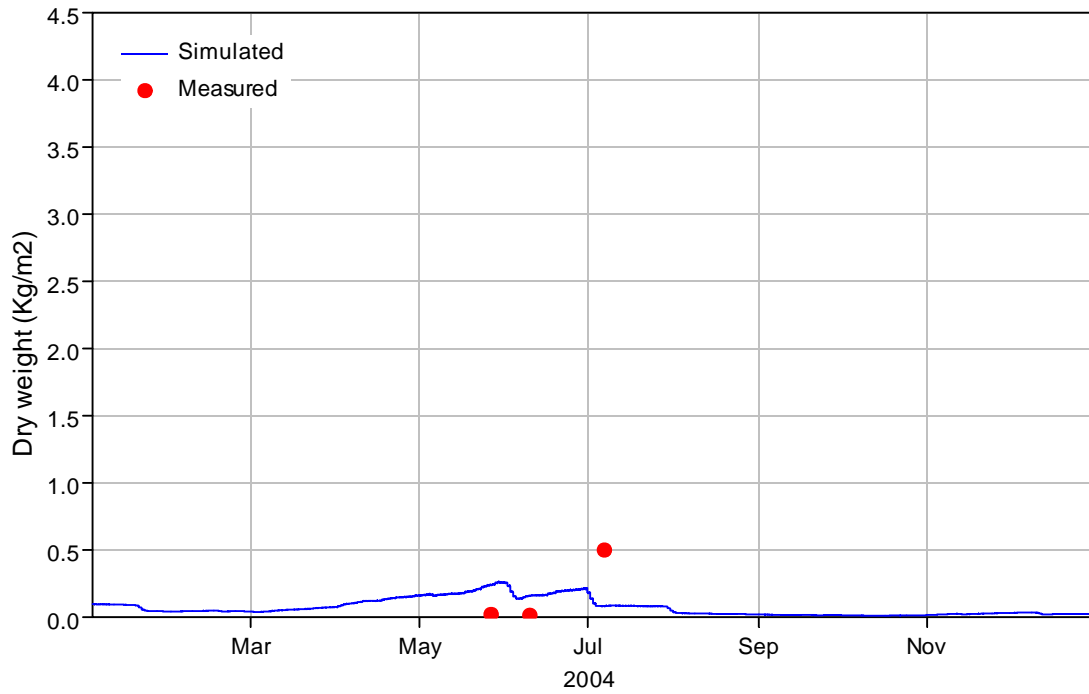


Figure 5-46 Comparison of computed macroalgae concentrations with the measured data at ALG9 in 2004.

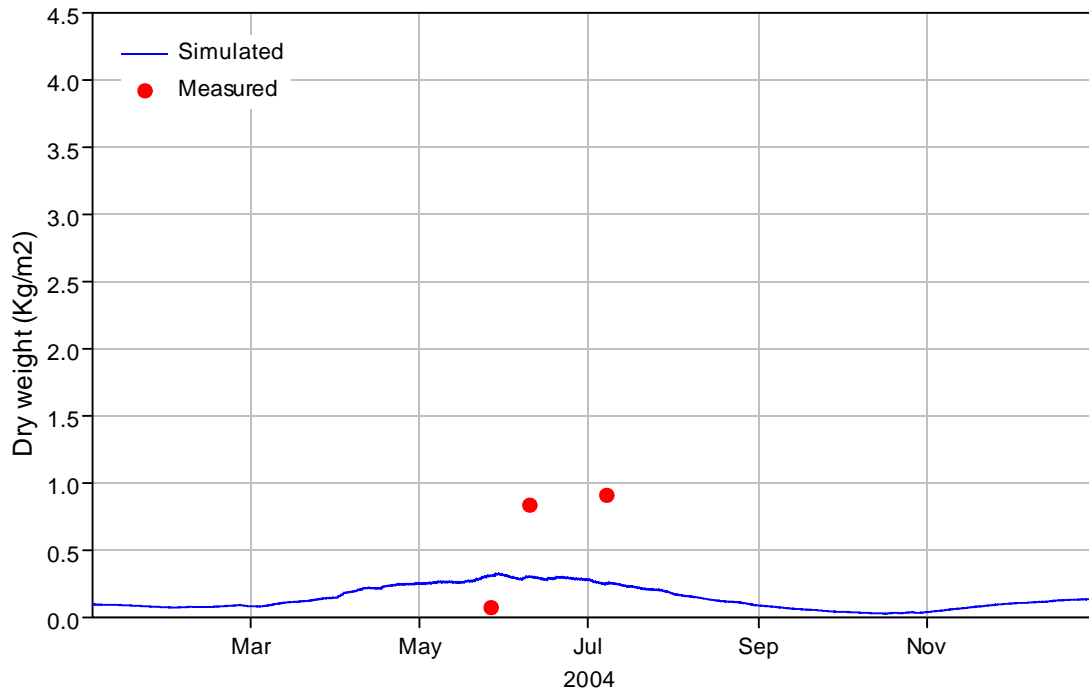


Figure 5-47 Comparison of computed macroalgae concentrations with the measured data at ALG7 in 2004.

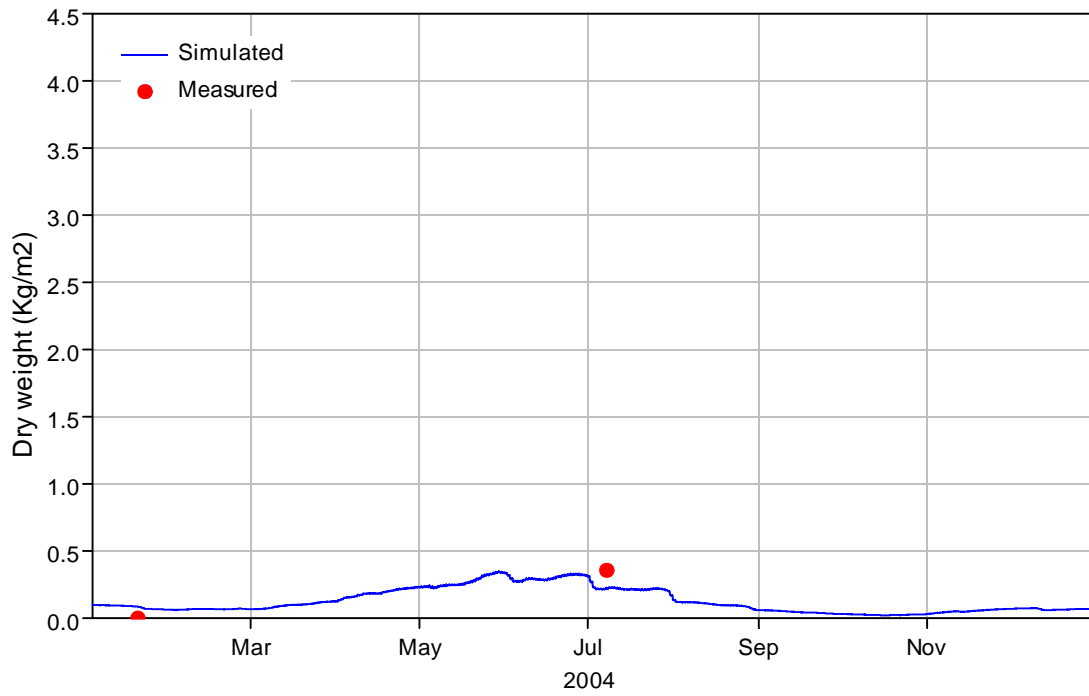


Figure 5-48 Comparison of computed macroalgae concentrations with the measured data at ALG4 in 2004.

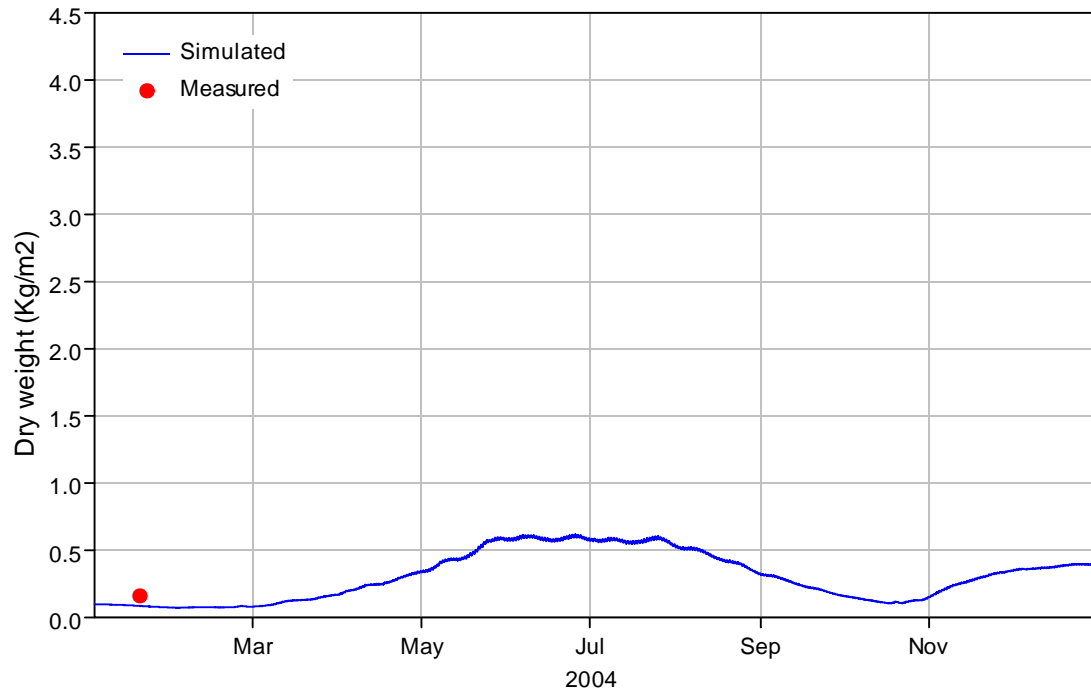


Figure 5-49 Comparison of computed macroalgae concentrations with the measured data at ALG2 in 2004.

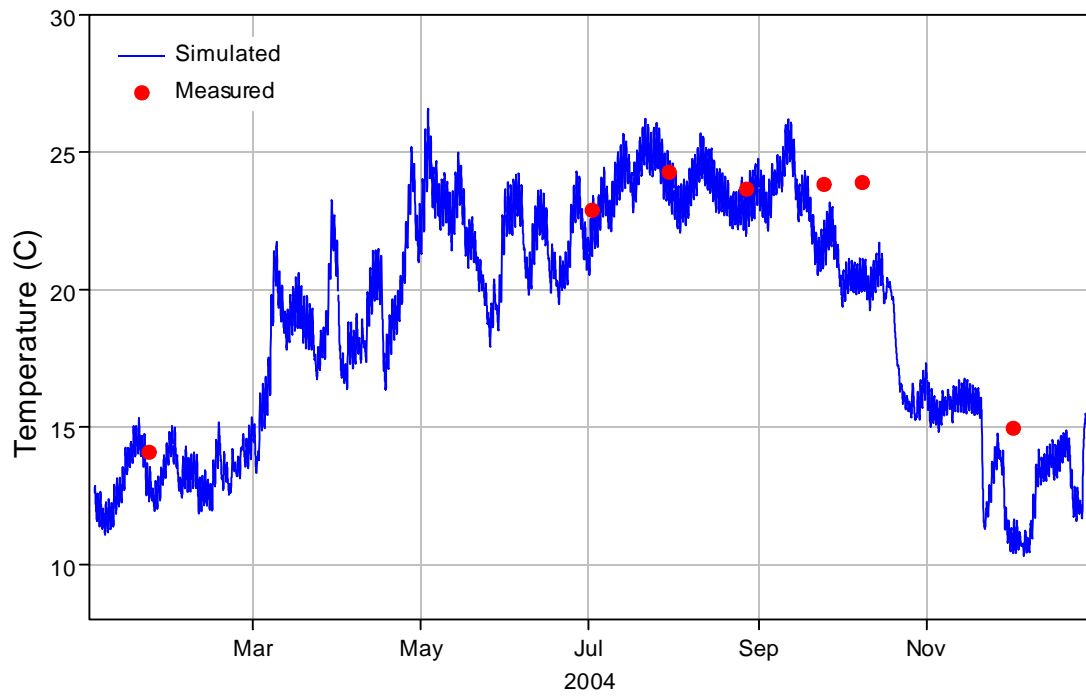


Figure 5-50 Comparison of computed temperature ($^{\circ}\text{C}$) with the measured data at UNBJAM in 2004.

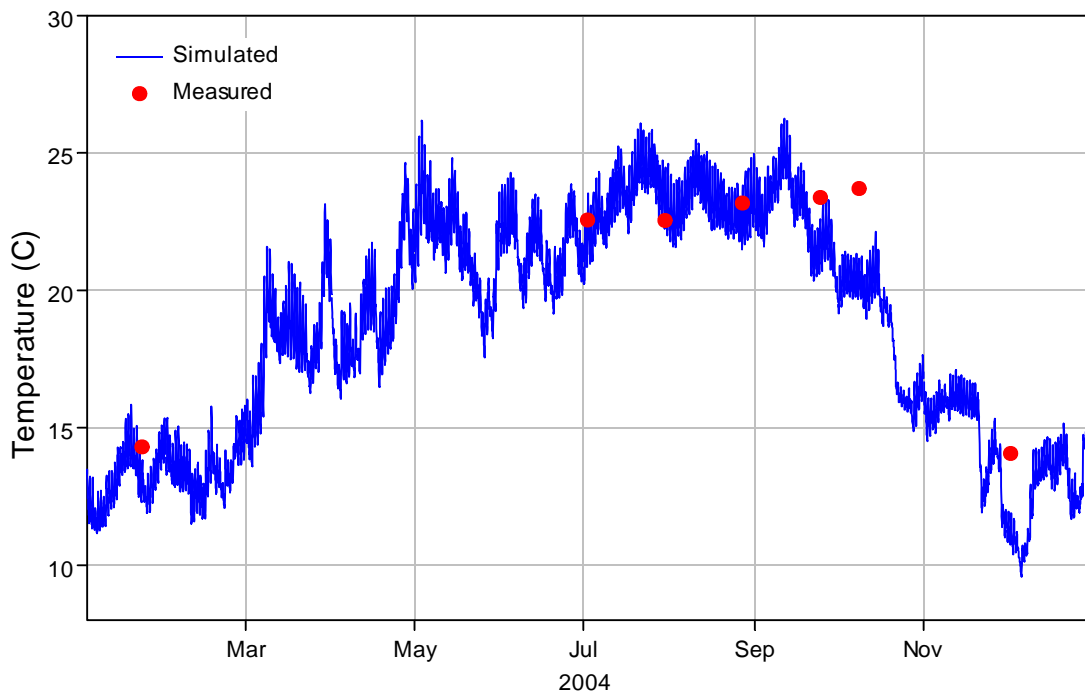


Figure 5-51 Comparison of computed temperature ($^{\circ}\text{C}$) with the measured data at UNBSDC in 2004.

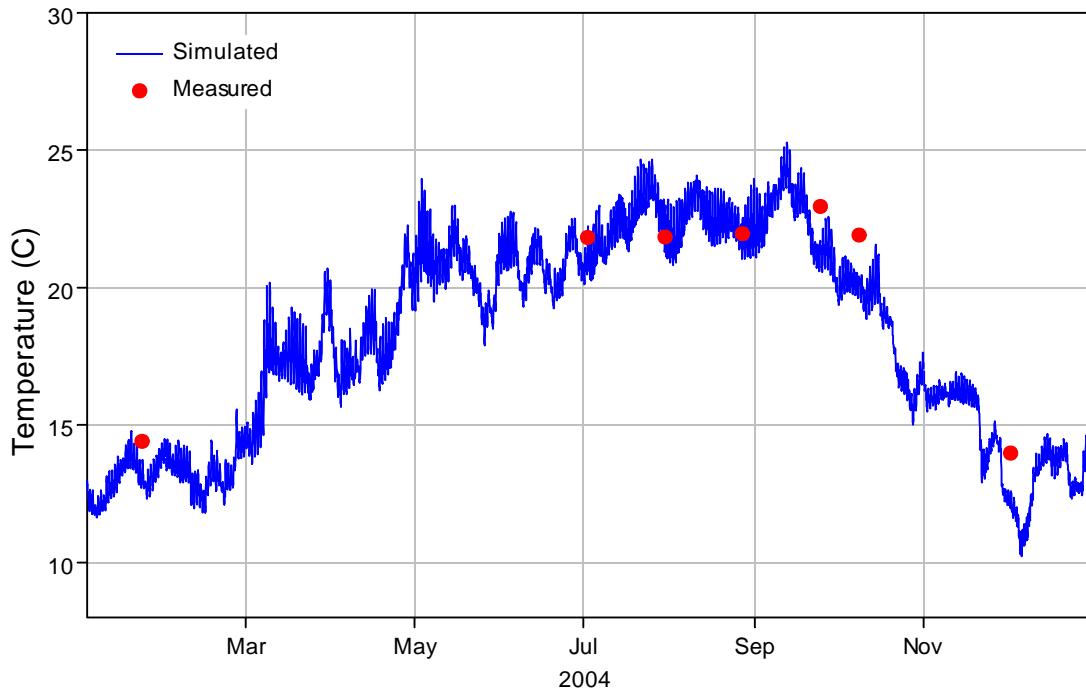


Figure 5-52 Comparison of computed temperature (°C) with the measured data at UNBNSB in 2004.

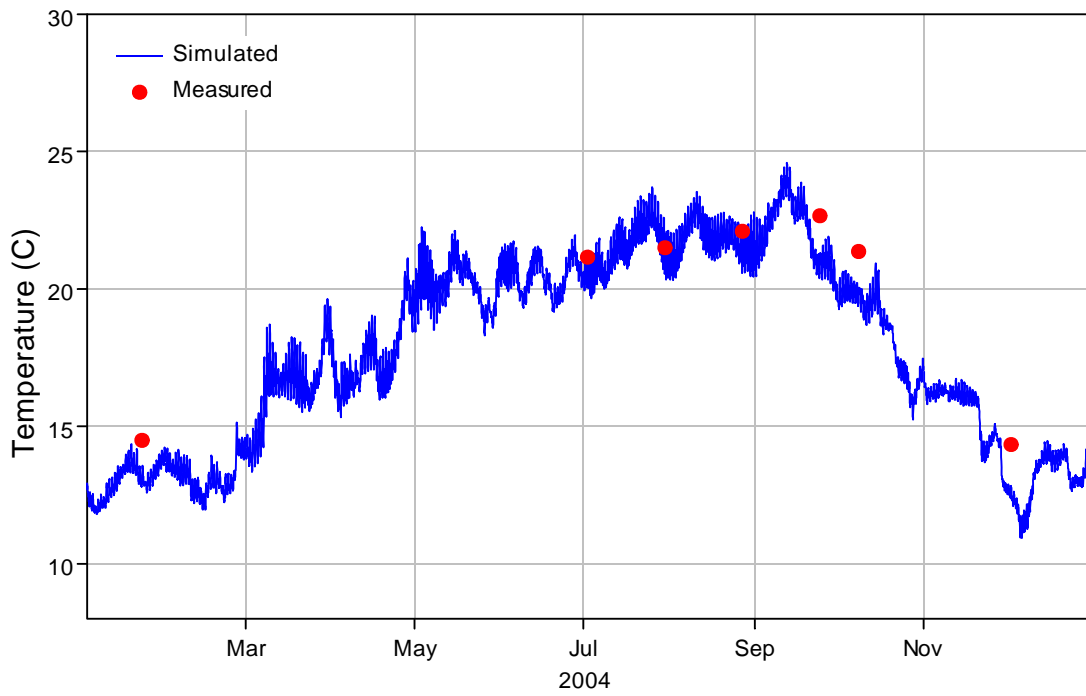


Figure 5-53 Comparison of computed temperature (°C) with the measured data at UNBCHB in 2004.

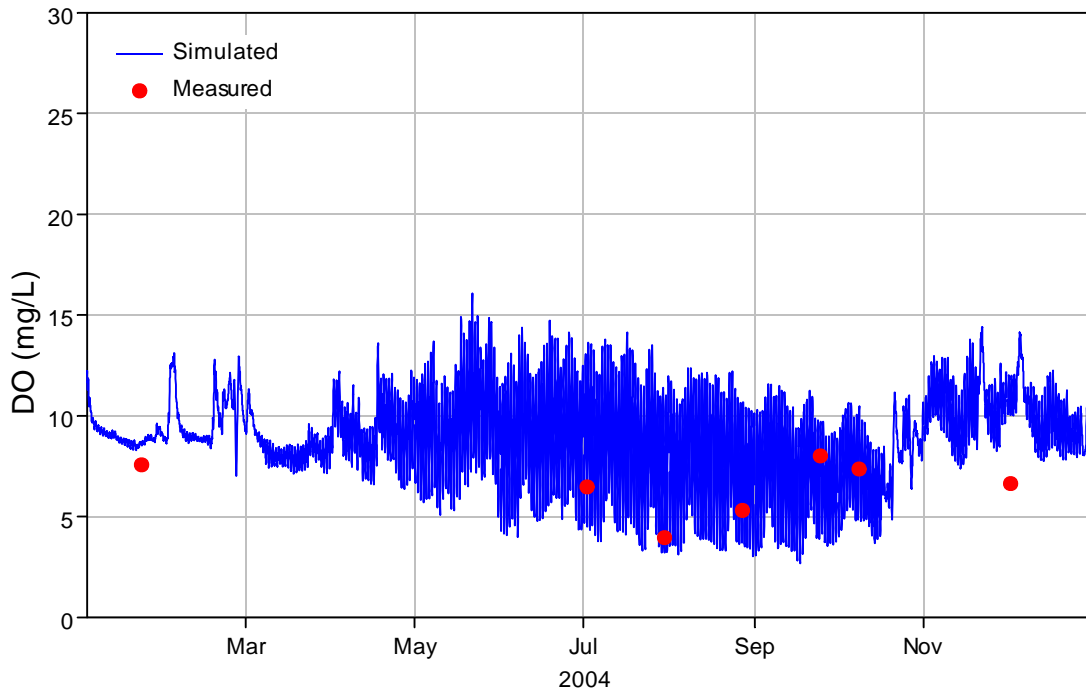


Figure 5-54 Comparison of computed DO concentrations with the measured data at UNBJAM in 2004.

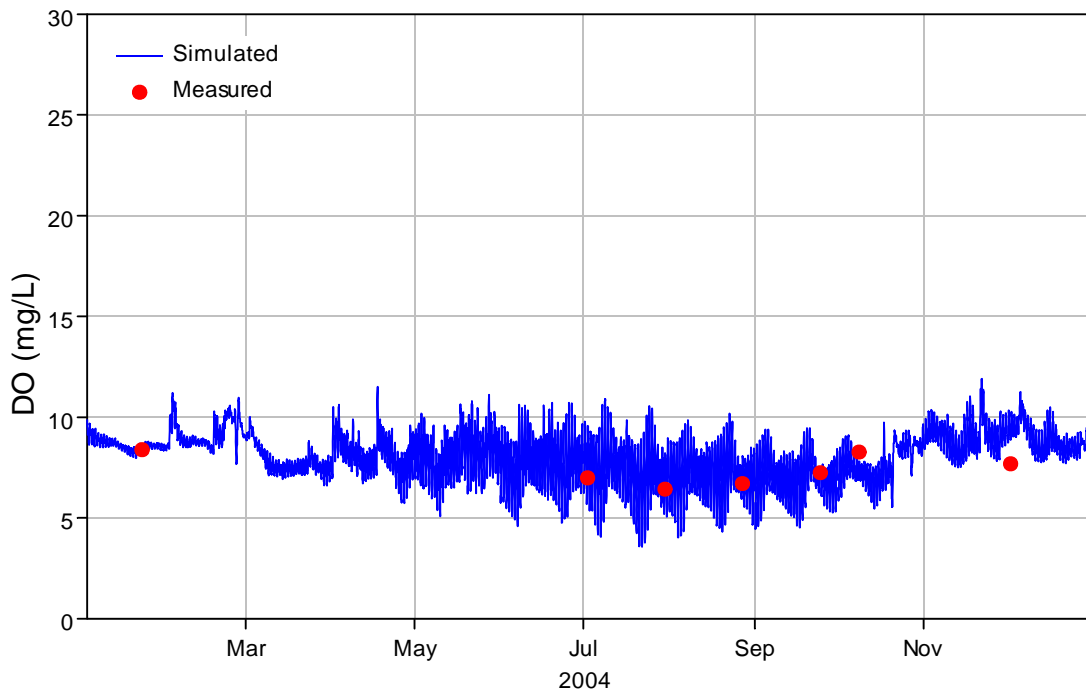


Figure 5-55 Comparison of computed DO concentrations with the measured data at UNBSDC in 2004.

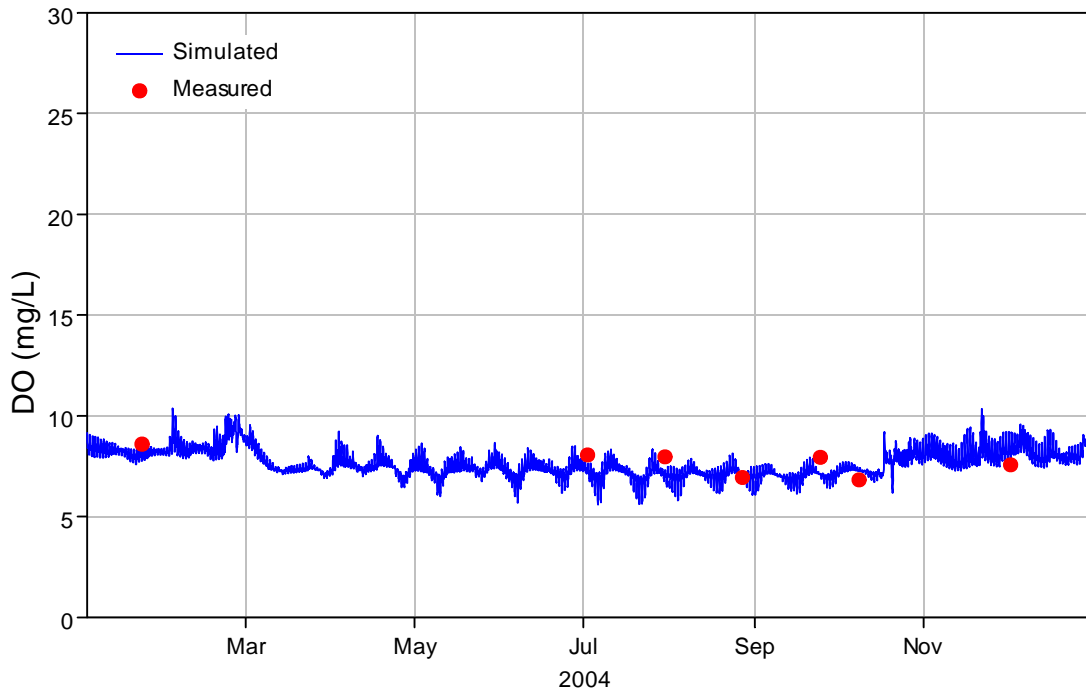


Figure 5-56 Comparison of computed DO concentrations with the measured data at UNBNSB in 2004.

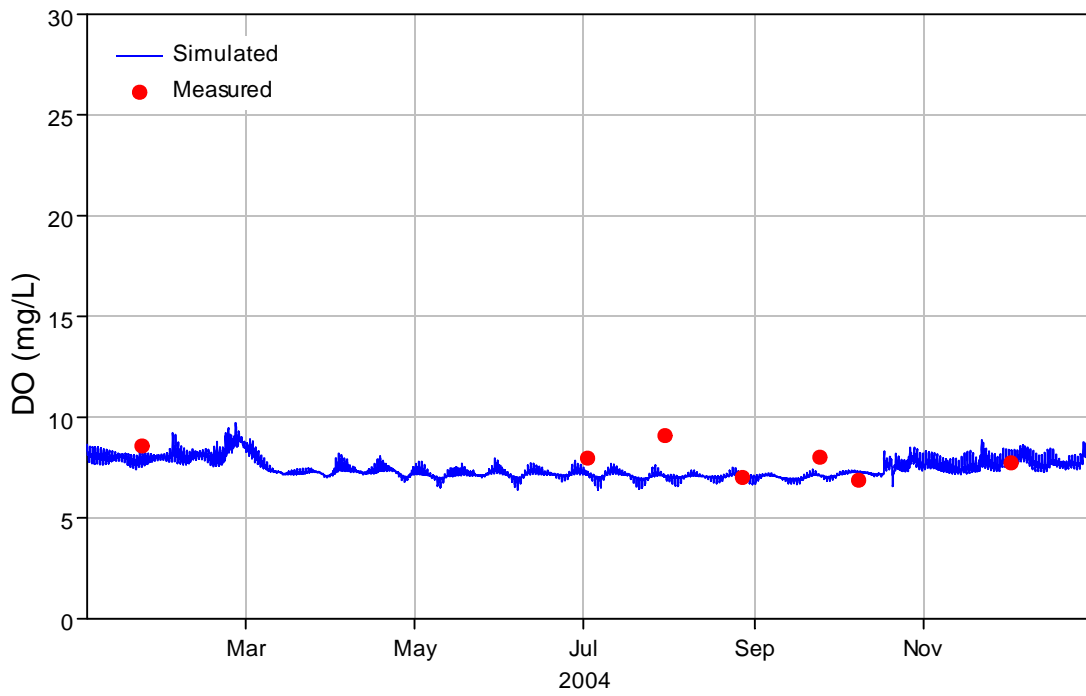


Figure 5-57 Comparison of computed DO concentrations with the measured data at UNBCHB in 2004.

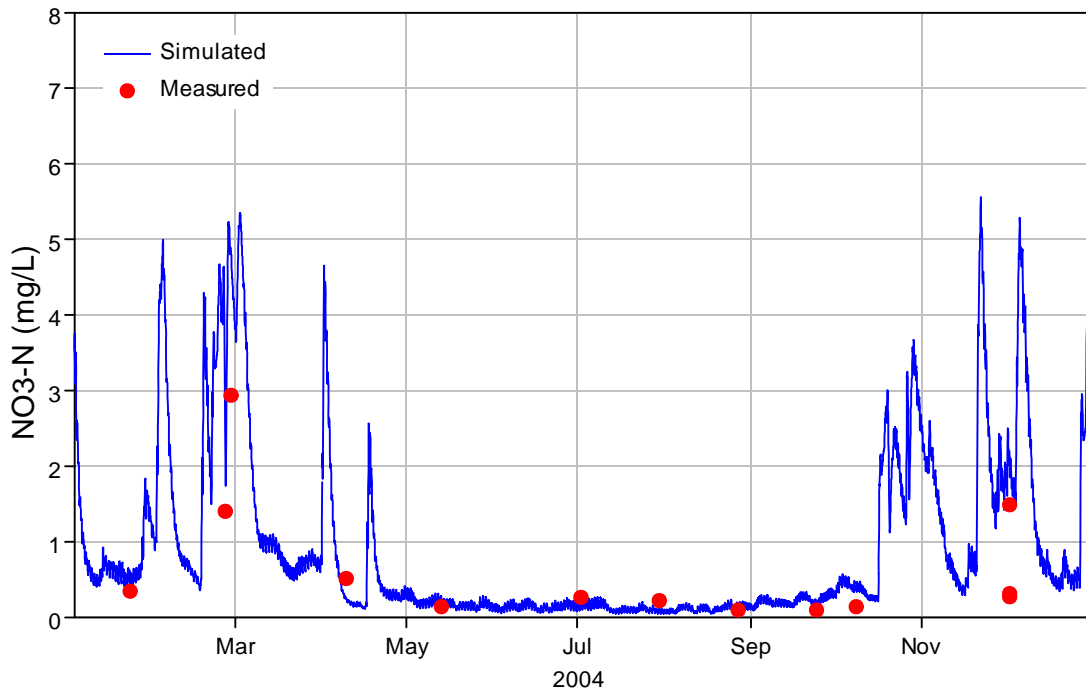


Figure 5-58 Comparison of computed NO₃ concentrations with the measured data at UNBJAM in 2004.

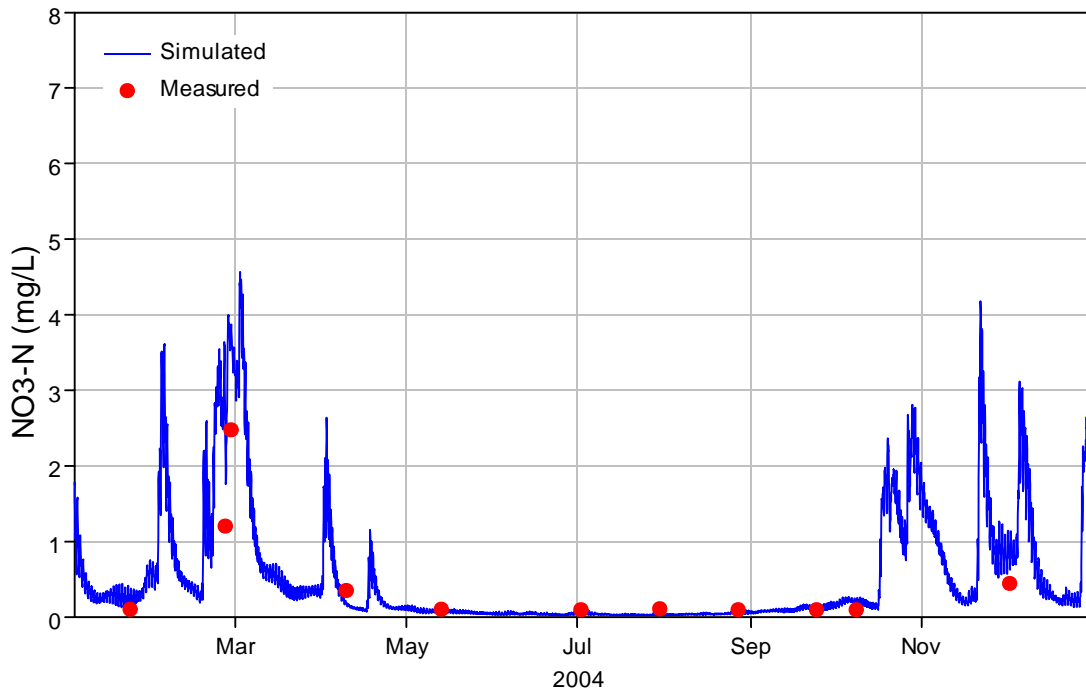


Figure 5-59 Comparison of computed NO₃ concentrations with the measured data at UNBSDC in 2004.

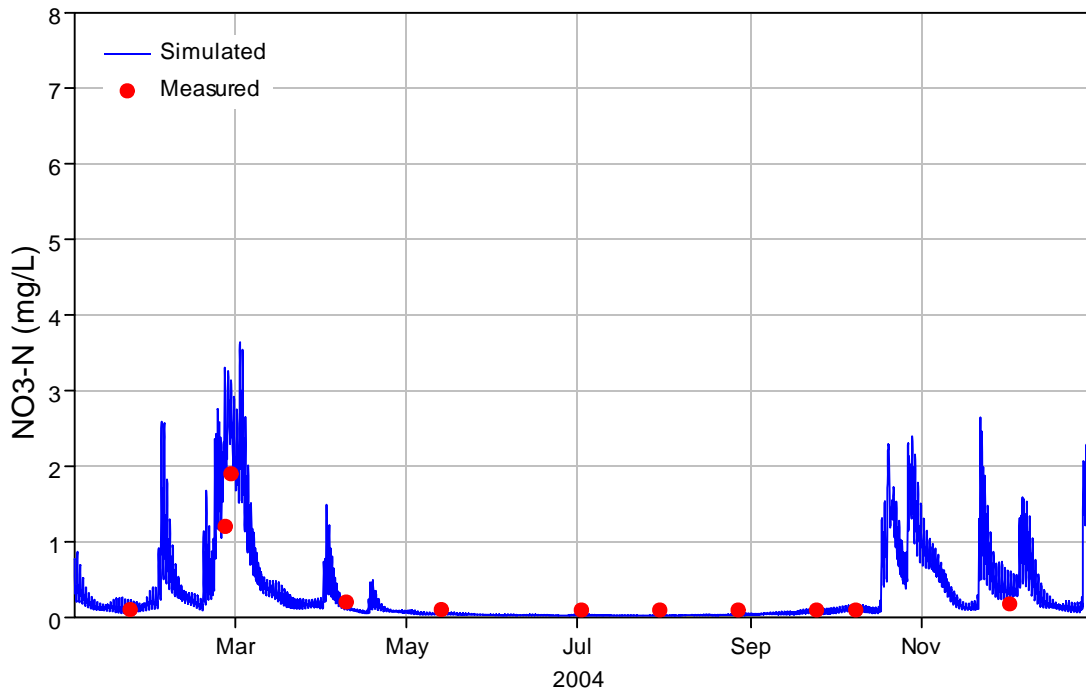


Figure 5-60 Comparison of computed NO3 concentrations with the measured data at UNBNSB in 2004.

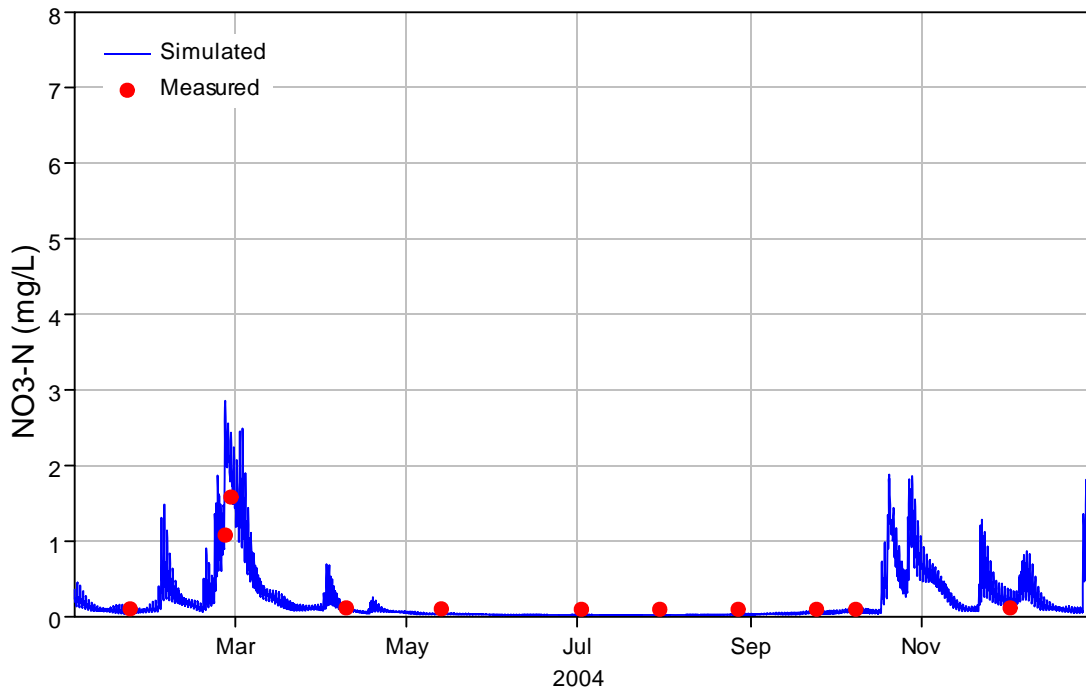


Figure 5-61 Comparison of computed NO3 concentrations with the measured data at UNBCHB in 2004.

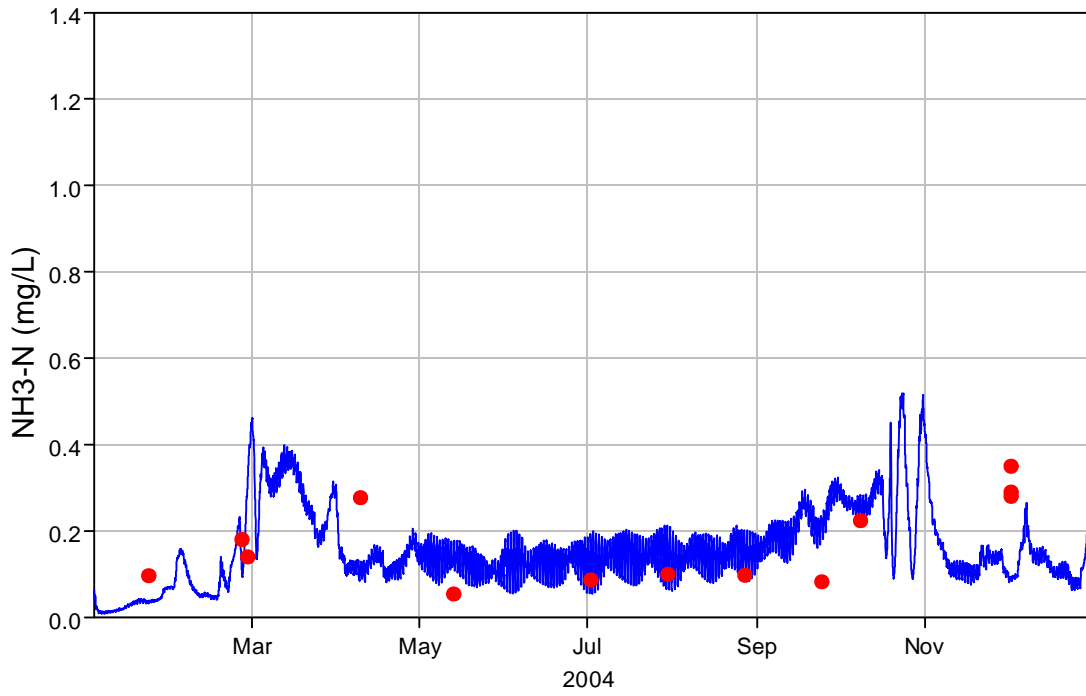


Figure 5-62 Comparison of computed NH3 concentrations with the measured data at UNBJAM in 2004.

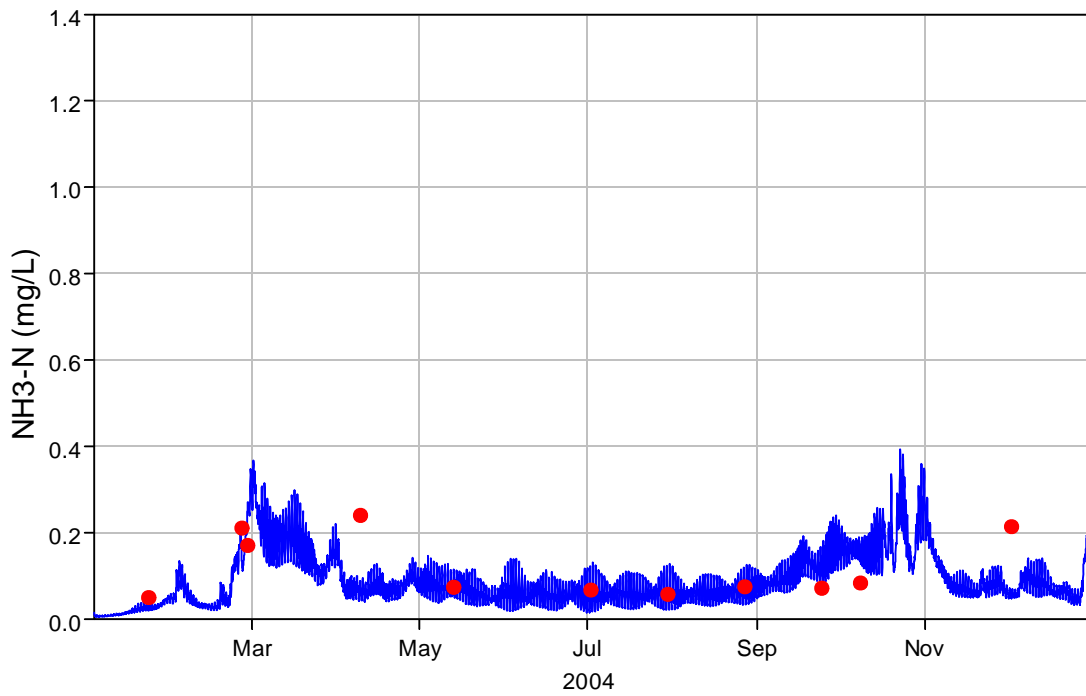


Figure 5-63 Comparison of computed NH3 concentrations with the measured data at UNBSDC in 2004.

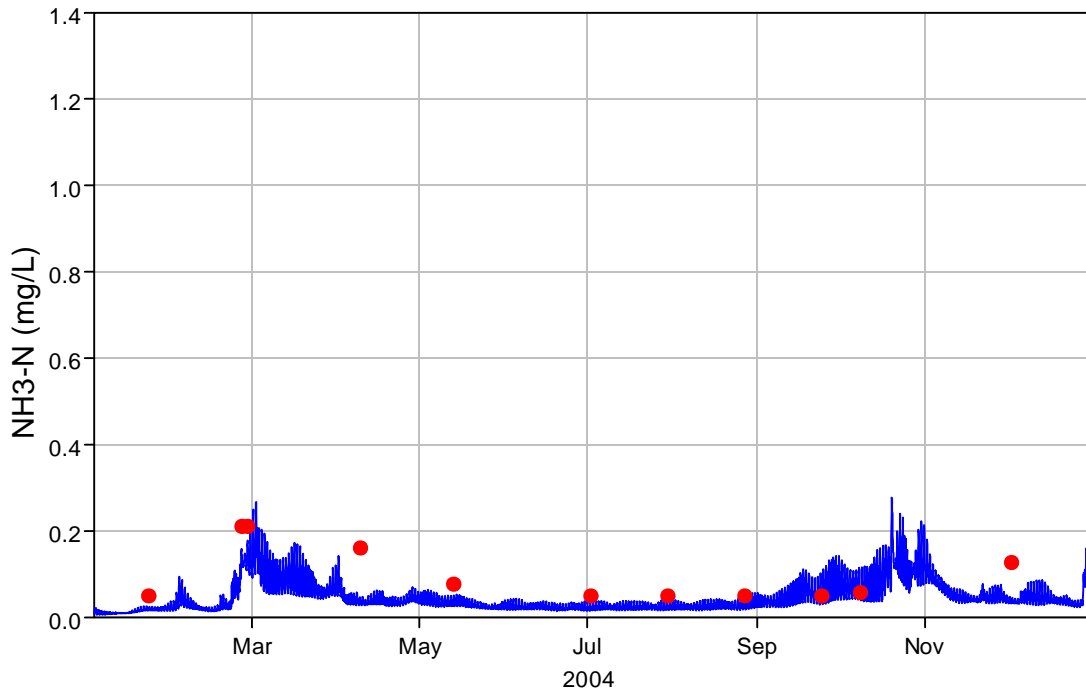


Figure 5-64 Comparison of computed NH3 concentrations with the measured data at UNBNSB in 2004.

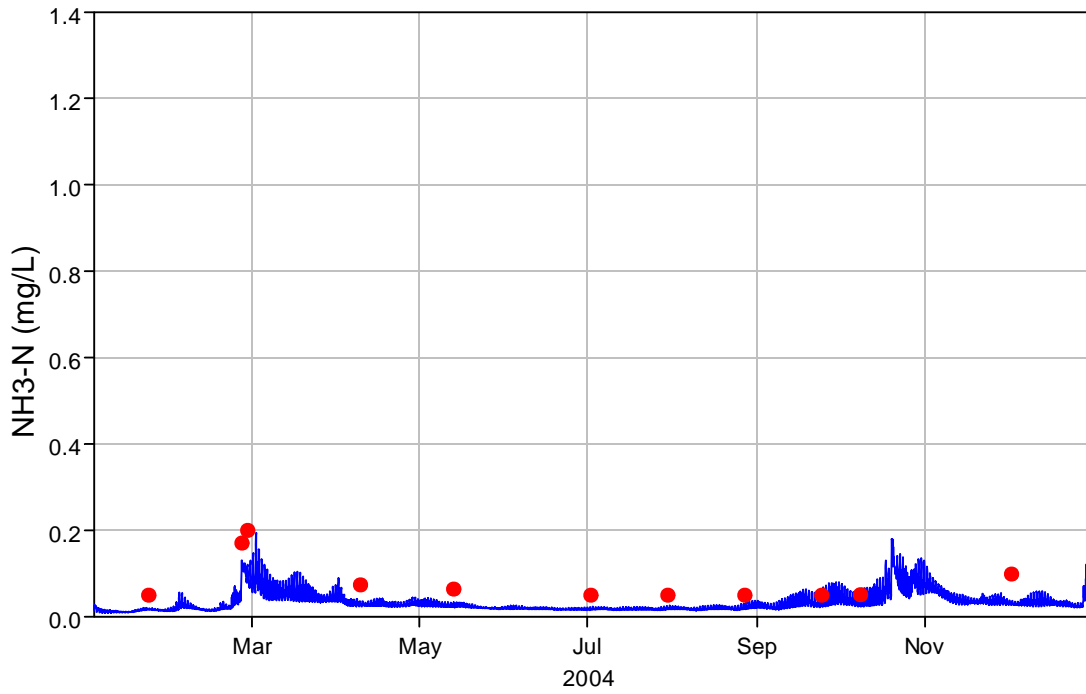


Figure 5-65 Comparison of computed NH3 concentrations with the measured data at UNBCHB in 2004.

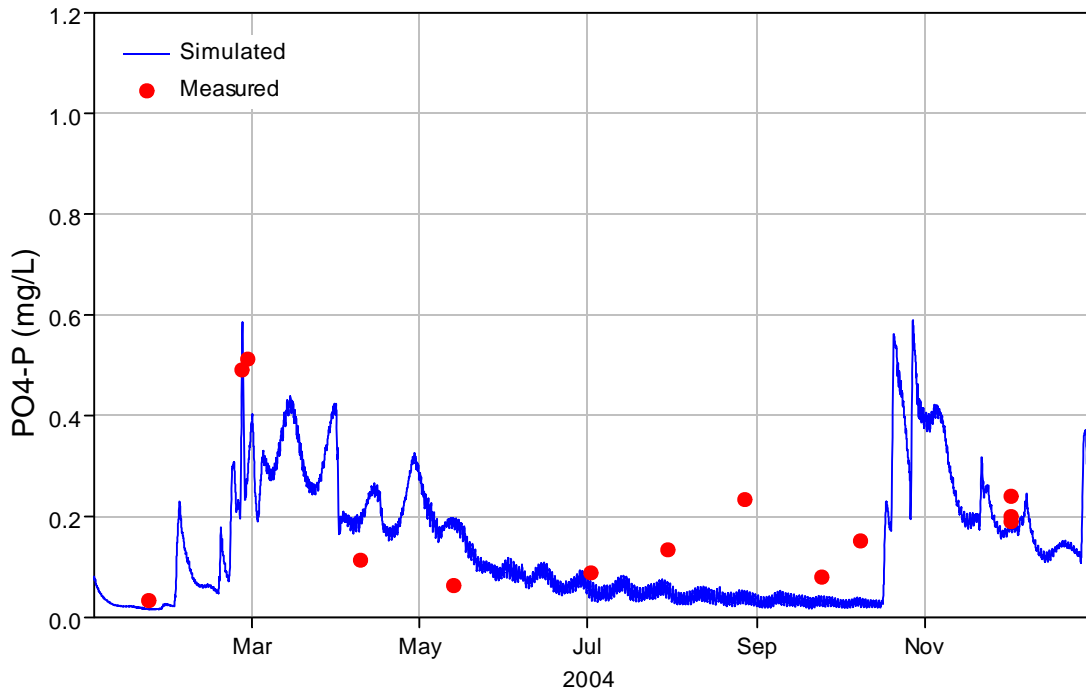


Figure 5-66 Comparison of computed PO4 concentrations with the measured data at UNBJAM in 2004.

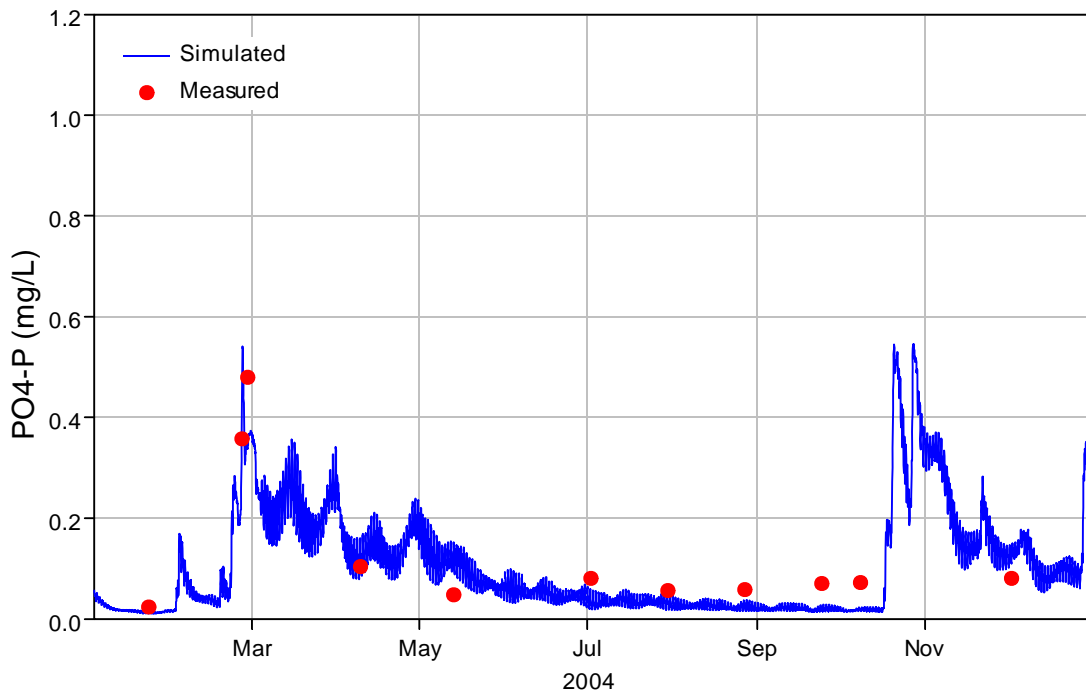


Figure 5-67 Comparison of computed PO4 concentrations with the measured data at UNBSDC in 2004.

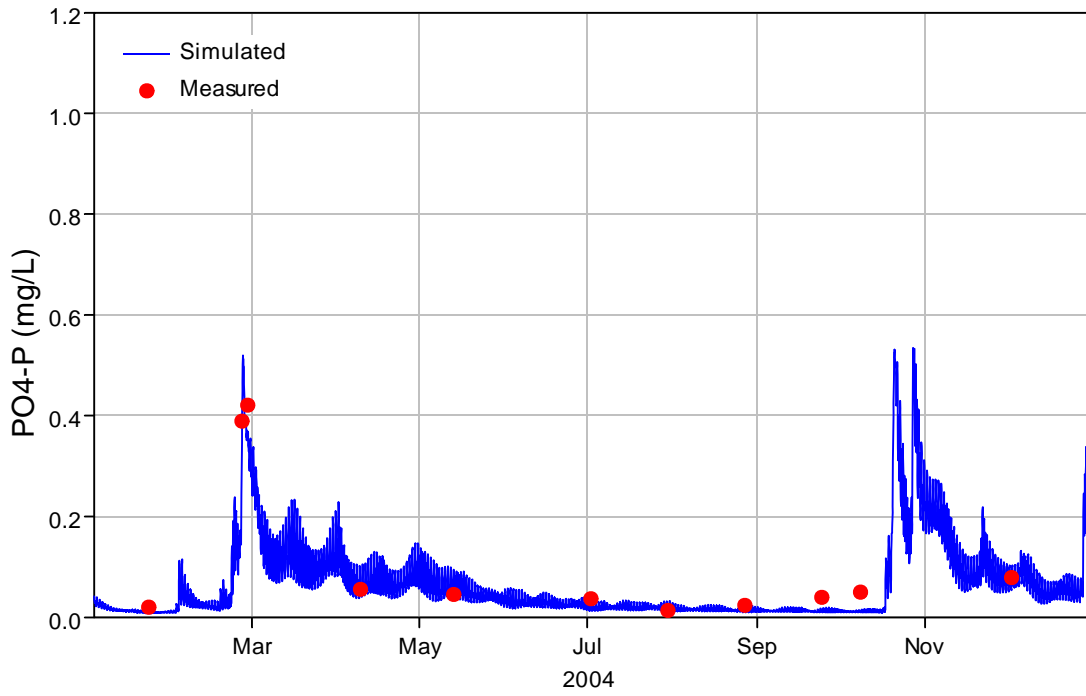


Figure 5-68 Comparison of computed PO4 concentrations with the measured data at UNBNSB in 2004.

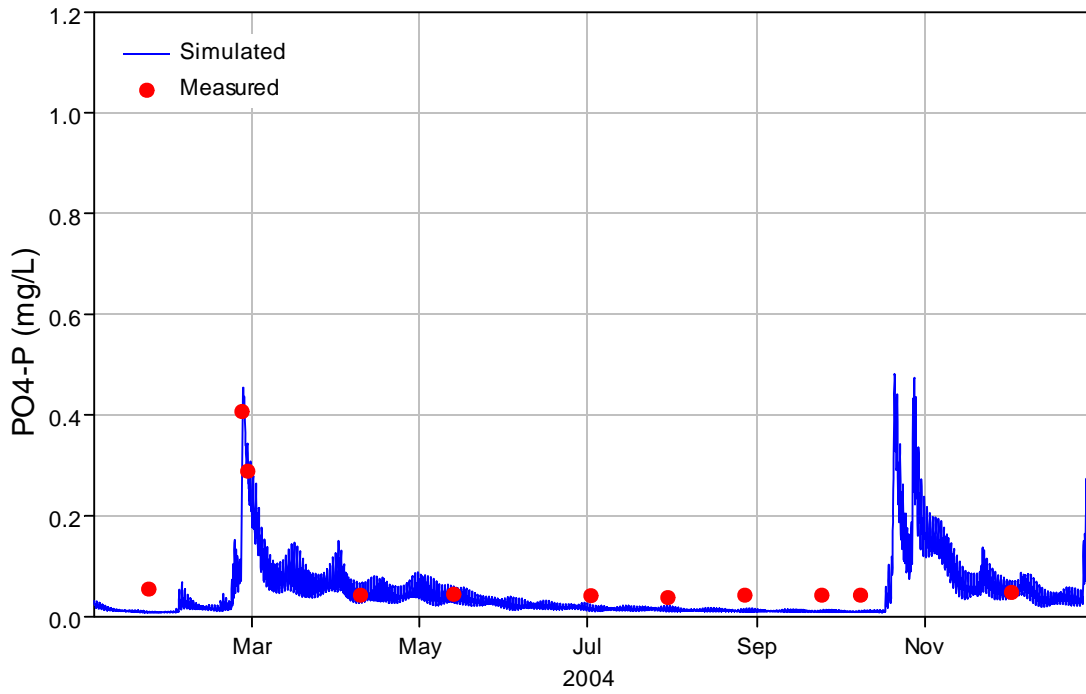


Figure 5-69 Comparison of computed PO4 concentrations with the measured data at UNBCHB in 2004.

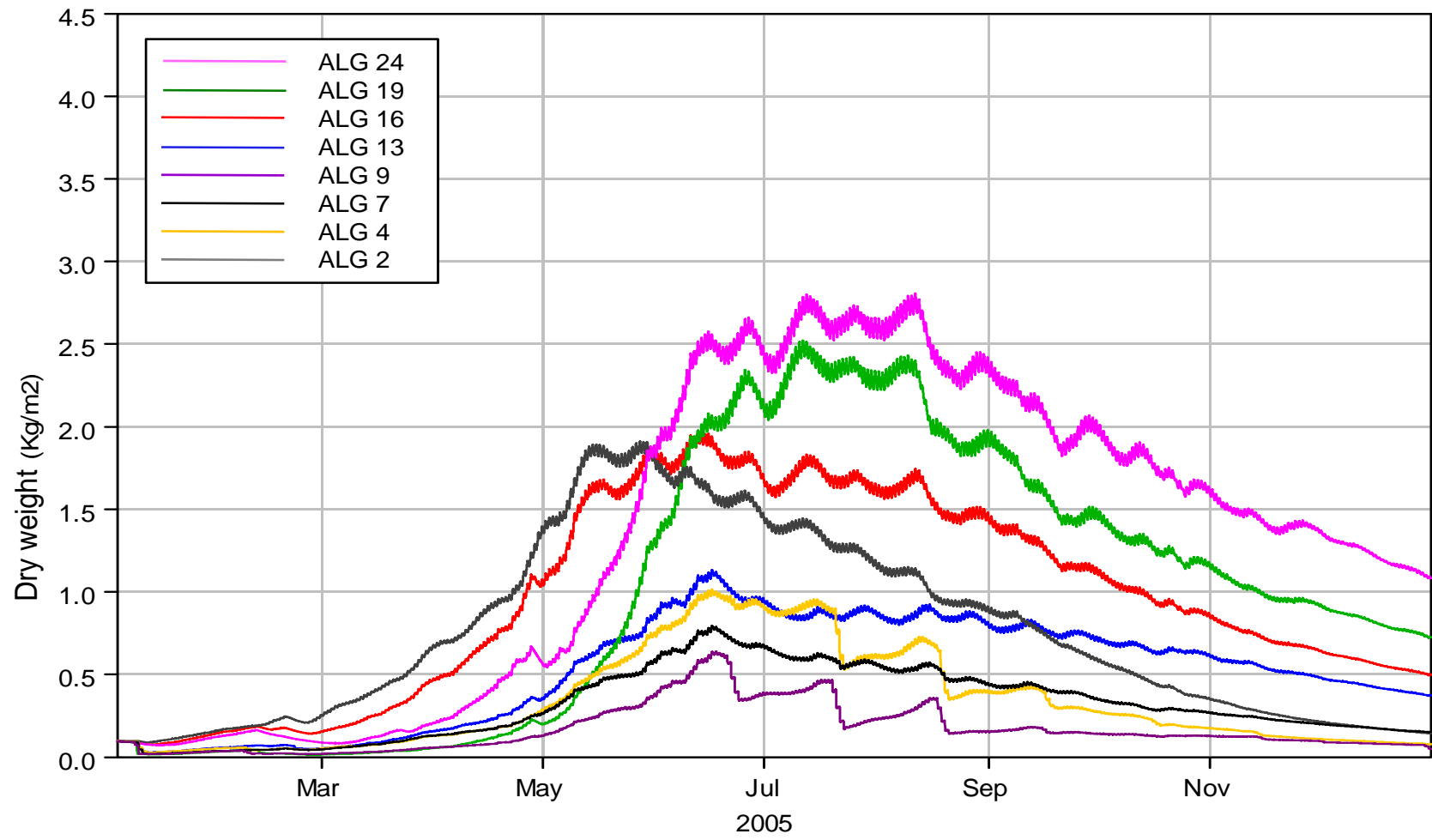


Figure 5-70 Comparison of computed macroalgae concentrations at sampling sites in 2005.

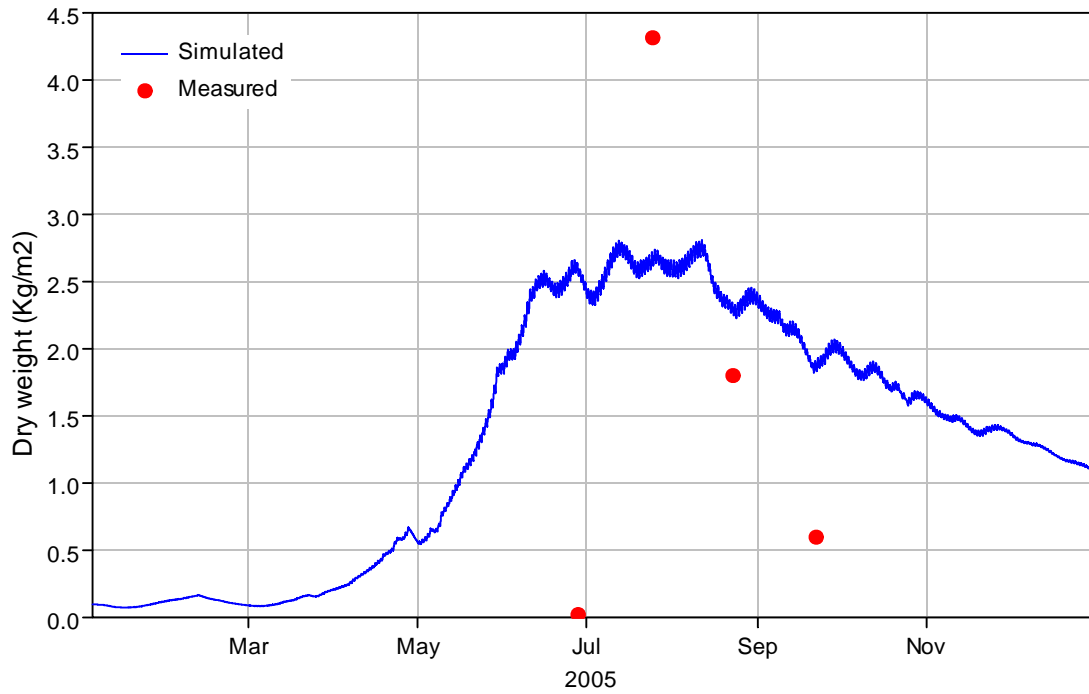


Figure 5-71 Comparison of computed macroalgae concentrations with the measured data at ALG24 in 2005.

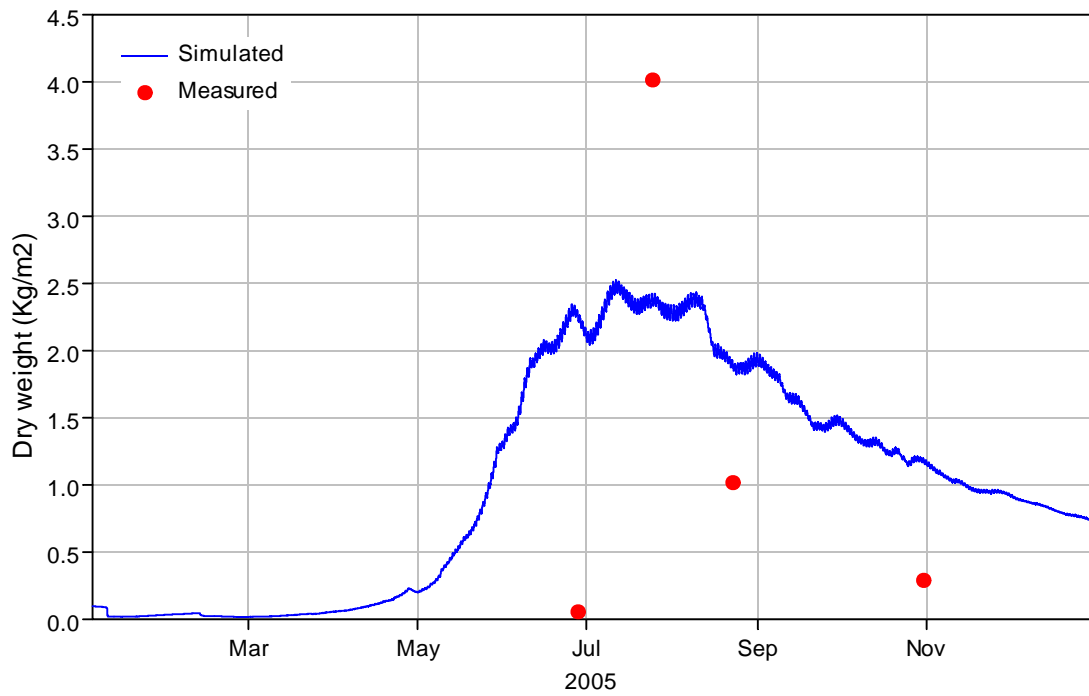


Figure 5-72 Comparison of computed macroalgae concentrations with the measured data at ALG19 in 2005.

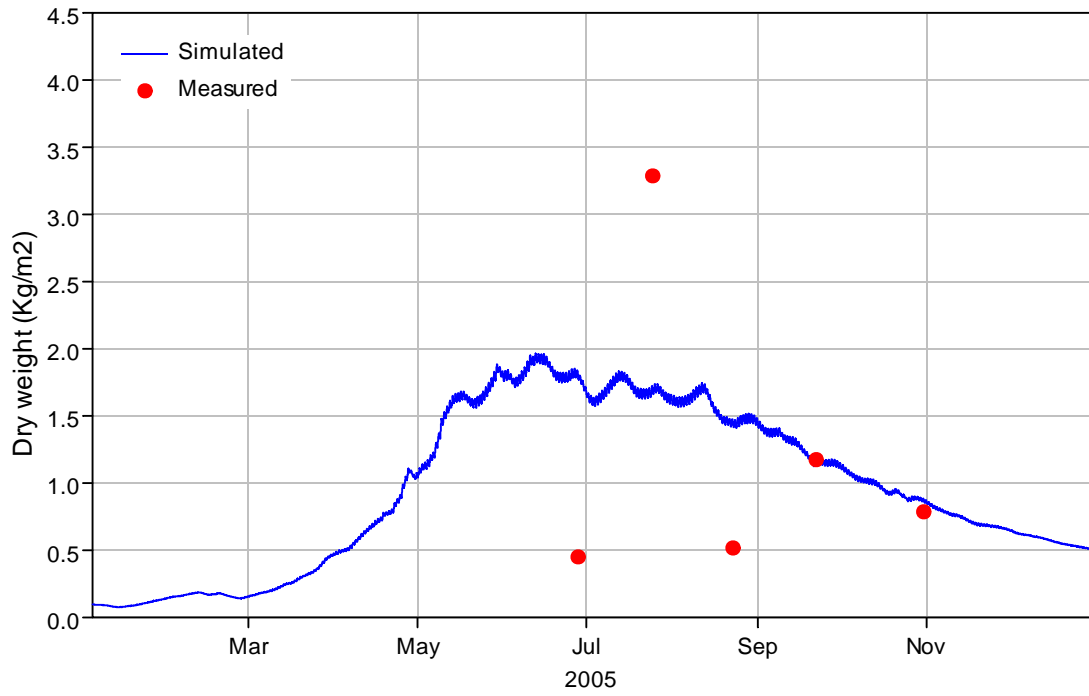


Figure 5-73 Comparison of computed macroalgae concentrations with the measured data at ALG16 in 2005.

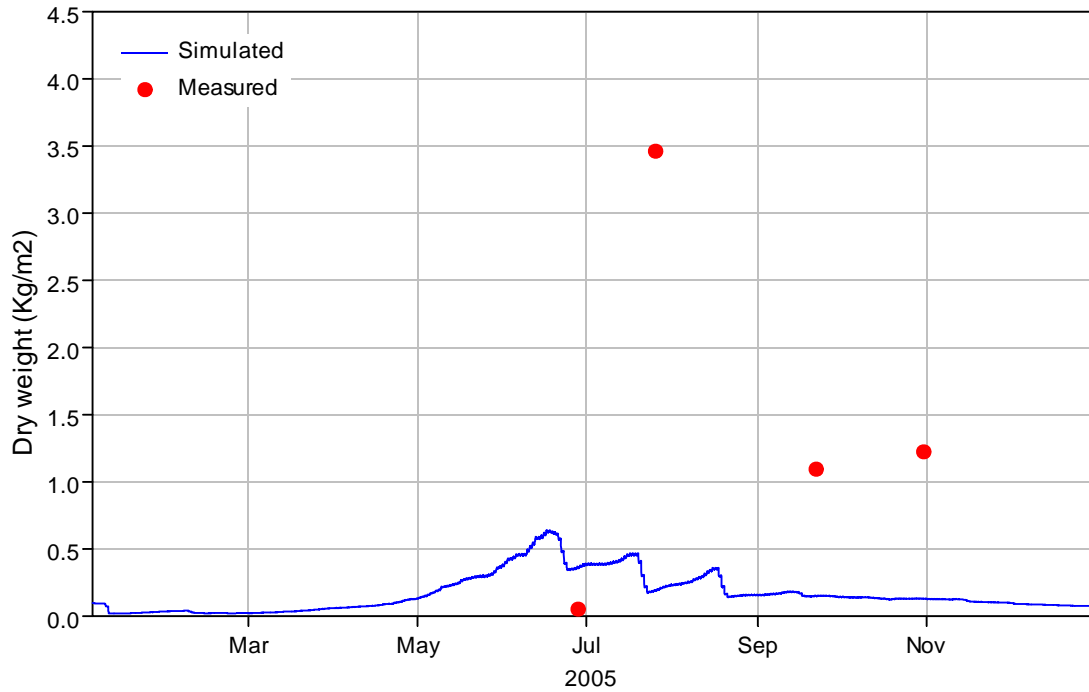


Figure 5-74 Comparison of computed macroalgae concentrations with the measured data at ALG9 in 2005.

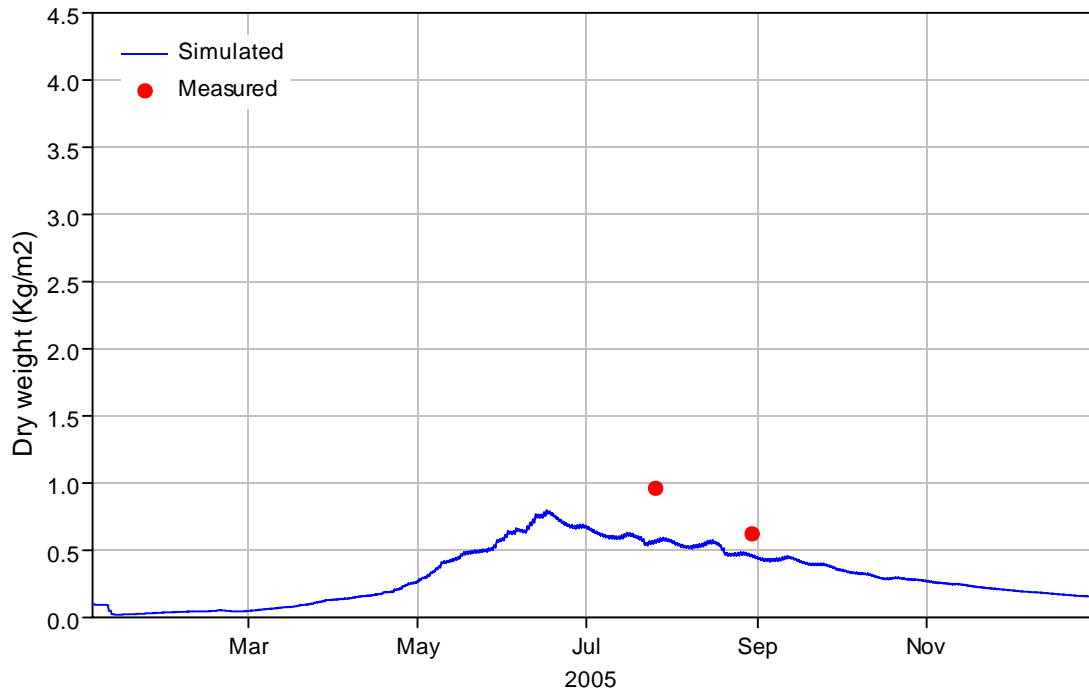


Figure 5-75 Comparison of computed macroalgae concentrations with the measured data at ALG7 in 2005.

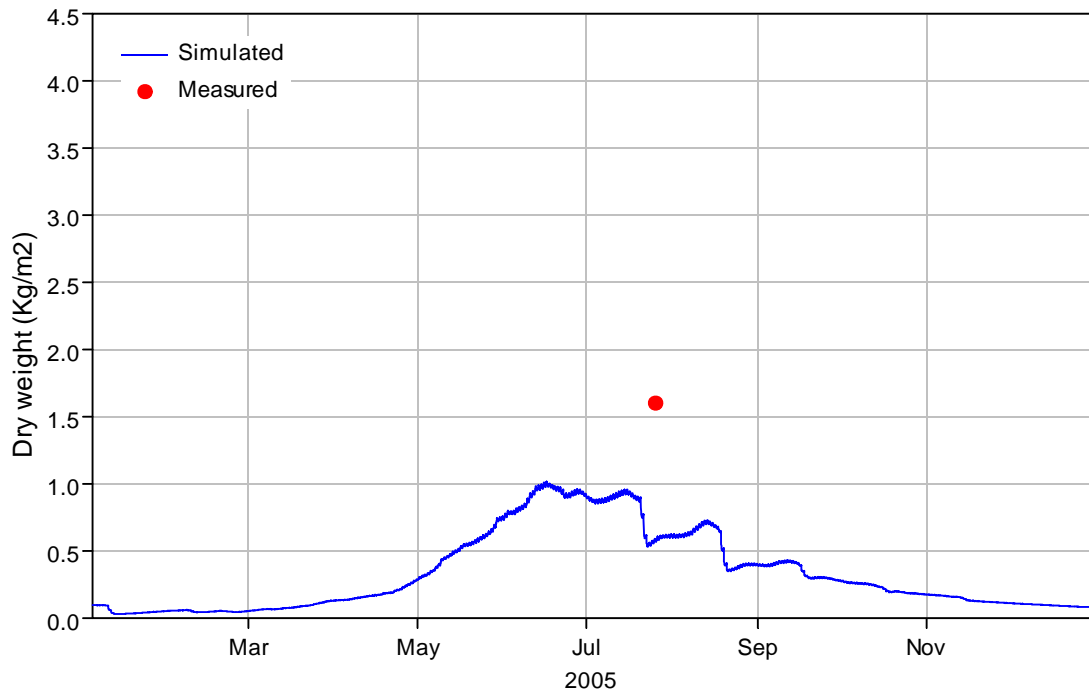


Figure 5-76 Comparison of computed macroalgae concentrations with the measured data at ALG4 in 2005.

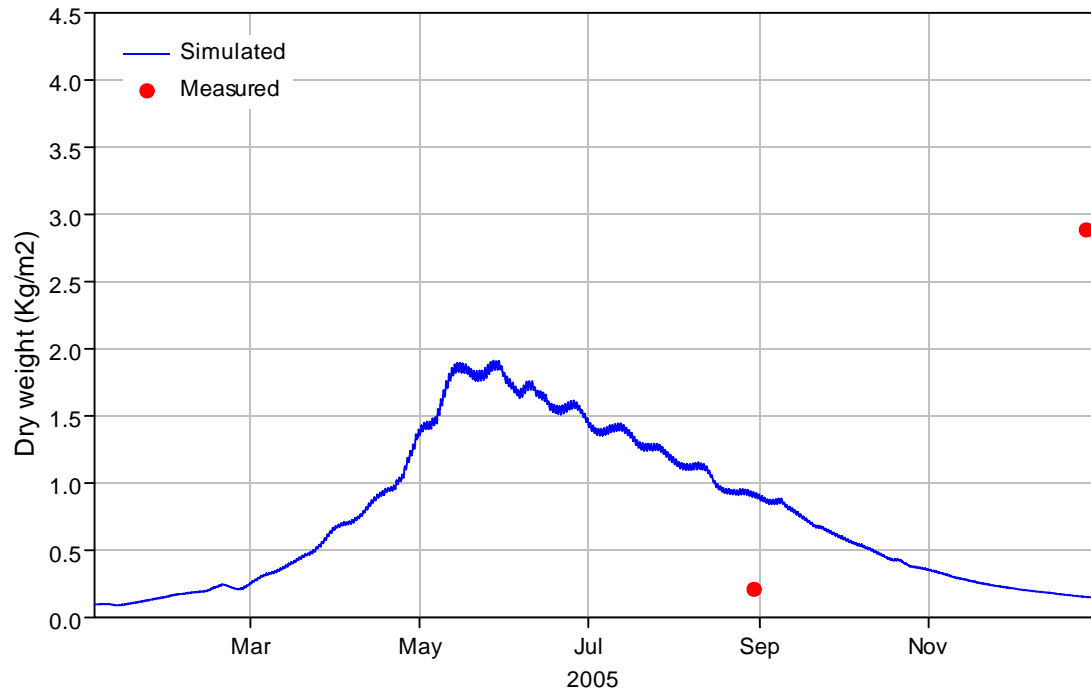


Figure 5-77 Comparison of computed macroalgae concentrations with the measured data at ALG2 in 2005.

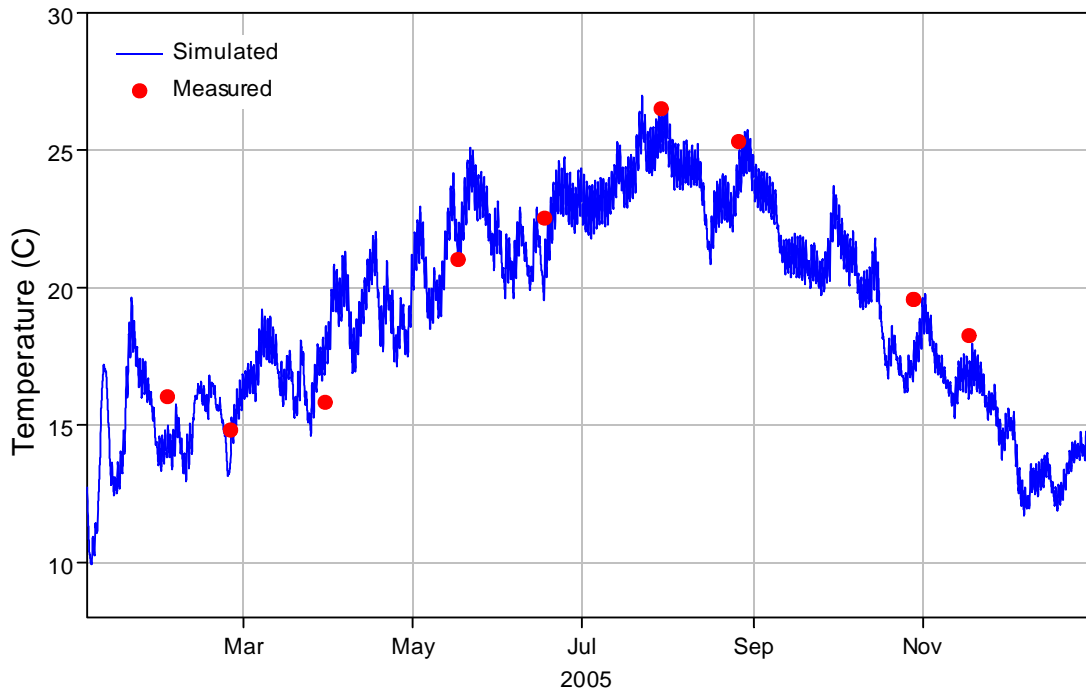


Figure 5-78 Comparison of computed temperature (°C) with the measured data at UNBJAM in 2005.

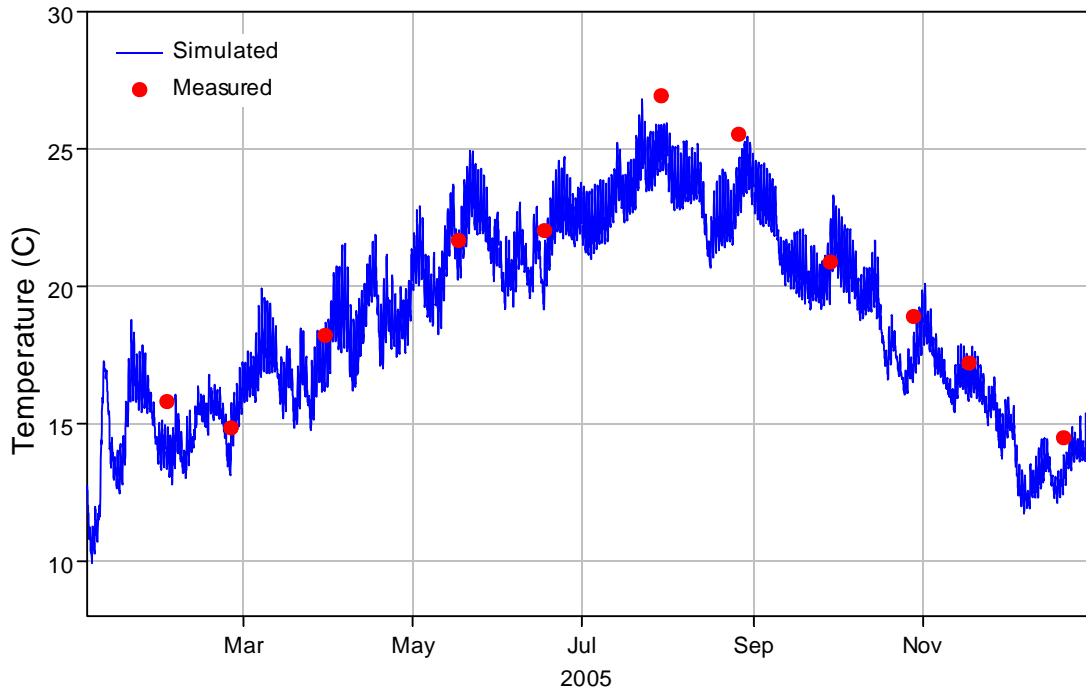


Figure 5-79 Comparison of computed temperature (°C) with the measured data at UNBSDC in 2005.

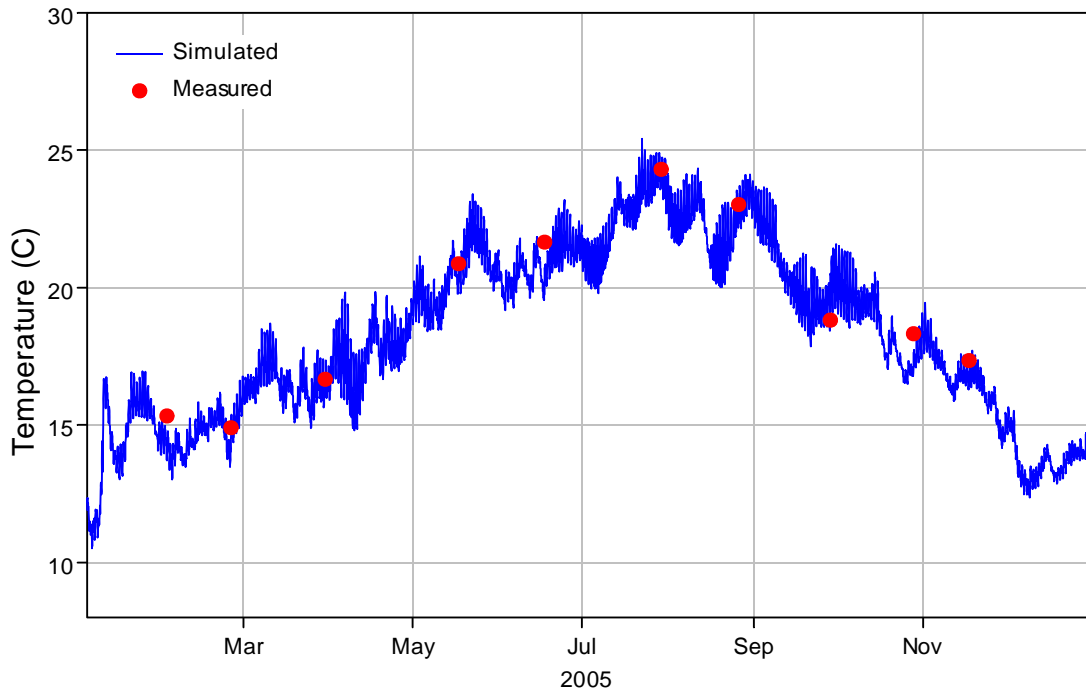


Figure 5-80 Comparison of computed temperature (°C) with the measured data at UNBNSB in 2005.

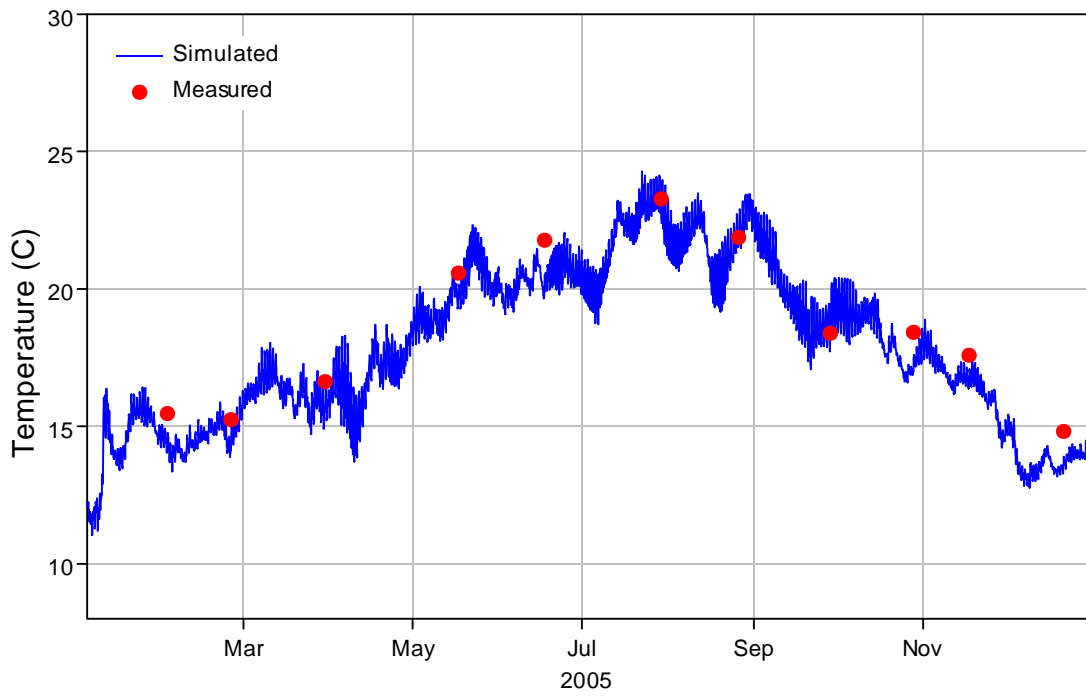


Figure 5-81 Comparison of computed temperature (°C) with the measured data at UNBCHB in 2005.



Figure 5-82 Location of continuous water quality measurements in Upper Newport Bay during 2005. Surface and bottom measurements are available for each station: one 0.5 m from the surface and one 0.5 m off the bottom.

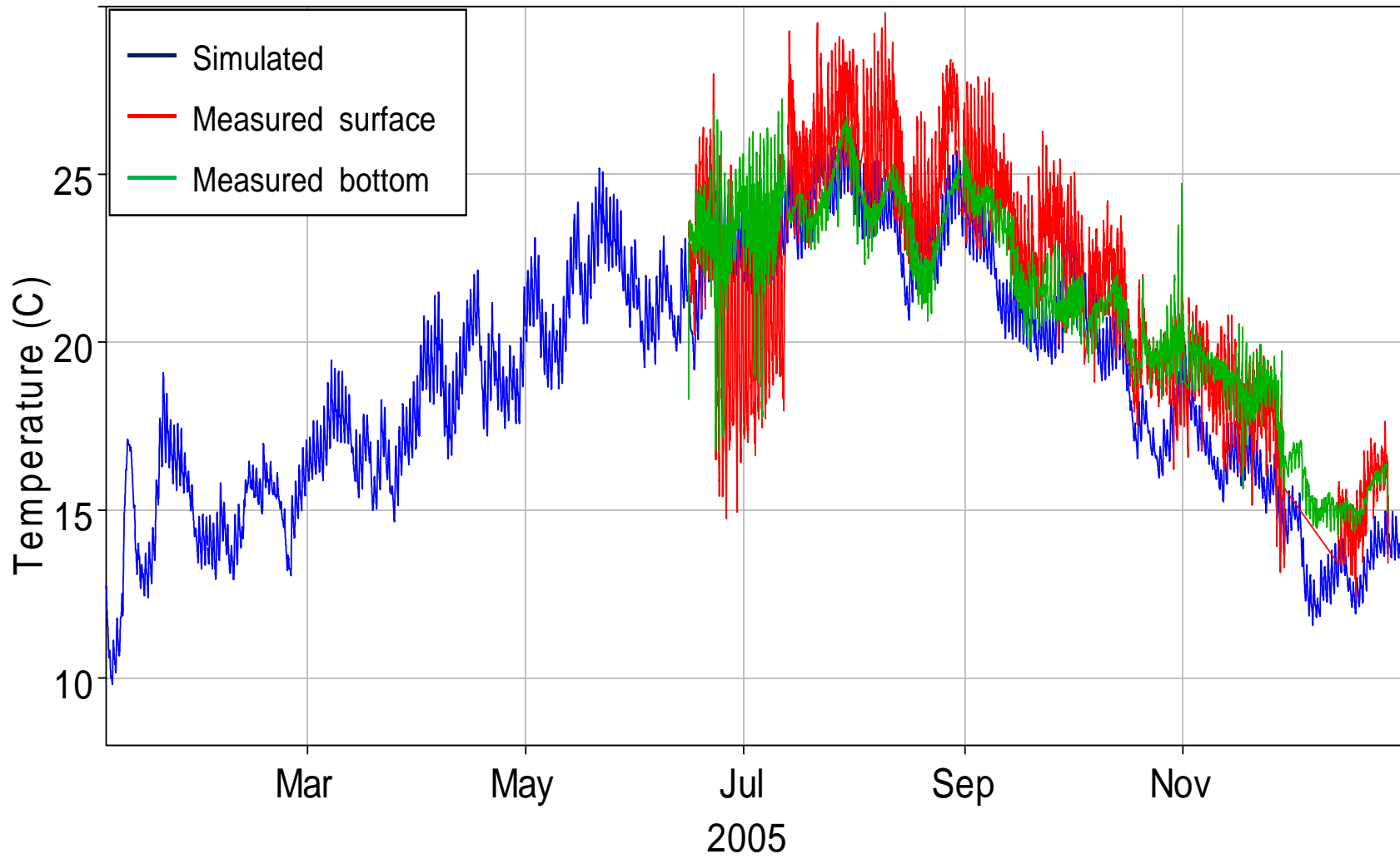


Figure 5-83 Comparison of computed temperature ($^{\circ}\text{C}$) with the measured data at S3 in 2005.

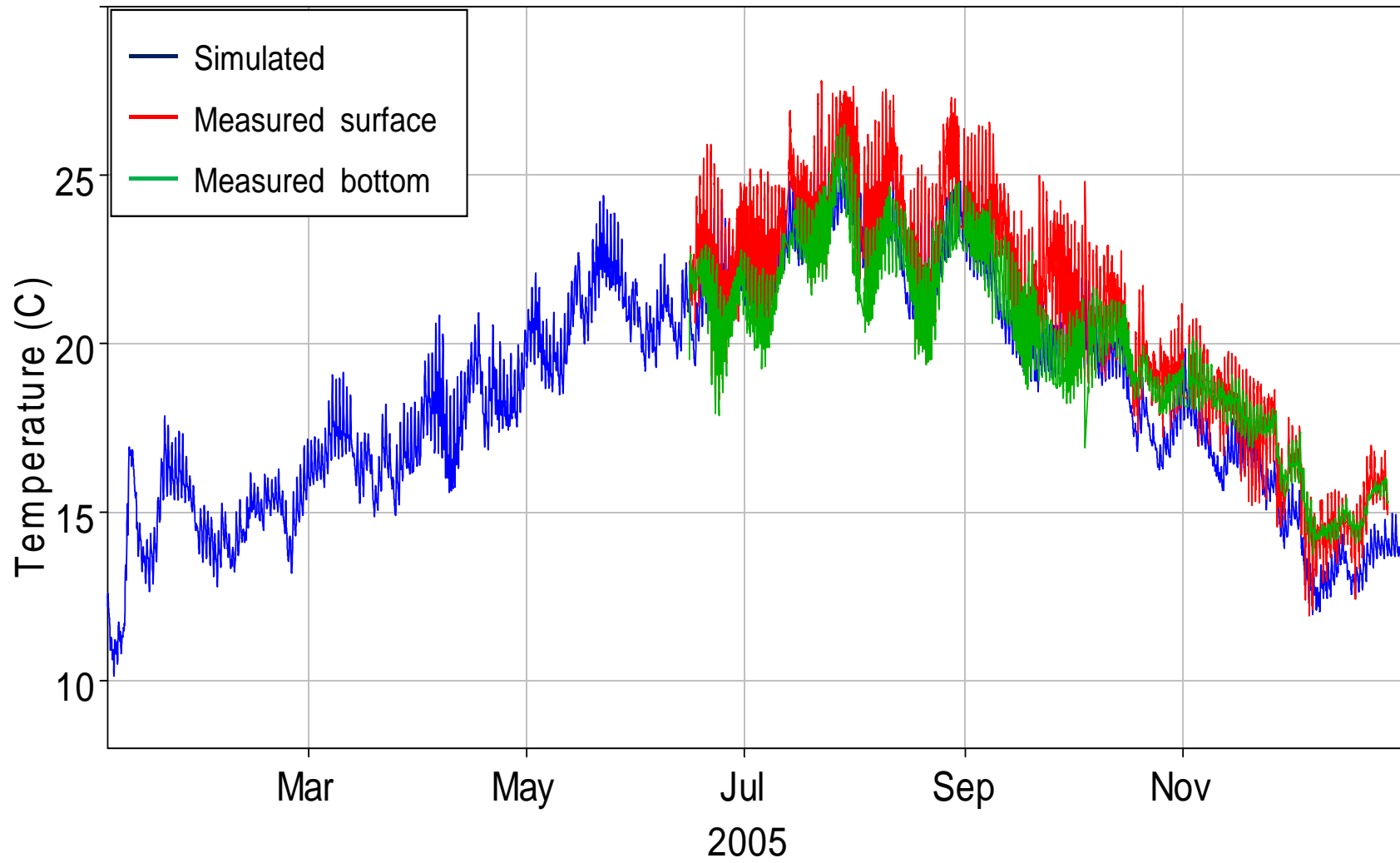


Figure 5-84 Comparison of computed temperature ($^{\circ}\text{C}$) with the measured data at S2 in 2005.

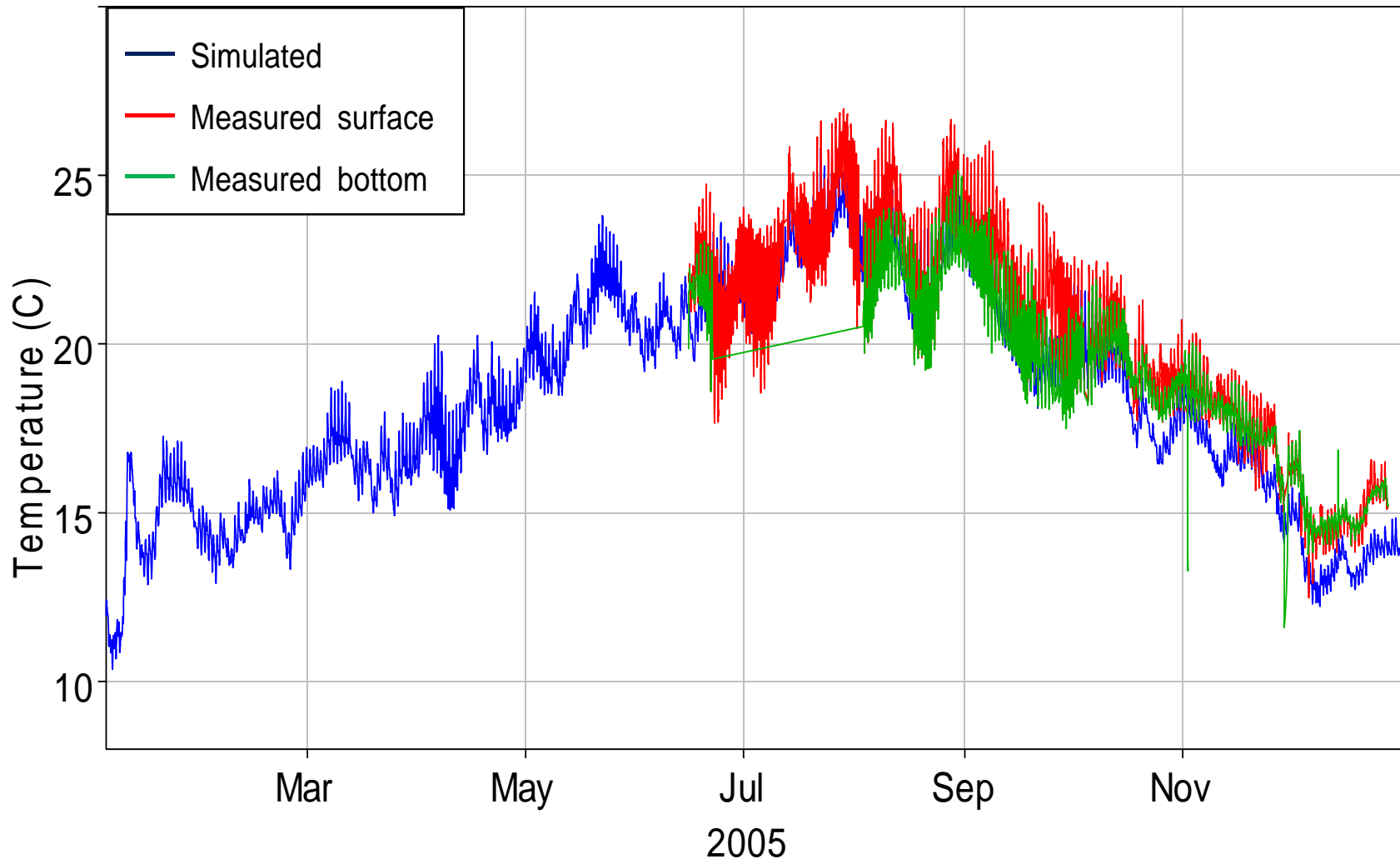


Figure 5-85 Comparison of computed temperature (°C) with the measured data at S1 in 2005.

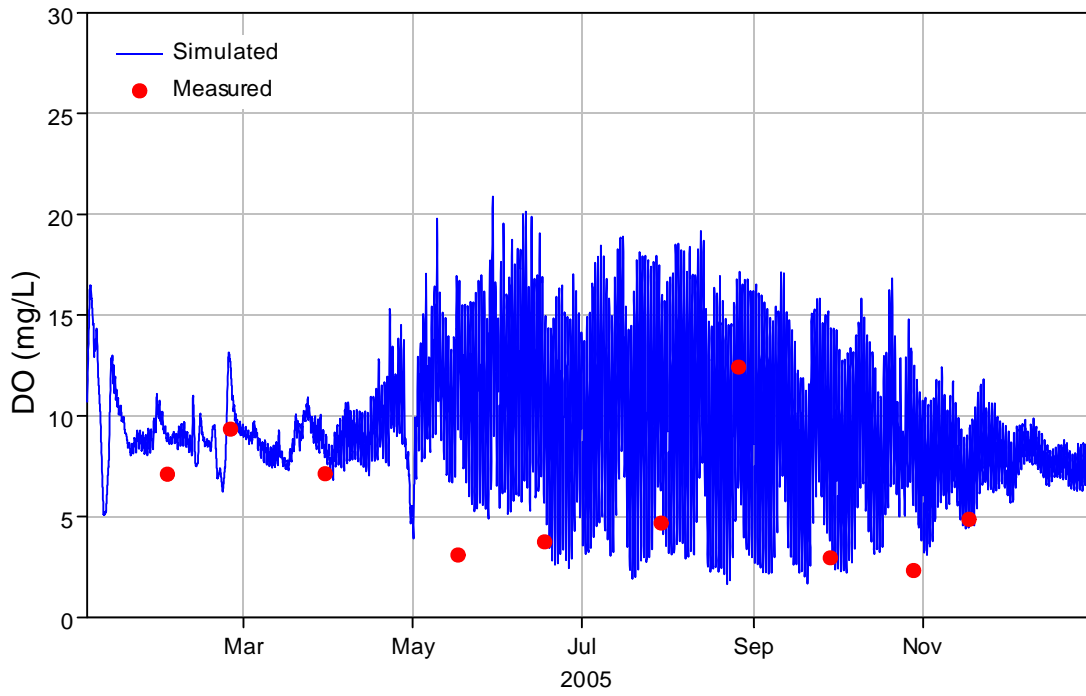


Figure 5-86 Comparison of computed DO concentrations with the measured data at UNBJAM in 2005.

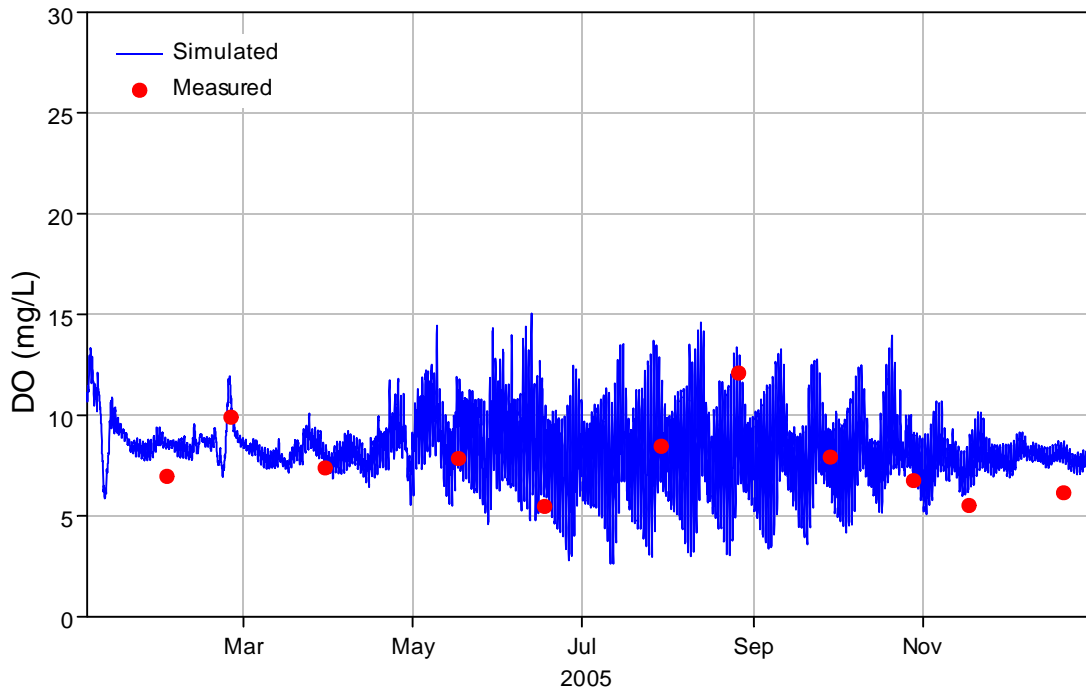


Figure 5-87 Comparison of computed DO concentrations with the measured data at UNBSDC in 2005.

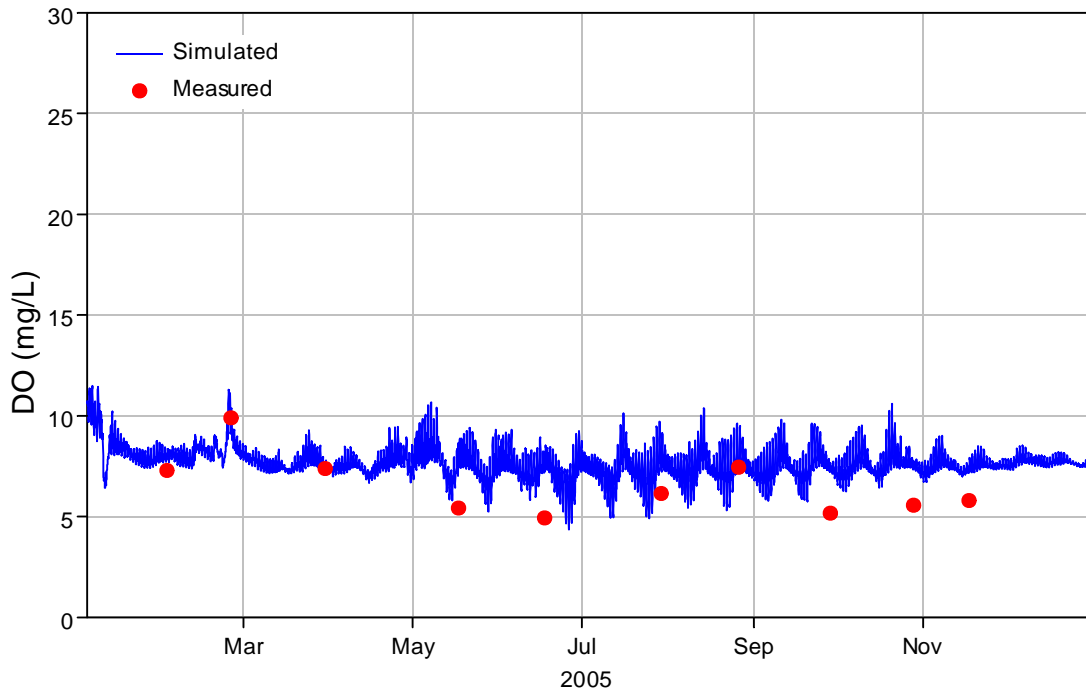


Figure 5-88 Comparison of computed DO concentrations with the measured data at UNBNSB in 2005.

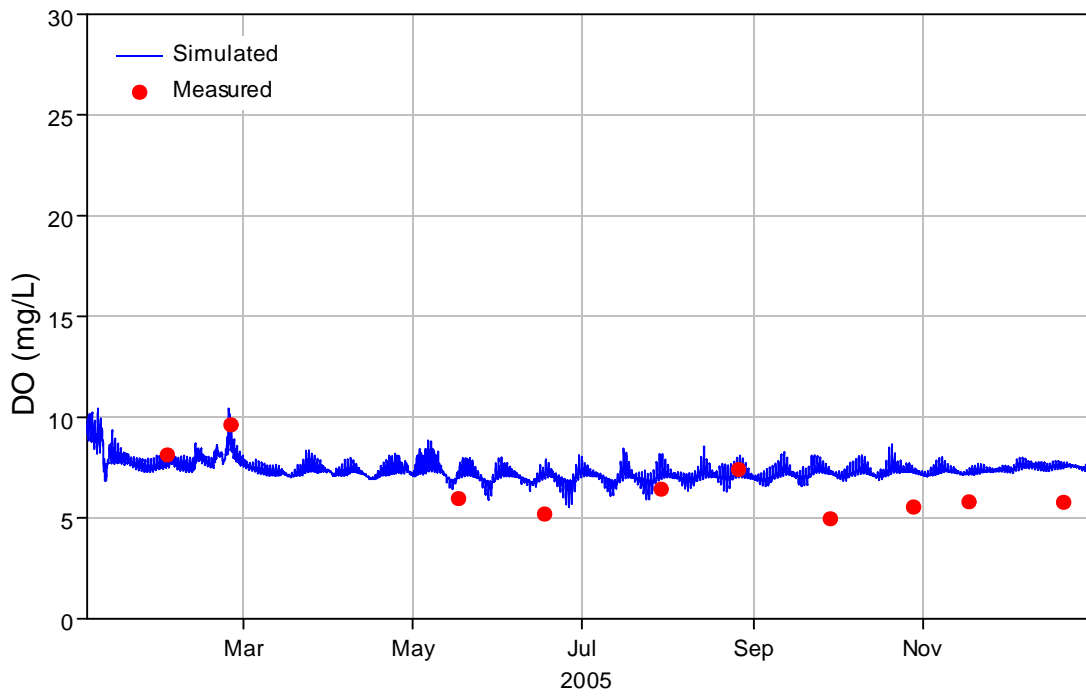


Figure 5-89 Comparison of computed DO concentrations with the measured data at UNBCHB in 2005.

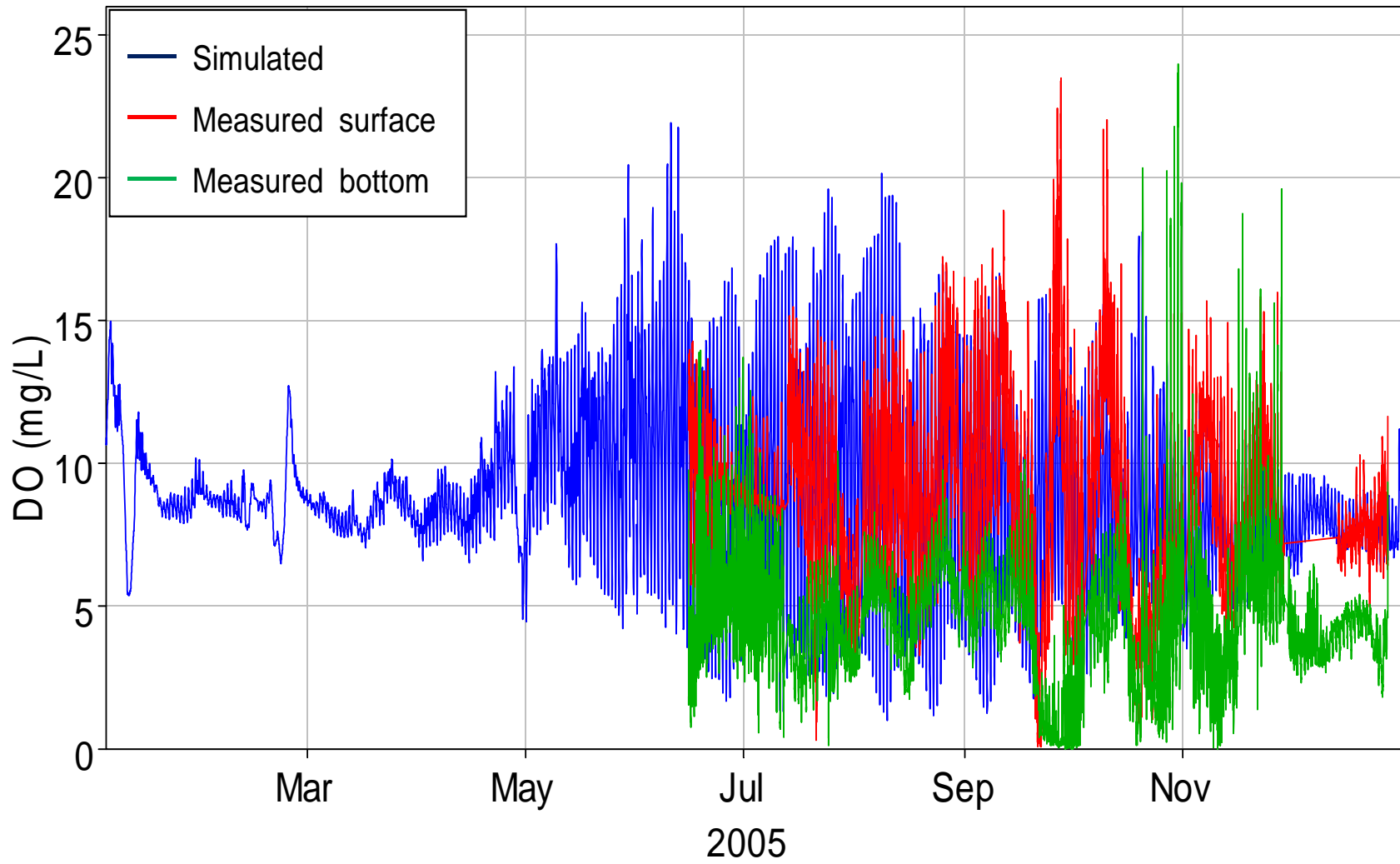


Figure 5-90 Comparison of computed DO concentrations with the measured data at S3 in 2005.

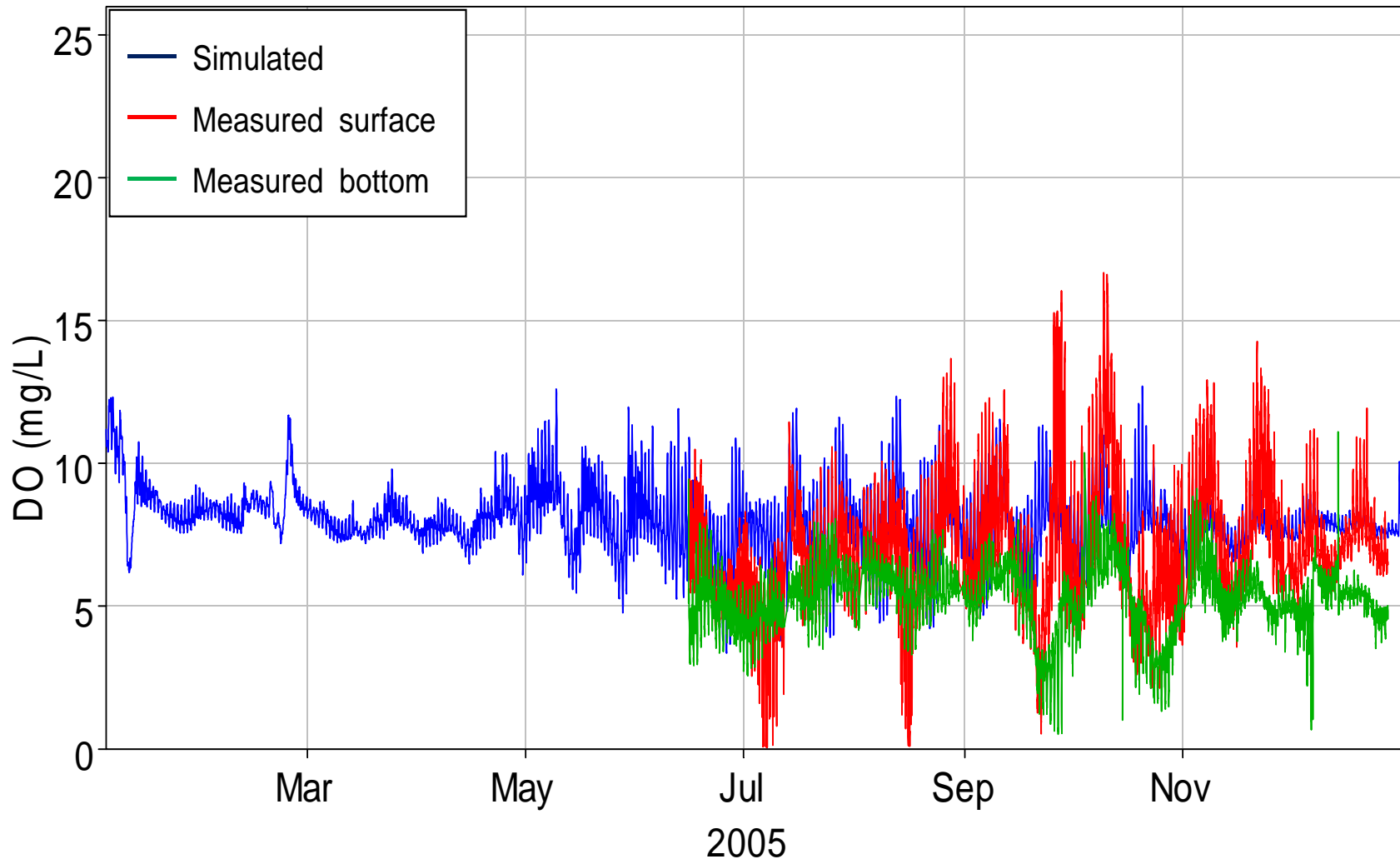


Figure 5-91 Comparison of computed DO concentrations with the measured data at S2 in 2005.

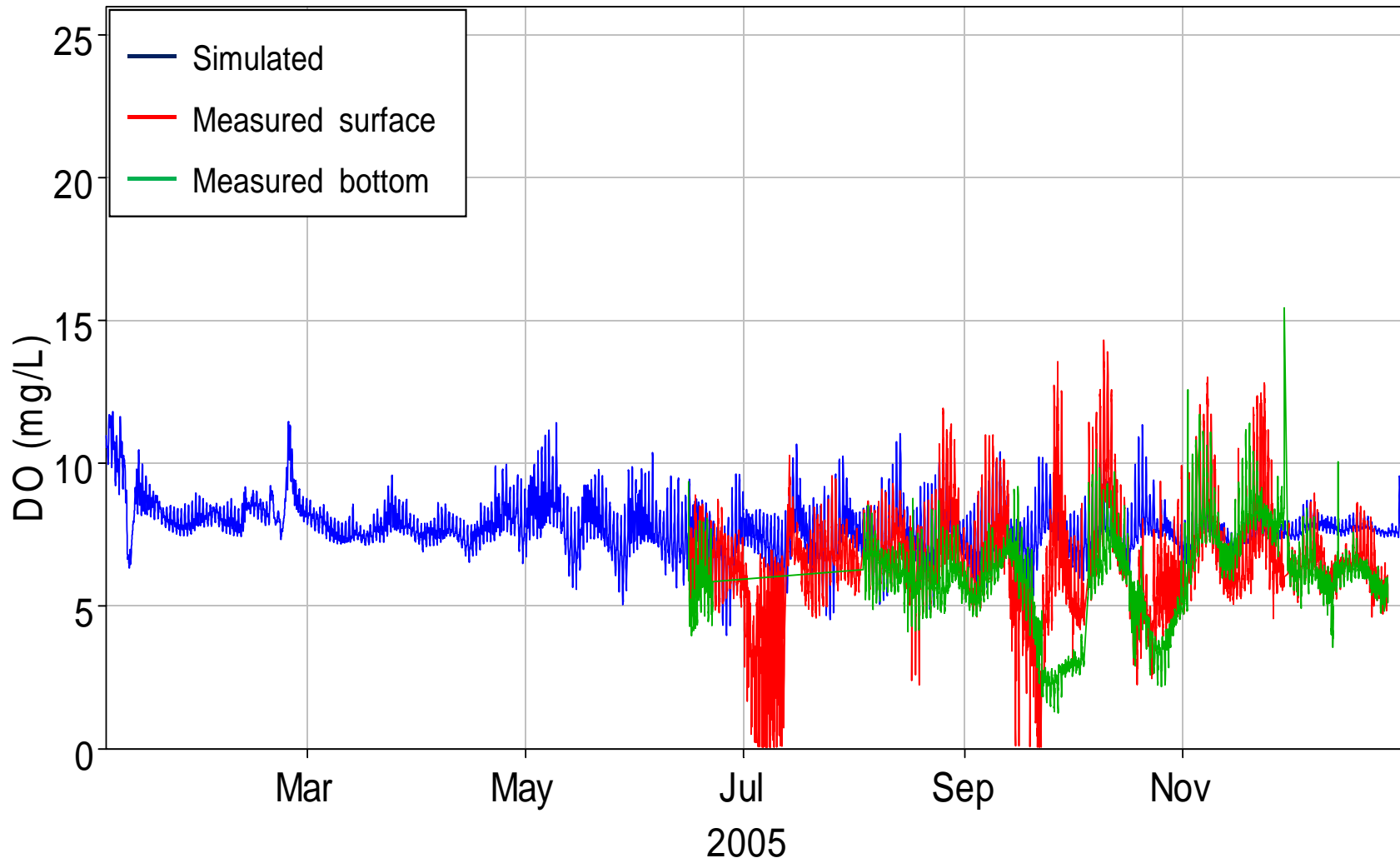


Figure 5-92 Comparison of computed DO concentrations with the measured data at S1 in 2005.

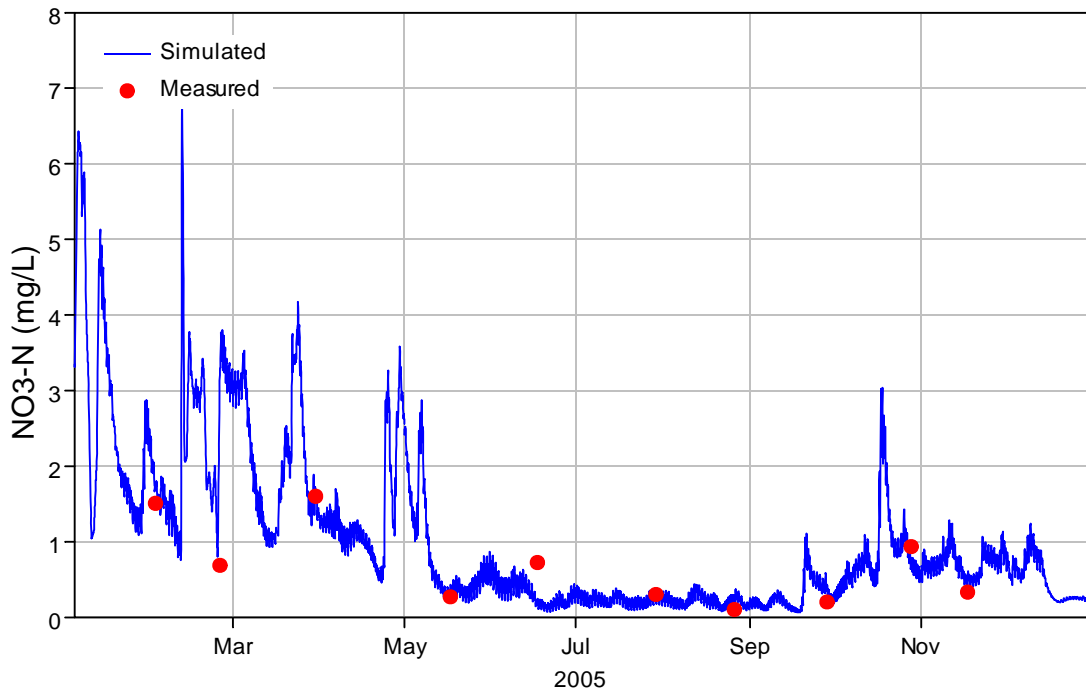


Figure 5-93 Comparison of computed NO₃ concentrations with the measured data at UNBJAM in 2005.

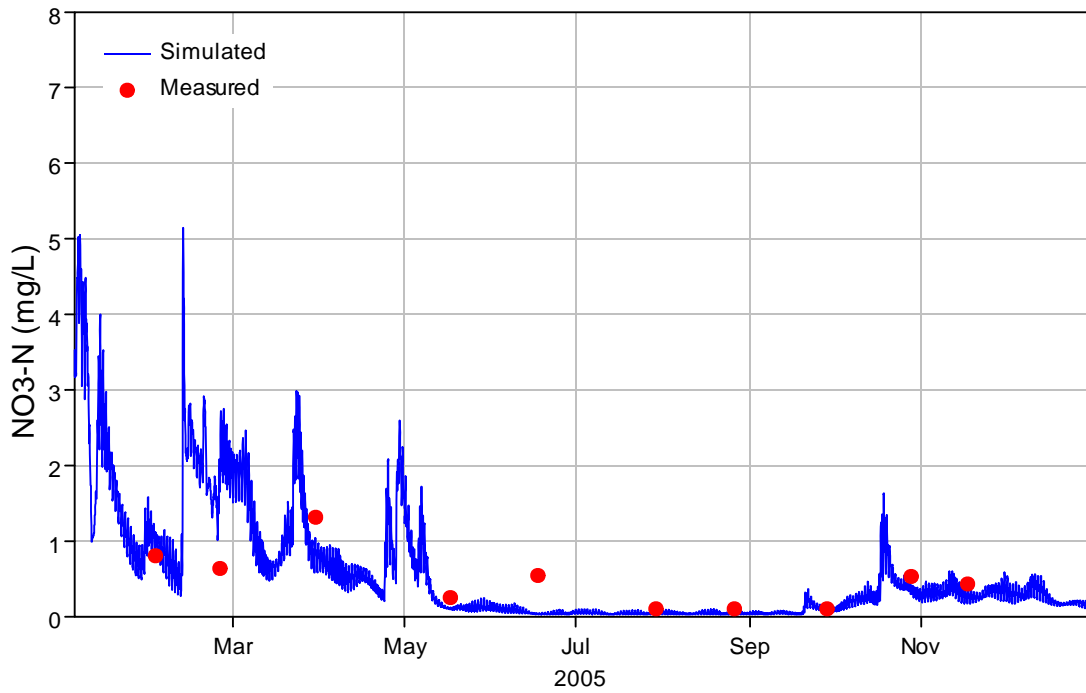


Figure 5-94 Comparison of computed NO₃ concentrations with the measured data at UNBSDC in 2005.

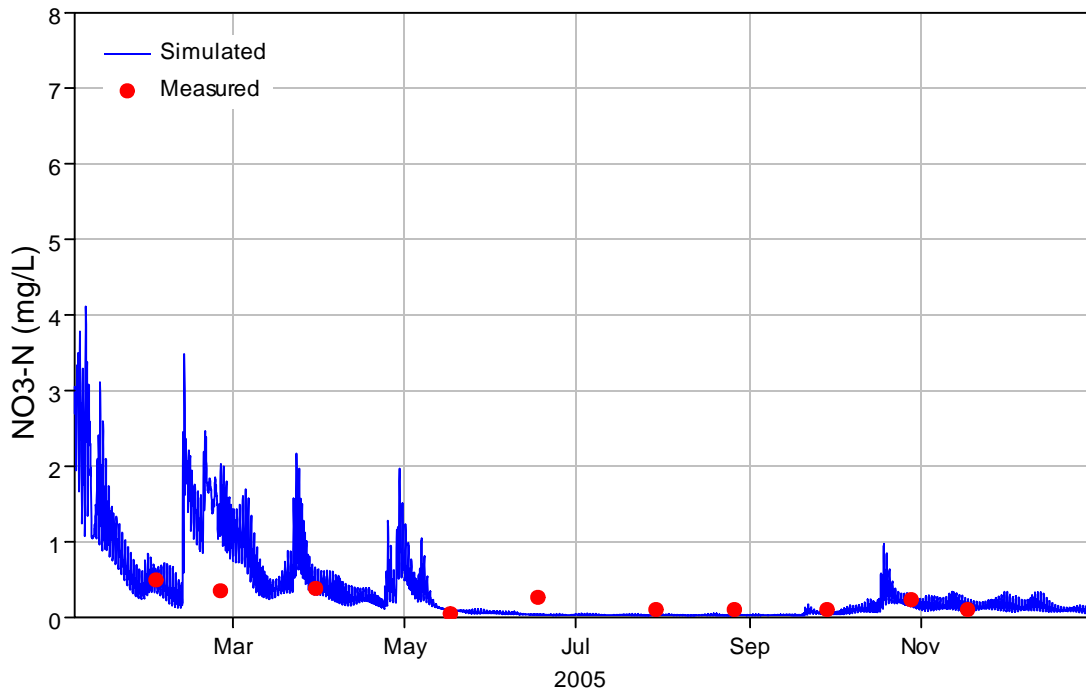


Figure 5-95 Comparison of computed NO₃ concentrations with the measured data at UNBNSB in 2005.

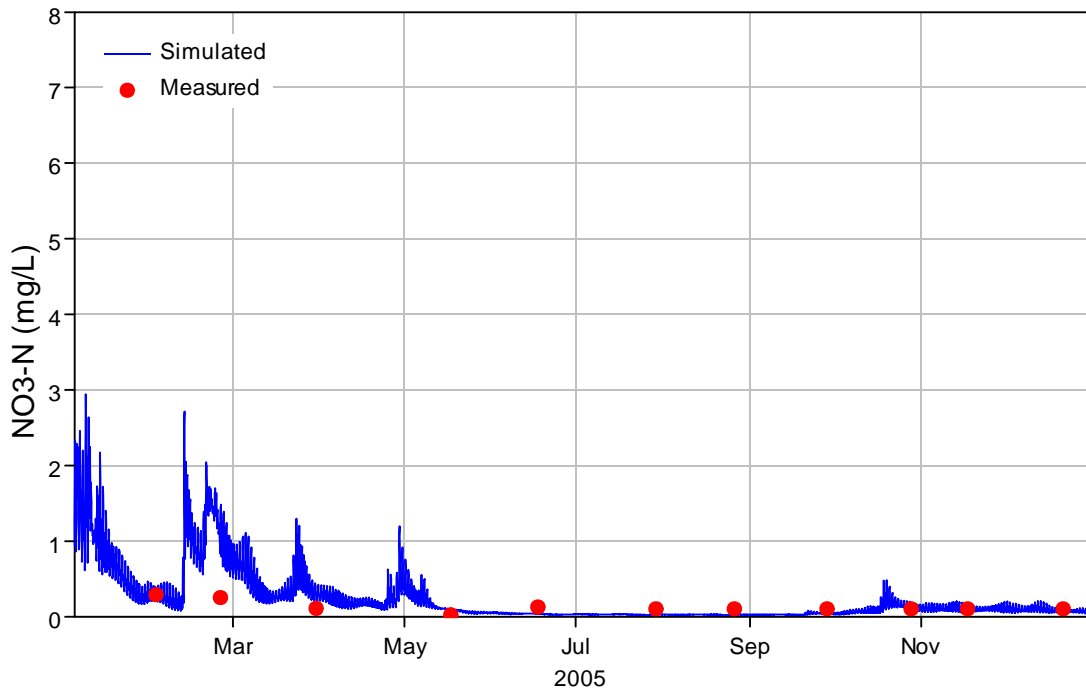


Figure 5-96 Comparison of computed NO₃ concentrations with the measured data at UNBCHB in 2005.

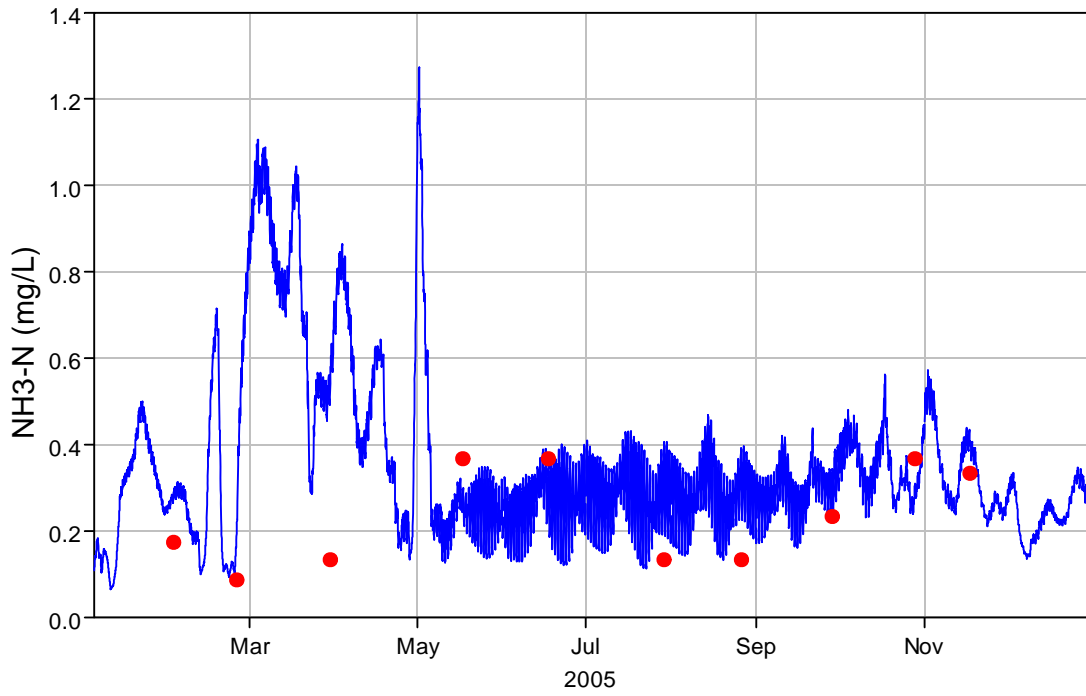


Figure 5-97 Comparison of computed NH3 concentrations with the measured data at UNBJAM in 2005.

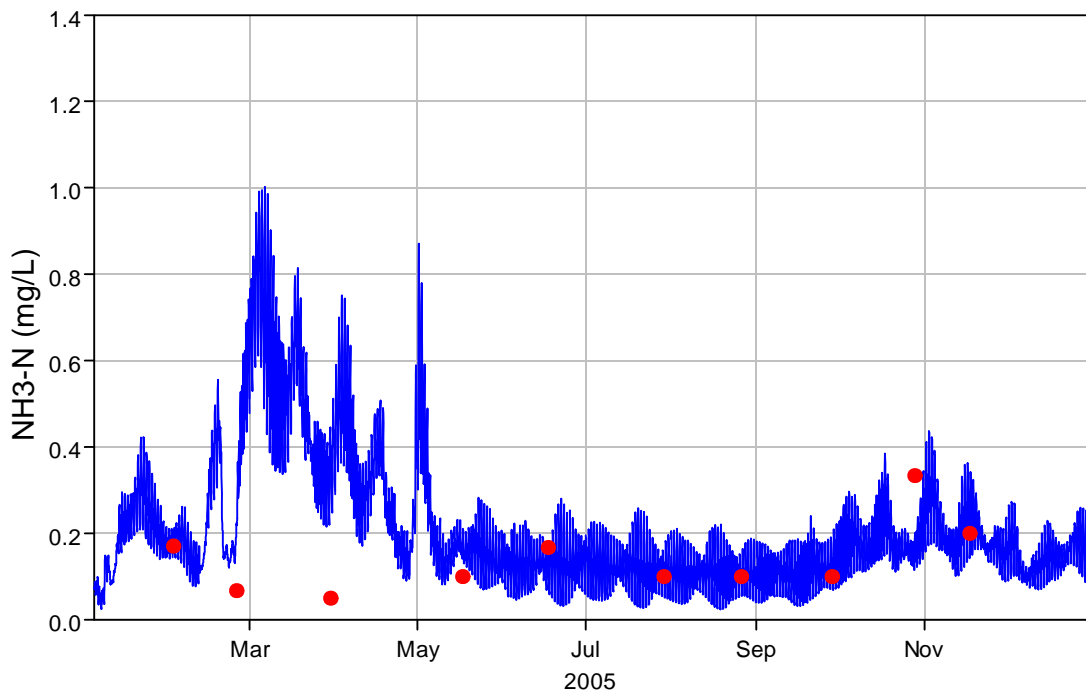


Figure 5-98 Comparison of computed NH3 concentrations with the measured data at UNBSDC in 2005.

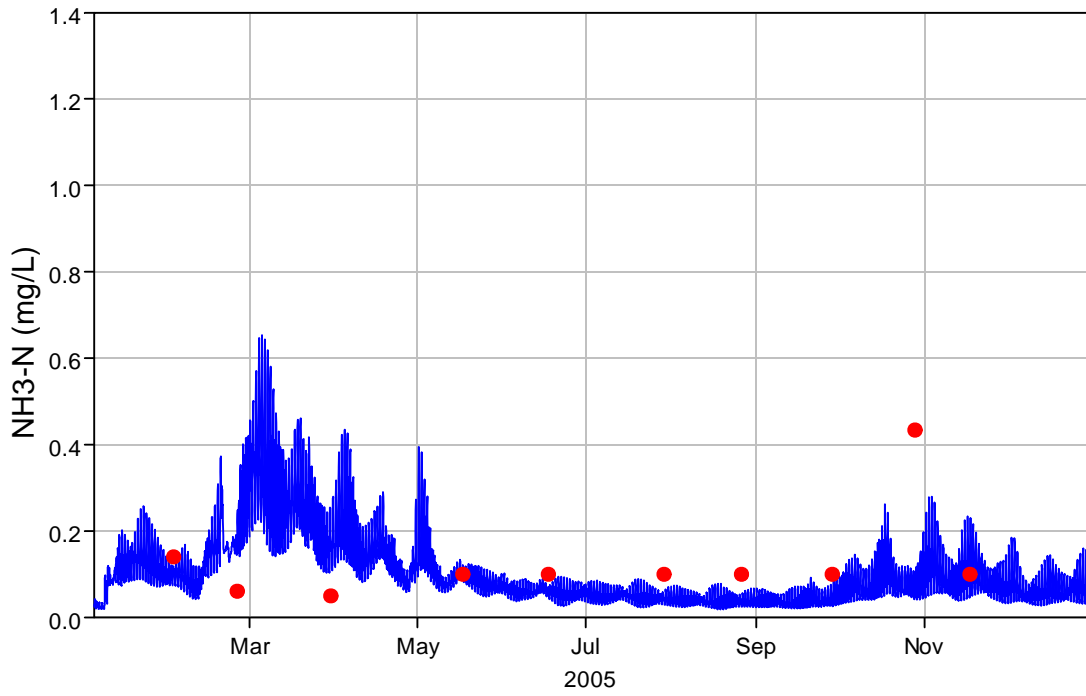


Figure 5-99 Comparison of computed NH₃ concentrations with the measured data at UNBNSB in 2005.

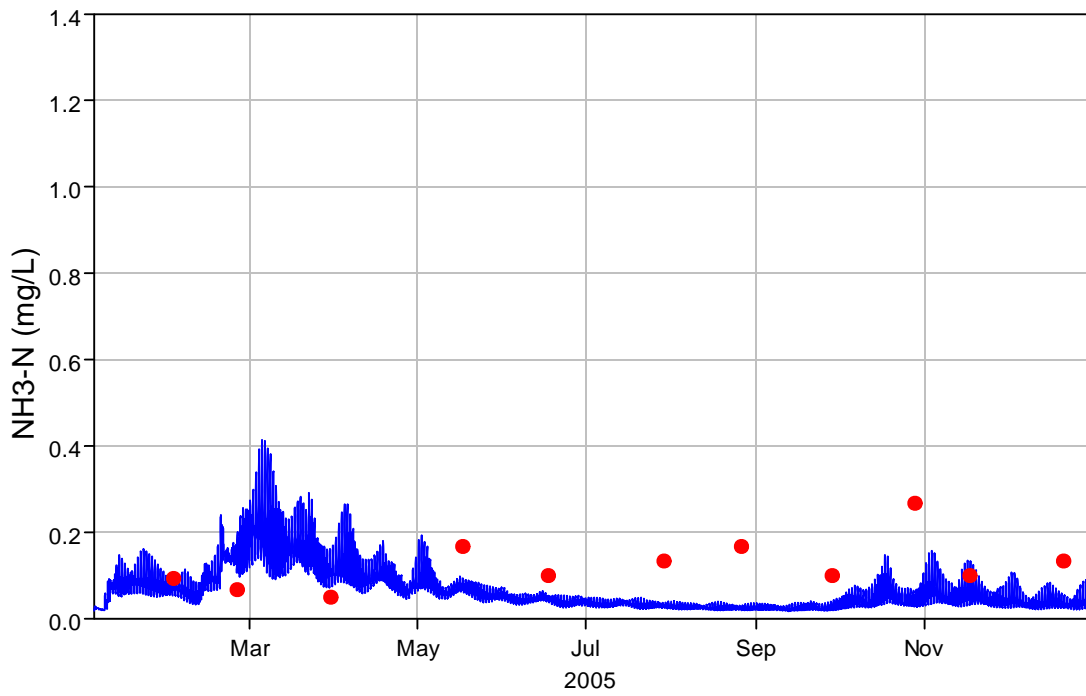


Figure 5-100 Comparison of computed NH₃ concentrations with the measured data at UNBCHB in 2005.

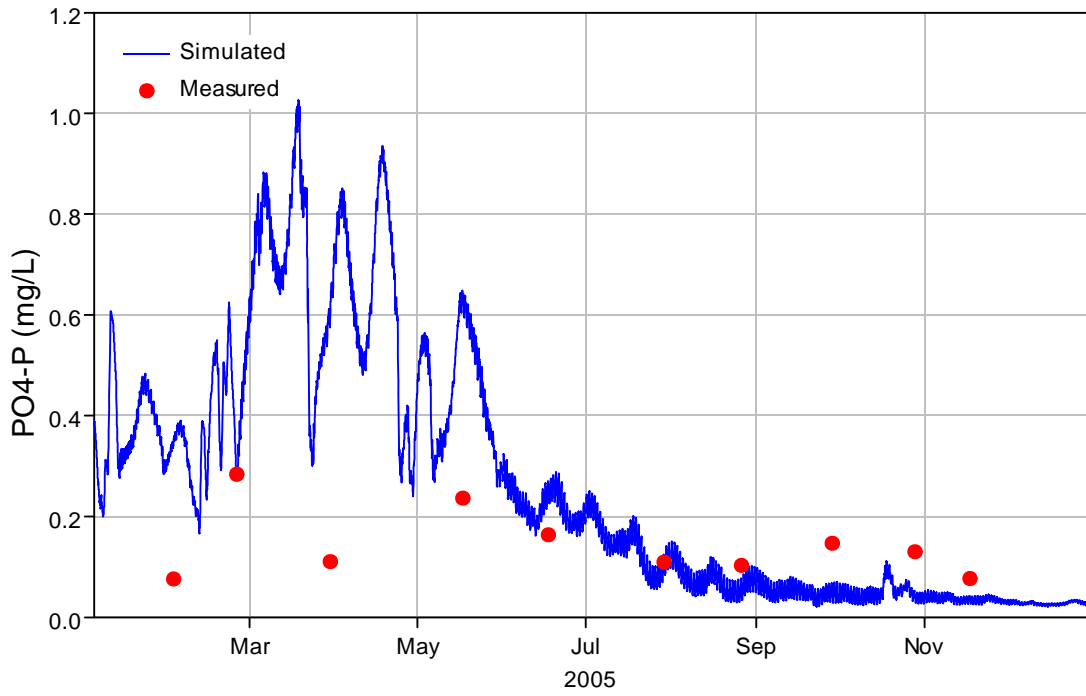


Figure 5-101 Comparison of computed PO4 concentrations with the measured data at UNBJAM in 2005.

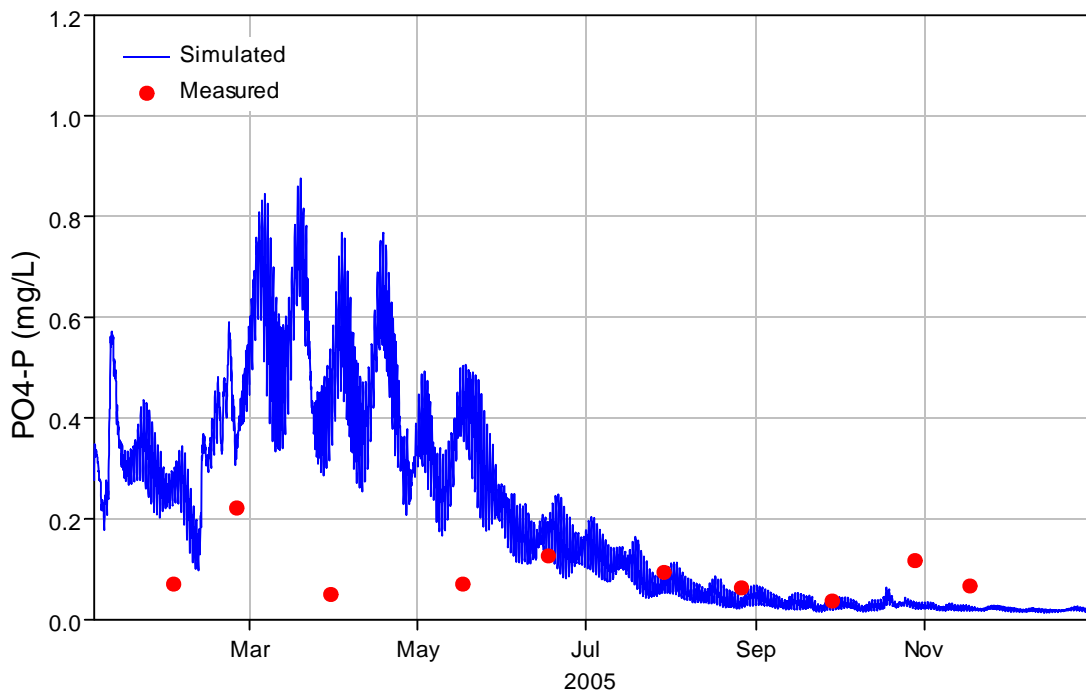


Figure 5-102 Comparison of computed PO4 concentrations with the measured data at UNBSDC in 2005.

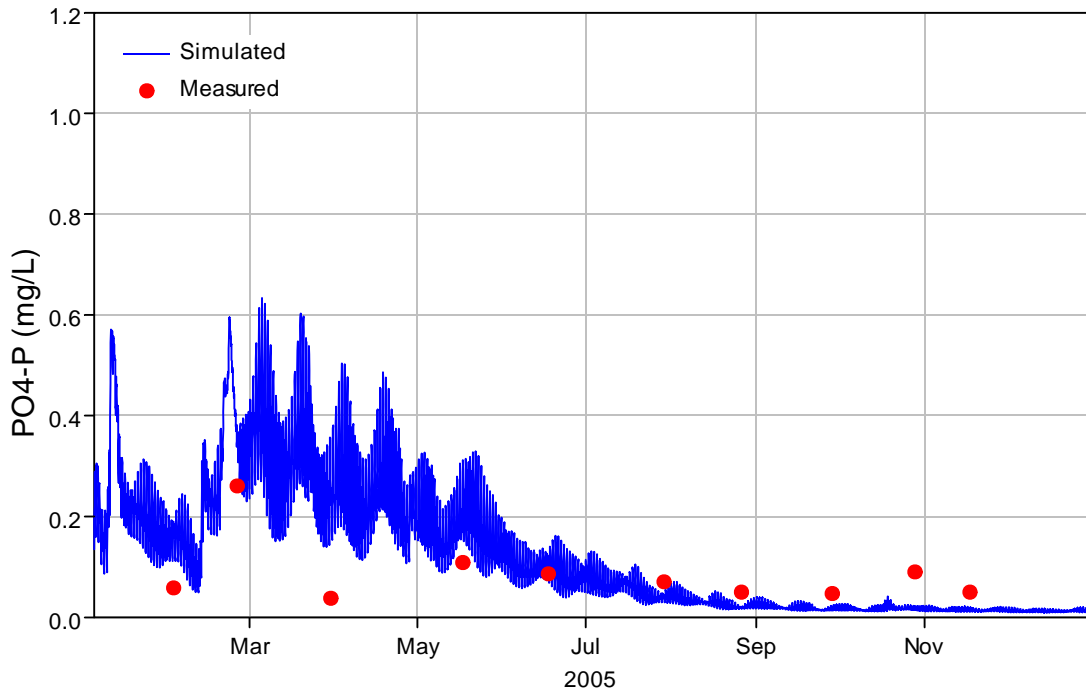


Figure 5-103 Comparison of computed PO4 concentrations with the measured data at UNBNSB in 2005.

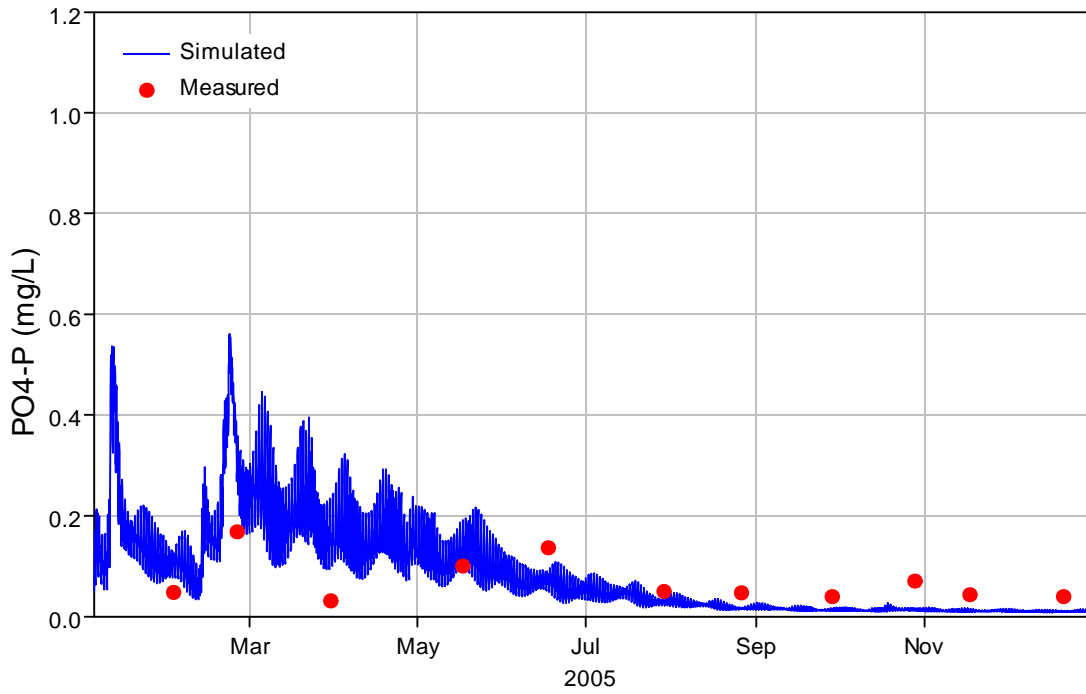


Figure 5-104 Comparison of computed PO4 concentrations with the measured data at UNBCHB in 2005.

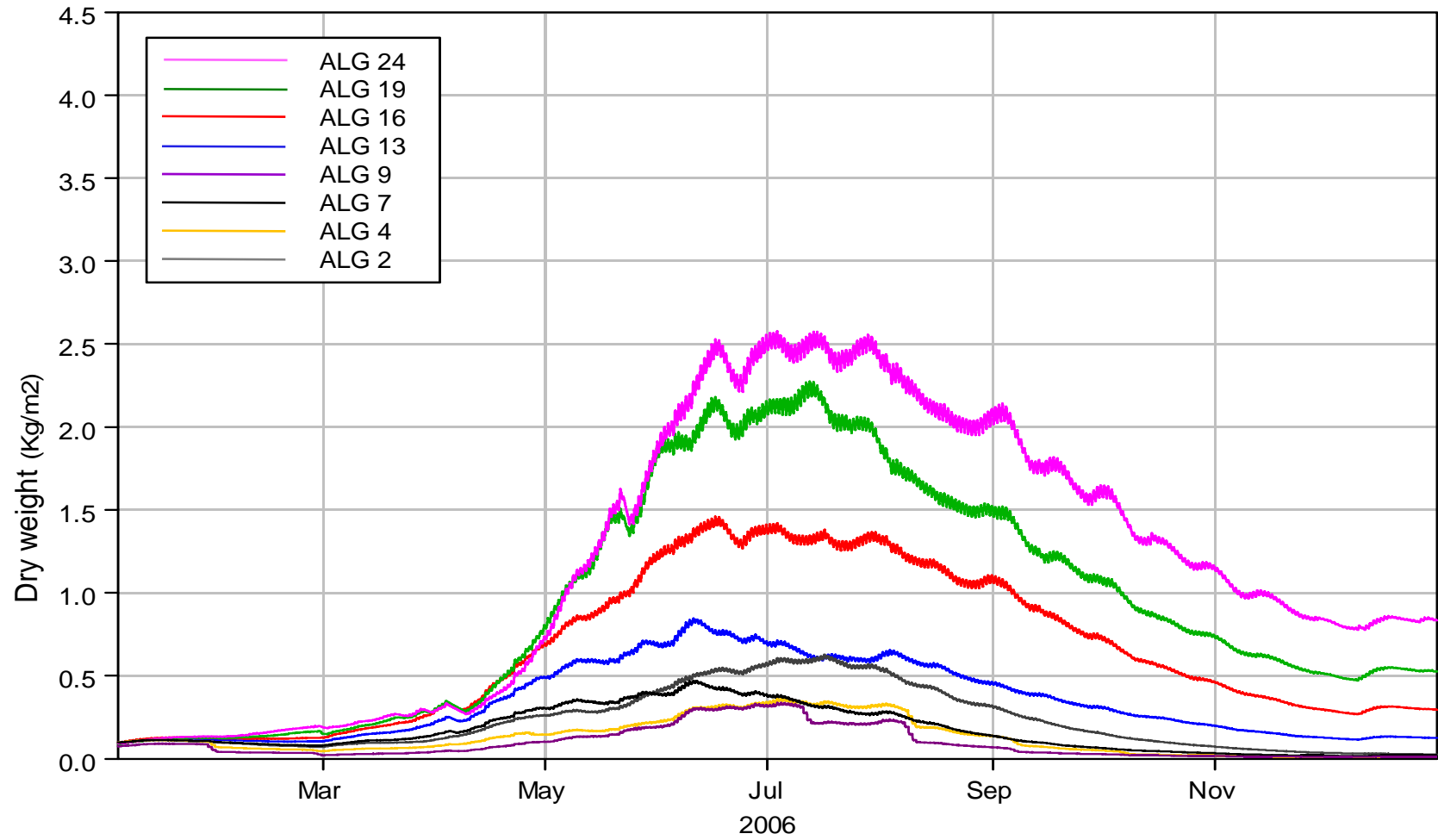


Figure 5-105 Comparison of computed macroalgae concentrations at sampling sites in 2006.

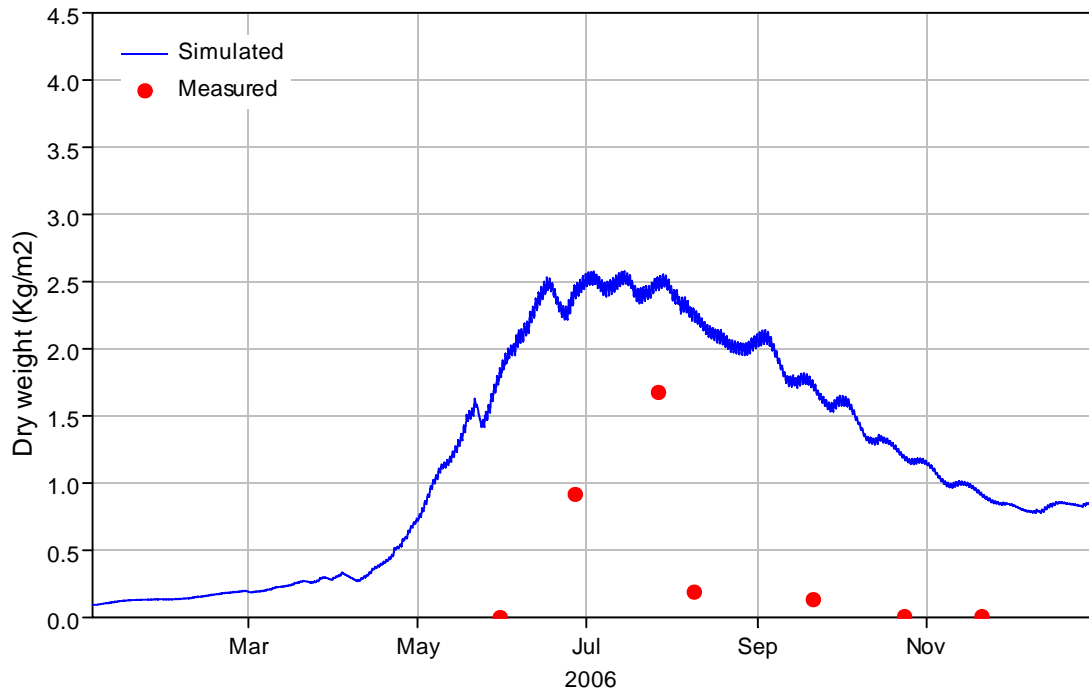


Figure 5-106 Comparison of computed macroalgae concentrations with the measured data at ALG24 in 2006.

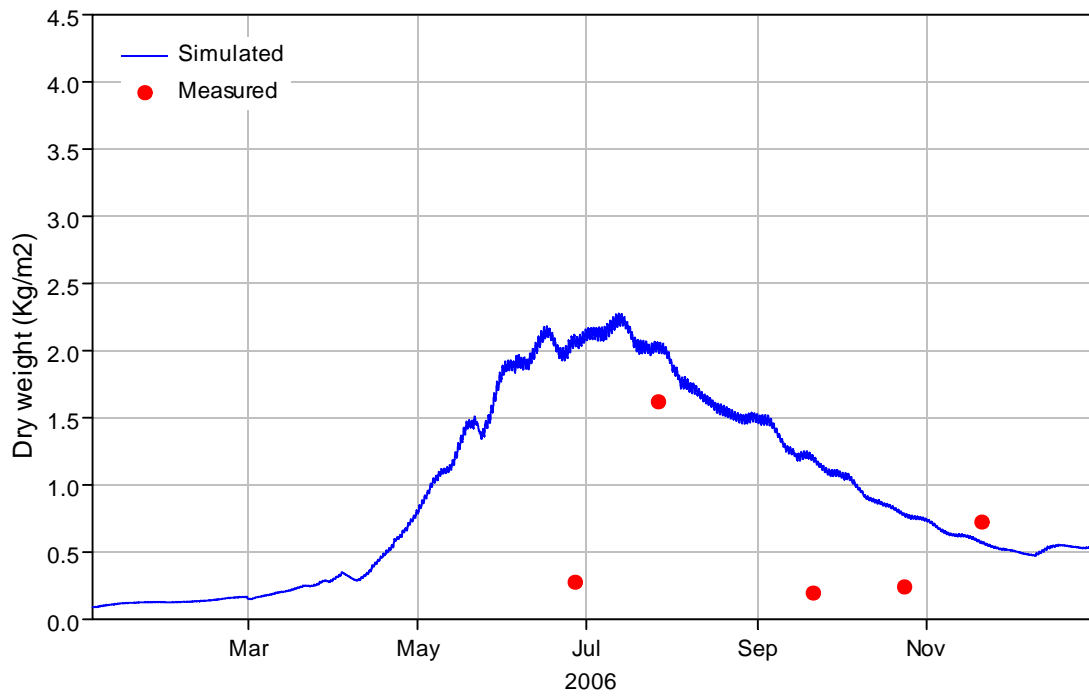


Figure 5-107 Comparison of computed macroalgae concentrations with the measured data at ALG19 in 2006.

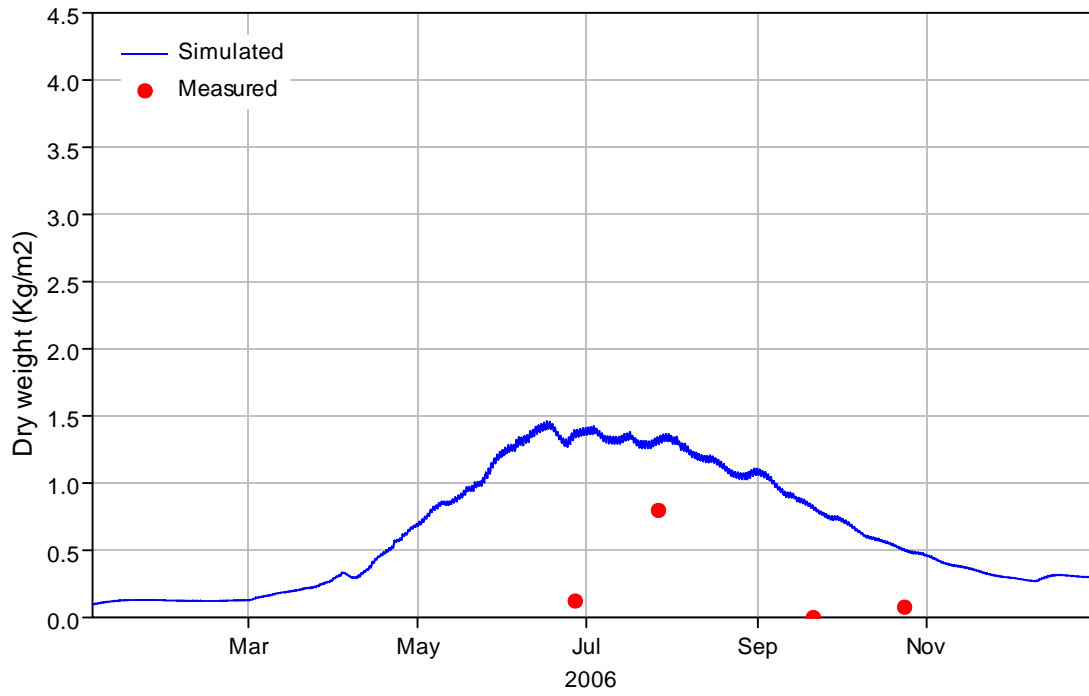


Figure 5-108 Comparison of computed macroalgae concentrations with the measured data at ALG16 in 2006.

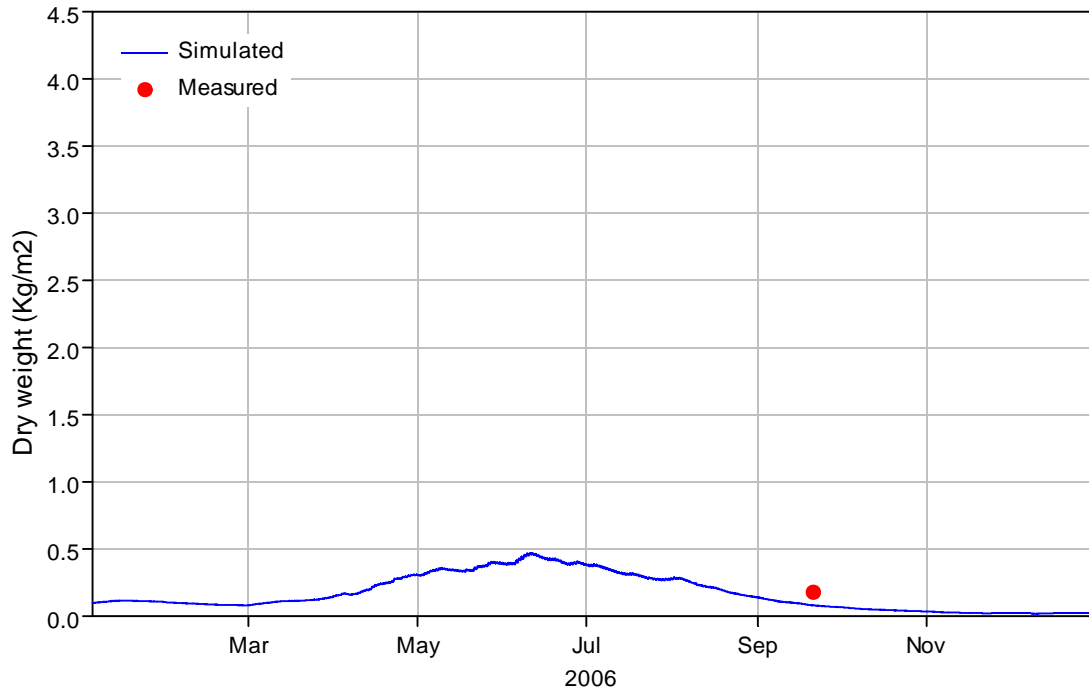


Figure 5-109 Comparison of computed macroalgae concentrations with the measured data at ALG7 in 2006.

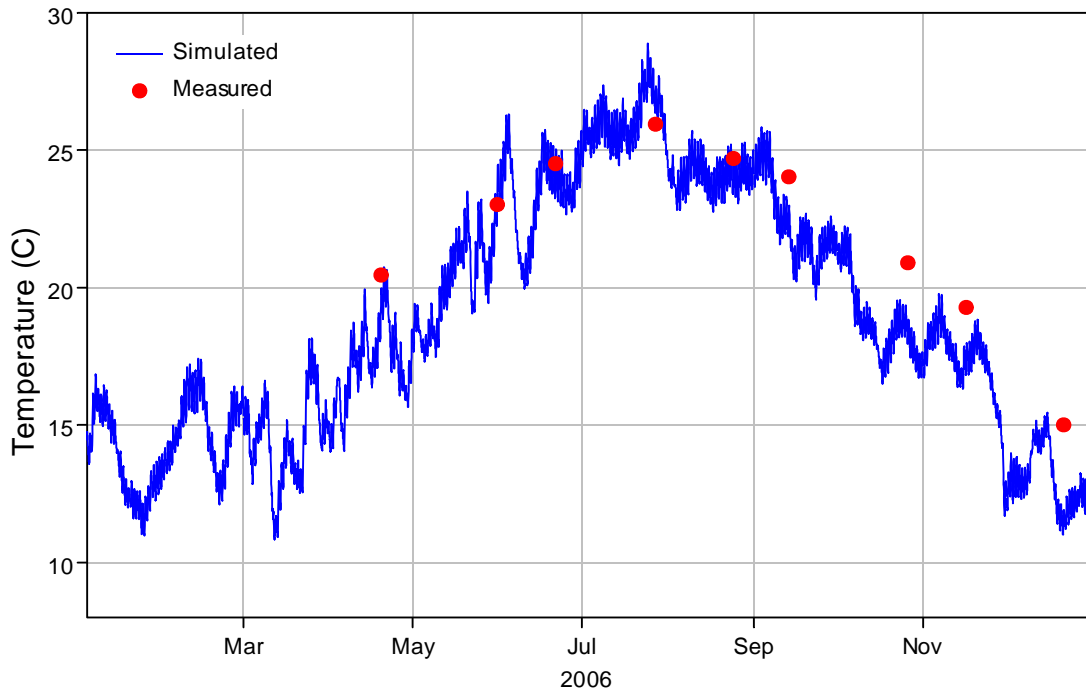


Figure 5-110 Comparison of computed temperature (°C) with the measured data at UNBJAM in 2006.

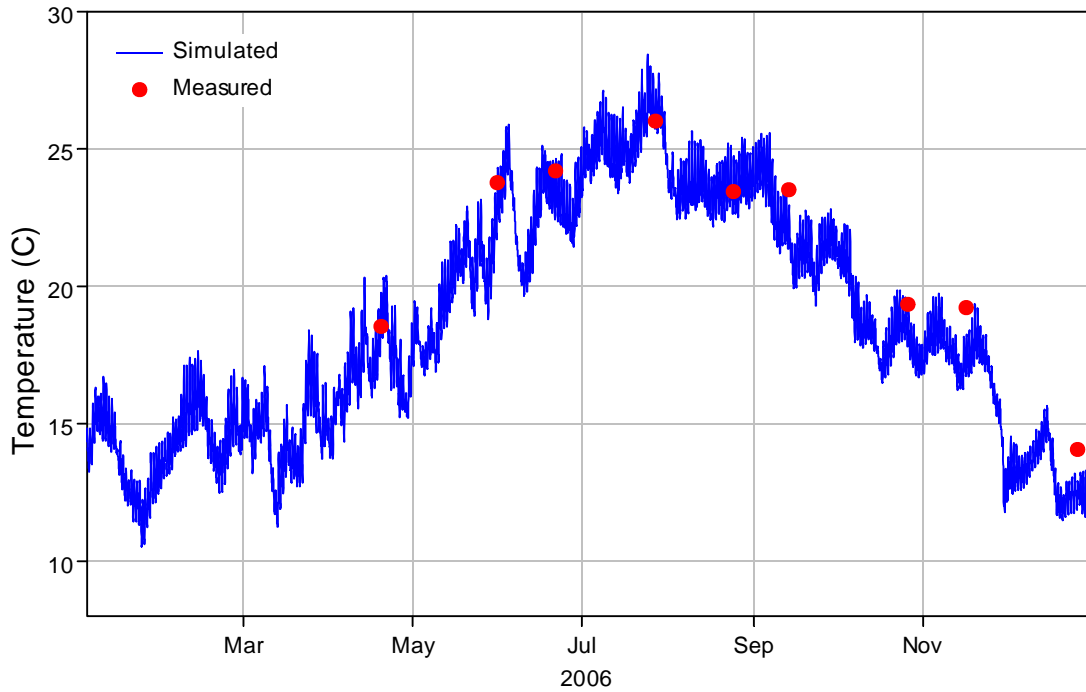


Figure 5-111 Comparison of computed temperature (°C) with the measured data at UNBSDC in 2006.

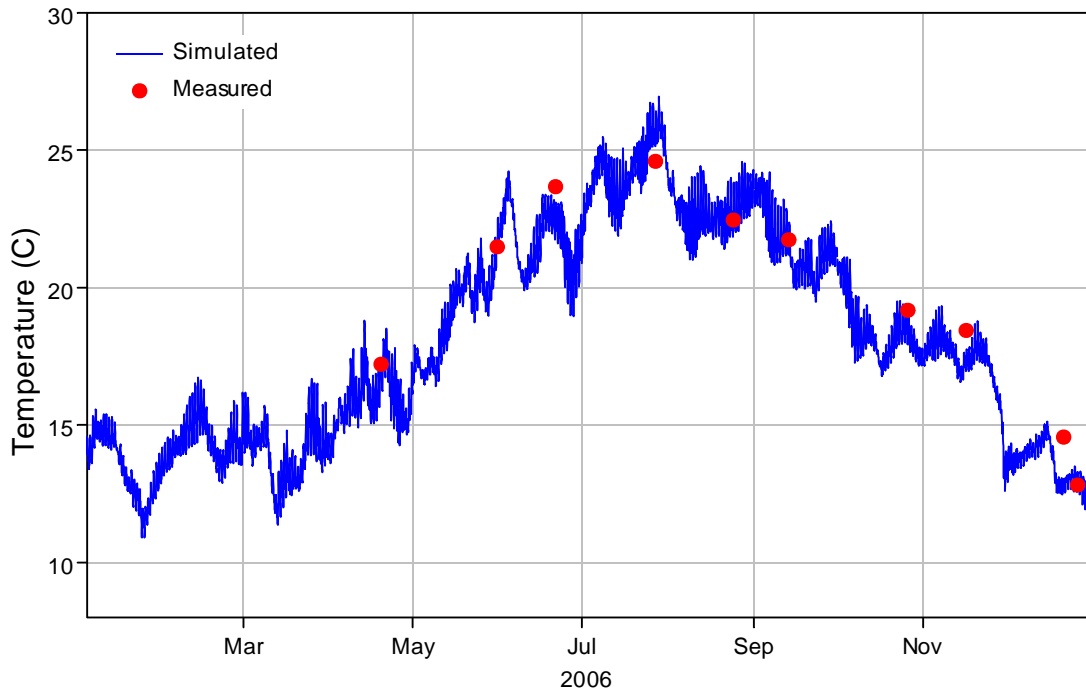


Figure 5-112 Comparison of computed temperature (°C) with the measured data at UNBNSB in 2006.

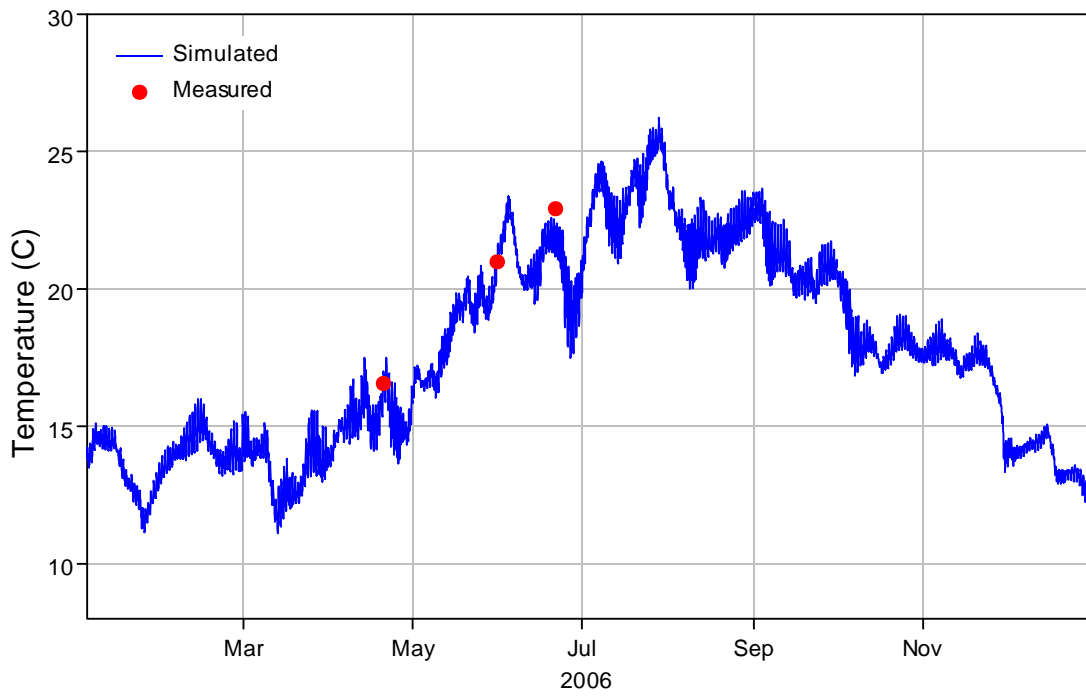


Figure 5-113 Comparison of computed temperature (°C) with the measured data at UNBCHB in 2006.

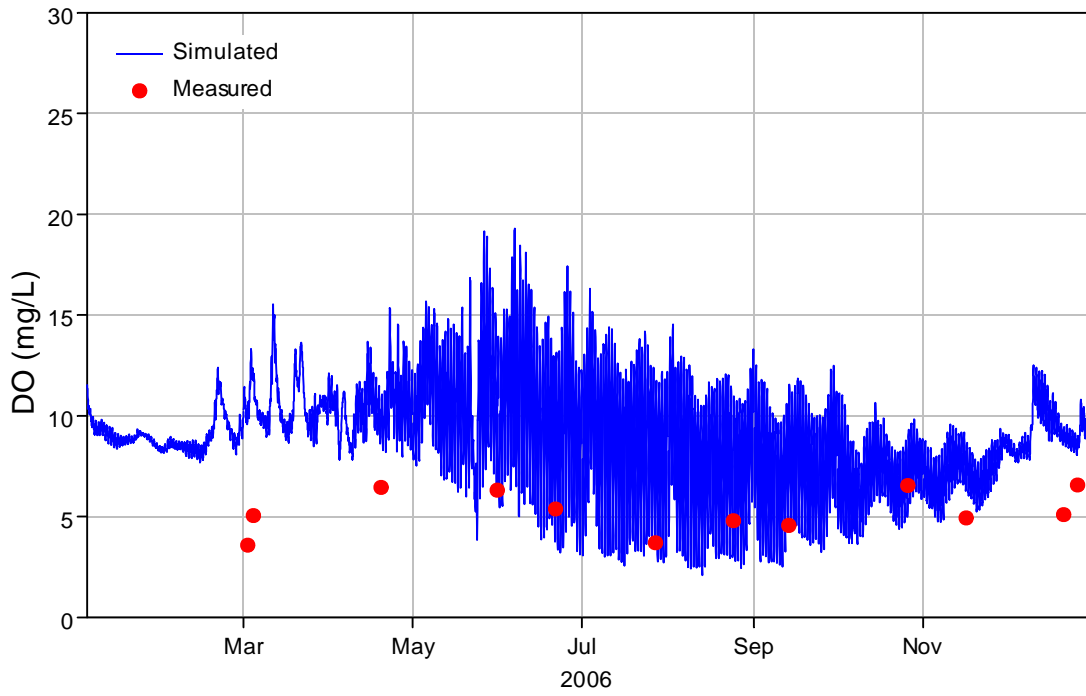


Figure 5-114 Comparison of computed DO concentrations with the measured data at UNBJAM in 2006.

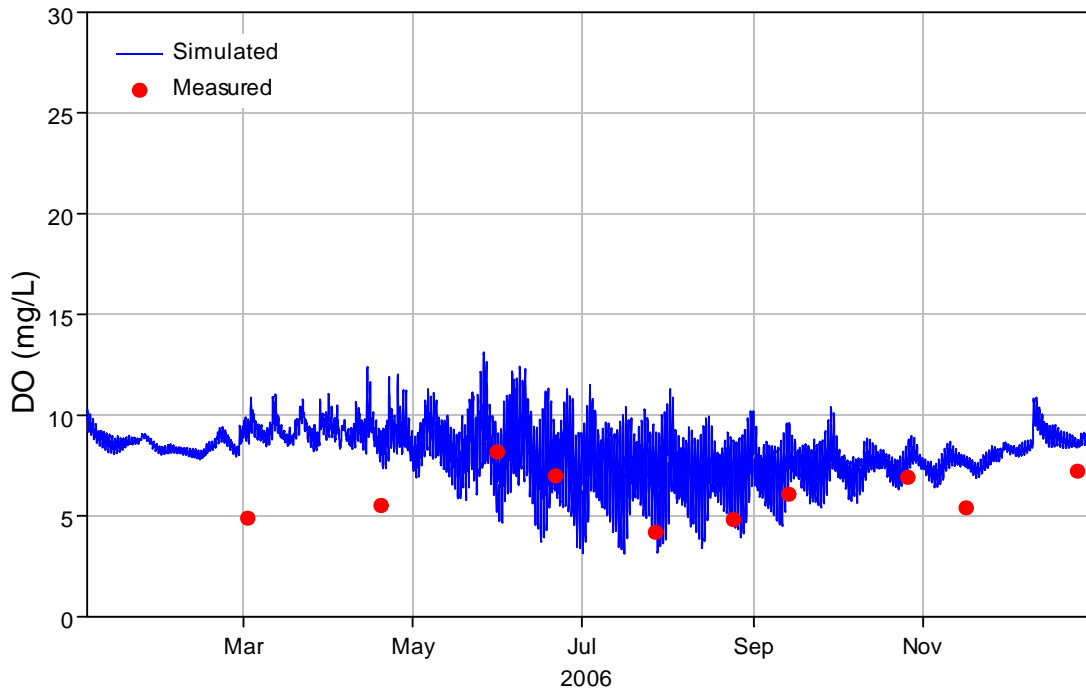


Figure 5-115 Comparison of computed DO concentrations with the measured data at UNBSDC in 2006.

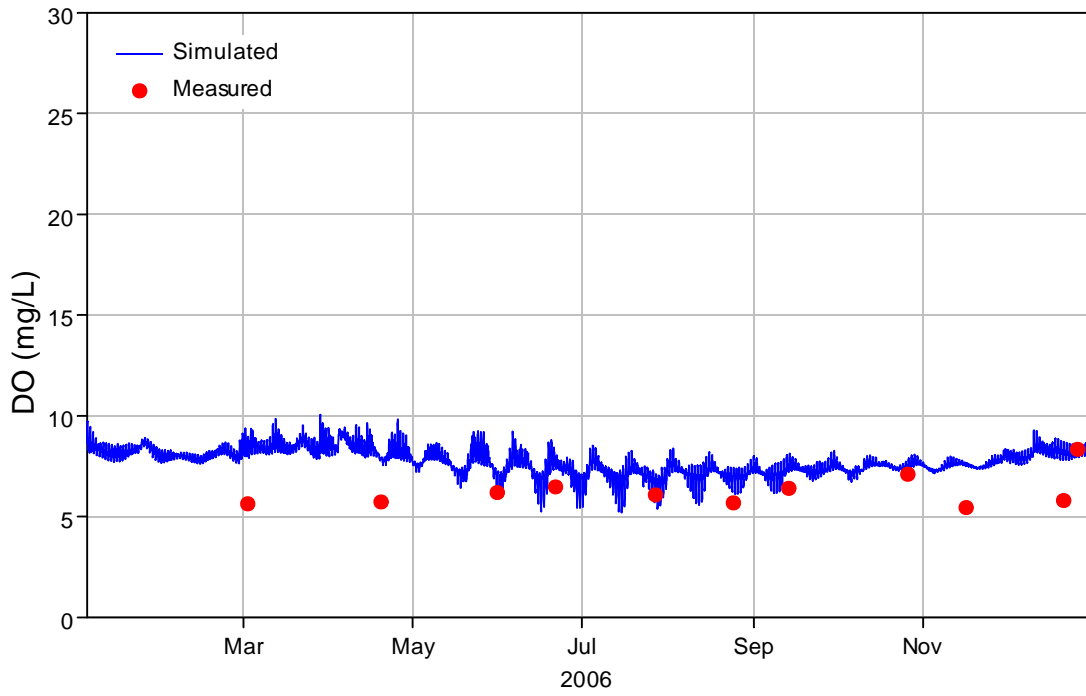


Figure 5-116 Comparison of computed DO concentrations with the measured data at UNBNSB in 2006.

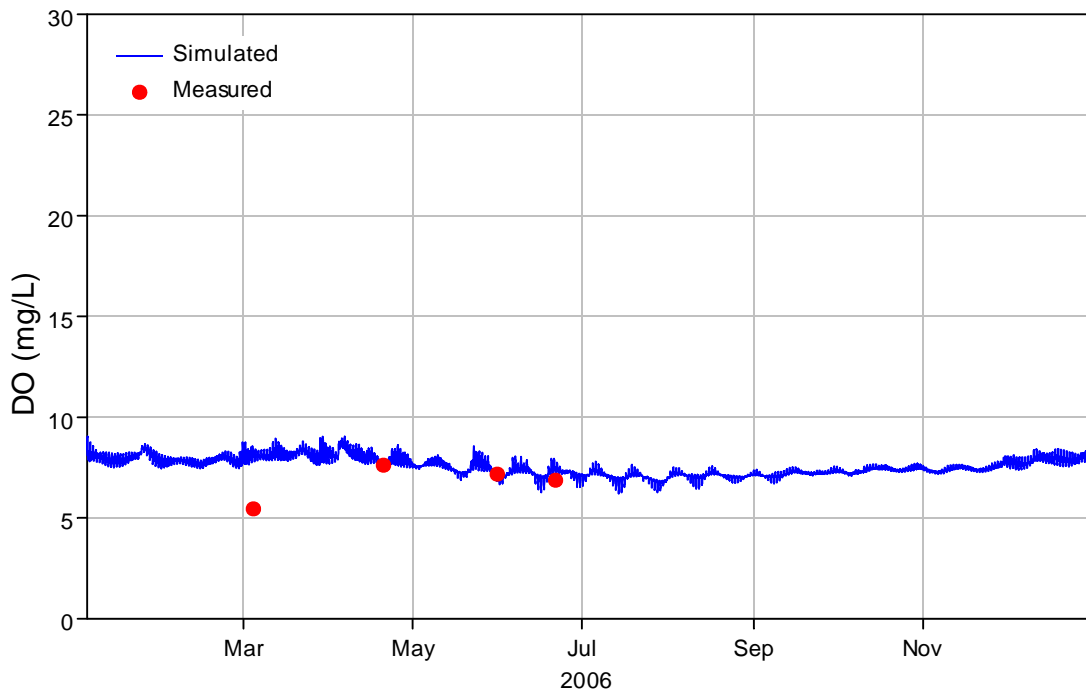


Figure 5-117 Comparison of computed DO concentrations with the measured data at UNBCHB in 2006.

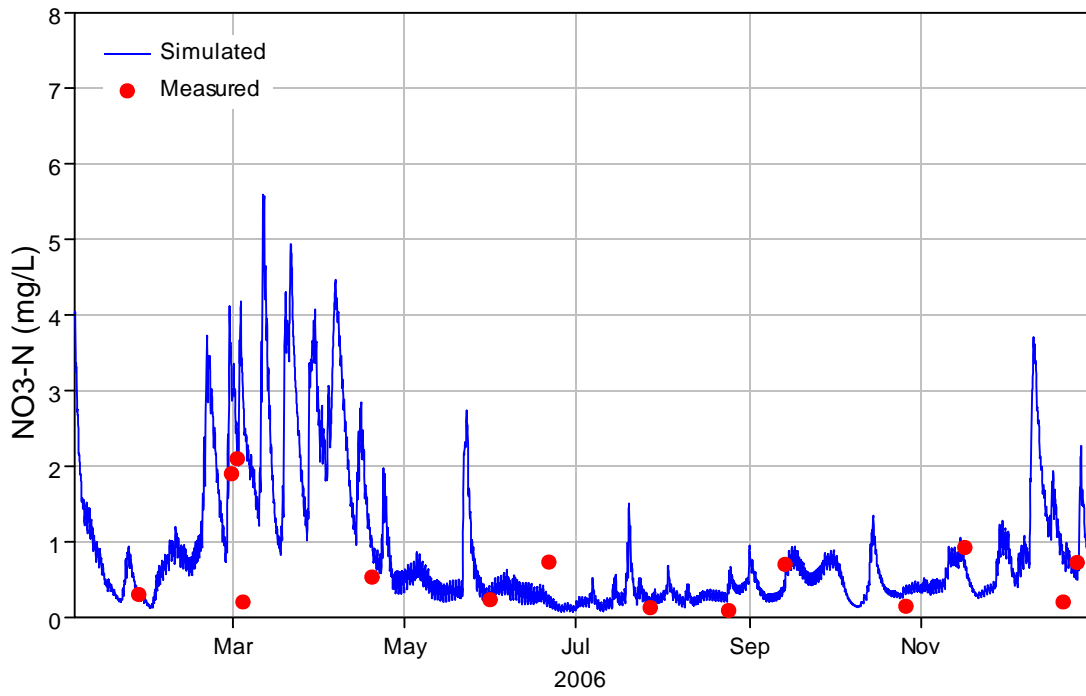


Figure 5-118 Comparison of computed NO₃ concentrations with the measured data at UNBJAM in 2006.

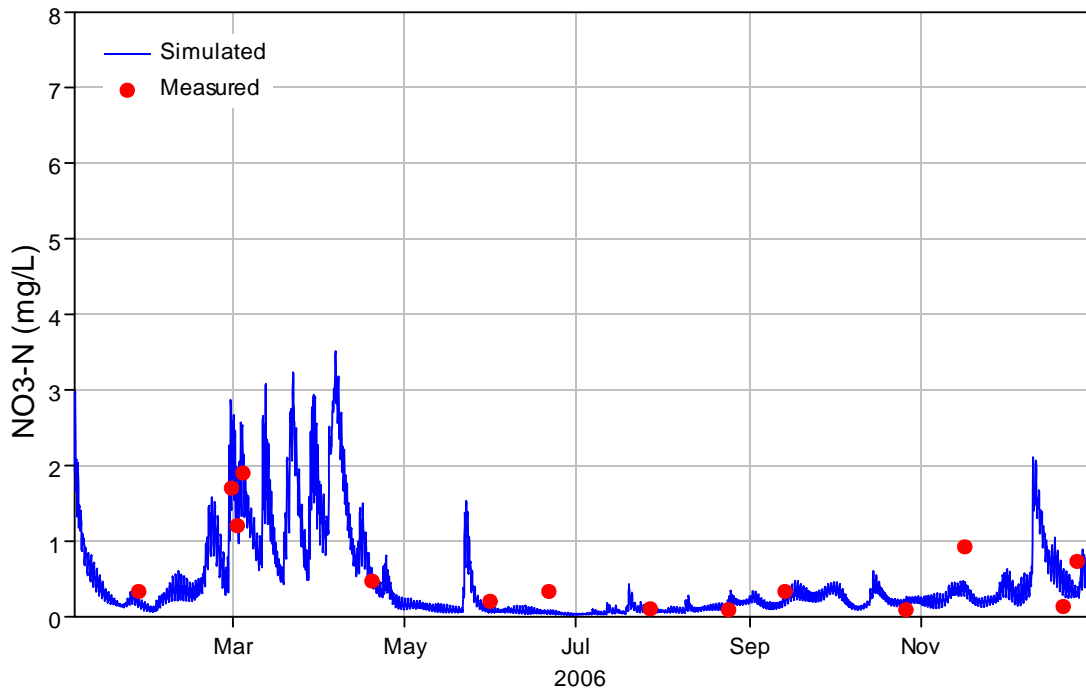


Figure 5-119 Comparison of computed NO₃ concentrations with the measured data at UNBSDC in 2006.

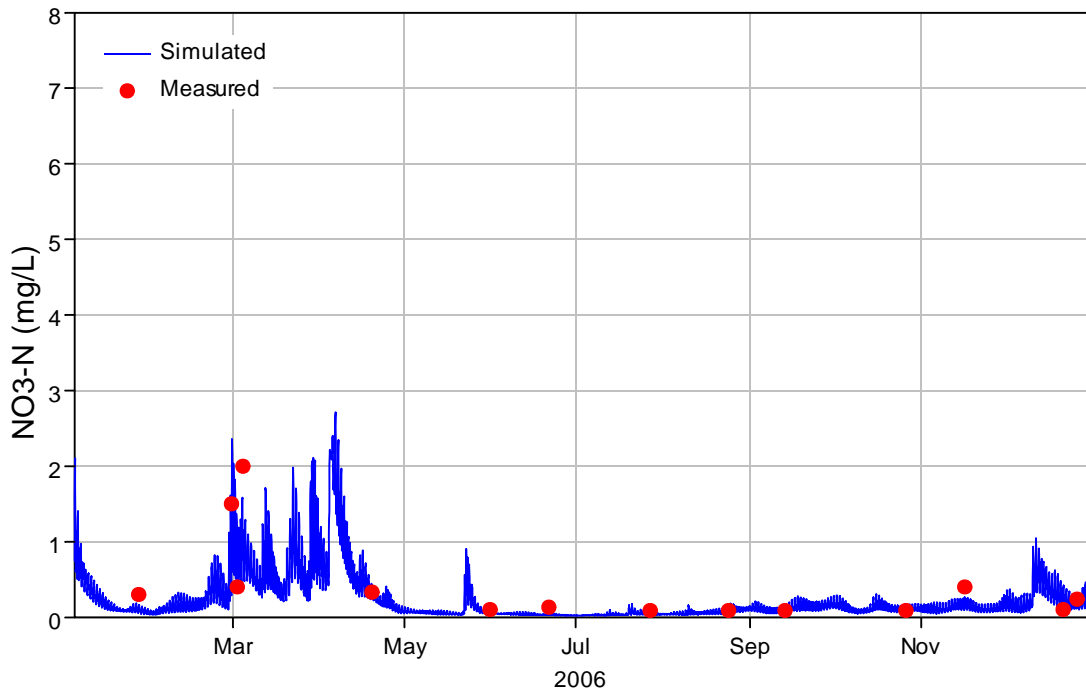


Figure 5-120 Comparison of computed NO₃ concentrations with the measured data at UNBNSB in 2006.

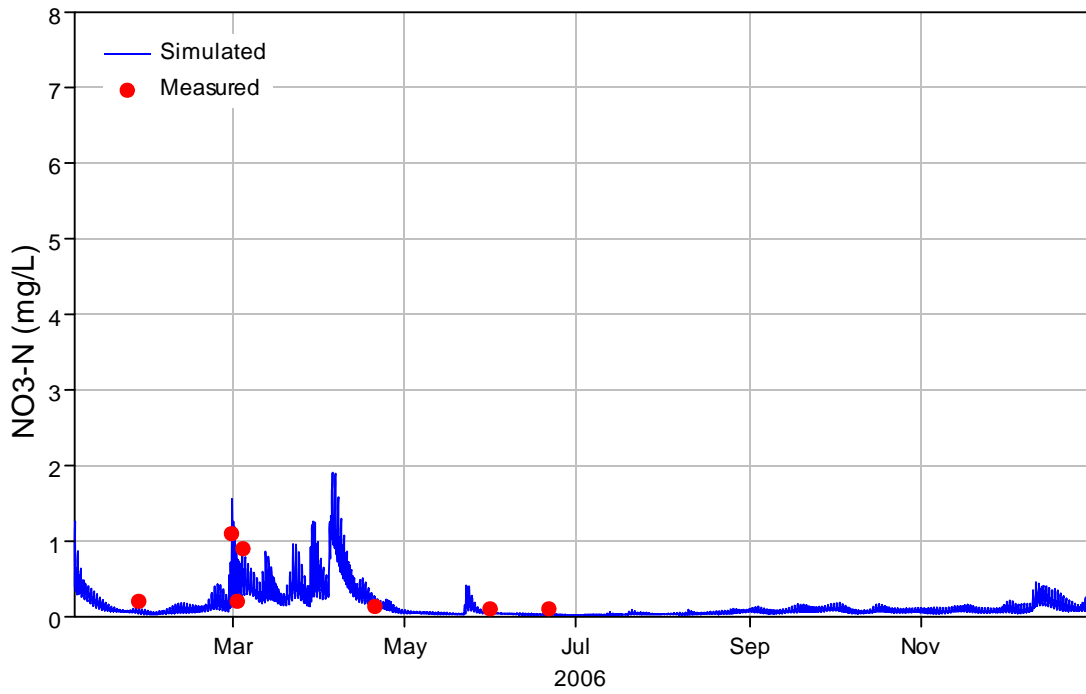


Figure 5-121 Comparison of computed NO₃ concentrations with the measured data at UNBCHB in 2006.

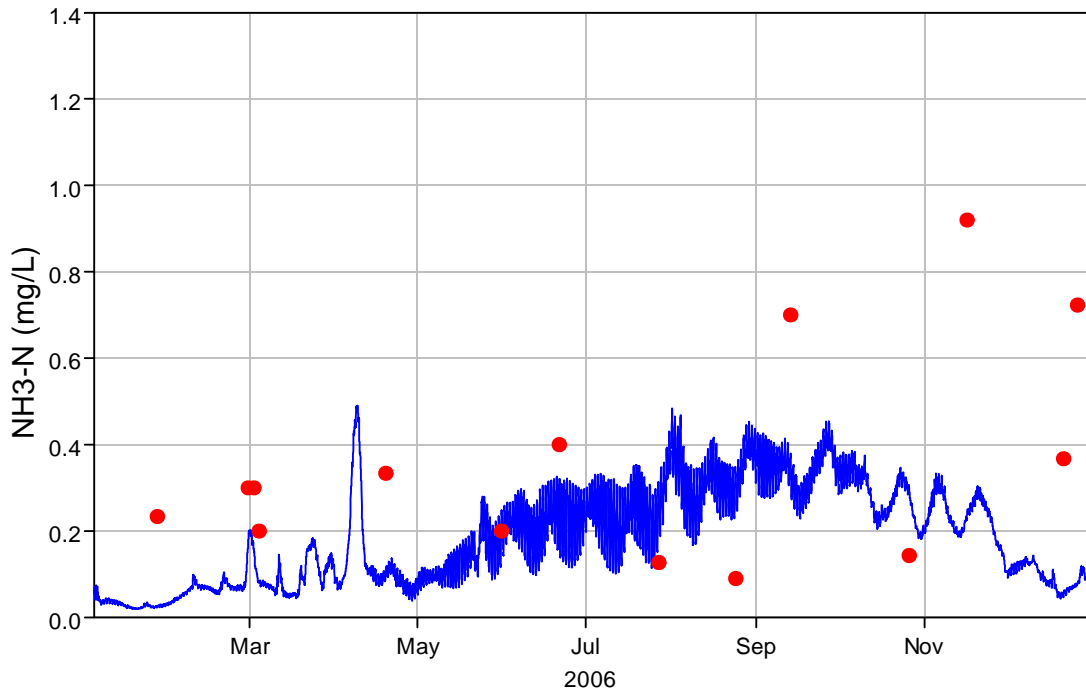


Figure 5-122 Comparison of computed NH3 concentrations with the measured data at UNBJAM in 2006.

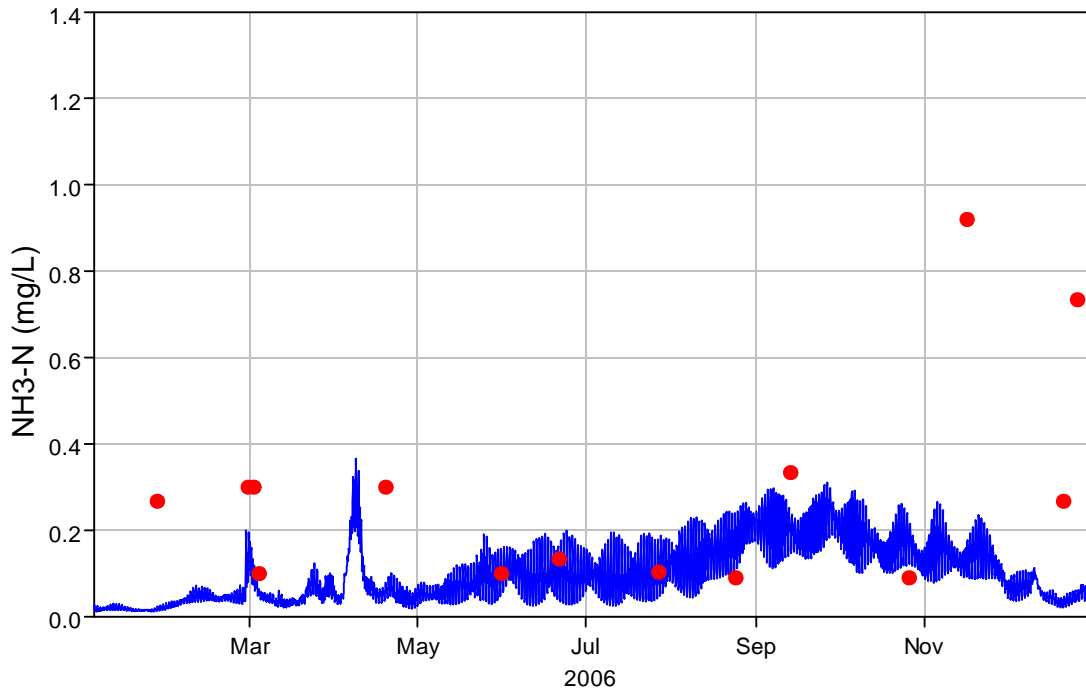


Figure 5-123 Comparison of computed NH3 concentrations with the measured data at UNBSDC in 2006.

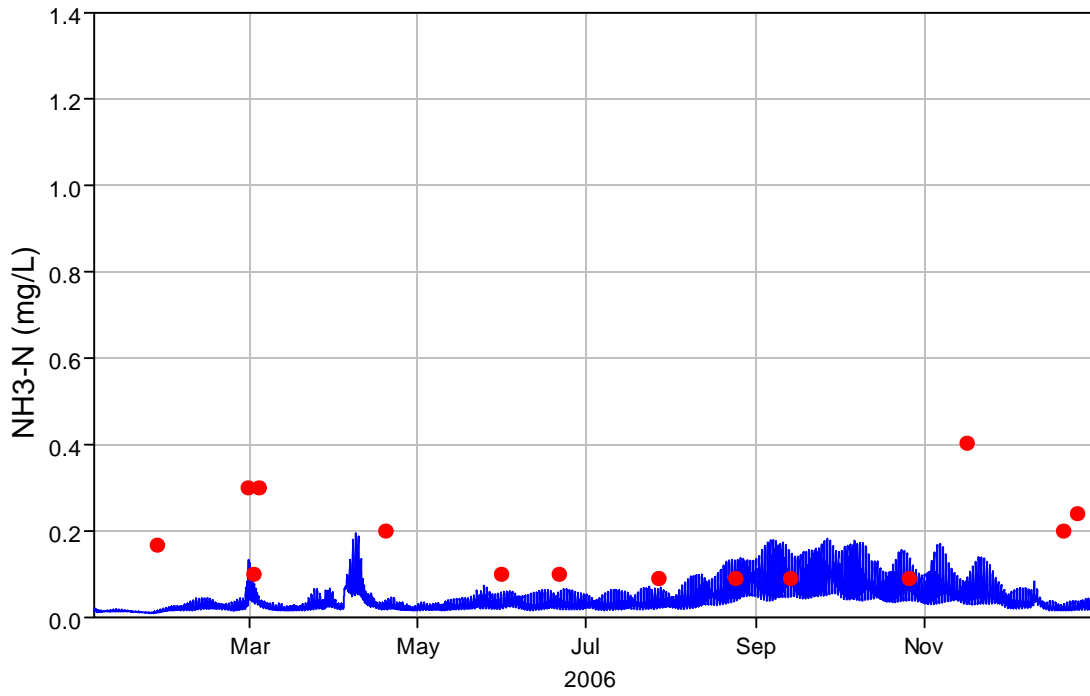


Figure 5-124 Comparison of computed NH₃ concentrations with the measured data at UNBNSB in 2006.

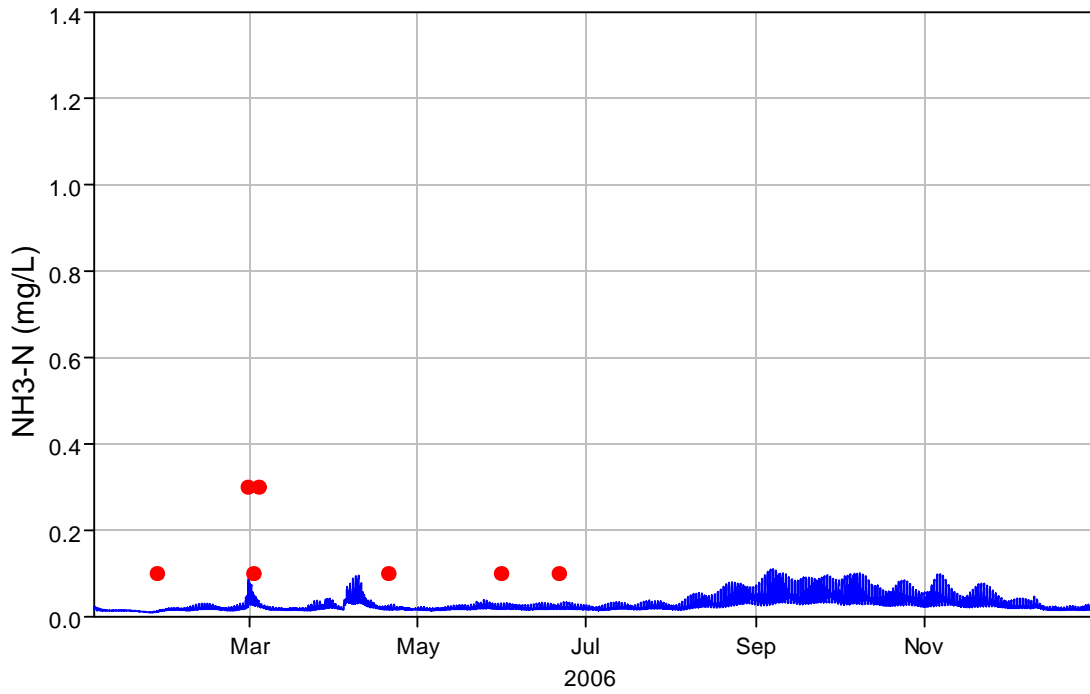


Figure 5-125 Comparison of computed NH₃ concentrations with the measured data at UNBCHB in 2006.

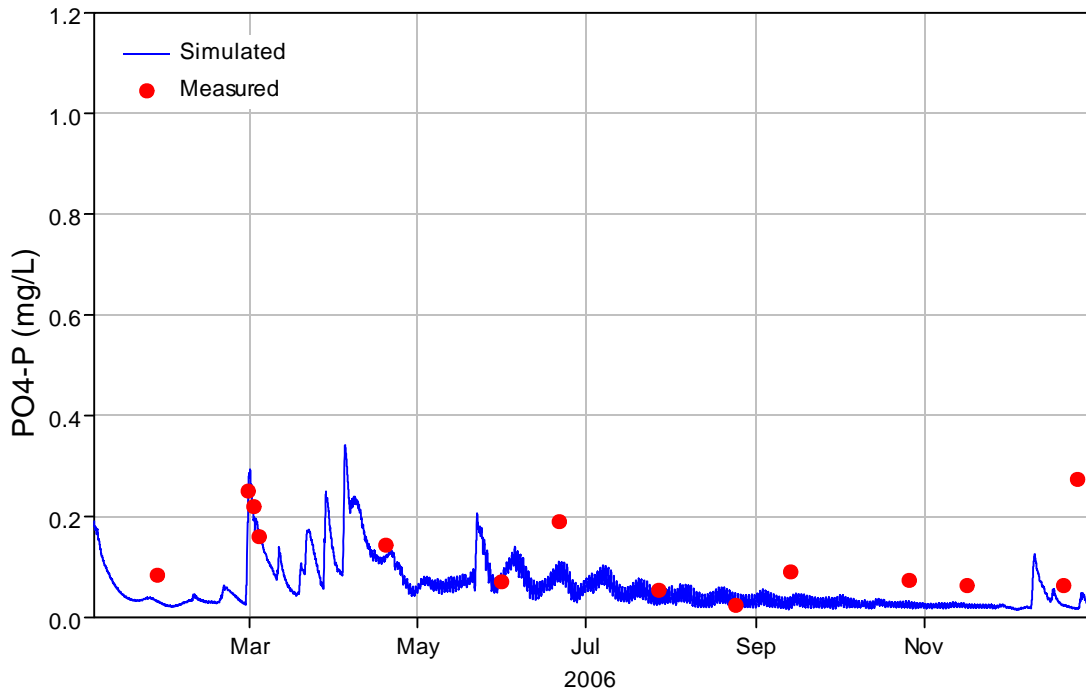


Figure 5-126 Comparison of computed PO4 concentrations with the measured data at UNBJAM in 2006.

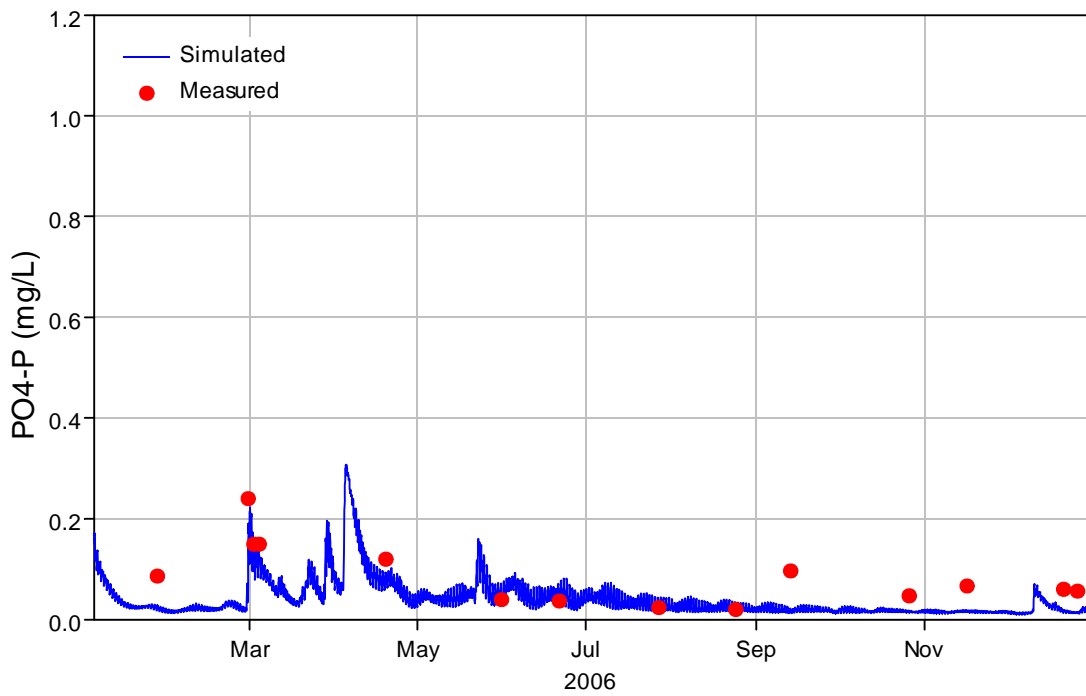


Figure 5-127 Comparison of computed PO4 concentrations with the measured data at UNBSDC in 2006.

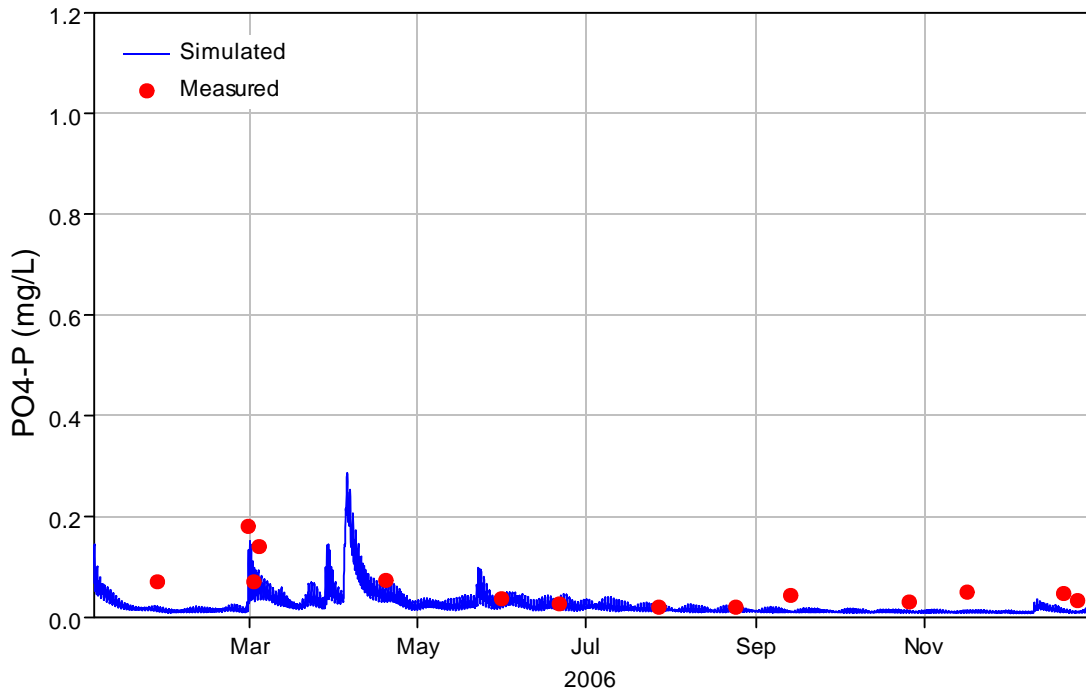


Figure 5-128 Comparison of computed PO4 concentrations with the measured data at UNBNSB in 2006.

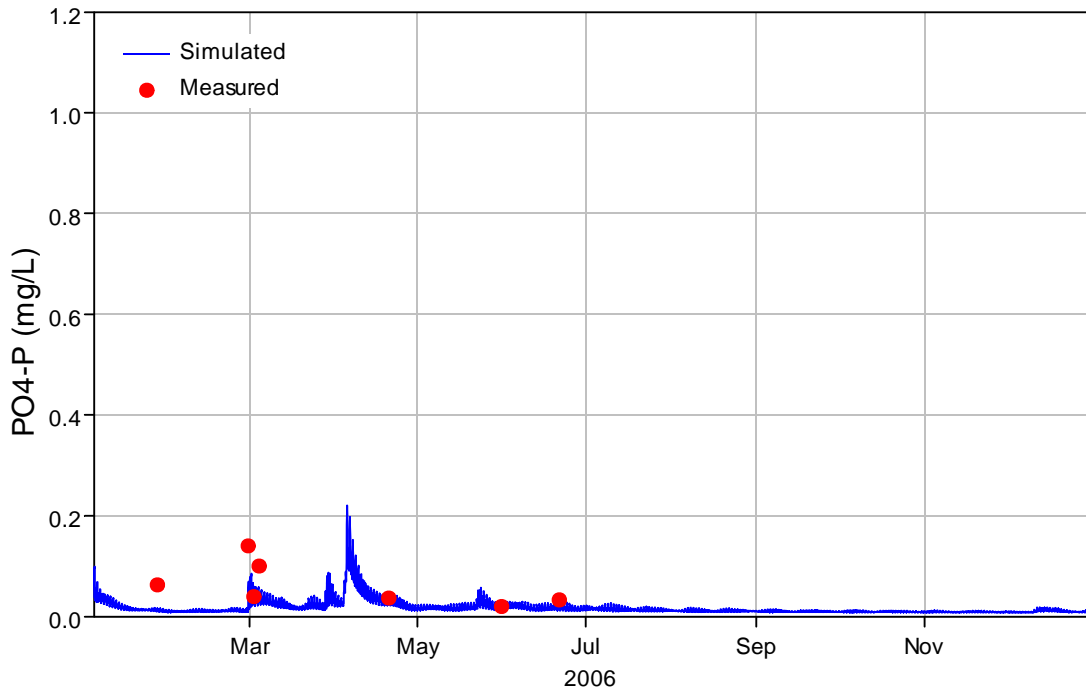


Figure 5-129 Comparison of computed PO4 concentrations with the measured data at UNBCHB in 2006.

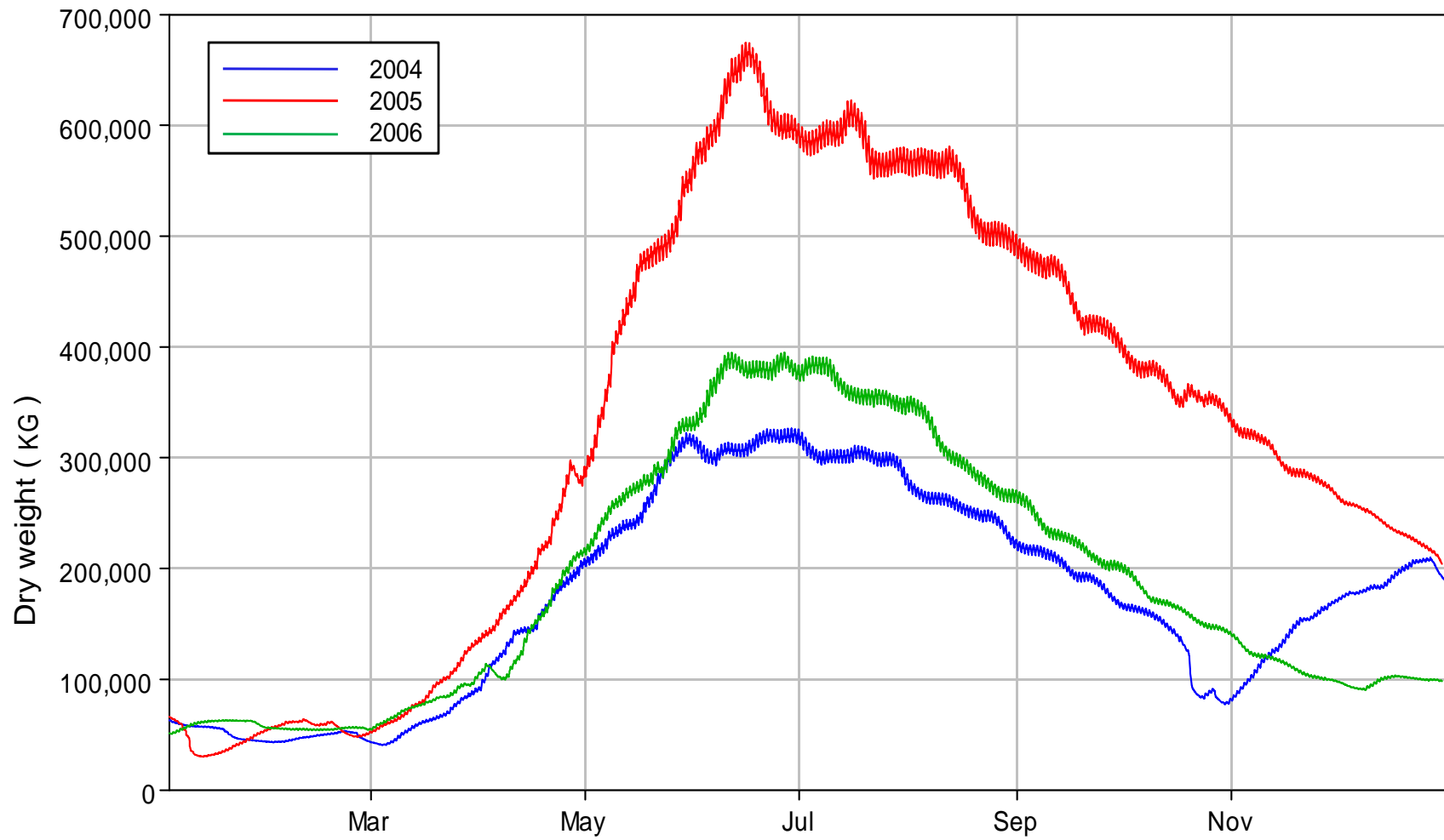


Figure 5-130 Comparison of computed total dry mass of macroalgae for calibration years of 2004, 2005 and 2006.

5.5 Comparison of Nutrient concentrations in the sediments

The model was not calibrated to measured porewater concentrations, however a post-calibration comparison with observed data shows reasonably good agreement. Sediment porewater samples of ammonia and phosphate were collected at the stations shown in Figure 5-131 during 2004 (Sutula, et al., 2004). Comparison plots between the collected data (at 0 to 1 cm sediment depth) and simulated porewater concentrations (from active sediment layer of 0 cm up to a maximum of approximately 10 cm sediment depth) are provided in

Figure 5-132 through Figure 5-143. These plots show that the model computes reasonable porewater concentrations of ammonia and phosphate.

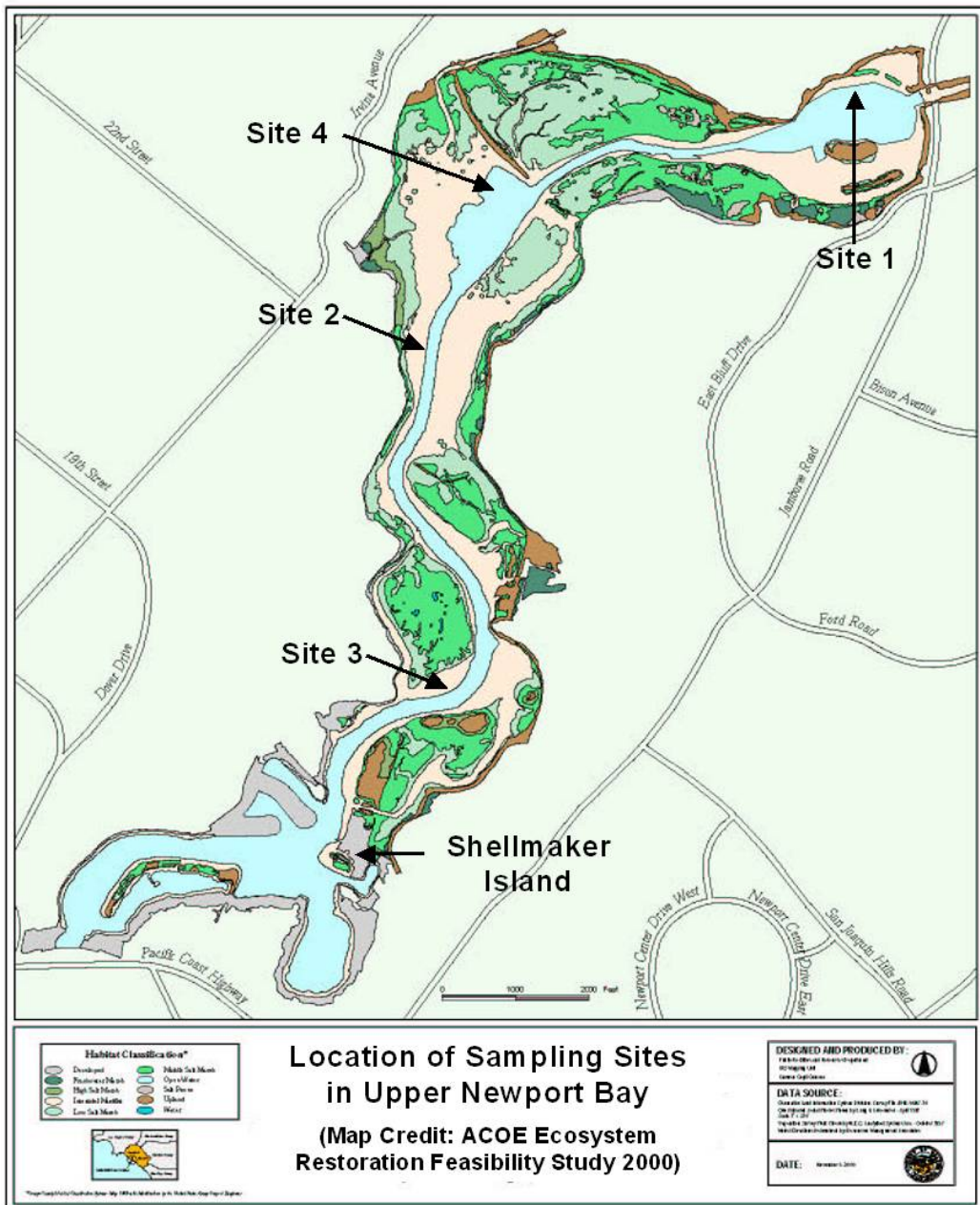


Figure 5-131 Map of sediment porewater sampling sites in Upper Newport Bay (UNB) (Source: Sutula et al., 2006).

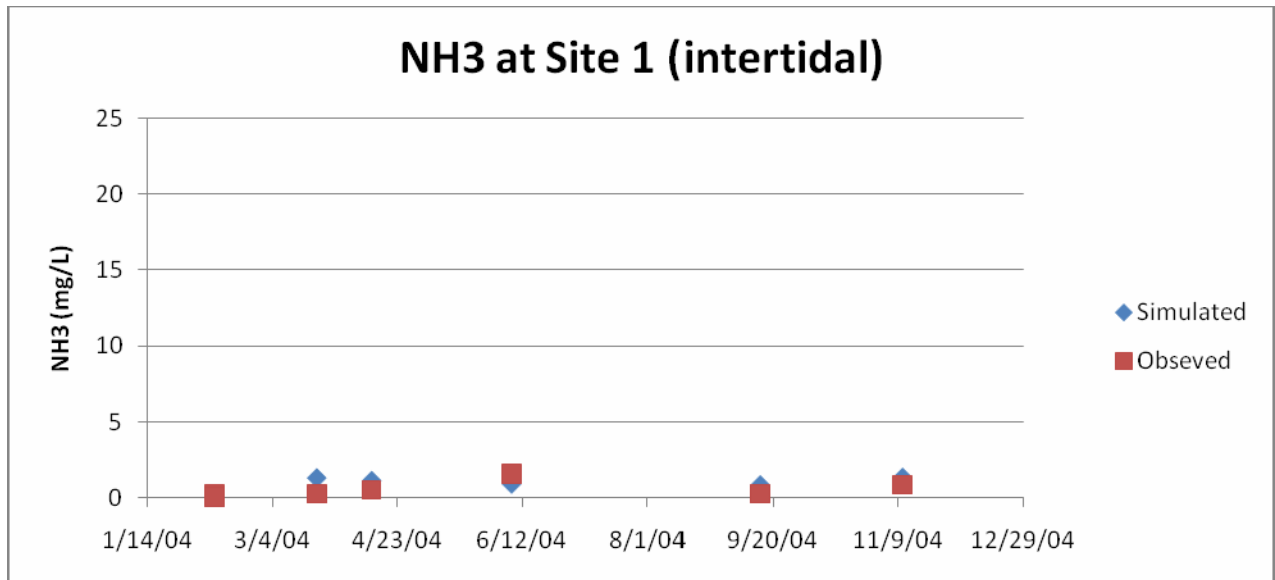


Figure 5-132 Comparison of surface sediment observed (0-1 cm) and computed (up to 10 cm) NH3 at the intertidal region of NB1 (Site 1 in Figure 5-131).

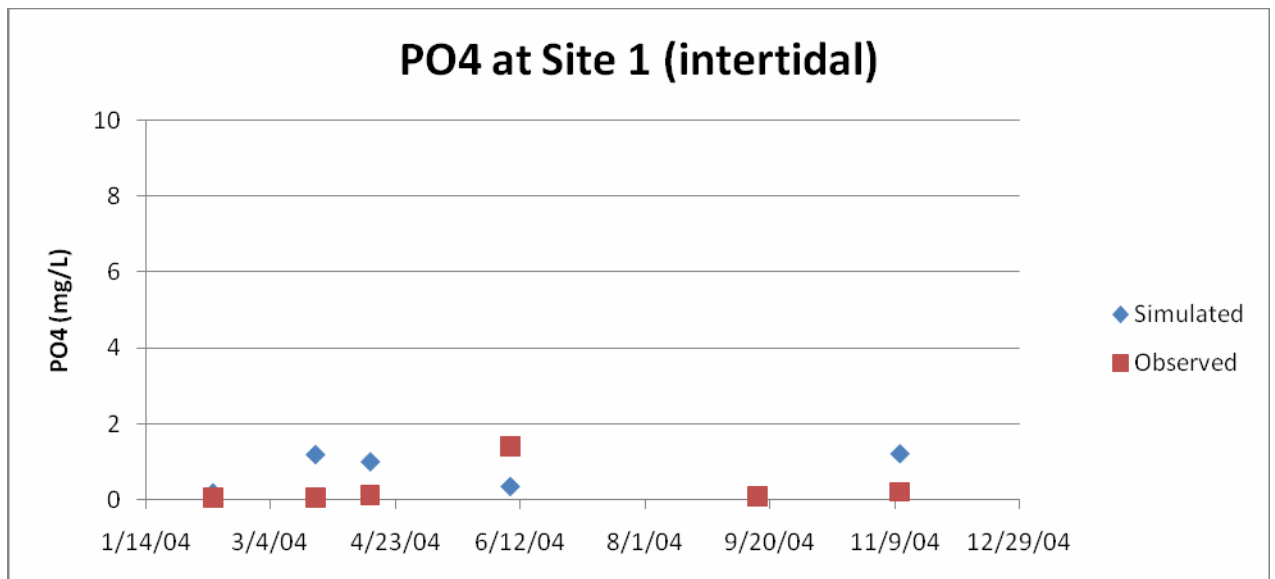


Figure 5-133 Comparison of surface sediment observed (0-1 cm) and computed (up to 10 cm) PO4 at the intertidal region of NB1 (Site 1 in Figure 5-131).

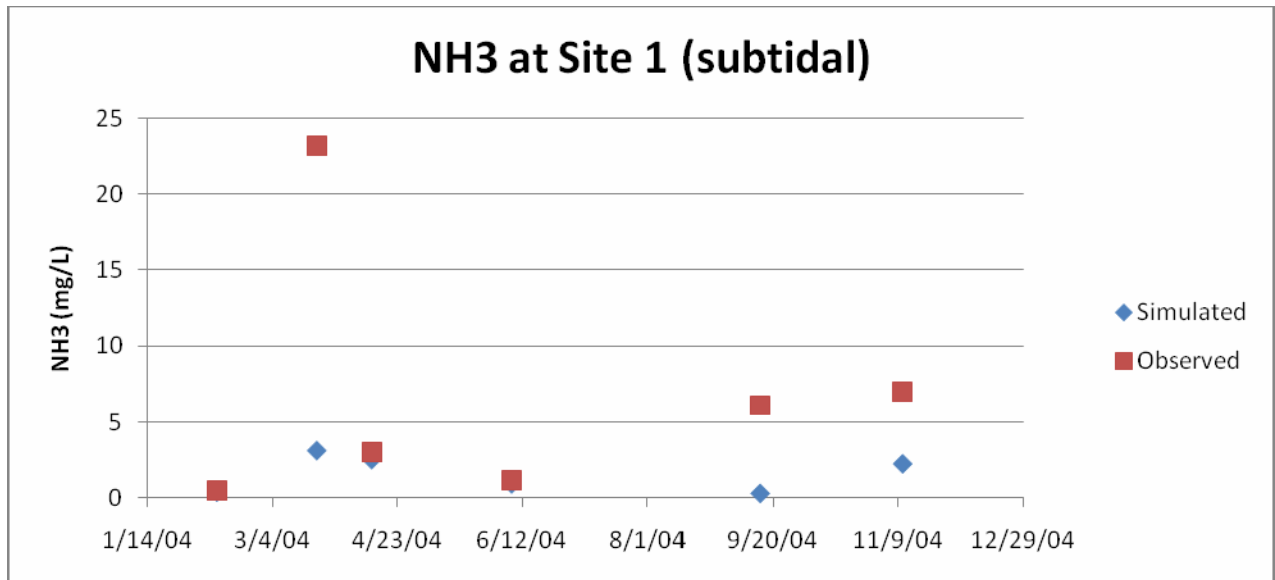


Figure 5-134 Comparison of surface sediment observed (0-1 cm) and computed (up to 10 cm) NH3 at the subtidal region of NB1 (Site 1 in Figure 5-131).

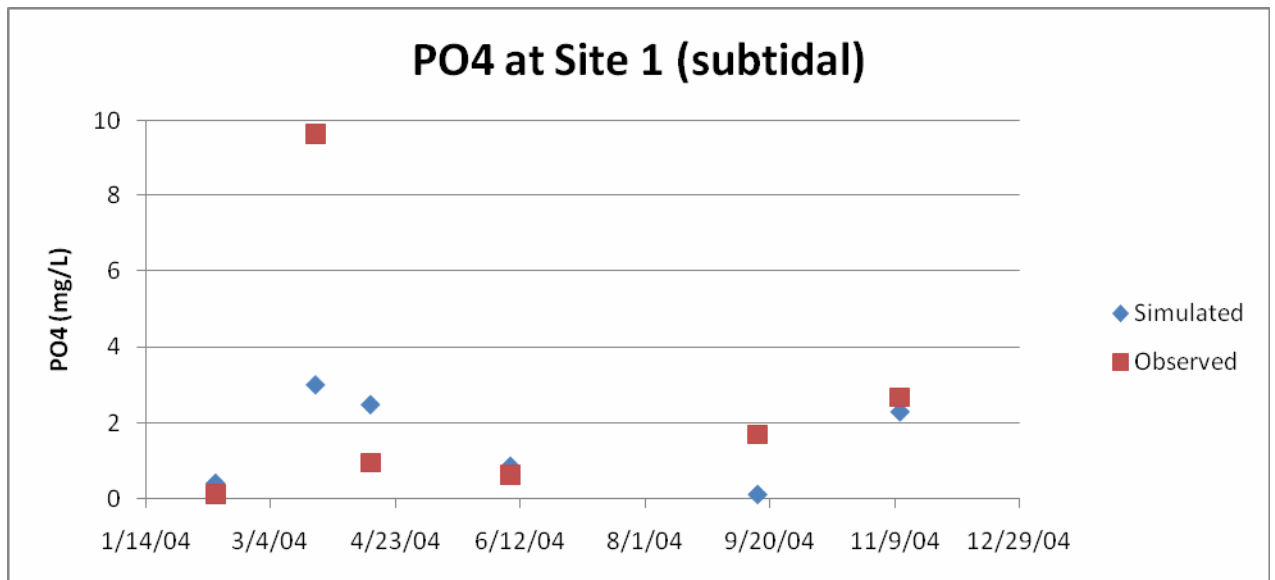


Figure 5-135 Comparison of surface sediment observed (0-1 cm) and computed (up to 10 cm) PO4 at the subtidal region of NB1 (Site 1 in Figure 5-131).

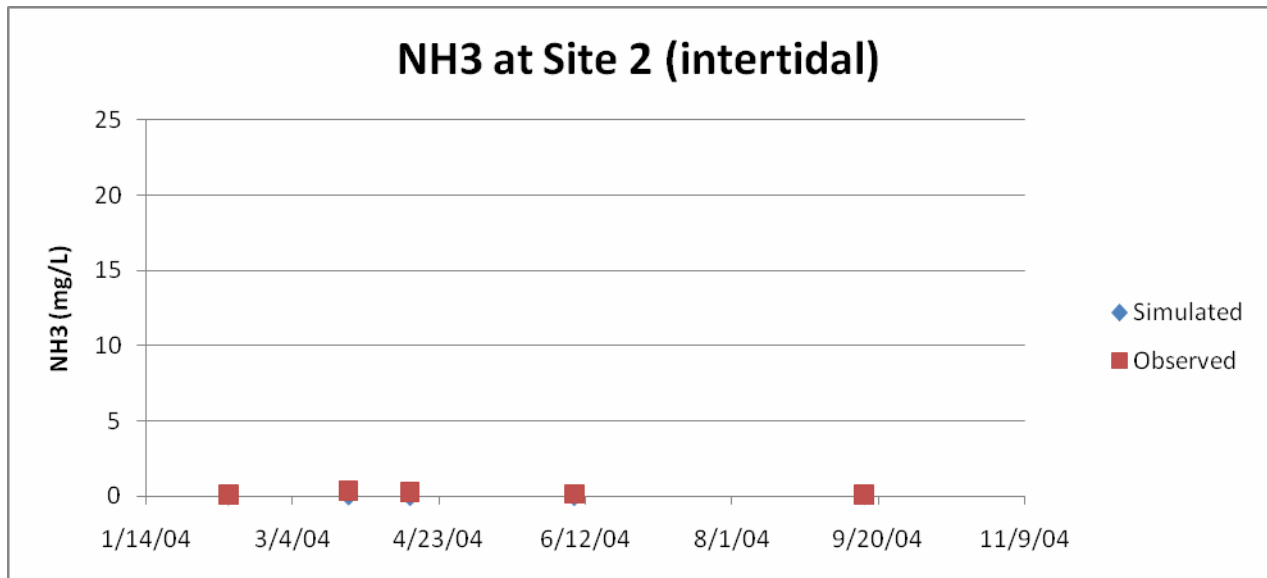


Figure 5-136 Comparison of surface sediment observed (0-1 cm) and computed (up to 10 cm) NH3 at the intertidal region of NB2 (Site 2 in Figure 5-131).

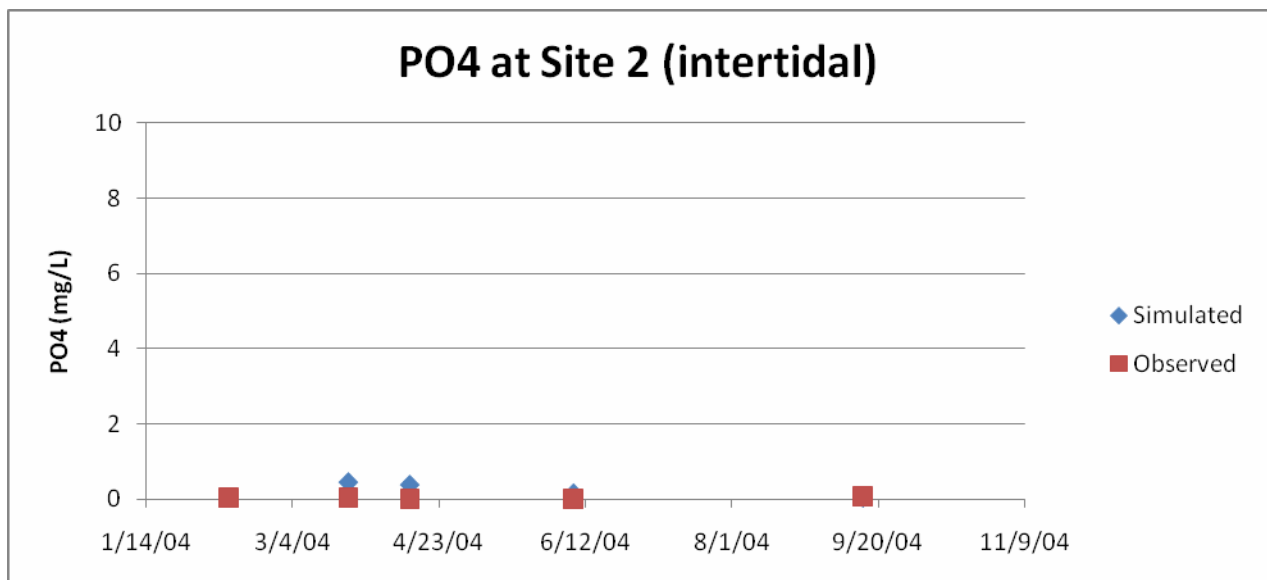


Figure 5-137 Comparison of surface sediment observed (0-1 cm) and computed (up to 10 cm) PO4 at the intertidal region of NB2 (Site 2 in Figure 5-131).

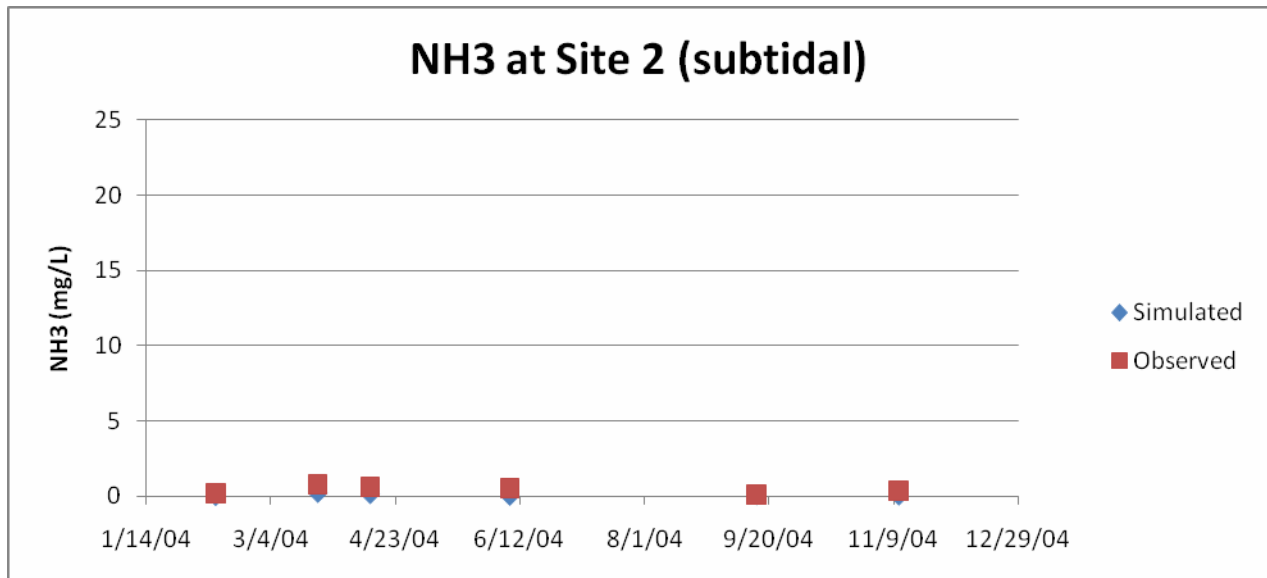


Figure 5-138 Comparison of surface sediment observed (0-1 cm) and computed (up to 10 cm) NH3 at the subtidal region of NB2 (Site 2 in Figure 5-131).

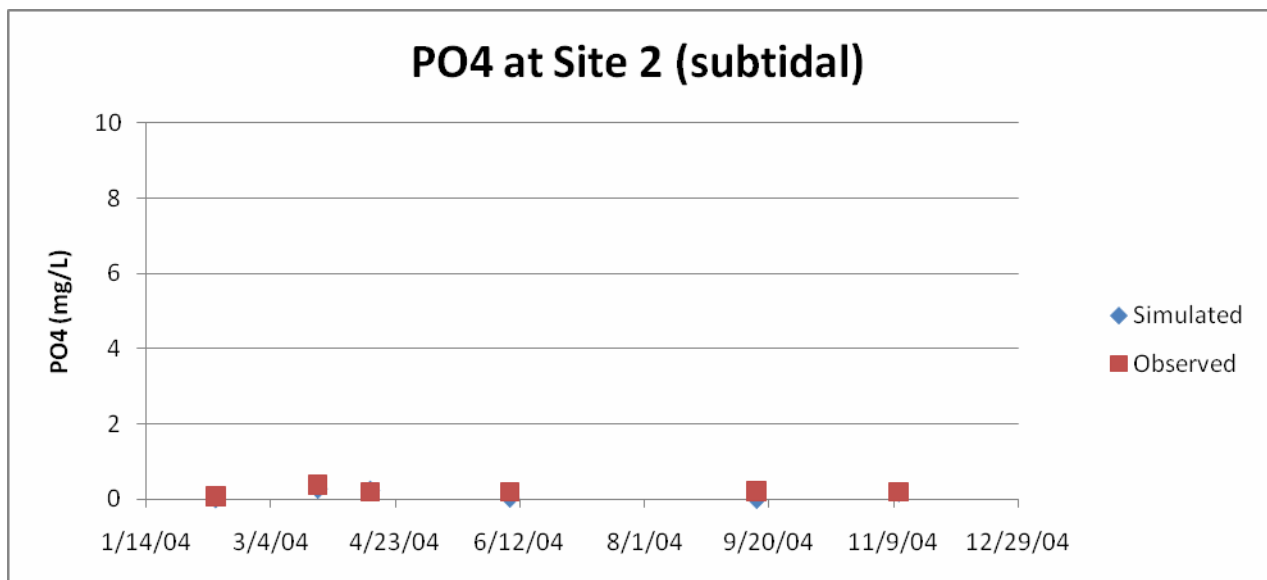


Figure 5-139 Comparison of surface sediment observed (0-1 cm) and computed (up to 10 cm) PO4 at the subtidal region of NB2 (Site 2 in Figure 5-131).

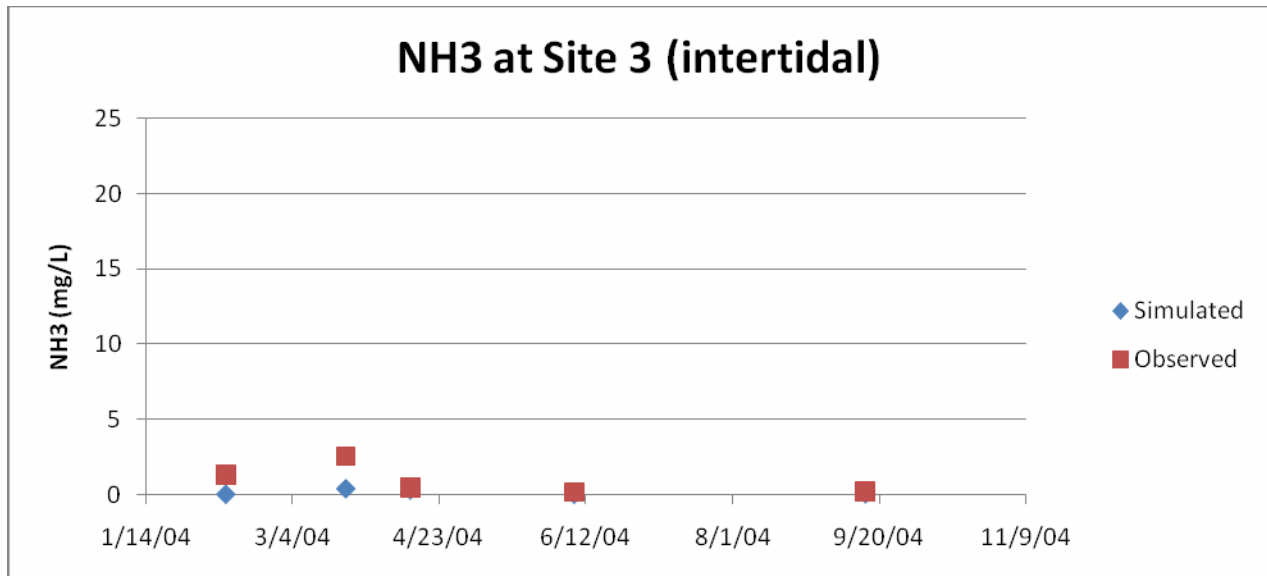


Figure 5-140 Comparison of surface sediment observed (0-1 cm) and computed (up to 10 cm) NH3 at the intertidal region of NB3 (Site 3 in Figure 5-131).

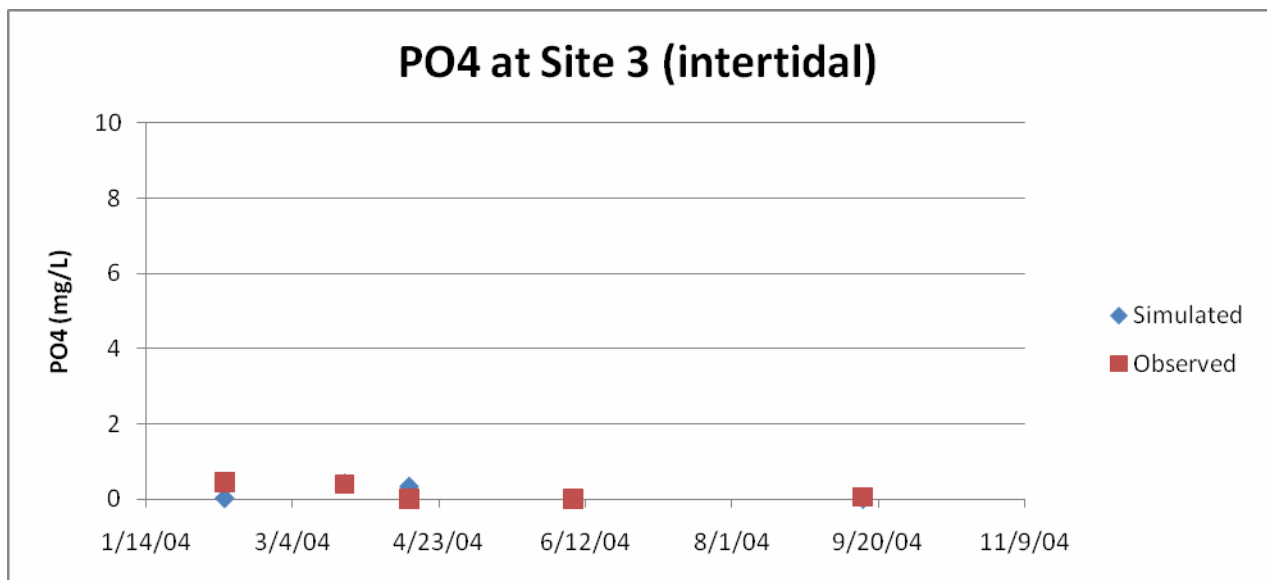


Figure 5-141 Comparison of surface sediment observed (0-1 cm) and computed (up to 10 cm) PO4 at the intertidal region of NB3 (Site 3 in Figure 5-131).

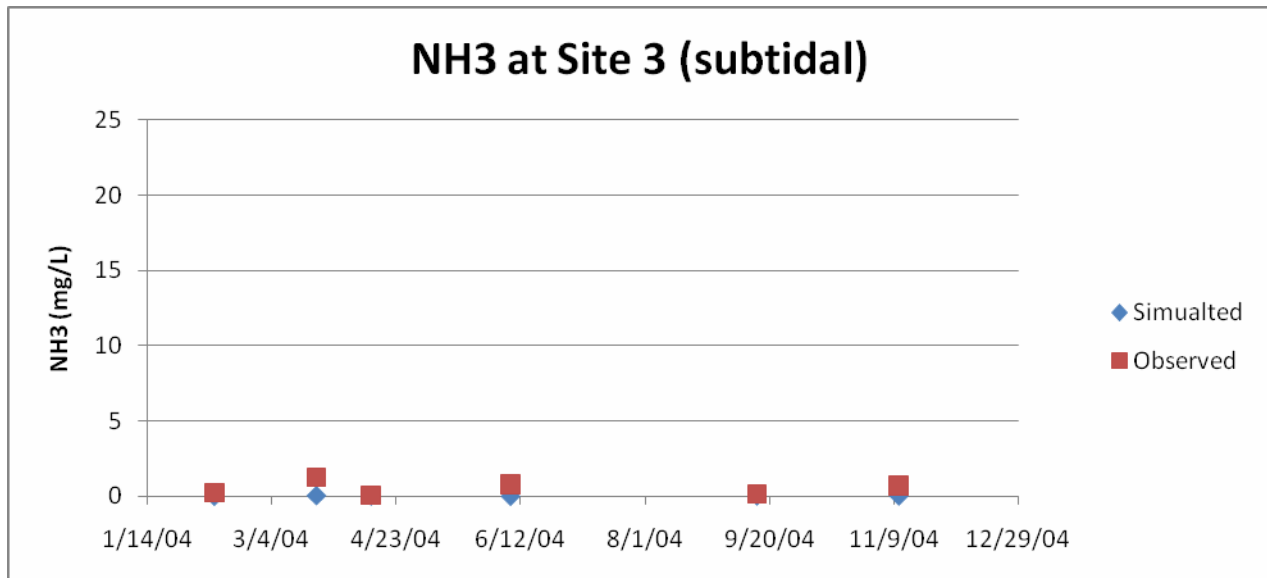


Figure 5-142 Comparison of surface sediment observed (0-1 cm) and computed (up to 10 cm) NH3 at the subtidal region of NB3 (Site 3 in Figure 5-131).

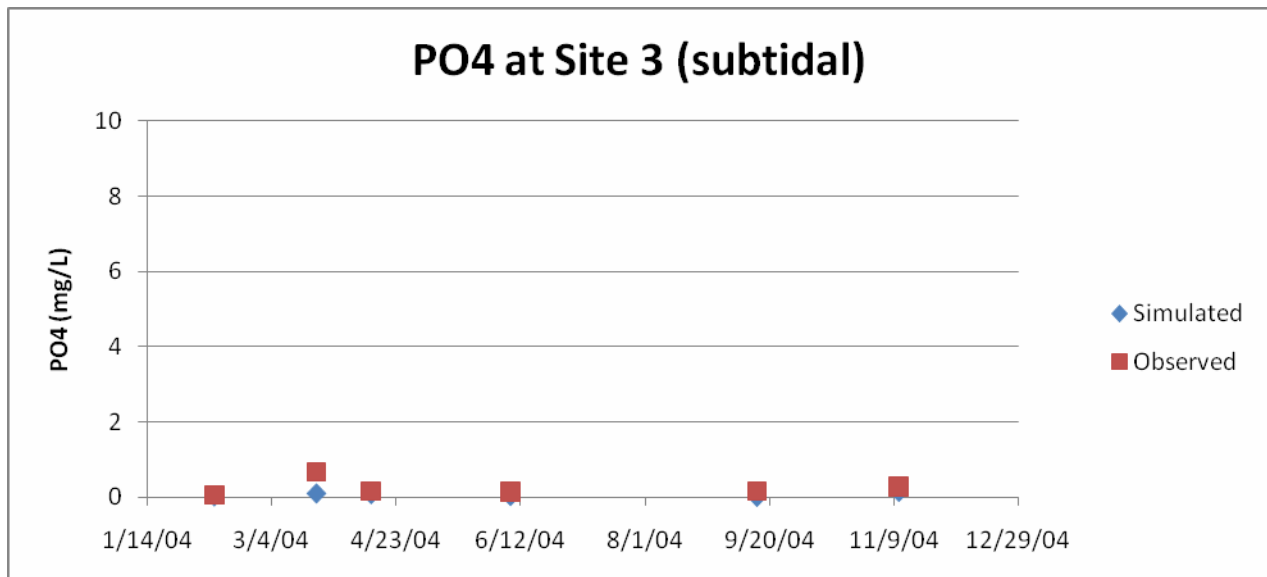


Figure 5-143 Comparison of surface sediment observed (0-1 cm) and computed (up to 10 cm) PO4 at the subtidal region of NB3 (Site 3 in Figure 5-131).

5.6 Limiting factors for macroalgae growth

Four of the limiting factors of macroalgae growth (light, internal nitrogen, phosphorus and freshwater stress) are plotted for each of the monitoring stations and for each year during the calibration/validation period in Figure 5-144 through Figure 5-147. These plots show the relative importance of each of the four factors. Note that these are not the only limitation factors in the model formulation. For example temperature limitation, not included in these plots, becomes of primary importance during the winter.

5.6.1 Limiting factors in 2004

Four limiting factors of macroalgae growth in 2004 are plotted for three macroalgae monitoring stations (i.e., head (Station ALG19), mid (Station ALG13) and lower part (Station ALG7) of the Bay) in Figure 5-144. These plots indicate that nitrogen is the primary limiting factor among the four during March through early June and November through December. Nitrogen has been considered as limiting nutrient in eutrophic coastal marine ecosystems (Howarth and Marino, 2006). During February and June through early August, nitrogen and phosphorus limitation are alternately important and dependent on location. During January and mid-August through mid-October, phosphorus limitation dominates. Phosphorus limitation occurs more often at locations lower in the Bay. Kamer et al. (2002) also found that nitrogen as the primary limiting nutrient with phosphorus being secondary in the Newport Bay. Even though none of the experiments produced biomass increases with phosphorus addition only, addition of phosphorus stimulated growth when supplied with nitrogen. Freshwater stress becomes important during storm periods. Light is limiting every night but seldom during the day.

5.6.2 Limiting factors in 2005

Four limiting factors of macroalgae growth in 2005 are plotted for three macroalgae monitoring stations (i.e., head, mid and lower part of the Bay) in Figure 5-145. These plots indicate that nitrogen is the primary limiting factor among the four during January through July except during storm periods when freshwater stress dominates. During August, nitrogen and phosphorus limitation are alternately important with phosphorus limitation occurring primarily at the uppermost stations. By September through the end of the year phosphorus limitation is the primary day time limitation factor. Light is limiting every night but seldom during the day.

The massive extent of the bloom in 2005 suggests that there was no significant nutrient limitation. Almost all of the available inter-tidal region was occupied by dense macroalgal mats during the peak bloom periods in summer and fall. To take a closer look at this period, Figure 5-146 shows a plot of the actual values of light, internal nitrogen, phosphorus, space and temperature limitation at the head of the Bay (ALG 19). What this plots show is that in this area of most dense macroalgal growth, the space limitation factor (not included in Figure 5-145) becomes dominant during July and August. Space limitation only becomes dominant at the head of the Bay during the summer of 2005, and not all elsewhere in the Bay, or during 2004 or 2006.

5.6.3 Limiting factors in 2006

Four limiting factors of macroalgae growth in 2006 are plotted for three macroalgae monitoring stations (i.e., head, mid and lower part of the Bay) in Figure 5-147. These plots indicate that phosphorus is the primary limiting factor among the four throughout the year at the stations lower in Newport Bay. At these stations there are some brief periods of nitrogen limitation during January, March and April. The uppermost stations are also primarily dominated by phosphorus limitation, however during March through mid-July nitrogen and phosphorus limitation are alternately important. Freshwater stress becomes important during storm periods. Light is limiting every night but seldom during the day.

This is a confounding result as nitrogen concentrations/loads in 2006 were reduced as compared to 2005. So there must have been a proportionally greater decline in phosphorus availability.

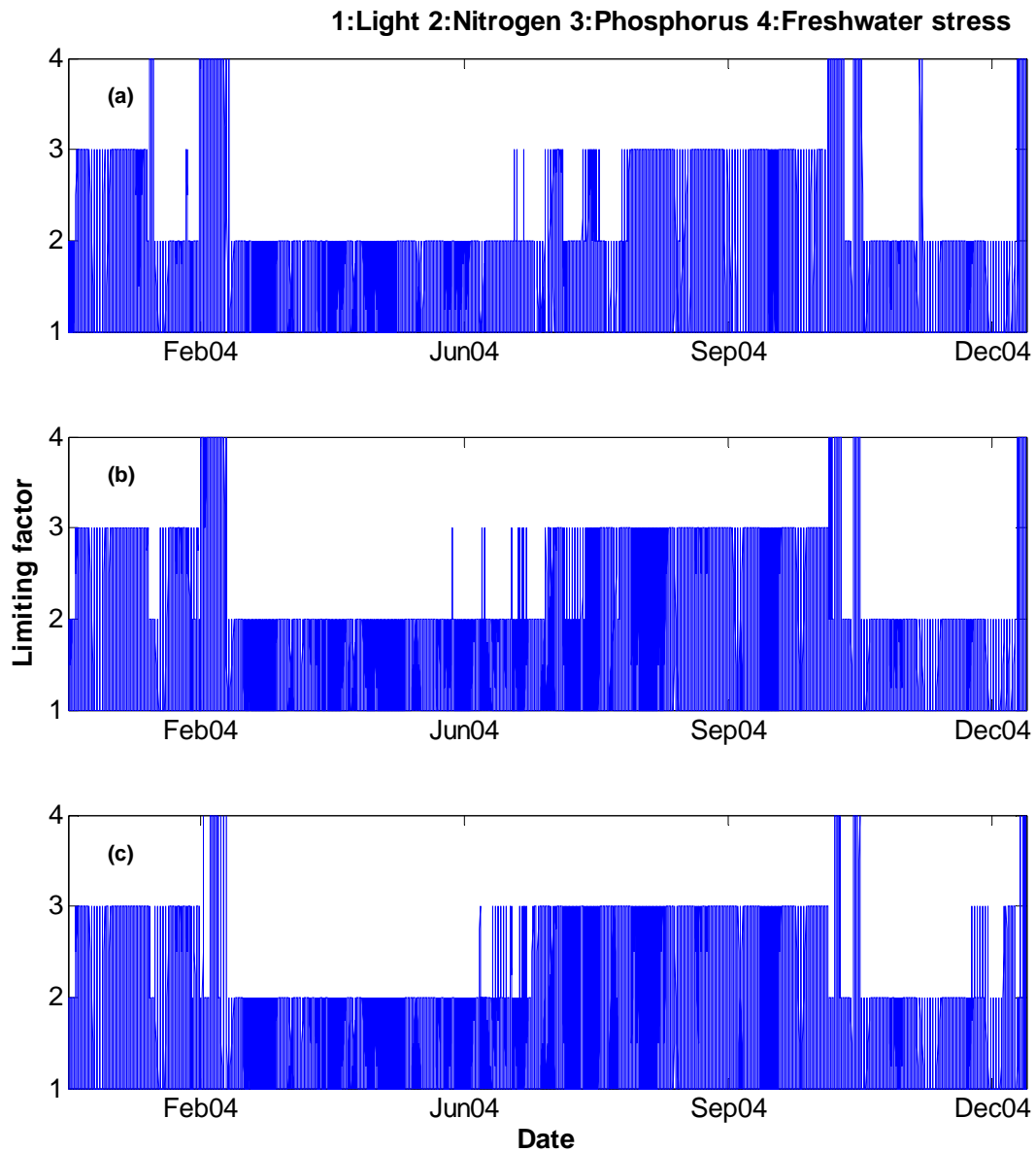


Figure 5-144 Limiting factors of macroalgae growth at each monitoring stations in 2004. The values of one, two, three and four indicate light limiting, internal nitrogen, phosphorus and freshwater stress, respectively. (a) Station ALG19; (b) Station ALG13; (c) Station ALG7.

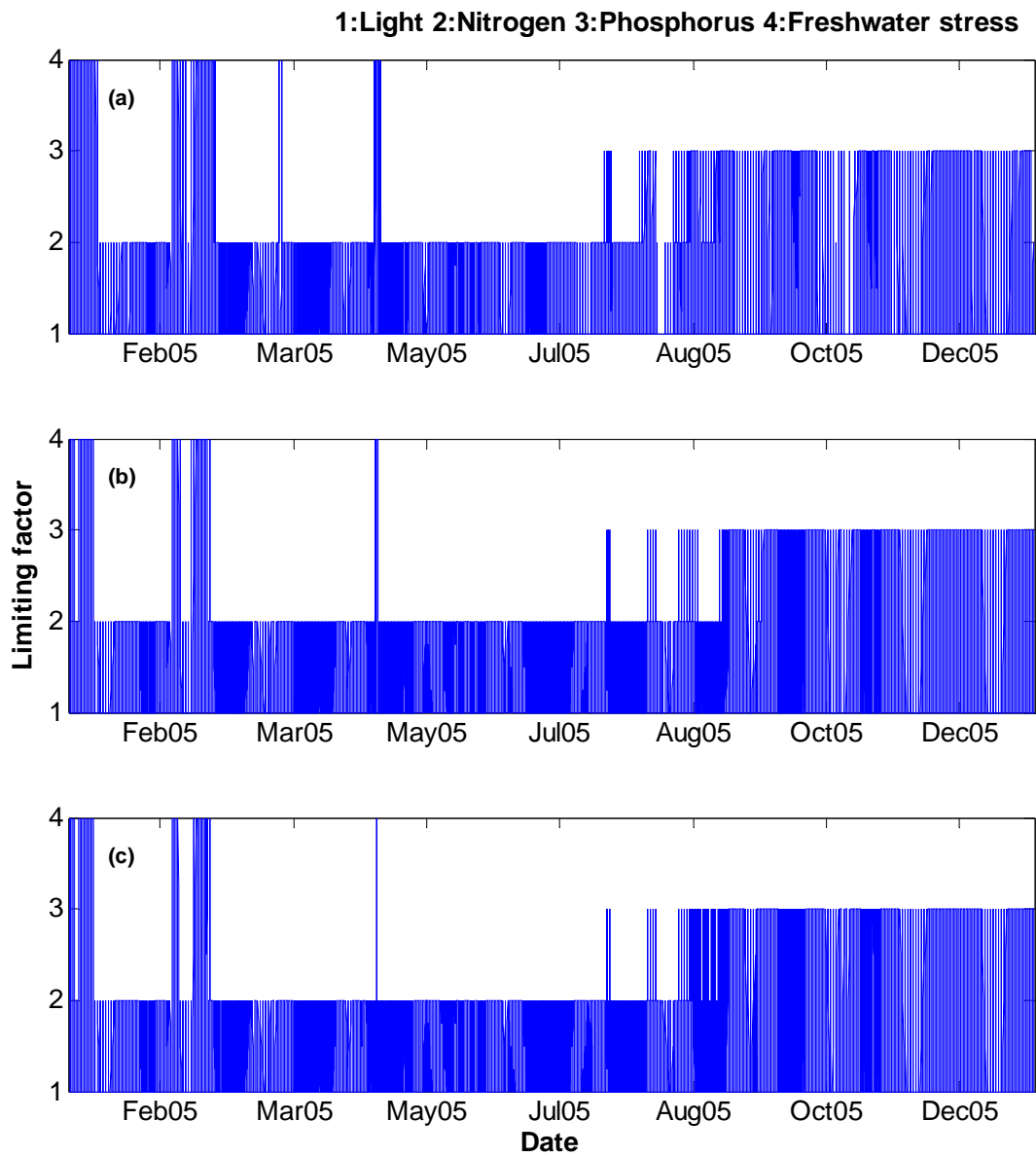


Figure 5-145 Limiting factors of macroalgae growth at each monitoring stations in 2005. The values of one, two, three and four indicate light limiting, internal nitrogen, phosphorus and freshwater stress, respectively. (a) Station ALG19; (b) Station ALG13; (c) Station ALG7.

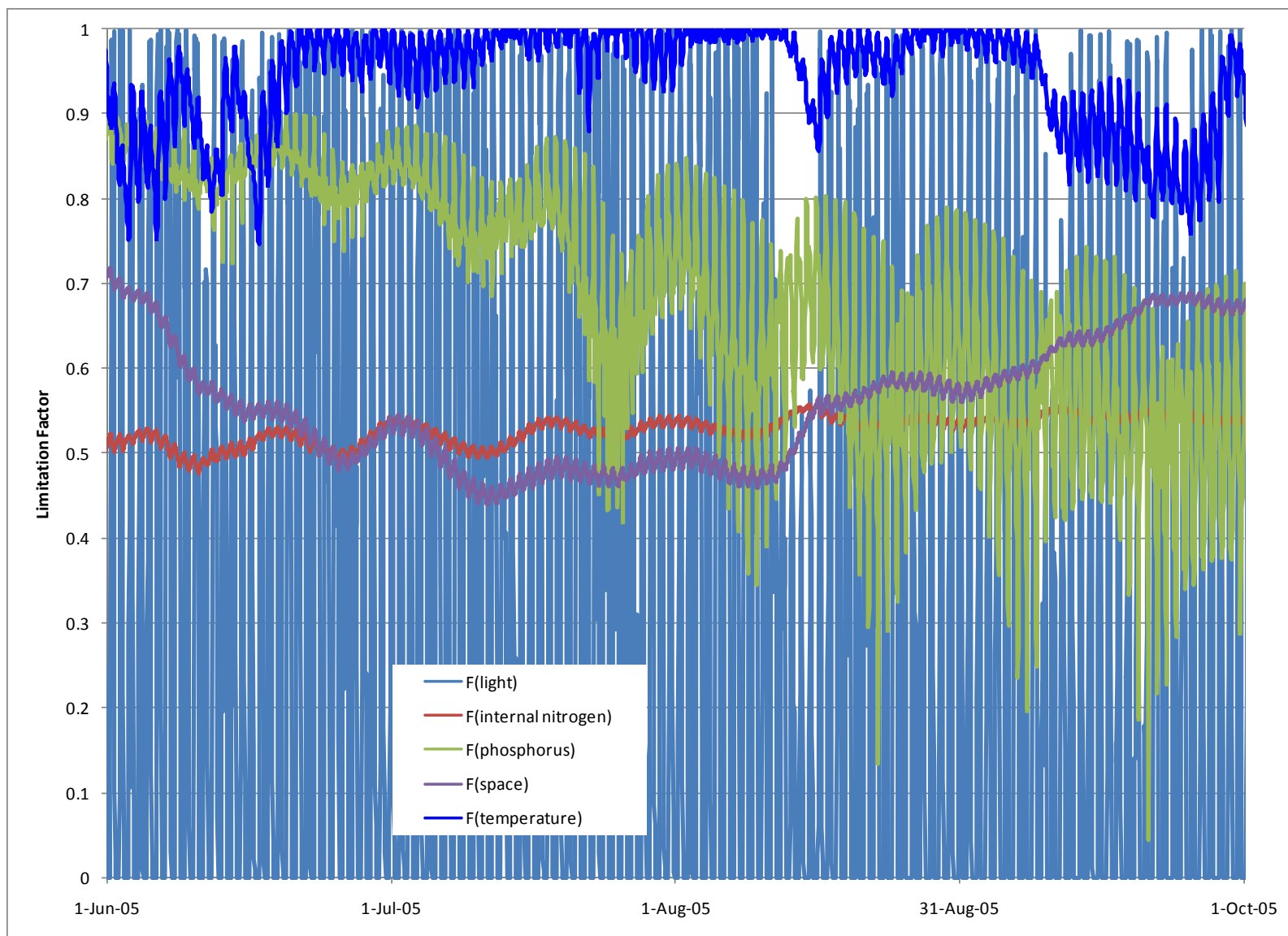


Figure 5-146 Time series plot of light, internal nitrogen, phosphorus, space and temperature limitation factors at Station ALG19 during summer 2005.

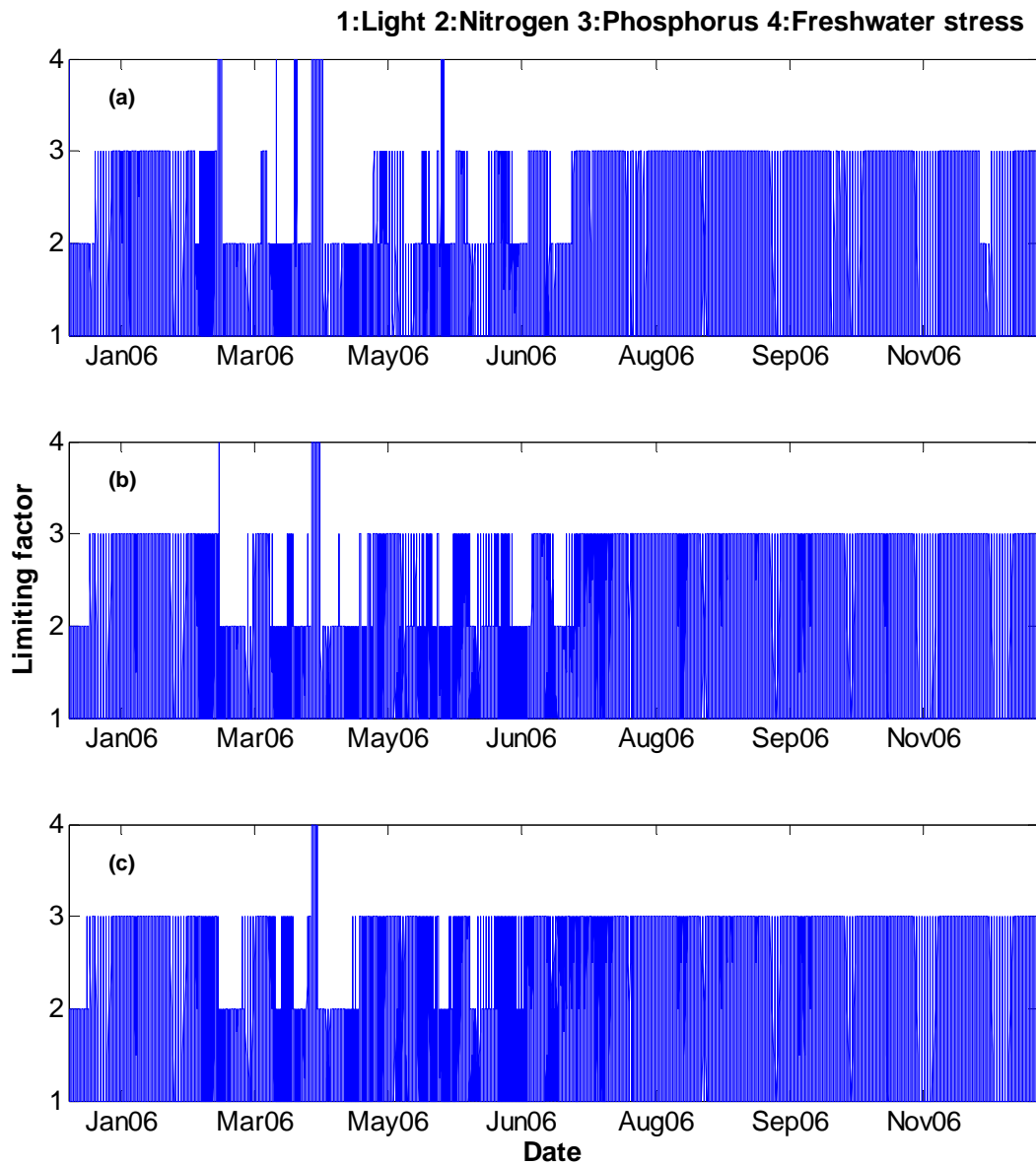


Figure 5-147 Limiting factors of macroalgae growth at each monitoring stations in 2006. The values of one, two, three and four indicate light limiting, internal nitrogen, phosphorus and freshwater stress, respectively. (a) Station ALG19; (b) Station ALG13; (c) Station ALG7.

5.7 Nutrient cycles in Newport Bay: Discussion of nutrient budgets

Nutrient budgets of nitrogen and phosphorus were estimated based on model simulations from 2004 through 2006. The regional area for the budgets is the same as that of the model simulation including from Unit 1 Basin to harbor entrance. The budgets consider two inflows including Santa Ana Delhi Channel and San Diego Creek, and a tidal outflow at the harbor entrance. The model was based on calendar years, therefore loads generated by the stormy winter of 2004-2005 are split between 2004 and 2005, assuming that late fall storms do not contribute significantly to nutrient supply for the following summer.

5.7.1 Nitrogen

The nitrogen budget consists of two inflows as sources, and one outflow and denitrification as sinks. The differences between sources and sinks for each year are the net changes in nitrogen in the water column and sediments plus nitrogen that has been taken up by macroalgae, which either remains in the Bay or has been removed from the system. The total inflows, outflows, denitrification and net changes for each year are listed in Table 5-5.

Nitrogen-containing suspended sediments coming from inflows are deposited on the bed. These deposited organic sediments are decayed and release dissolved nitrogen into the water, adding to the water column dissolved nitrogen from the creek flows. The cumulative contributions of total nitrogen to the system for each of the three calibration years are shown as time series in Figure 5-148, Figure 5-150 and Figure 5-152.

Time series of nitrogen distribution in the Bay are plotted for each year in Figure 5-149, Figure 5-151 and Figure 5-153, respectively. As nitrogen enters the system, these plots show how it is distributed in the Bay. Any buried sediment is cumulative because once it is buried it is permanently lost from the system. The active sediment layer increases when storm inflows deposit sediment, and decreases as nitrogen is released to the water column. Sloughing and non-recycled dead macroalgae is cumulative because nitrogen is permanently lost from the system. Nitrogen in the macroalgae rises and falls based on macroalgae growth dynamics. Water column concentrations vary, with the largest changes resulting from increased inflows. Nitrogen that exits the ocean boundary and denitrification are both cumulative as they are permanent losses from the system.

The final cumulative total of nitrogen at the end of each year in the distribution plots is equal to the end of year total of nitrogen in the inflows for each year in Figure 5-148, Figure 5-150 and Figure 5-152. Looking back at the net changes in Table 5-5, the net change for each year is equal to the sum of the nitrogen in the buried sediment, active sediment layer, macroalgae, sloughed and non-recycled dead macroalgae and the water column.

5.7.1.1 Sources

- **Inflows**

Daily discharges of Santa Ana Delhi Channel (SADF01) and San Diego Creek at Campus Drive (SDMF05) were multiplied by their nitrogen constituent concentrations. These concentrations are the same as the inflow inputs. The amount of total nitrogen of inflows is shown in Table 5-5.

- **Minor sources**

Potential sources of unknown magnitude include groundwater and non-point sources. Groundwater can be considered negligible at less than 24 m³/day (Worsnopp et al). In addition, nitrogen data from wells adjacent to the bay show nitrogen concentrations average less than 1 mg/L (personal communication with Santa Ana Regional Water Quality Control Board). Combining these two sources of information, the max load would be less than 10 kg/yr (22 lbs/yr). Other minor sources that have been neglected include small drainages – Bonita Canyon, Costa Mesa Channel, Santa Isabella Channel, Big Canyon, and seepage from bluffs at south end of bay (e.g., for Costa Mesa Channel is 259 kg/yr (572 lbs/yr) TN dry season average, 389 kg/yr (858 lbs/yr) wet season average). In the nitrogen budget, minor sources are not considered.

Tidal mixing is a source of nitrogen in the Bay, however this is difficult to quantify with available data.

5.7.1.2 Sinks

- **Outflow**

Daily discharge from Newport Bay was calculated in the model. This discharge was multiplied by the computed nitrogen constituent concentrations at the tidal boundary. The amount of total nitrogen in the outflow is about 299,506,215 lbs/yr.

- **Denitrification**

Denitrification of nitrate to N₂ is estimated in the model as previously described in section 3.2. The amount of total nitrogen lost from the system due to denitrification is about 40,045,021 lbs/yr. It is interesting that the denitrification rate didn't increase greatly in 2005, which could be explained by the efficient uptake of nitrate by the large macroalgal bloom that year. This likely minimized the pool of nitrate available for denitrification. Low denitrification rates were also observed in the intertidal region of the Bay (personal communication with Peggy Fong and Tonya Kane).

5.7.2 Phosphorus

The phosphorus budget consists of two sources (i.e., two inflows) and a sink (one outflow) and includes phosphate and particulate phosphorus. As with the nitrogen budget, the differences between sources and sinks for each year are the net changes in phosphorus in the water column and sediments plus phosphorus that has been taken up by macroalgae, which either remains in the Bay or has been removed from the system. The total inflows, outflows and net changes for each year are listed in Table 5-6.

Phosphorus-containing suspended sediments coming from inflows are deposited on the bed. These deposited organic sediments are decayed and release dissolved phosphorus into the water, adding to water column dissolved phosphorus from the creek flows. The cumulative contributions of phosphorus to the system for each of the three calibration years are shown as time series in Figure 5-154, Figure 5-156 and Figure 5-158.

Time series of phosphorus distribution in the Bay are plotted for each year in Figure 5-155, Figure 5-157 and Figure 5-159, respectively. As phosphorus enters the system, these plots show how it is distributed in the Bay. Any buried sediment is cumulative because once it is buried it is permanently lost from the system. The active sediment layer increases when storm inflows deposit sediment, and decreases as phosphorus is released to the water column. Sloughing and non-recycled dead macroalgae is cumulative because phosphorus is permanently lost from the system. Phosphorus in the macroalgae rises and falls based on macroalgae growth dynamics. Water column concentrations vary, with the largest changes resulting from increased inflows. Phosphorus that exits the ocean boundary is cumulative as it is a permanent loss from the system.

The final cumulative total of phosphorus at the end of each year in the distribution plots is equal to the end of year total of phosphorus in the inflows for each year in Figure 5-154, Figure 5-156 and Figure 5-158. Looking back at the net changes in Table 5-6, the net change for each year is equal to the sum of the phosphorus in the buried sediment, active sediment layer, macroalgae, sloughed and non-recycled dead macroalgae and the water column.

5.7.2.1 Sources

- **Inflows**

Daily discharges of Santa Ana Delhi Channel (SADF01) and San Diego Creek at Campus Drive (SDMF05) were multiplied by their phosphorus constituent concentrations. The amount of total nitrogen of inflows is shown in Table 5-6.

Tidal mixing is an important source of phosphorus in the Bay, however this is difficult to quantify with available data.

5.7.2.2 Sinks

- **Outflow**

Daily discharge from Newport Bay was calculated in the model. This discharge was multiplied by the computed phosphorus constituent concentrations. The amount of total phosphorus of outflows is shown in Table 5-6.

Table 5-5 Newport Bay nitrogen budget for calibration years.

	Inflows (lbs)	Outflow (lbs)	Denitrification (lbs)	Net changes (lbs)
Jan, 2004 – Dec, 2004	527,000	319,000	63,000	145,000
Jan, 2005 – Dec, 2005	725,000	538,000	71,000	115,000
Jan, 2006 – Dec, 2006	271,000	174,000	54,000	43,000

Table 5-6 Newport Bay phosphorus budget for calibration years.

	Inflows (lbs)	Outflow (lbs)	Net changes (lbs)
Jan, 2004 – Dec, 2004	86,000	65,000	21,000
Jan, 2005 – Dec, 2005	172,000	169,000	3,000
Jan, 2006 – Dec, 2006	15,000	14,000	1,000

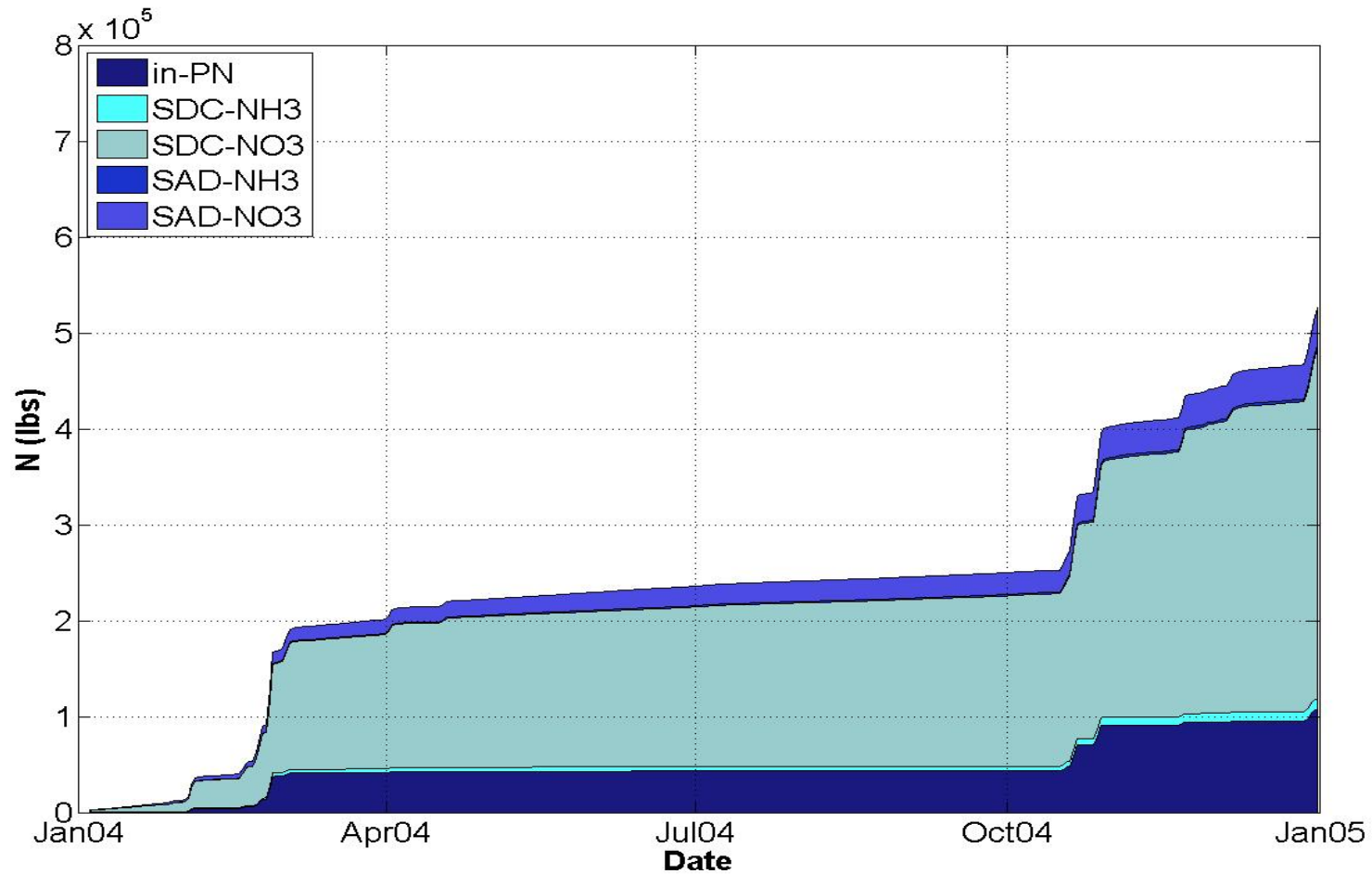


Figure 5-148. Time series of accumulated nitrogen mass into Newport Bay from January, 2004 to December, 2004 as input to the model. Very dark blue indicates particulate nitrogen from two inflows, cyan and light blue indicate NH₃ and NO₃ of San Diego Creek, respectively, and dark blue and blue indicate NH₃ and NO₃ of Santa Ana Delhi.

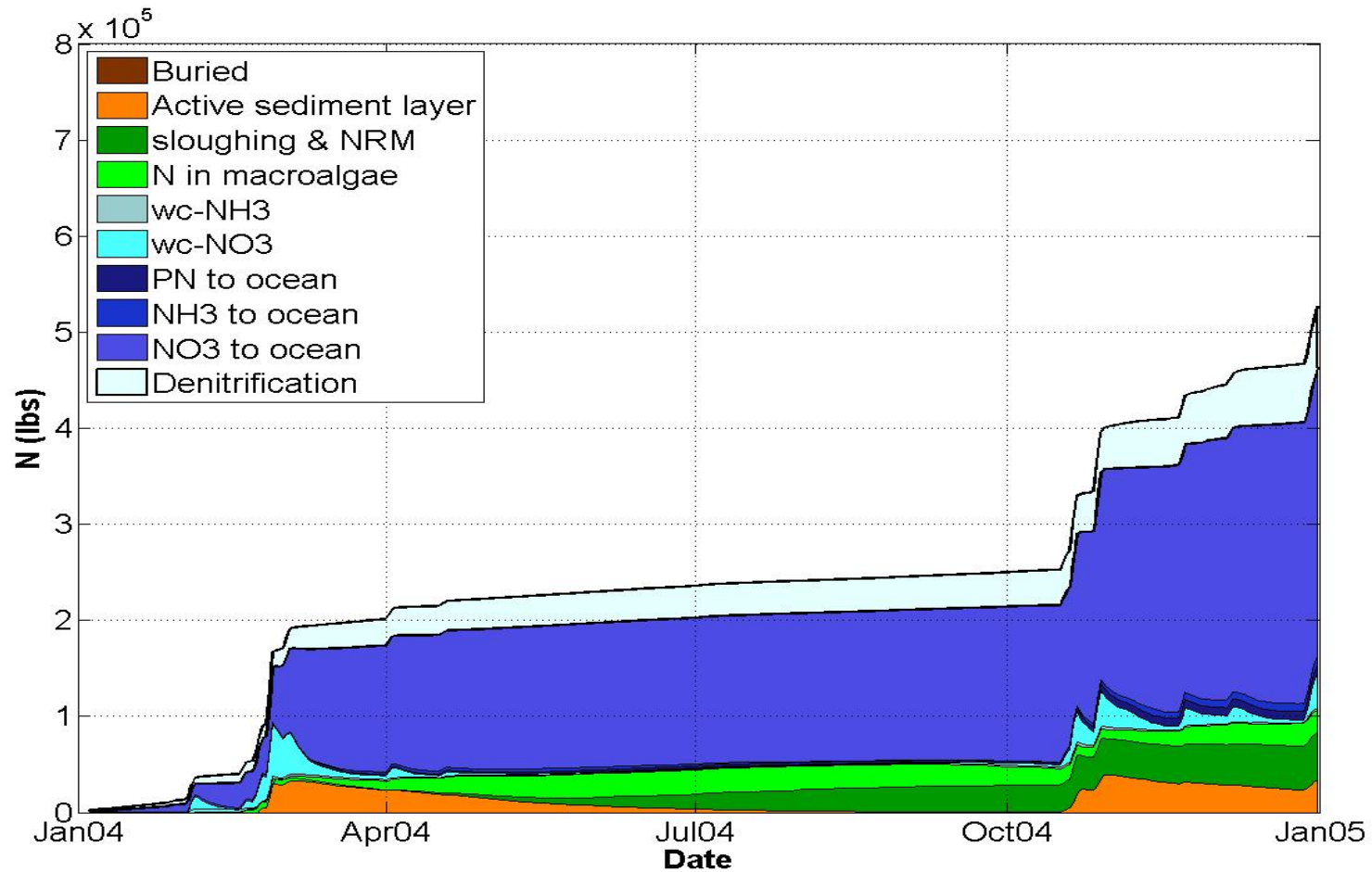


Figure 5-149. Time series of distribution of nitrogen in Newport Bay as computed in the model from January, 2004 to December, 2004. Dark brown indicates buried sediments, light brown indicates active sediment layer including N-POM, dark green indicates sloughing and non-recycled dead macroalgae (NRM), light green indicates internal nitrogen, light blue indicates NH₃ in the water column, cyan indicates NO₃ in the water column, very dark blue indicates particulate nitrogen out to the ocean, dark blue indicates NH₃ out to the ocean, blue indicates NO₃ out to the ocean and pale blue indicates denitrification.

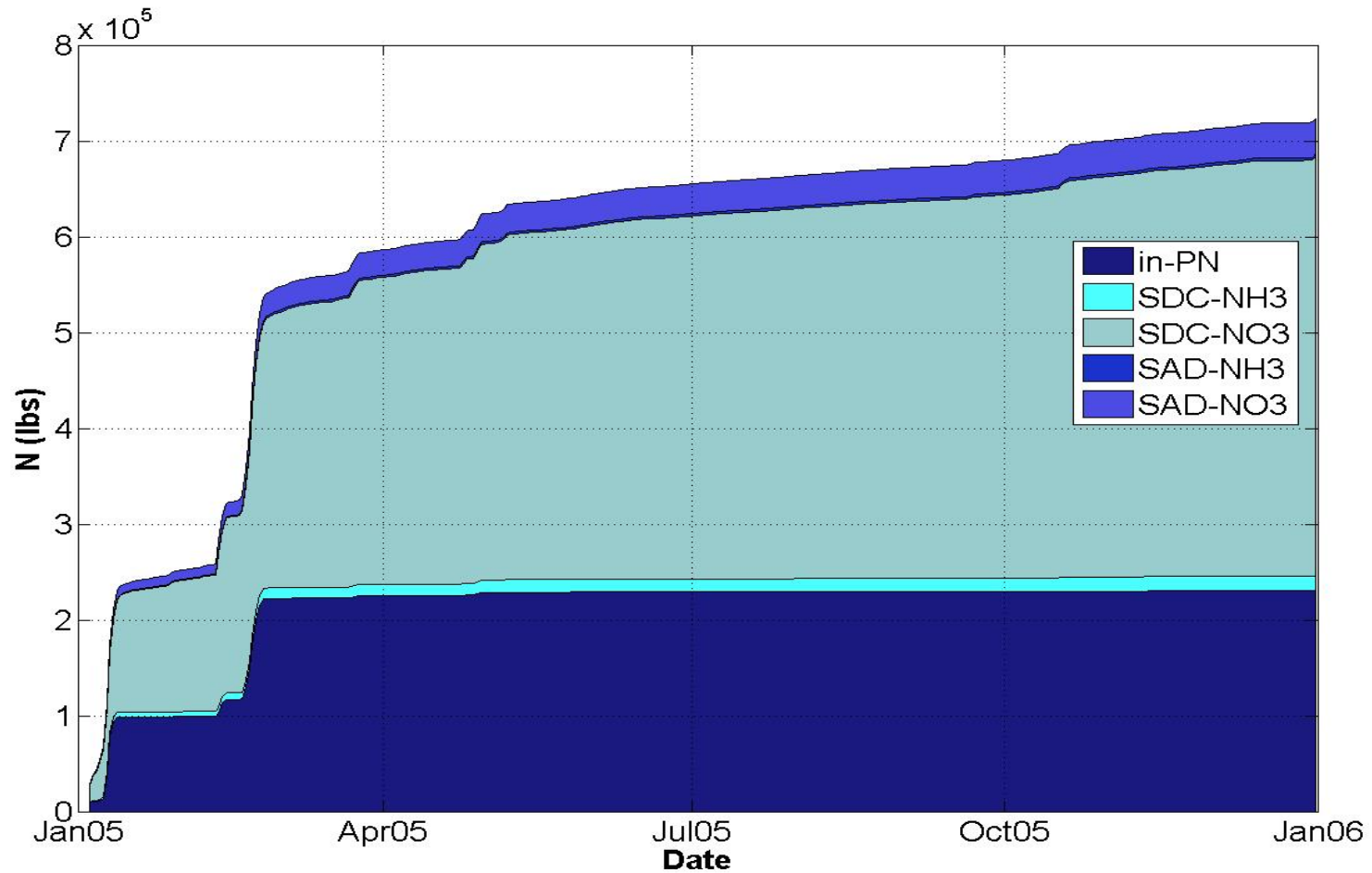


Figure 5-150. Time series of accumulated nitrogen mass into Newport Bay from January, 2005 to December, 2005 as input to the model. Very dark blue indicates nitrogen from two inflows, cyan and light blue indicate NH₃ and NO₃ of San Diego Creek, respectively, and dark blue and blue indicate NH₃ and NO₃ of Santa Ana Delhi.

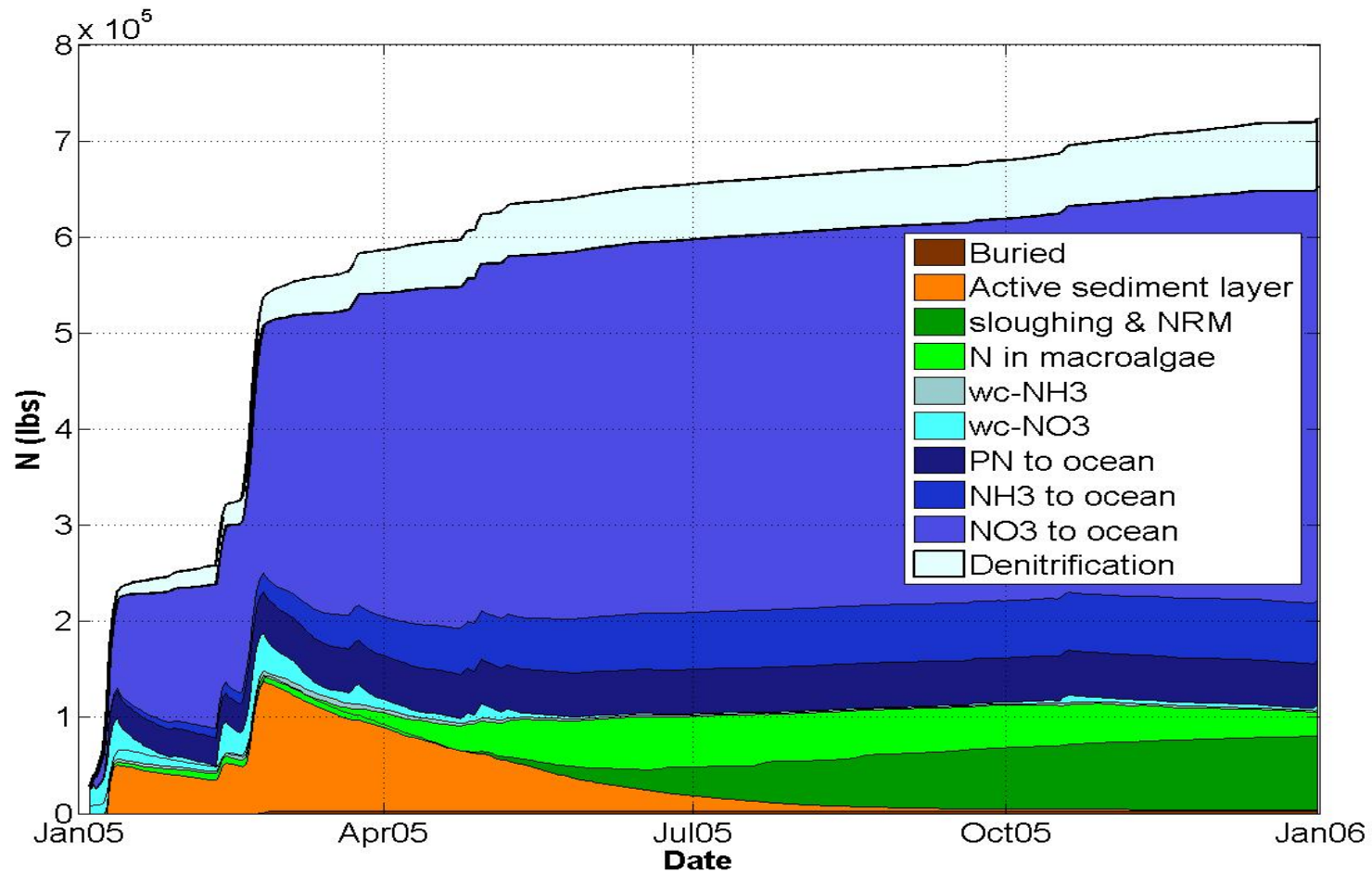


Figure 5-151. Time series of distribution of nitrogen in Newport Bay as computed in the model from January, 2005 to December, 2005. Dark brown indicates buried sediments, light brown indicates active sediment layer including N-POM, dark green indicates sloughing and non-recycled dead macroalgae (NRM), light green indicates internal nitrogen, light blue indicates NH₃ in the water column, cyan indicates NO₃ in the water column, very dark blue indicates particulate nitrogen out to the ocean, dark blue indicates NH₃ out to the ocean, blue indicates NO₃ out to the ocean and pale blue indicates denitrification.

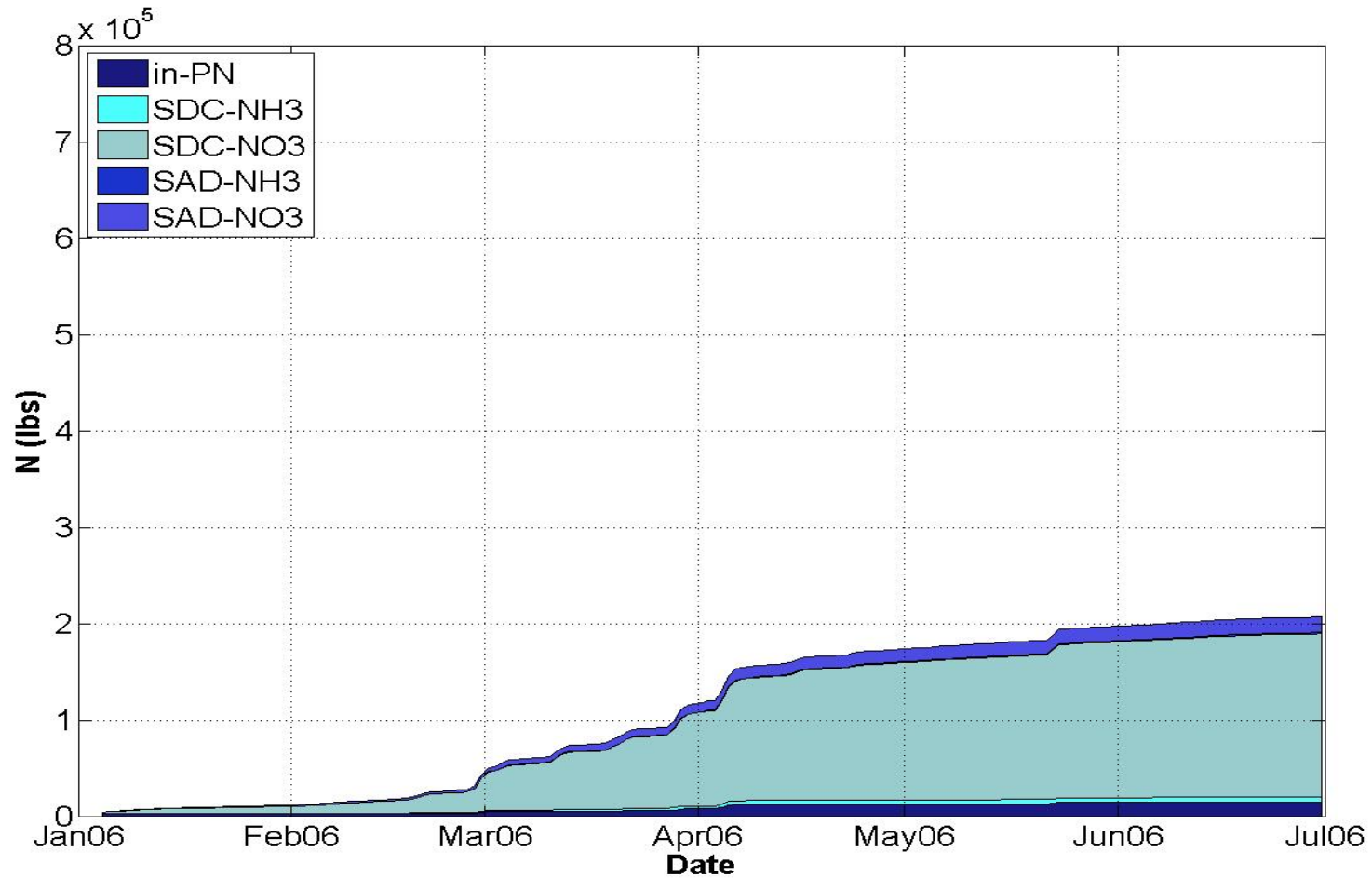


Figure 5-152. Time series of accumulated nitrogen mass into Newport Bay from January, 2006 to June, 2006 as input to the model. Very dark blue indicates nitrogen from two inflows, cyan and light blue indicate NH₃ and NO₃ of San Diego Creek, respectively, and dark blue and blue indicate NH₃ and NO₃ of Santa Ana Delhi.

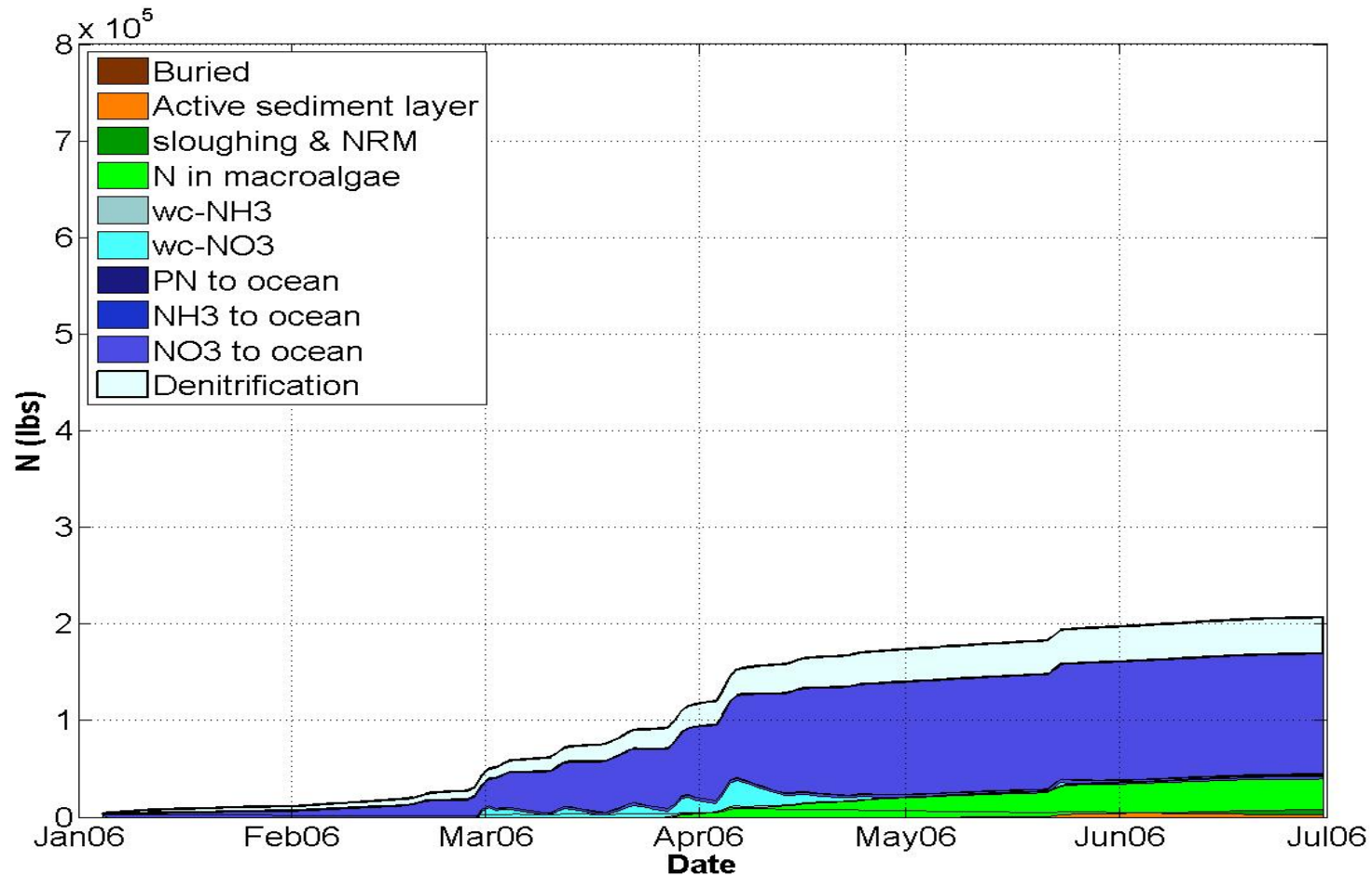


Figure 5-153. Time series of distribution of nitrogen in Newport Bay as computed in the model from January, 2006 to June, 2006. Dark brown indicates buried sediments, light brown indicates active sediment layer including N-POM, dark green indicates sloughing and non-recycled dead macroalgae (NRM), light green indicates internal nitrogen, light blue indicates NH_3 in the water column, cyan indicates NO_3 in the water column, very dark blue indicates particulate nitrogen out to the ocean, dark blue indicates NH_3 out to the ocean, blue indicates NO_3 out to the ocean and pale blue indicates denitrification.

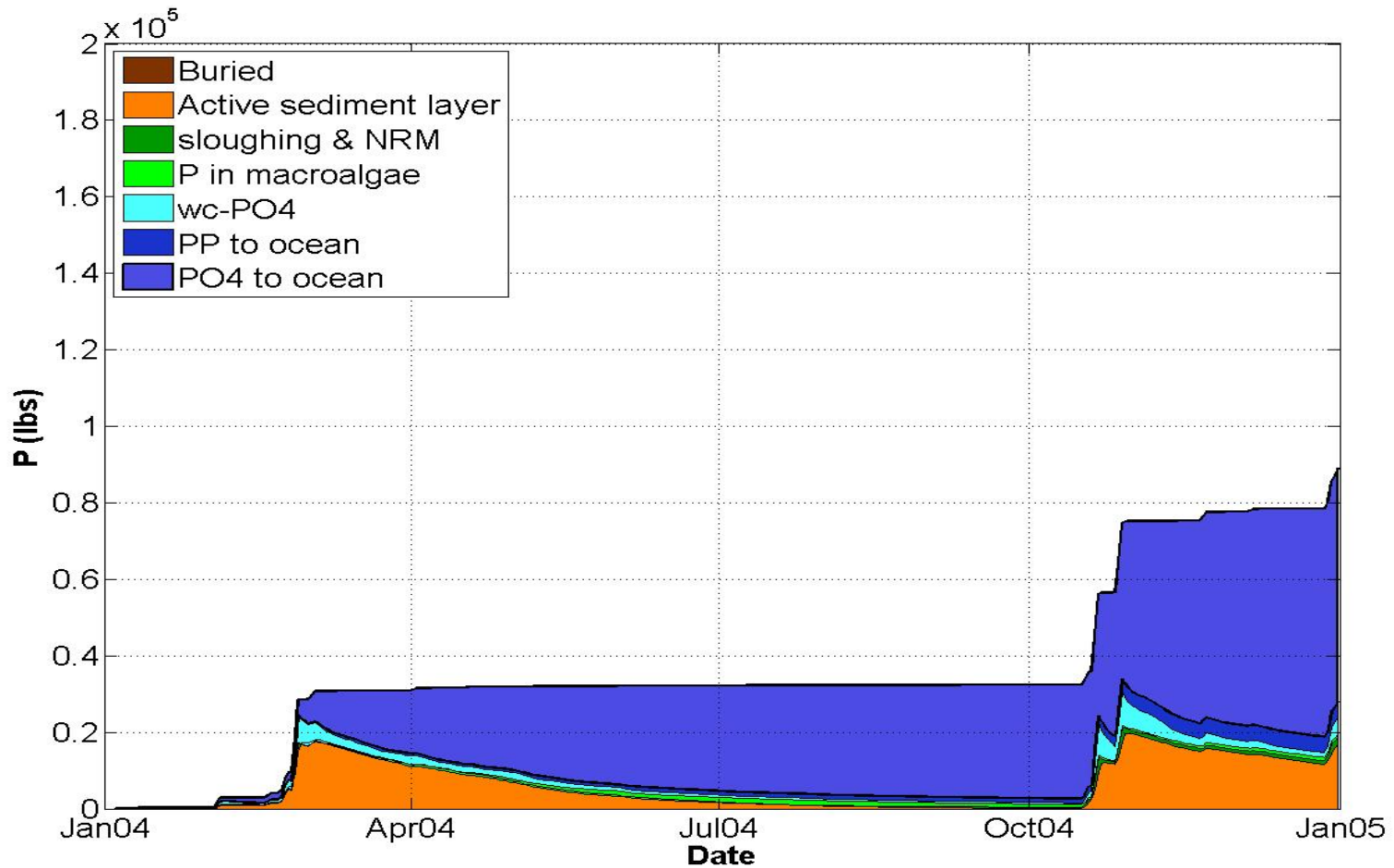


Figure 5-154. Time series of distribution of phosphorus in Newport Bay as computed in the model from January, 2004 to December, 2004. Dark brown indicates buried sediments, light brown indicates active sediment layer including P-POM, dark green indicates sloughing and non-recycled dead macroalgae (NRM), light green indicates phosphorus in macroalgae, cyan indicates PO4 in the water column, very dark blue indicates particulate phosphorus out to the ocean, and blue indicates PO4 out to the ocean.

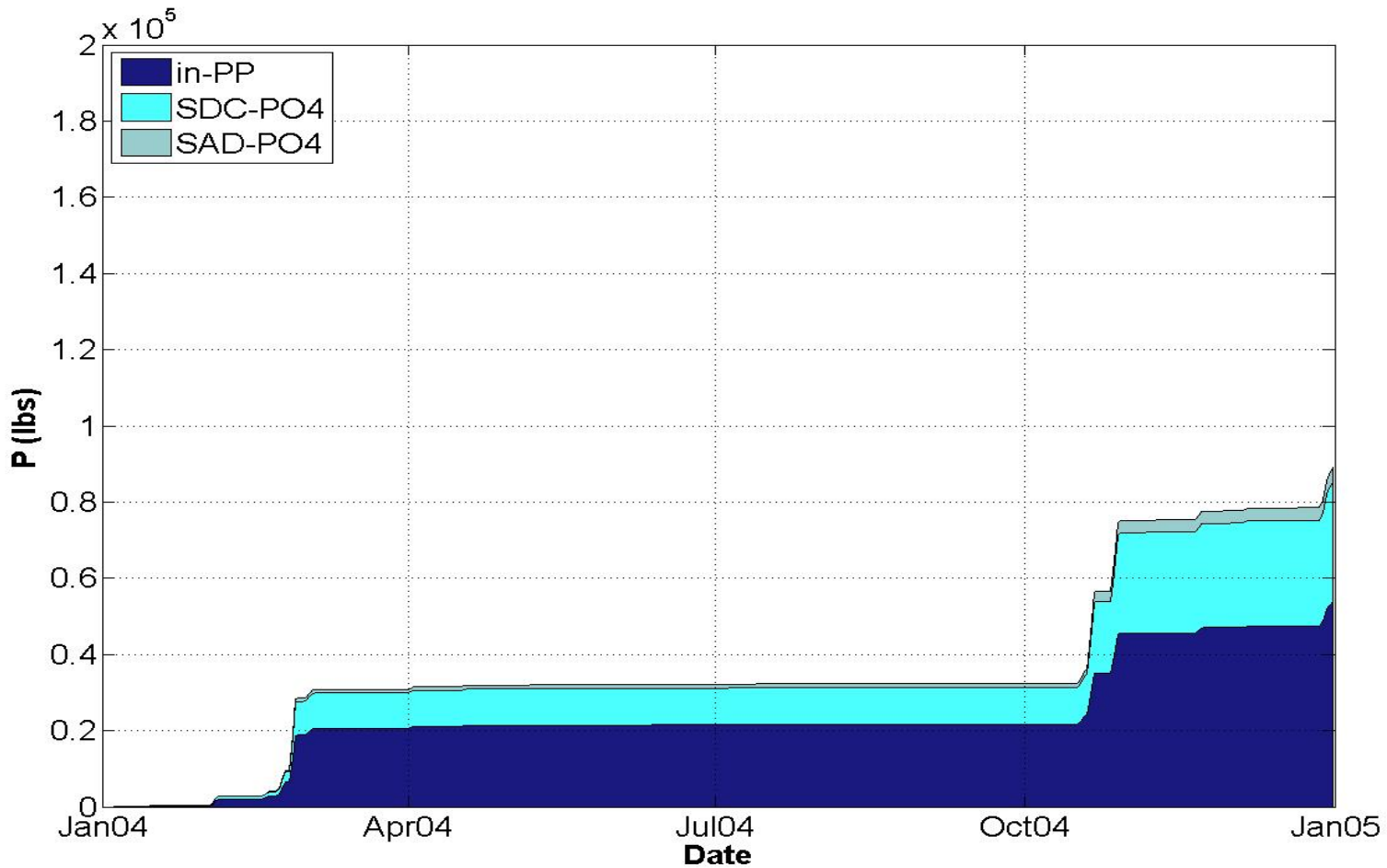


Figure 5-155. Time series of accumulated phosphorus mass into Newport Bay from January, 2004 to December, 2004 as input to the model. Very dark blue indicates particulate phosphorus from two inflows, cyan and light blue indicate NH₃ and NO₃ of San Diego Creek, respectively, and dark blue and blue indicate NH₃ and NO₃ of Santa Ana Delhi.

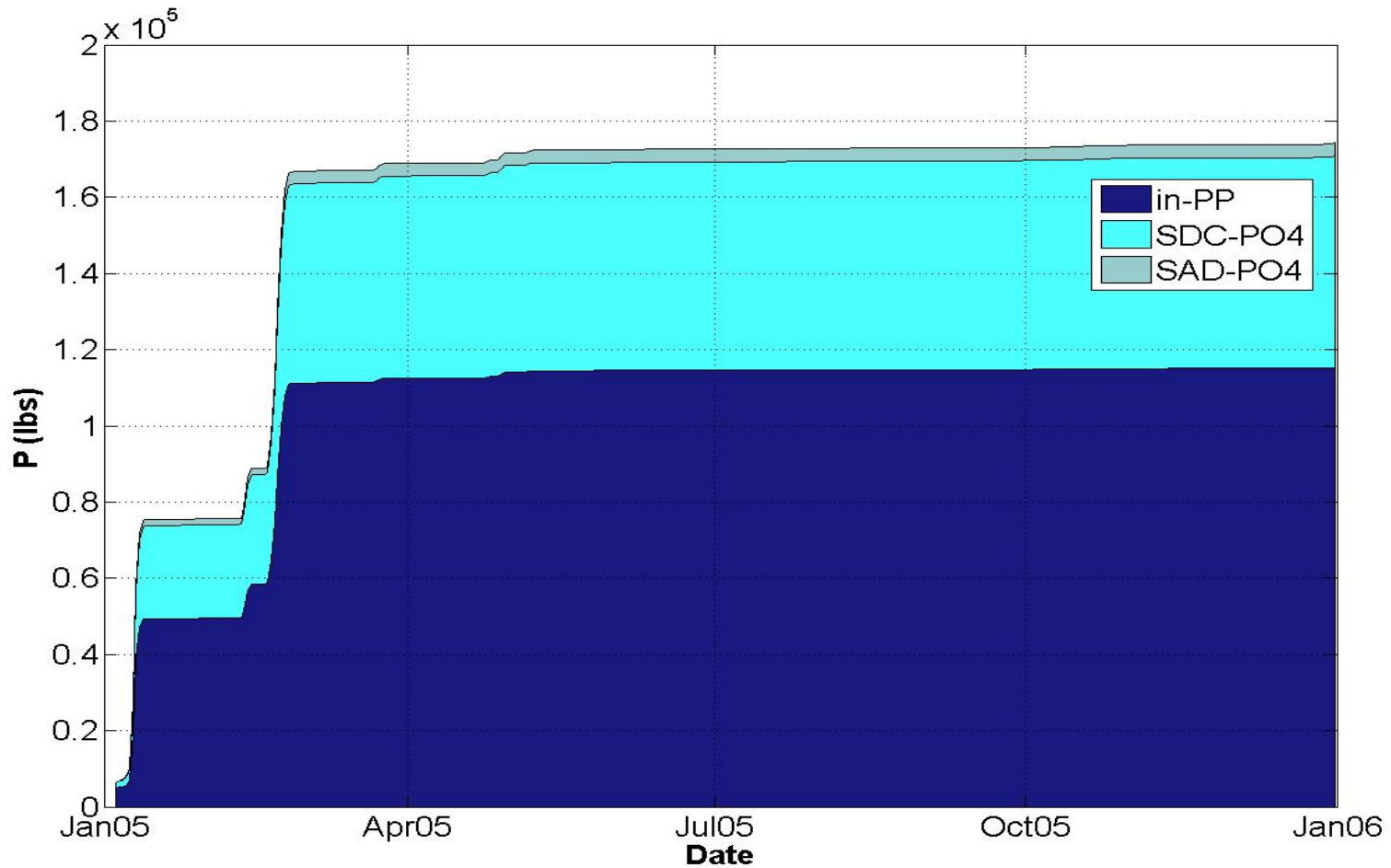


Figure 5-156. Time series of accumulated phosphorus mass into Newport Bay from January, 2005 to December, 2005 as input to the model. Very dark blue indicates particulate phosphorus from two inflows, cyan and light blue indicate NH₃ and NO₃ of San Diego Creek, respectively, and dark blue and blue indicate NH₃ and NO₃ of Santa Ana Delhi.

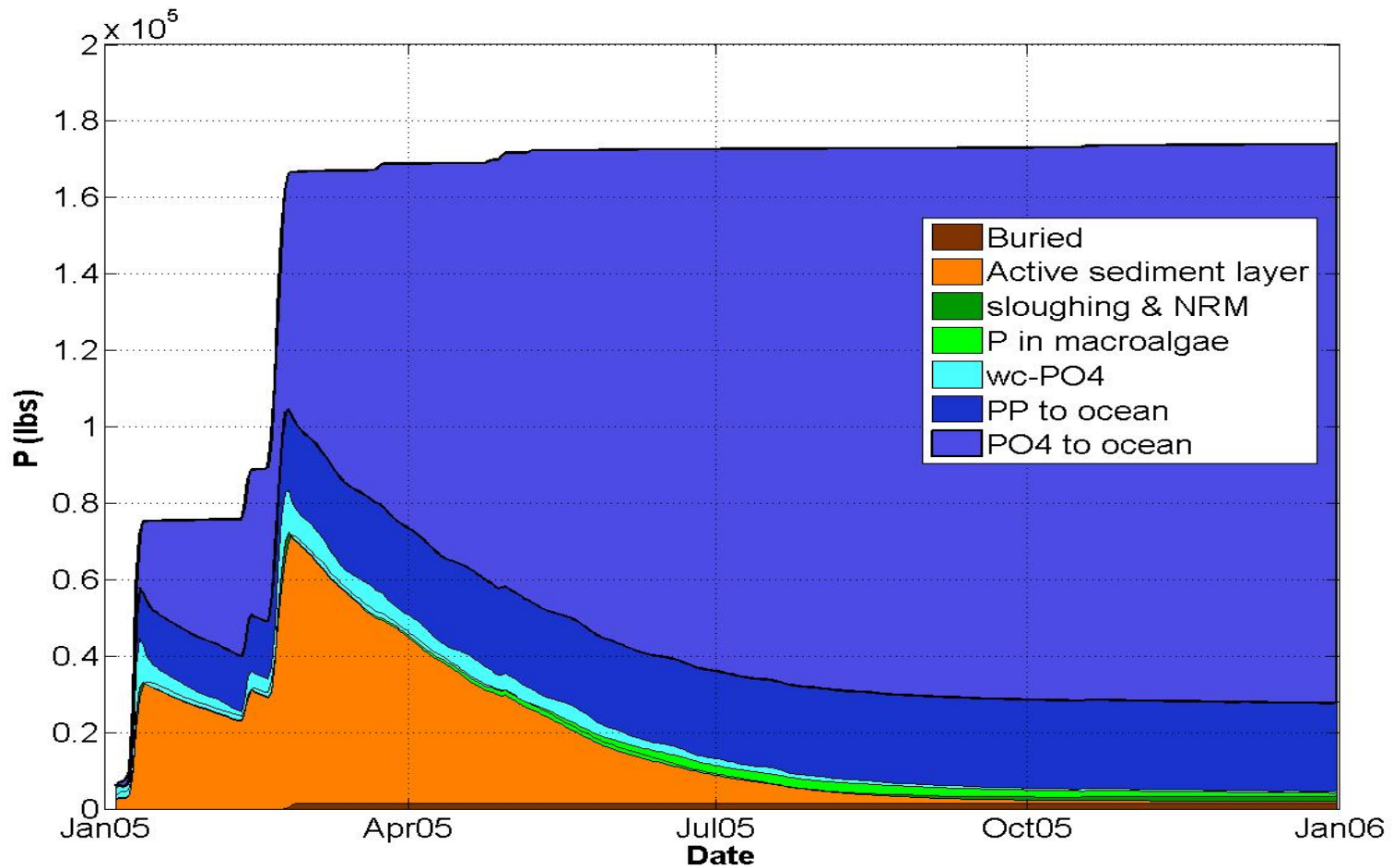


Figure 5-157. Time series of distribution of phosphorus in Newport Bay as computed in the model from January, 2005 to December, 2005. Dark brown indicates buried sediments, light brown indicates active sediment layer including P-POM, dark green indicates sloughing and non-recycled dead macroalgae (NRM), light green indicates phosphorus in macroalgae, cyan indicates PO₄ in the water column, very dark blue indicates particulate phosphorus out to the ocean, and blue indicates PO₄ out to the ocean.

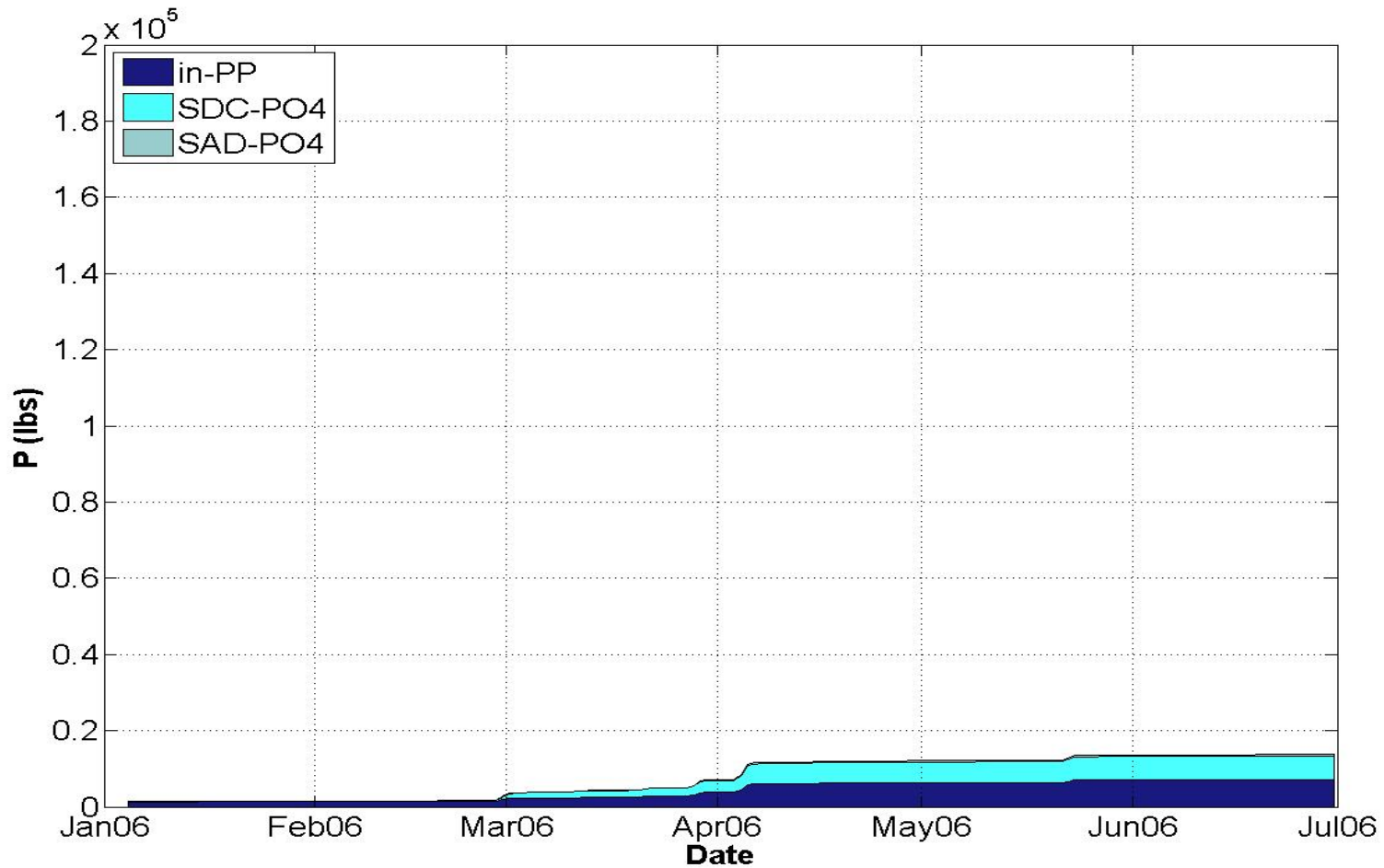


Figure 5-158. Time series of accumulated phosphorus mass into Newport Bay from January, 2006 to June, 2006 as input to the model. Very dark blue indicates particulate phosphorus from two inflows, cyan and light blue indicate NH₃ and NO₃ of San Diego Creek, respectively, and dark blue and blue indicate NH₃ and NO₃ of Santa Ana Delhi.

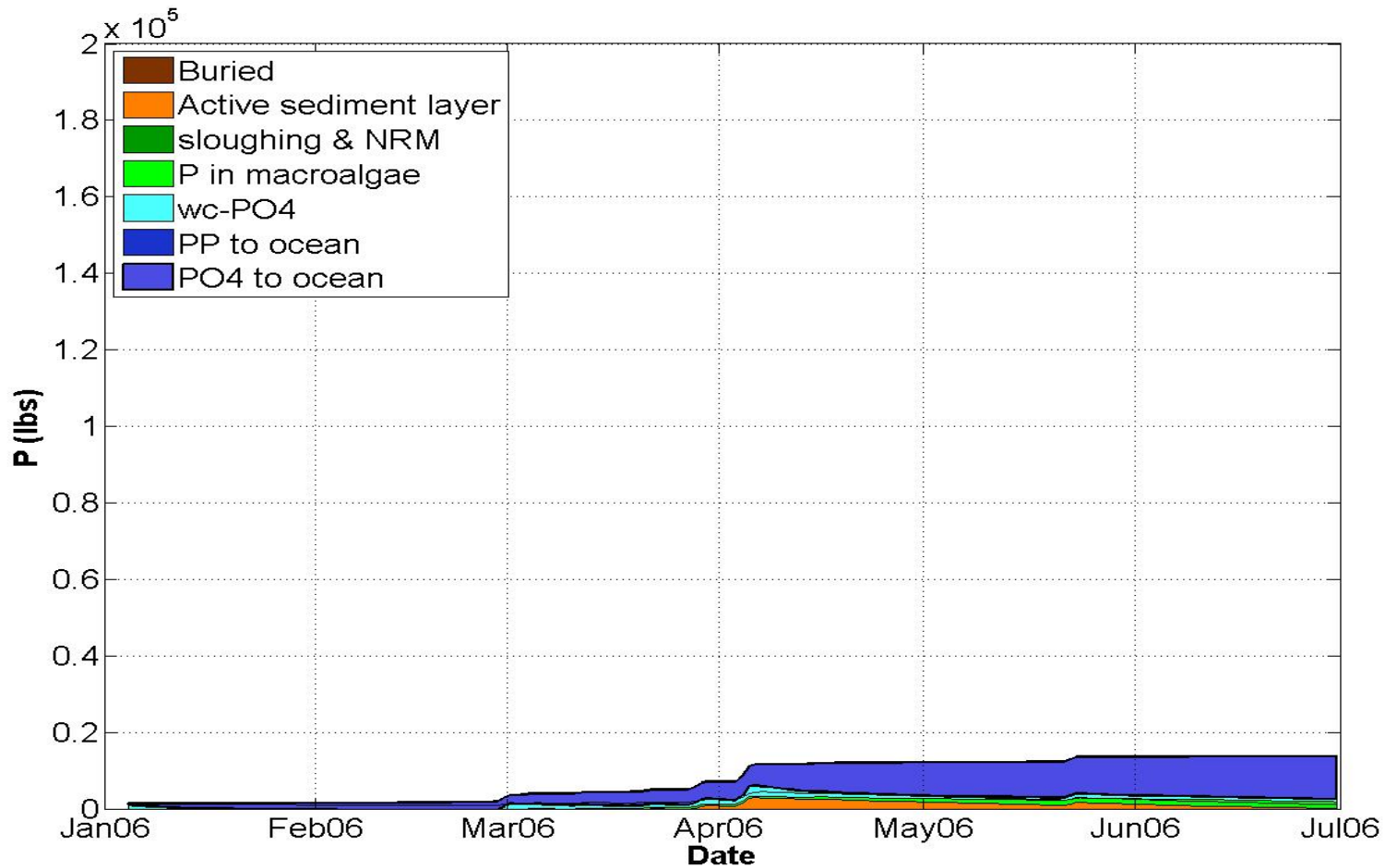


Figure 5-159. Time series of distribution of phosphorus in Newport Bay as computed in the model from January, 2006 to June, 2006. Dark brown indicates buried sediments, light brown indicates active sediment layer including P-POM, dark green indicates sloughing and non-recycled dead macroalgae (NRM), light green indicates phosphorus in macroalgae, cyan indicates PO4 in the water column, very dark blue indicates particulate phosphorus out to the ocean, and blue indicates PO4 out to the ocean.

5.7.3 Nitrate loading during a storm period

To take a closer look at that fate of nitrate loading during storm periods, the two-month wet weather period of January – February 2004 is analyzed. Plots are provided in Figure 5-160 that show nitrate inflow, outflow and water column concentration. A time series of creek inflow is provided to show corresponding flow conditions. These plots show a rapid increase in water column nitrate concentrations during storm events. The nitrate passes quickly through the Bay and discharges to the ocean allowing water column concentrations to return to pre-storm levels. Thus it appears that the storm-related nitrate load has little long-term impact on the system.

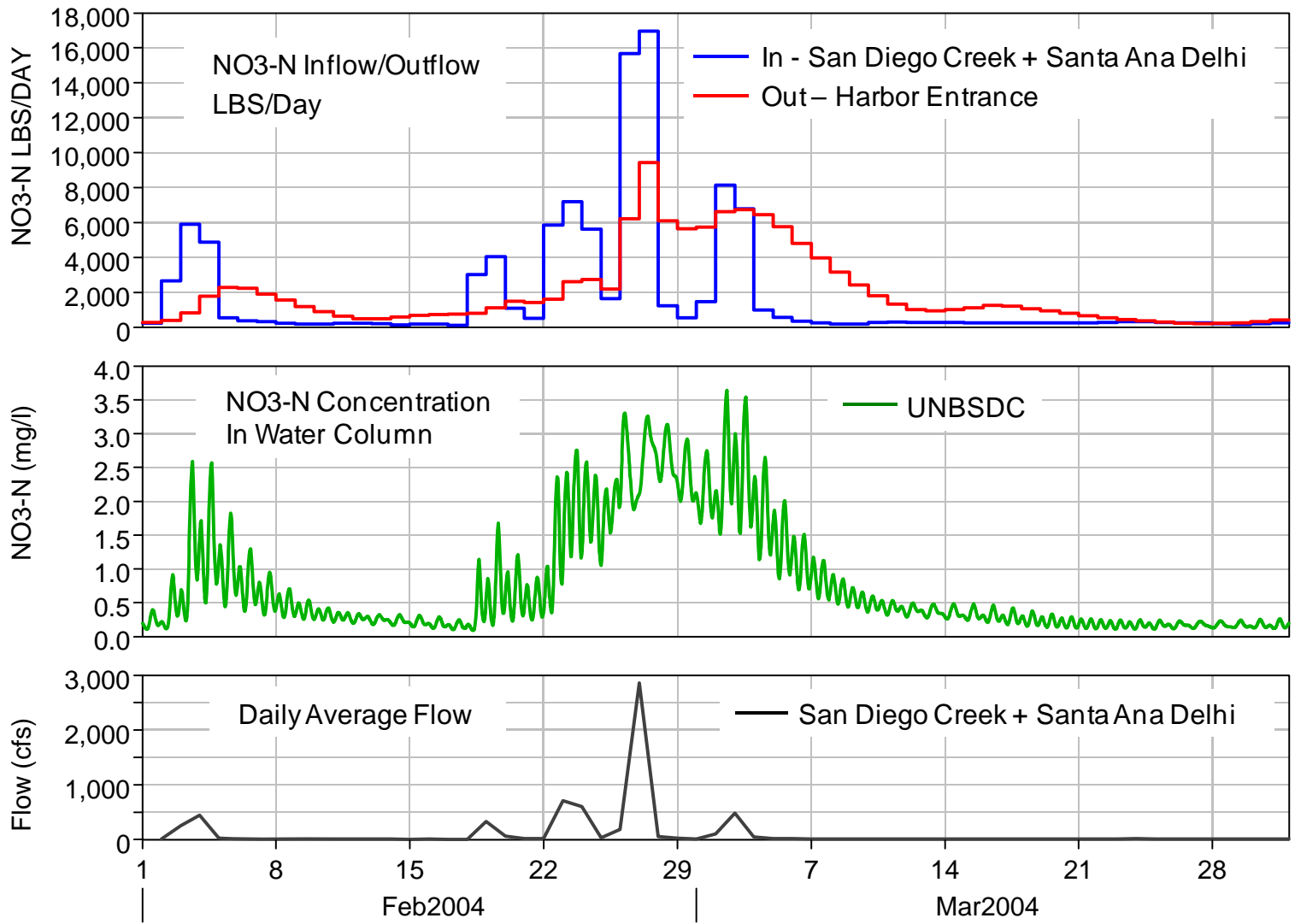


Figure 5-160 NO3-N for storm events between February and March 2004.

6. Additional model simulations, results and discussion

6.1 Scenarios with conservative constituents

Model simulations were run with nutrients (nitrate, ammonia and phosphate) simulated as conservative constituents. There was no interaction among the nutrients, or with macroalgae or other constituents, and heat budget was not considered. Two simulations were run for each constituent: one with boundary conditions set as described in section 4.1.2; and one with the same creek inflow boundaries, but tidal boundary concentrations set to zero. Comparison of results from these two types of simulations and comparisons between simulation results and observed data can help determine the relative importance of the tidal and creek inflow boundary contributions to total nutrient concentrations in the Bay.

Conservatively computed NO_3 is plotted with observed data in Figure 6-1 through Figure 6-4 at stations shown in Figure 5-1. In these simulations, the impact of the ocean boundary condition is least important at the most upstream station (UNBJAM) and becomes more important at the furthest downstream station (UNBCHB) as expected. At UNBJAM and UNBSDC, computed concentrations are higher than observed much of the time, although computed results correspond well with several data points. At UNBNSB, the simulation results correspond well with much of the observed data. At UNBCHB, the observed data points fall in between the two simulations during the dry season and the wet season results vary by year.

These conservative NO_3 simulation results indicate that the ocean boundary concentrations do not dominate the system. Compared with the observed data, it also appears that there is a sink of NO_3 in the system, as predicted from the nitrogen mass balance discussed in section 5.7.1. Macroalgal uptake and/or sediments (i.e., probably via denitrification) are likely to be the primary sink for NO_3 .

Conservatively computed NH_3 is plotted with observed data in Figure 6-5 through Figure 6-8 at stations shown in Figure 5-1. In these simulations, the impact of the ocean boundary condition is fairly important throughout the Bay, but particularly further downstream. Even with concentrations set for the ocean boundary, simulation results are lower than observed data, with very few exceptions, at all stations. Compared with the observed data, it is apparent that there is a source of NH_3 in the system, which increases the importance of the NO_3 sink, given that the nitrogen mass balance discussed in section 5.7.1 shows a net loss of nitrogen in the system. Sediments (e.g., diagenesis of POM) are likely to be the primary source of NH_3 .

Conservatively computed PO_4 is plotted with observed data in Figure 6-9 through Figure 6-12 at stations shown in Figure 5-1. In these simulations, the impact of the ocean boundary condition is

quite important throughout the Bay, to the point that ocean input alone can produce summertime concentrations at UNBSDC that are in the range of observed values and, and concentrations even higher than observed at the further downstream stations. An internal source of PO₄ is indicated at UNBJAM, given that computed concentrations are lower than observed. This is in line with the predictions in the mass balance. Sediments (e.g., diagenesis of POM) are the likely source, especially in summer. At the stations further downstream, however, a net sink is indicated. Although there are both sources and sinks of all nutrients in the system, another likely explanation is that the tidal boundary is actually set too high, thus causing the elevated concentrations lower in the Bay. Nutrient data for the ocean boundary are very limited (collected quarterly by from a different location - LA Harbor) and therefore add a higher level of uncertainty, which could be an important factor affecting the ability to closely calibrate the model. Moreover, upwelling events in the west coast of the Pacific Ocean (which are not always captured in the ocean nutrient data) potentially add uncertainty of tidal boundary conditions to the nutrient cycles of the Bay, since the driven surface waters from the coast are replaced by denser, cold water below carrying dissolved nutrients. The use of lower Bay phosphate data as the ocean boundary condition may have improved the results.

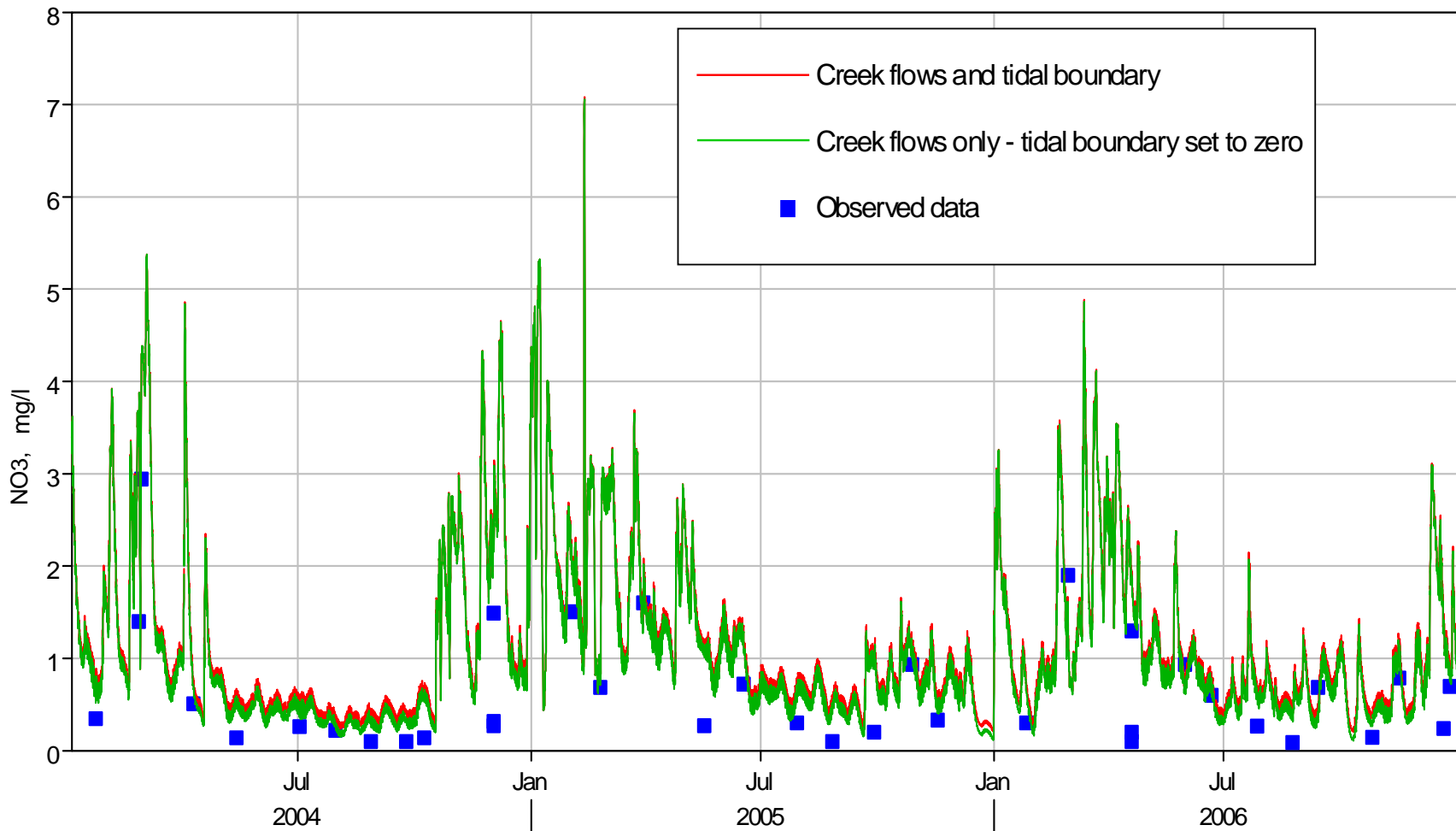


Figure 6-1 Observed and conservatively computed NO₃ at UNBJAM for years 2004 - 2006. Conservative simulations were performed both with tidal boundaries set using observed data, and set to zero.

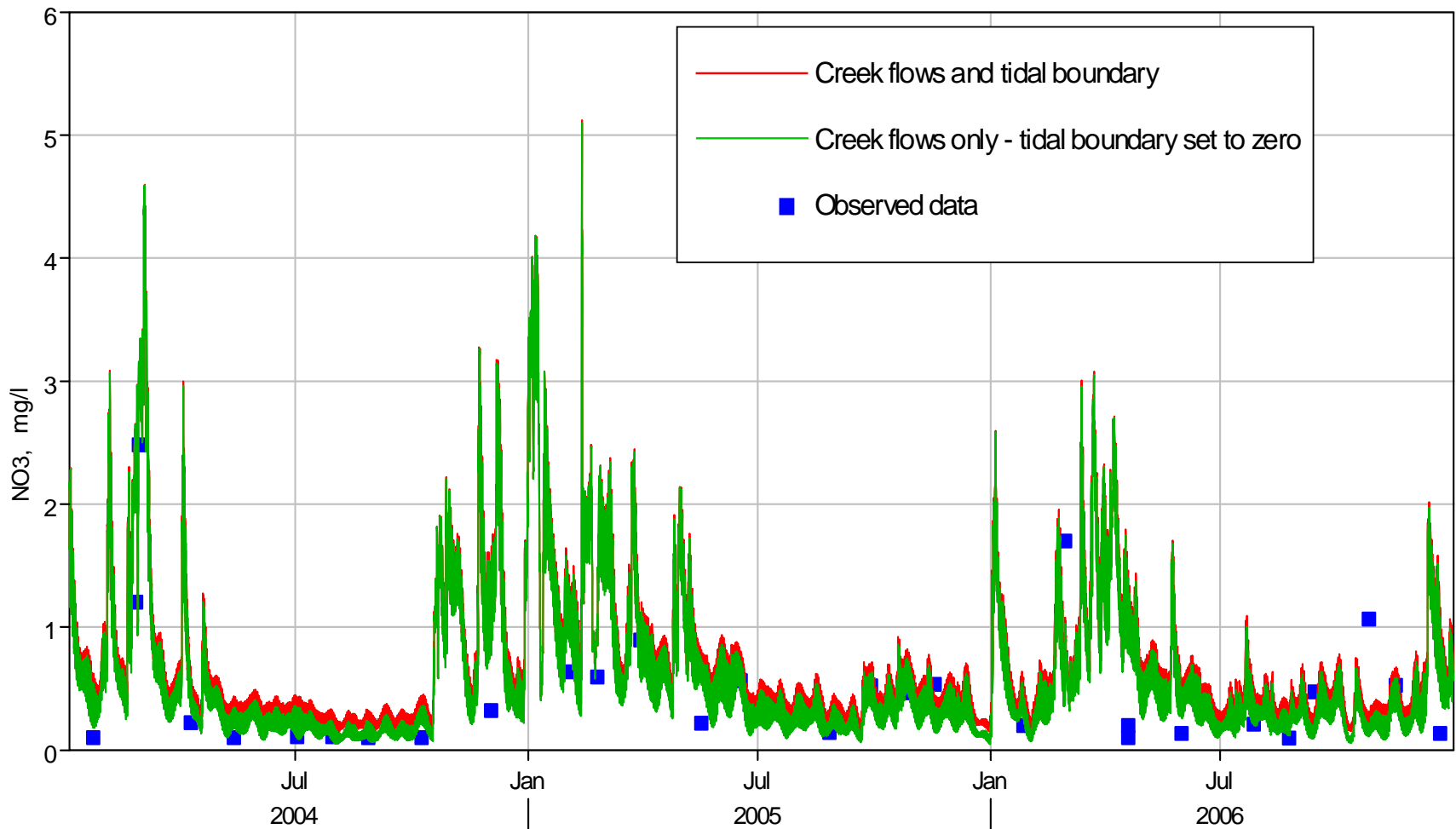


Figure 6-2 Observed and conservatively computed NO₃ at UNBSDC for years 2004 - 2006. Conservative simulations were performed both with tidal boundaries set using observed data, and set to zero.

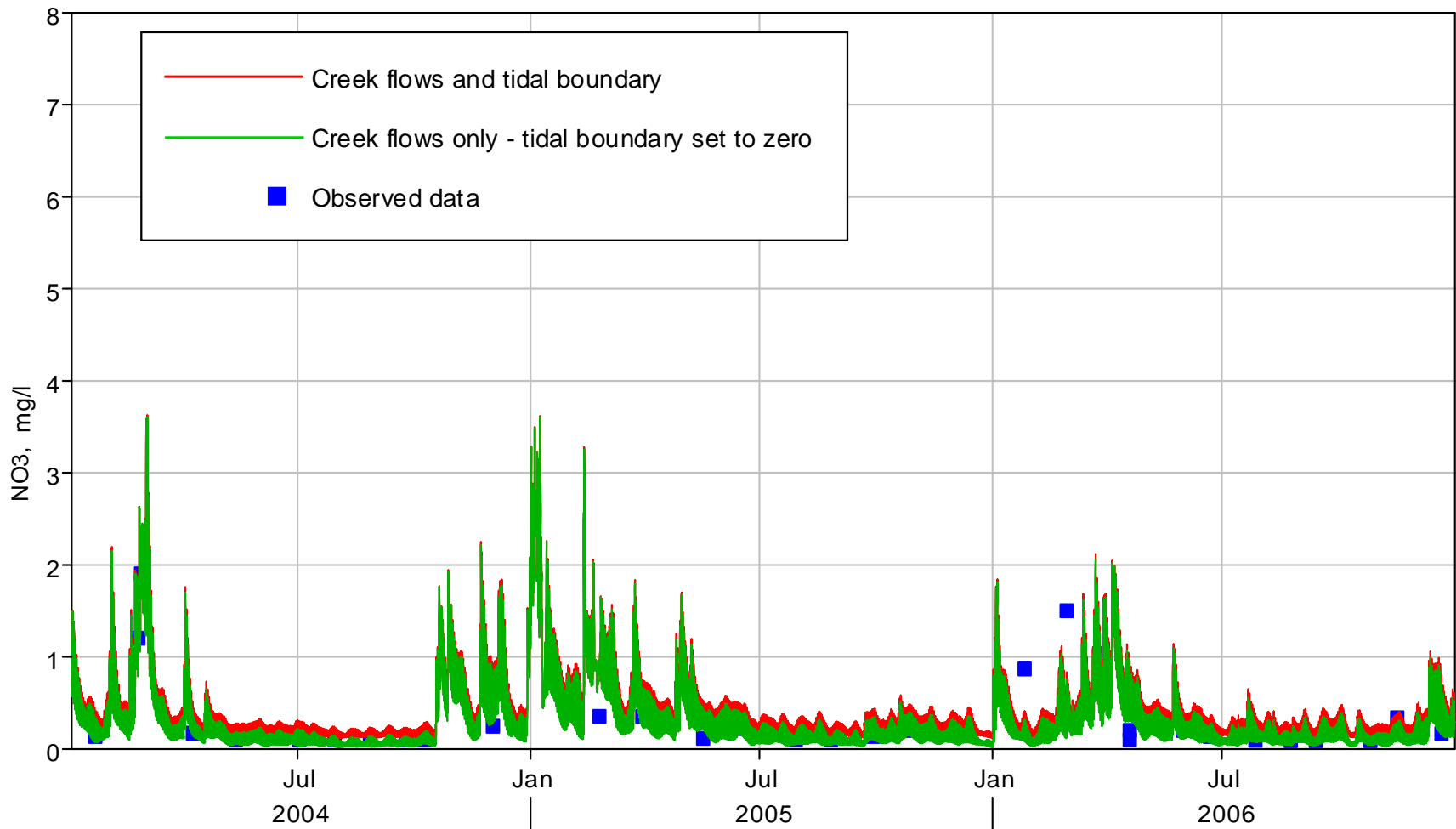


Figure 6-3 Observed and conservatively computed NO₃ at UNBNSB for years 2004 - 2006. Conservative simulations were performed both with tidal boundaries set using observed data, and set to zero.

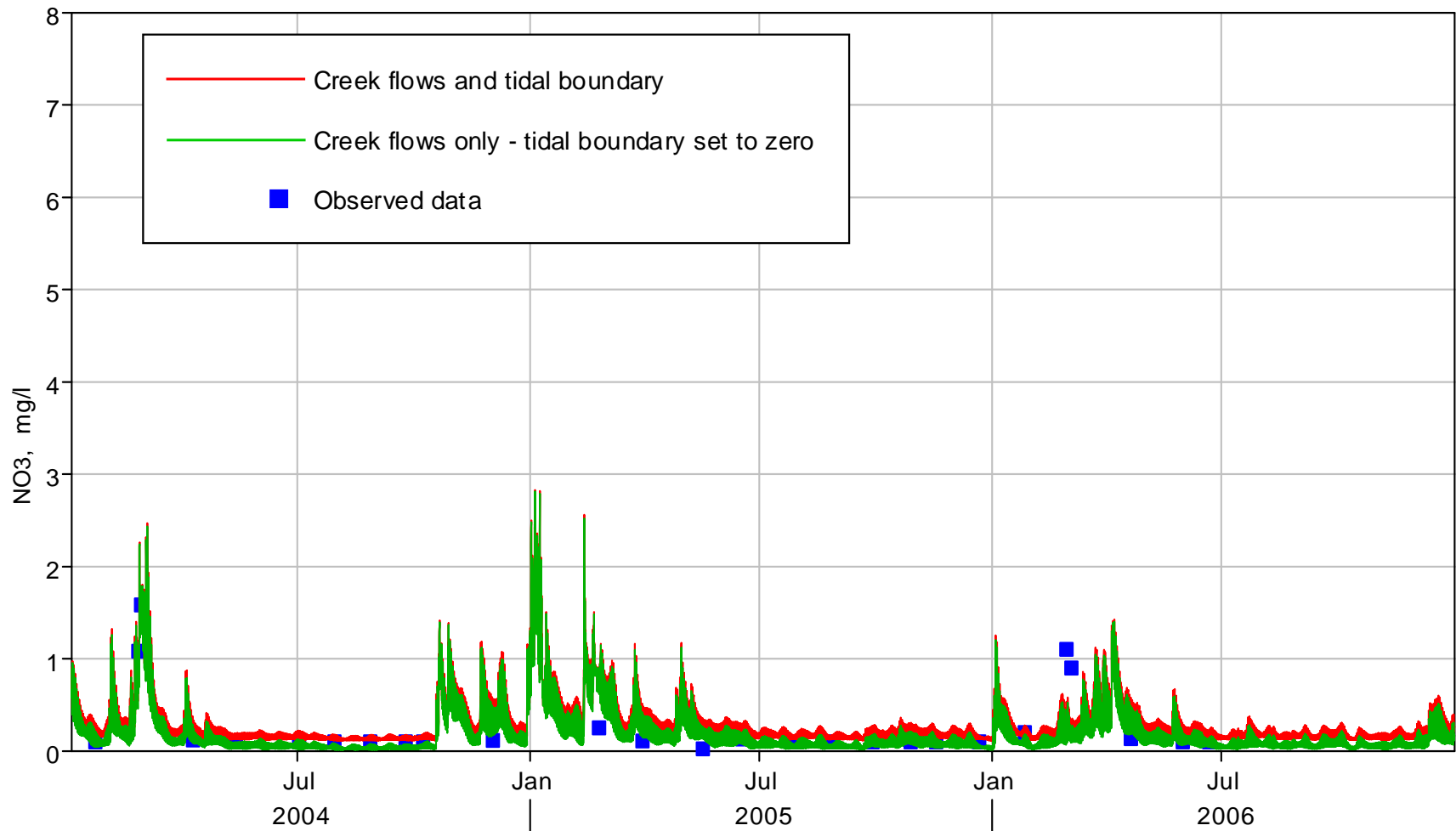


Figure 6-4 Observed and conservatively computed NO₃ at UNBCHB for years 2004 - 2006. Conservative simulations were performed both with tidal boundaries set using observed data, and set to zero.

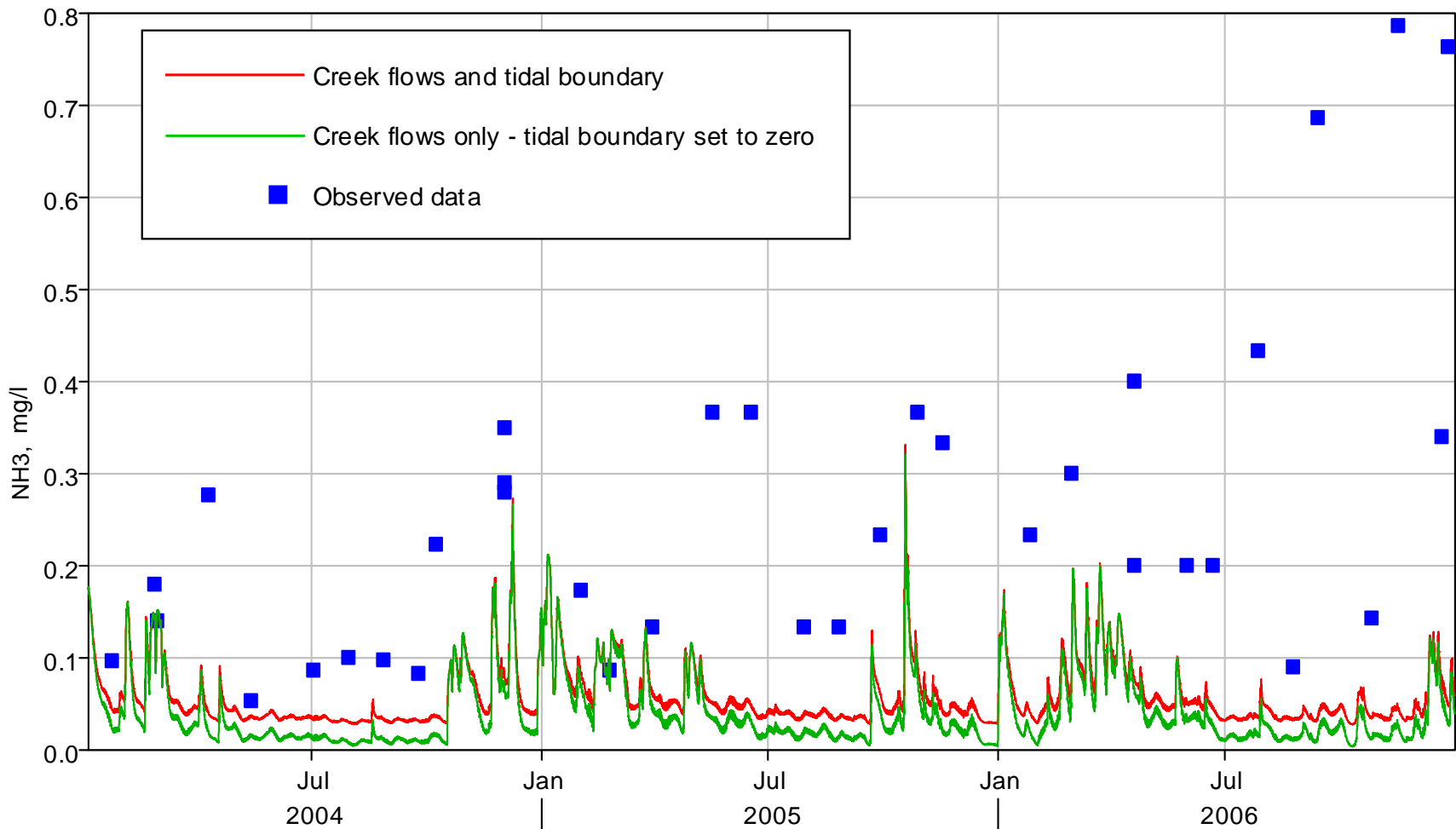


Figure 6-5 Observed and conservatively computed NH3 at UNBJAM for years 2004 - 2006. Conservative simulations were performed both with tidal boundaries set using observed data, and set to zero.

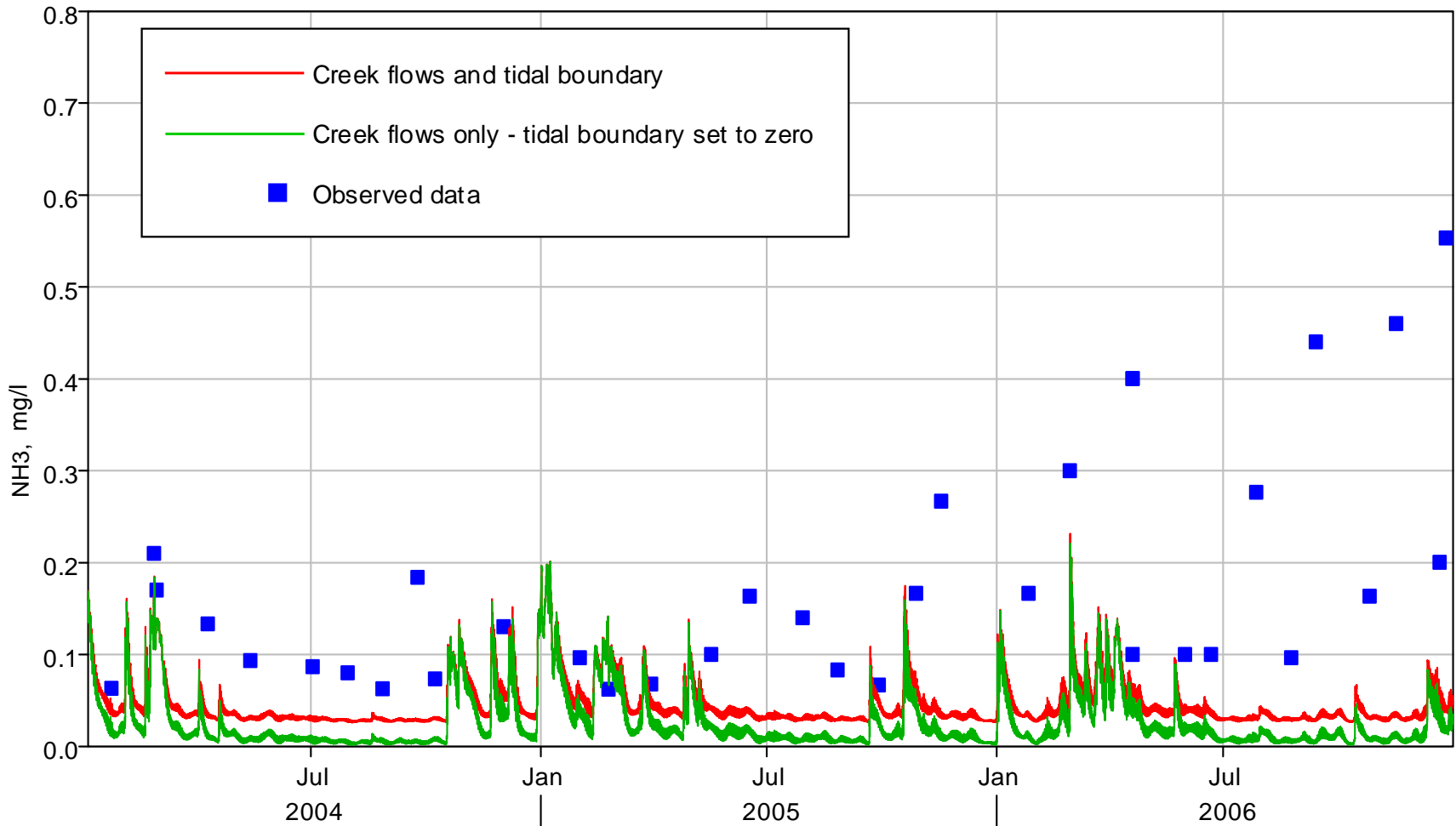


Figure 6-6 Observed and conservatively computed NH3 at UNBSDC for years 2004 - 2006. Conservative simulations were performed both with tidal boundaries set using observed data, and set to zero.

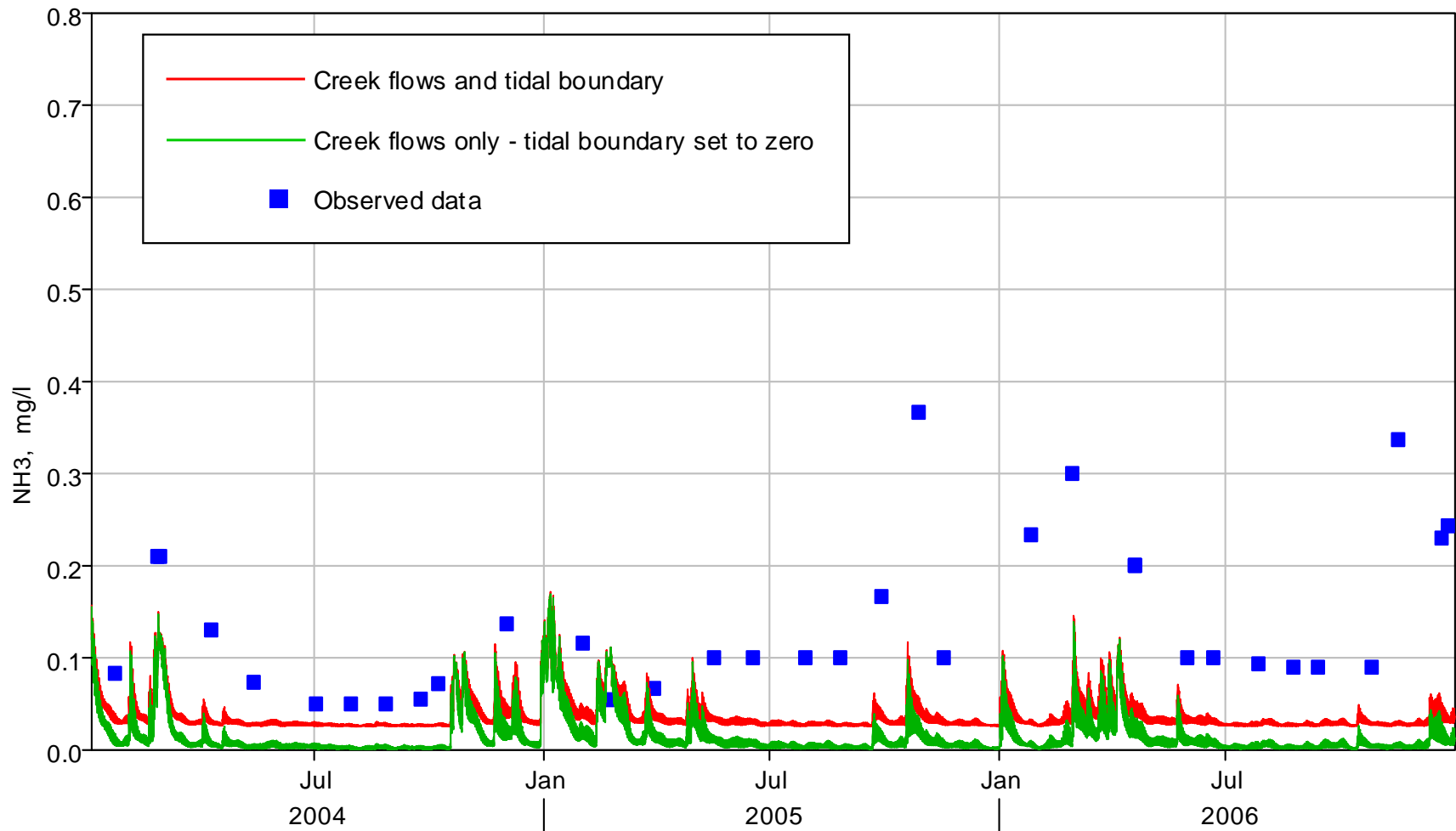


Figure 6-7 Observed and conservatively computed NH₃ at UNBNSB for years 2004 - 2006. Conservative simulations were performed both with tidal boundaries set using observed data, and set to zero.

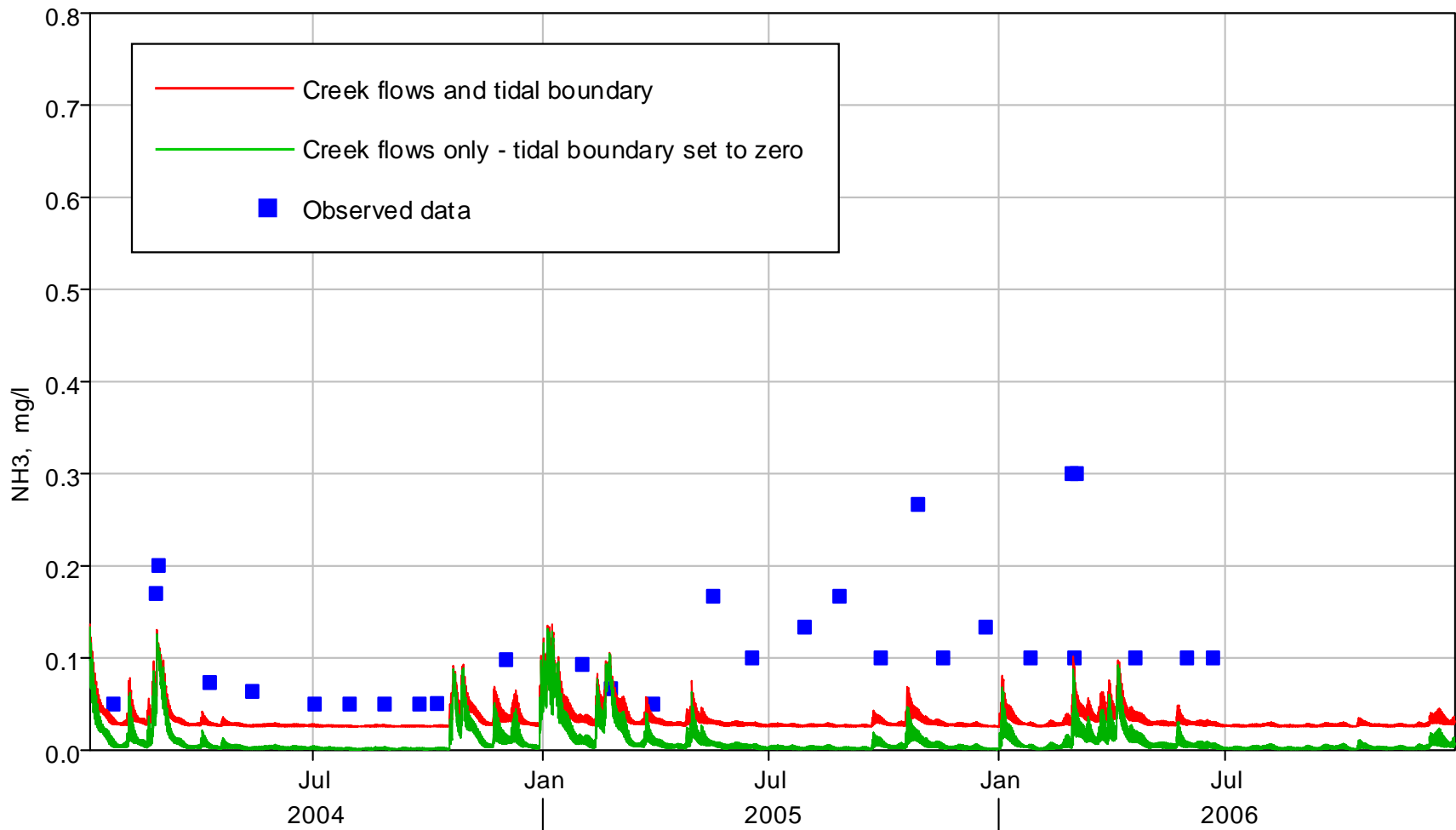


Figure 6-8 Observed and conservatively computed NH₃ at UNBCHB for years 2004 - 2006. Conservative simulations were performed both with tidal boundaries set using observed data, and set to zero.

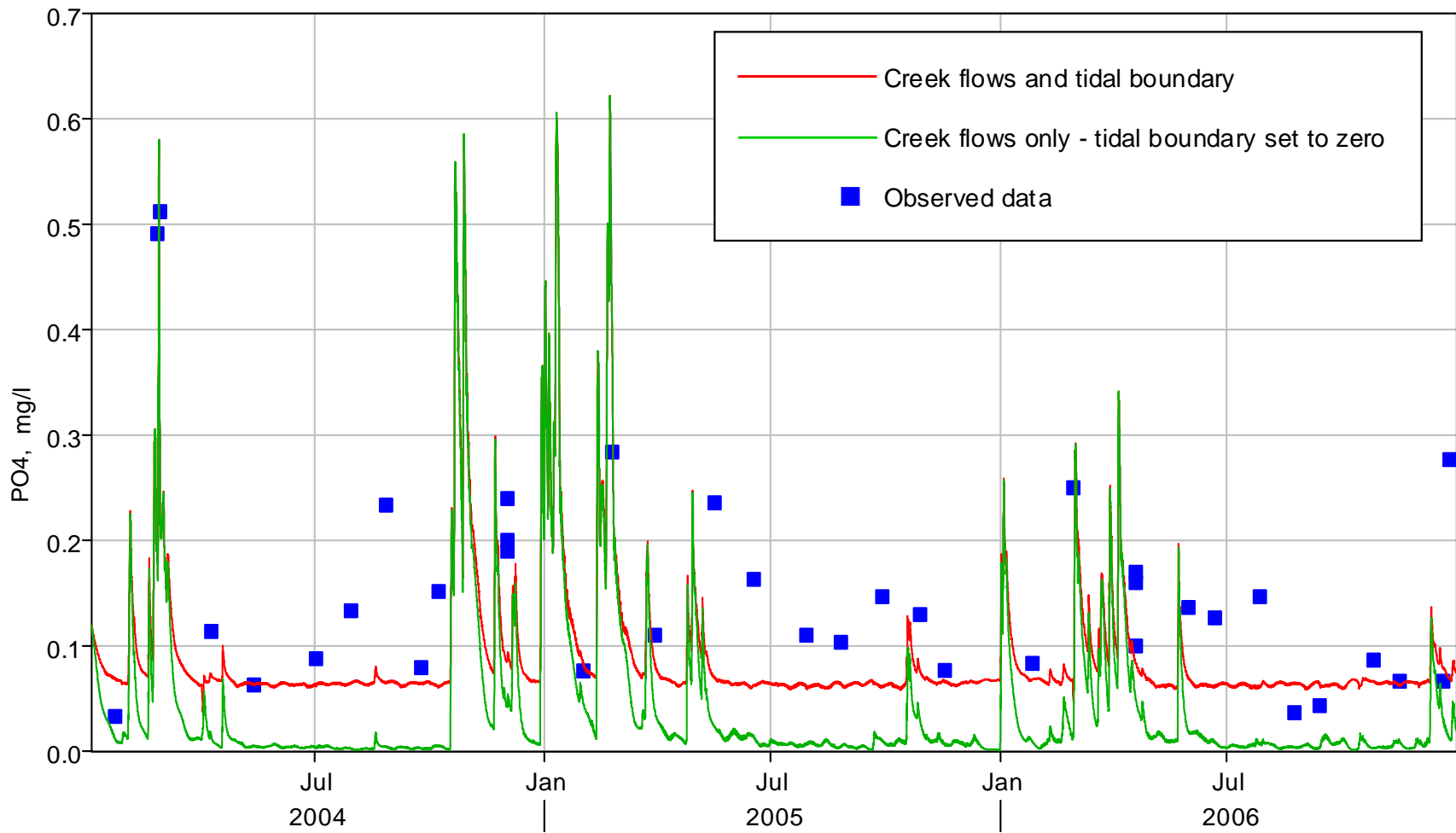


Figure 6-9 Observed and conservatively computed PO4 at UNBJAM for years 2004 - 2006. Conservative simulations were performed both with tidal boundaries set using observed data, and set to zero.

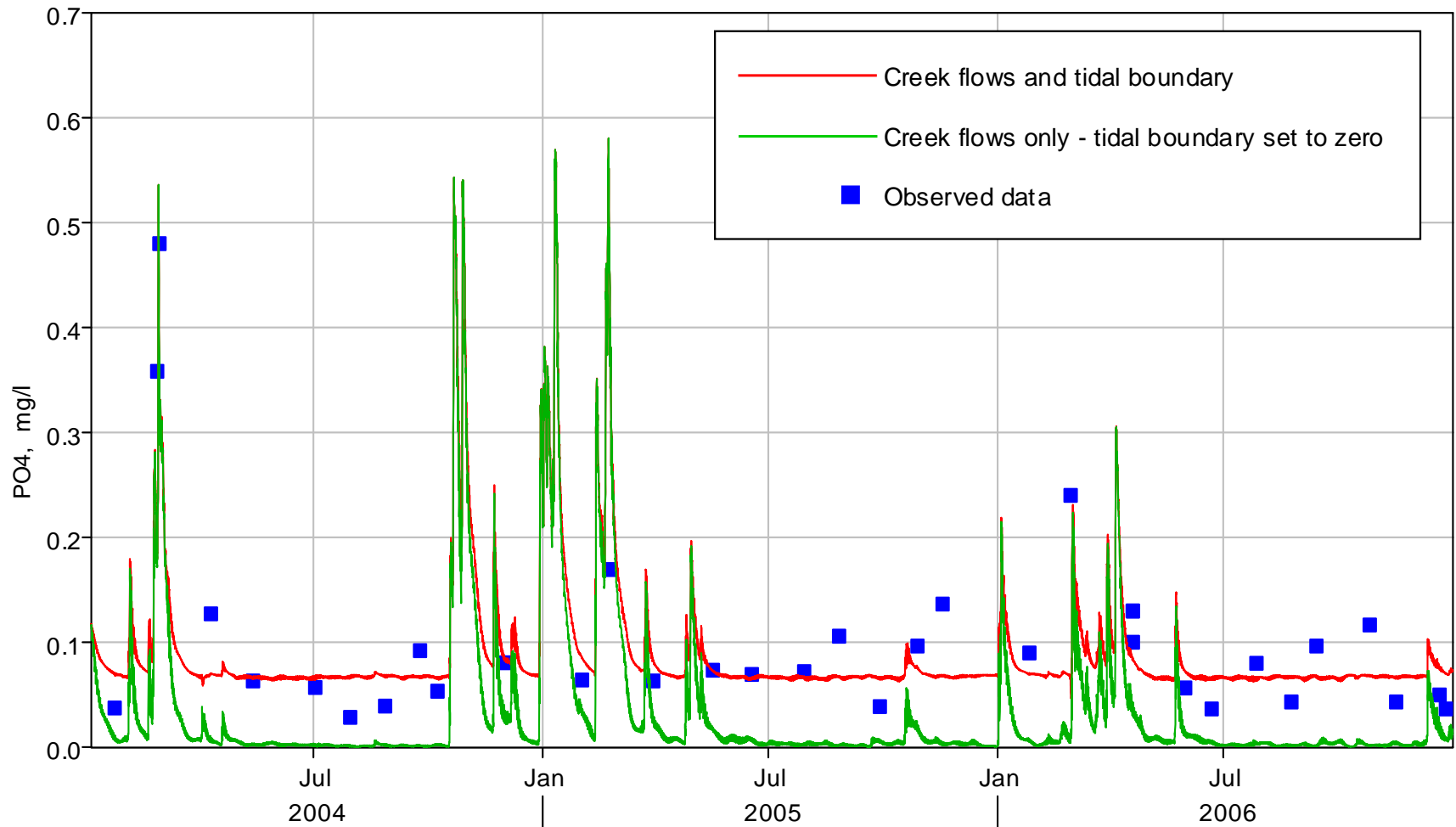


Figure 6-10 Observed and conservatively computed PO4 at UNBSDC for years 2004 - 2006. Conservative simulations were performed both with tidal boundaries set using observed data, and set to zero.

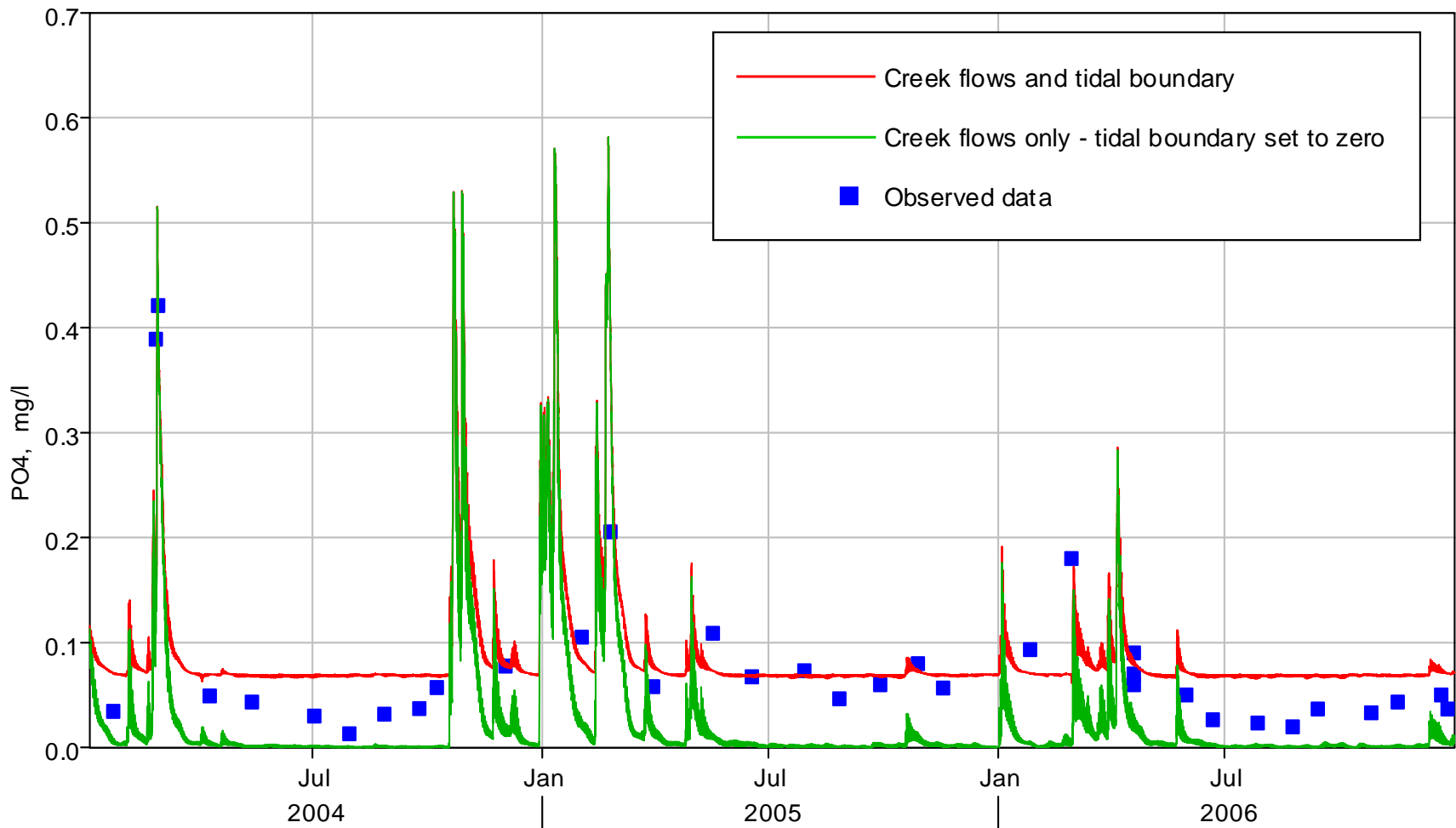


Figure 6-11 Observed and conservatively computed PO4 at UNBNSB for years 2004 - 2006. Conservative simulations were performed both with tidal boundaries set using observed data, and set to zero.

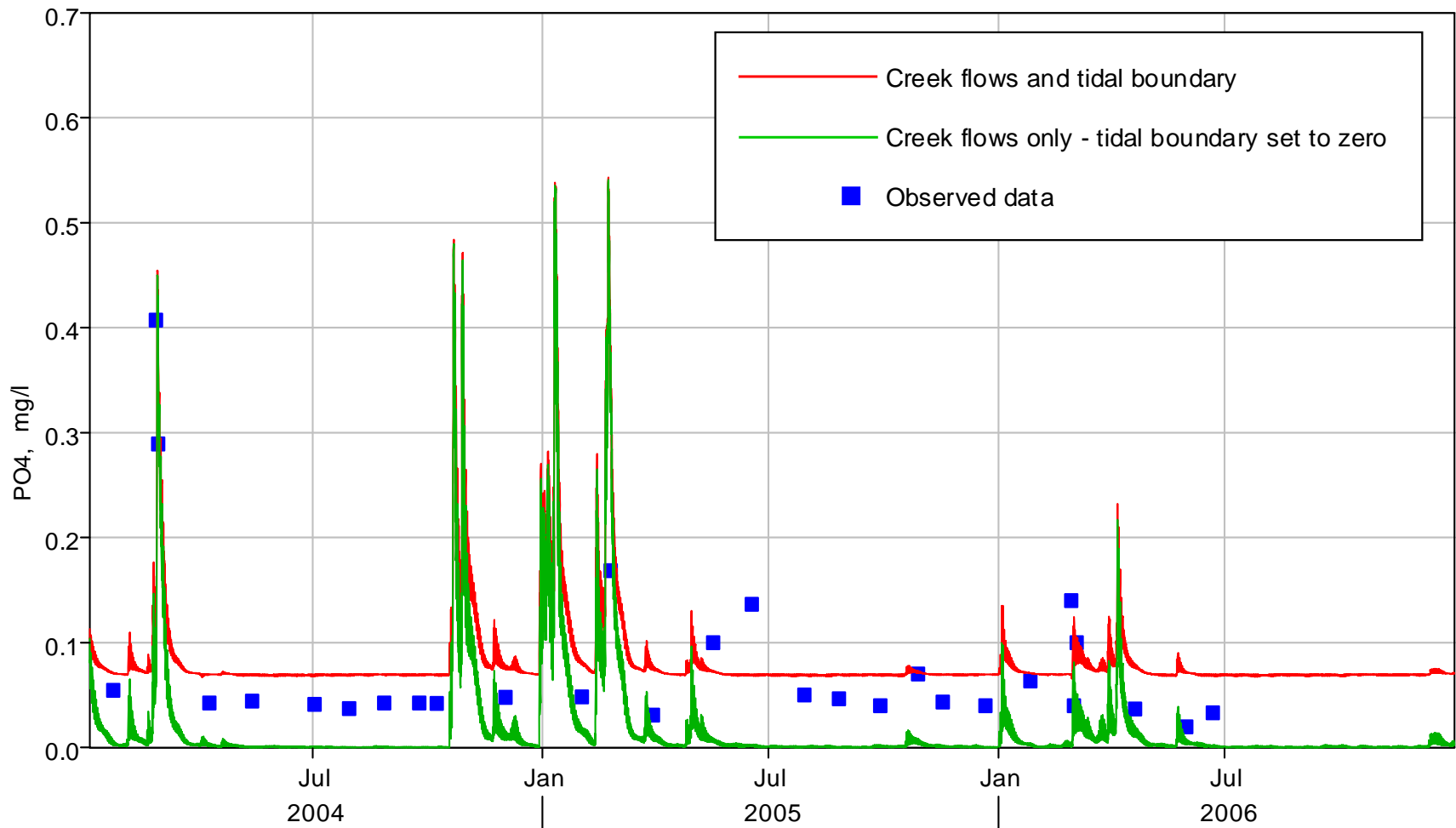


Figure 6-12 Observed and conservatively computed PO4 at UNBCHB for years 2004 - 2006. Conservative simulations were performed both with tidal boundaries set using observed data, and set to zero.

6.2 Scenarios with biological and chemical reactions

To analyze the relative importance of sediment processes, simulations were run with biological and chemical reactions but no sediment interactions. All other model parameters, were set the same as for the calibrated model.

In Figure 6-13 through Figure 6-15 total dry weight macroalgae, computed with no sediment interactions, is compared with the calibrated model result (with sediment interactions) for years 2004 through 2006. In 2004, macroalgae mass declines continually from the initial condition on January first, nearing zero by September. In 2005 and 2006, peak macroalgae mass occurs in the spring at very small fractions of the peaks in the calibrated model, then declines to minimal values by the end of the year.

These results give strong evidence that sediments provide an important source of nutrients for macroalgae blooms in Newport Bay.

The relative importance of NO₃ inputs from two main inflows was also analyzed. Simulations were run under the same conditions as the calibration but with no NO₃ coming from inflows. In Figure 7-16, Figure 7-17 and Figure 7-18, total dry weight of macroalgae simulated for each calibration year is plotted with and without NO₃ inputs from inflows. The model simulations indicate that removal of NO₃ from inflows could decrease total dry weight by 30% to 50% of the peak biomass in a year. It may be presumed that an ideal approach to manage macroalgal blooms would be complete removal of NO₃ from the inflows. However, these simulation results in comparison with results from the simulations without sediments indicate that control of particulate nitrogen could have a more significant impact than NO₃ reductions on management of macroalgal blooms.

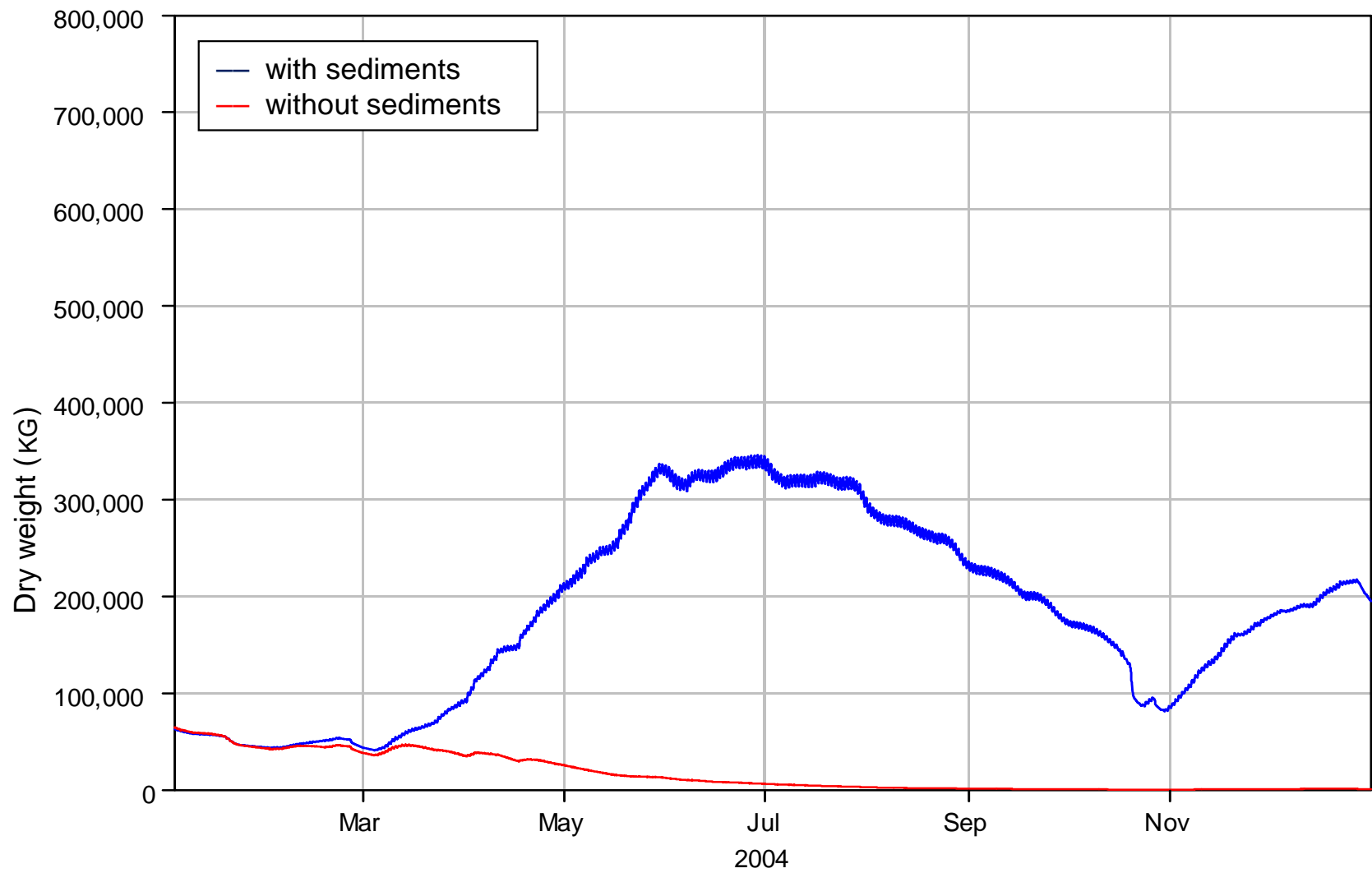


Figure 6-13 Comparison of total dry mass of macroalgae simulated with and without sediment fluxes in 2004.

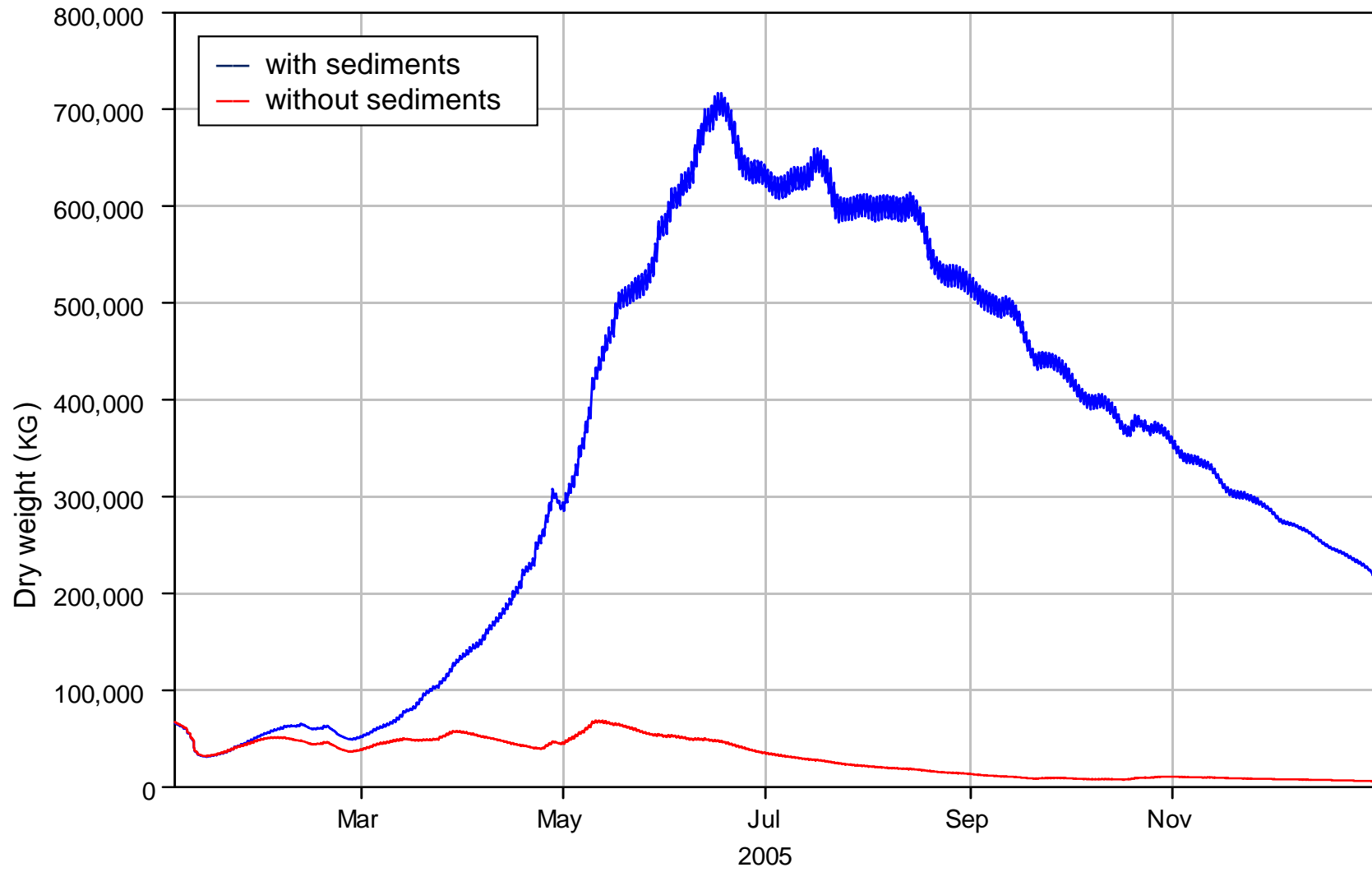


Figure 6-14 Comparison of total dry mass of macroalgae simulated with and without sediment fluxes in 2005.

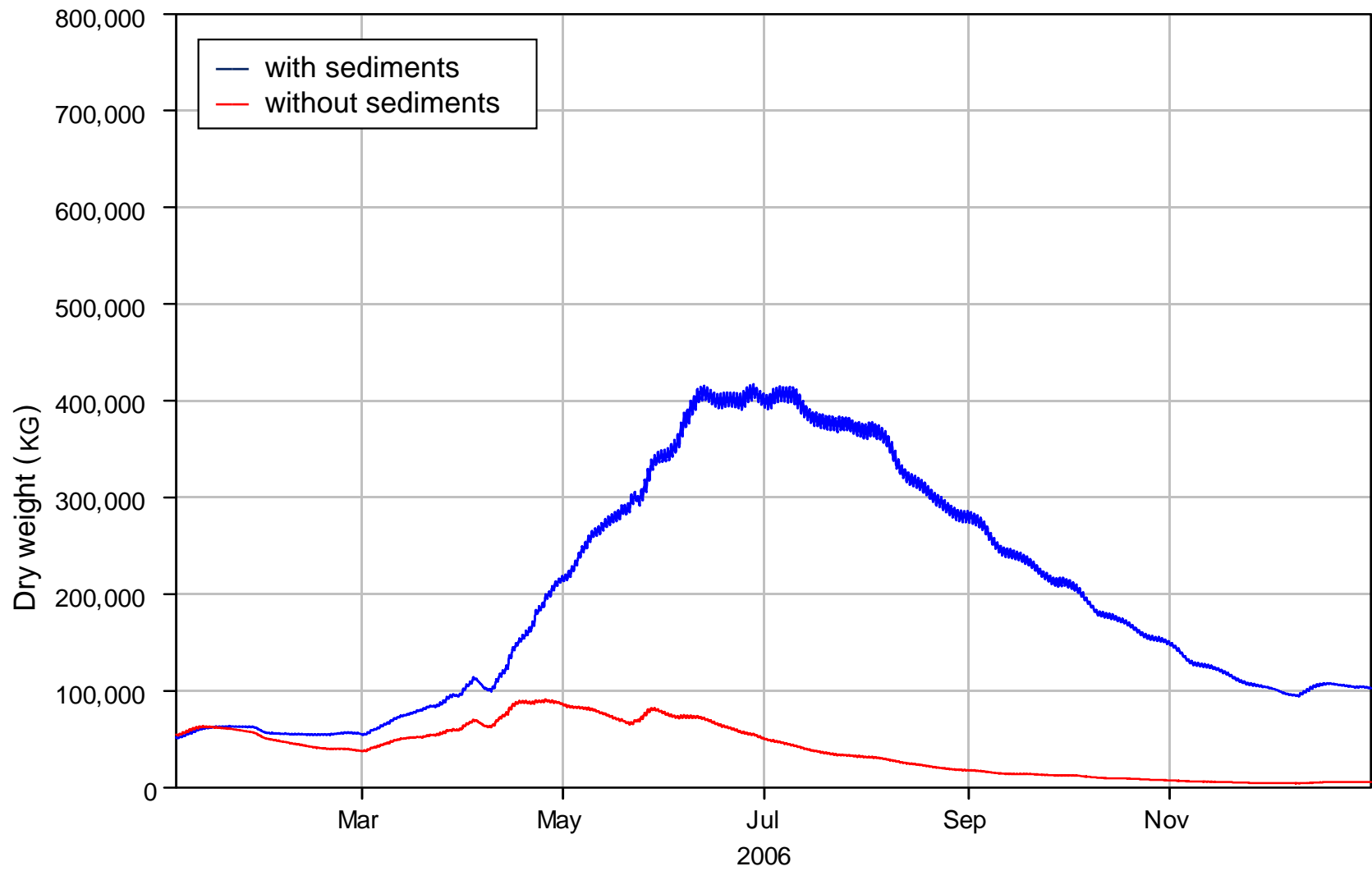


Figure 6-15 Comparison of total dry mass of macroalgae simulated with and without sediment fluxes in 2006.

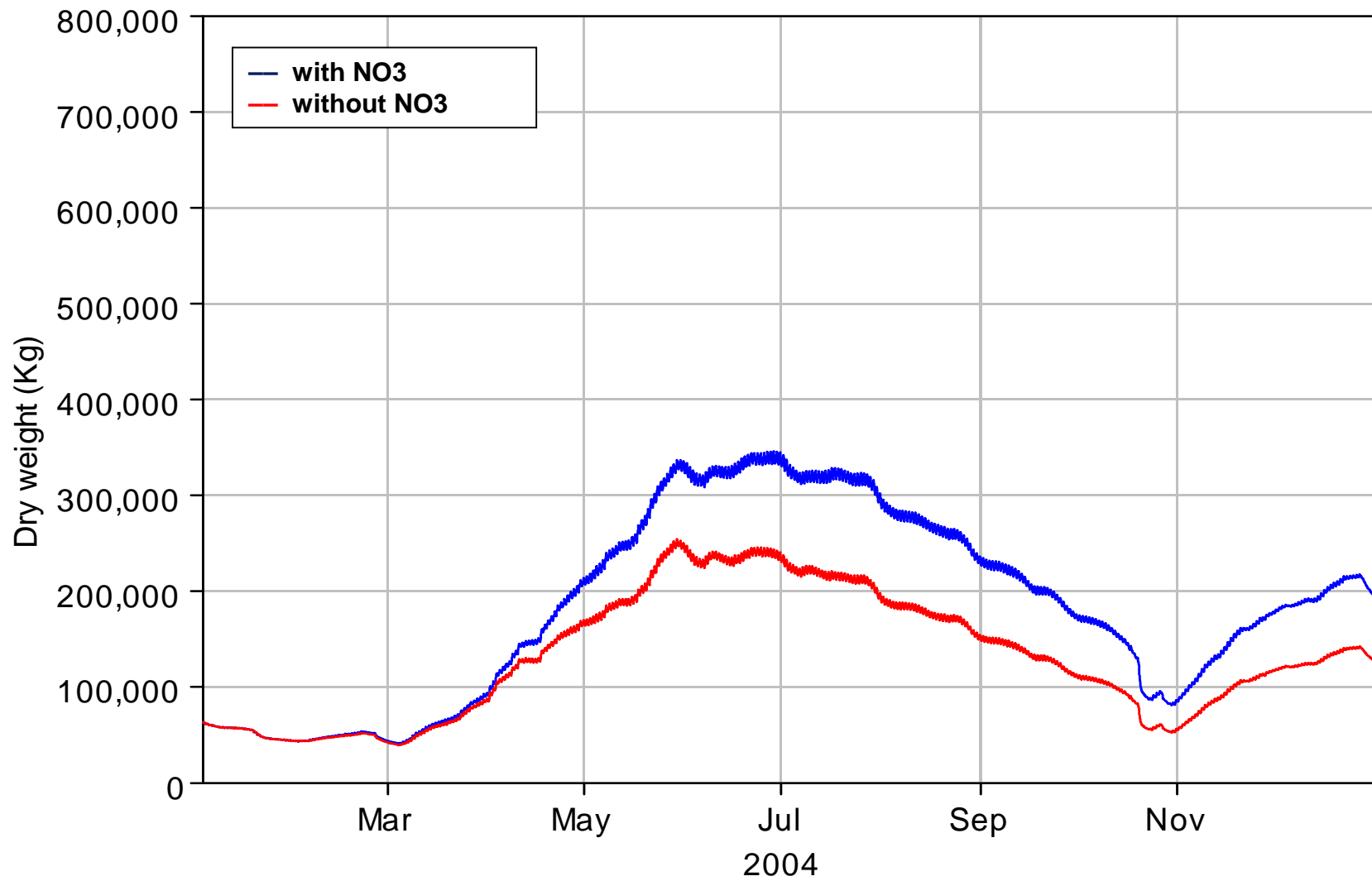


Figure 6-16 Comparison of total dry mass of macroalgae simulated with and without NO₃ inputs from inflows in 2004.

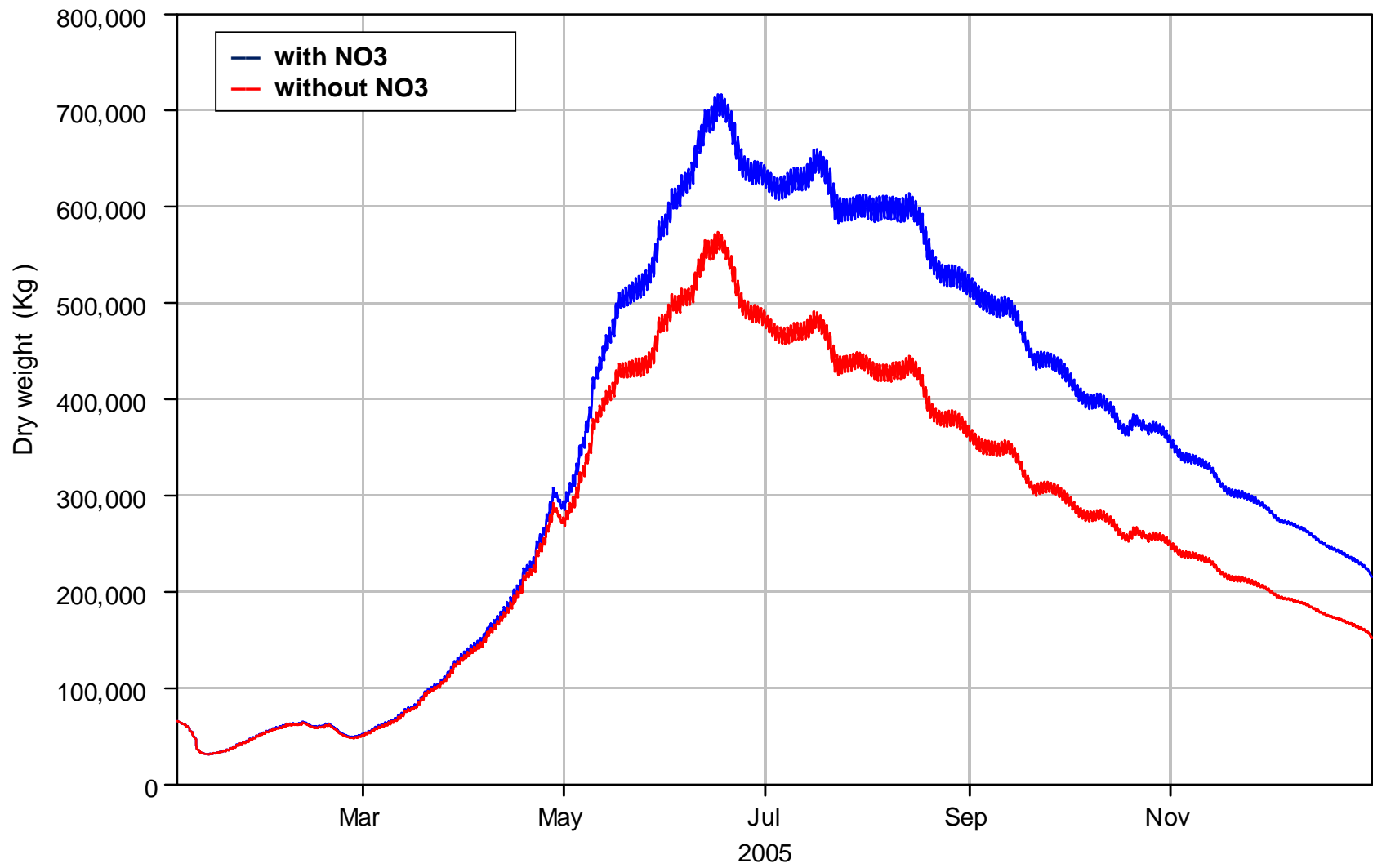


Figure 6-17 Comparison of total dry mass of macroalgae simulated with and without NO3 inputs from inflows in 2005.

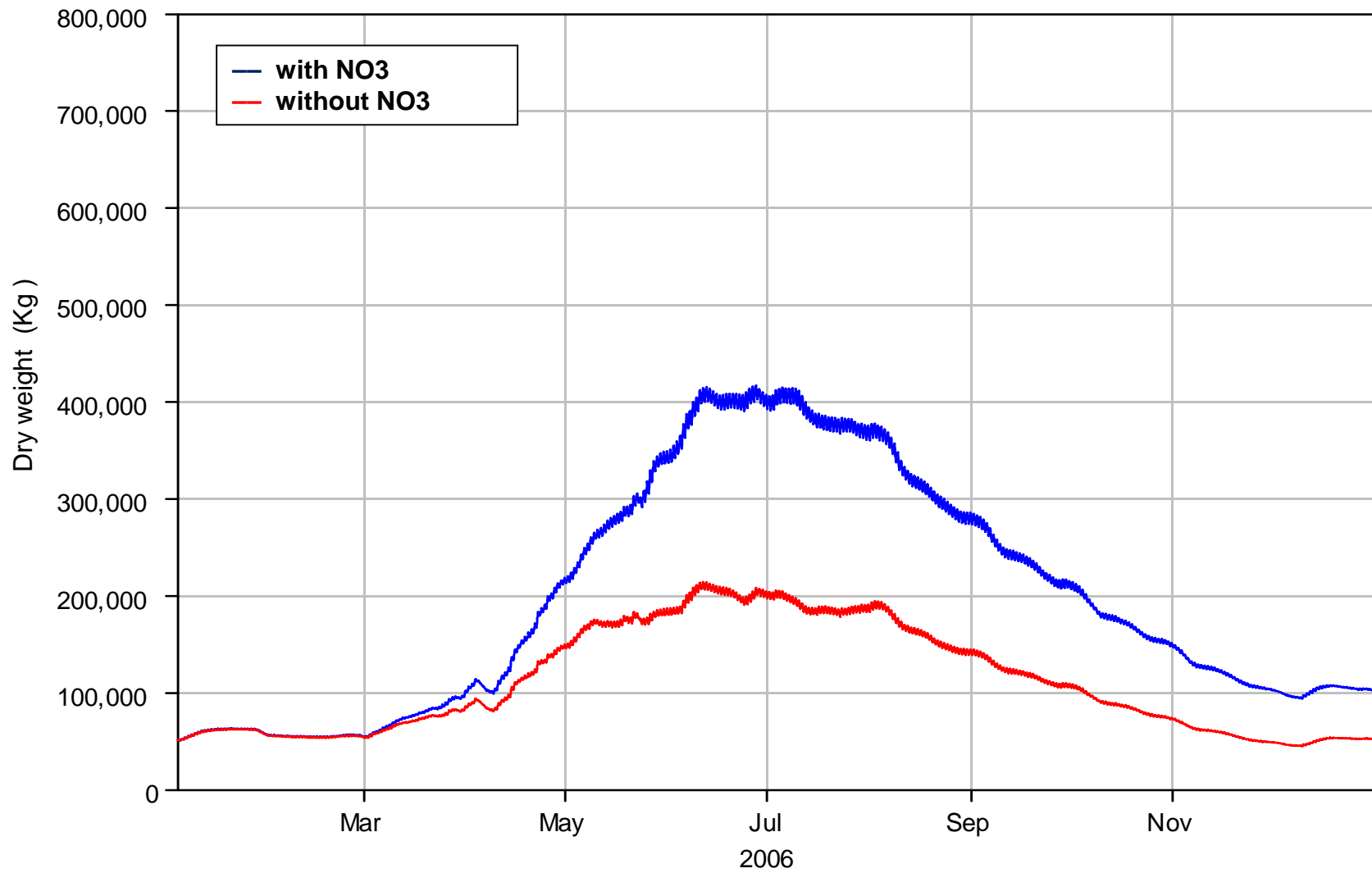


Figure 6-18 Comparison of total dry mass of macroalgae simulated with and without NO3 inputs from inflows in 2006.

6.3 Residence time simulations

Residence time simulations were performed for the dry weather period of July – August 2004. To compute residence time, all flows entering at the creek inflow or tidal boundaries are considered “new” water with a residence time of zero. The water volume in the 2-D area of the model is loaded with a tracer at 1 g/m³-day. The computed tracer concentration in the Bay is a direct measure of residence time (in days) of water within that area.

The Bay is initialized with zero tracer concentration throughout. Over time, tracer concentration – residence time – approaches an equilibrium concentration that varies with spring-neap tidal variation. During the summer, when tributary inflows are low, residence time increases through the neap tide and decreases through the spring tide. Lowest residence times follow the strongest spring tides. Color contour plots of residence time in Figure 6-19 bracket the range in residence time through the spring-neap tidal cycle. Figure 6-20 shows the timing of these plots relative to the tidal cycle. The highest residence time, about 12 days, occurs in Rhine Channel after the neap tide.

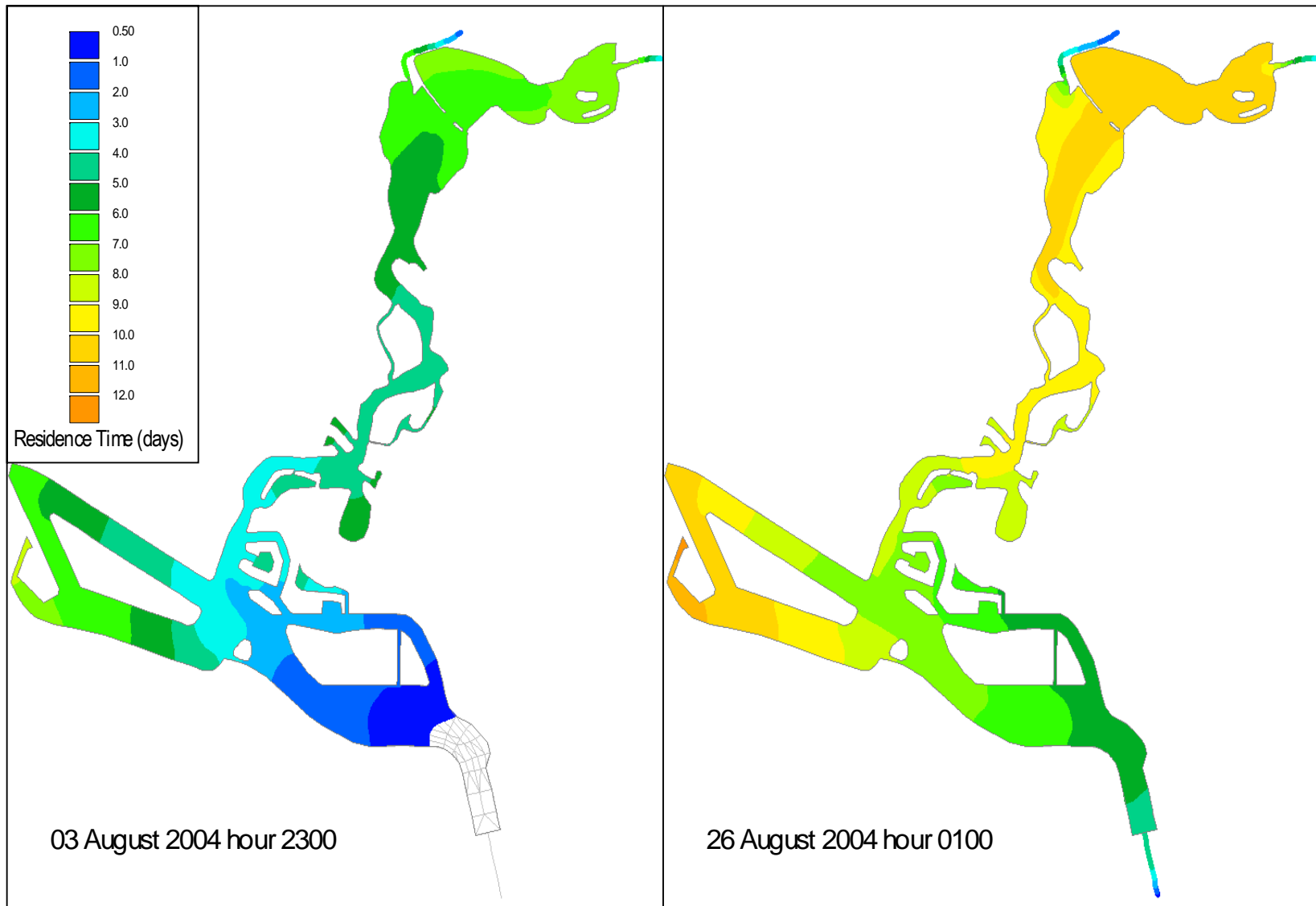


Figure 6-19 Color contour plots showing the range of residence times occurring during the 01 July – 31 August 2004 simulation period. Tidal phase and stage at the times of these plots can be seen in Figure 6-20.

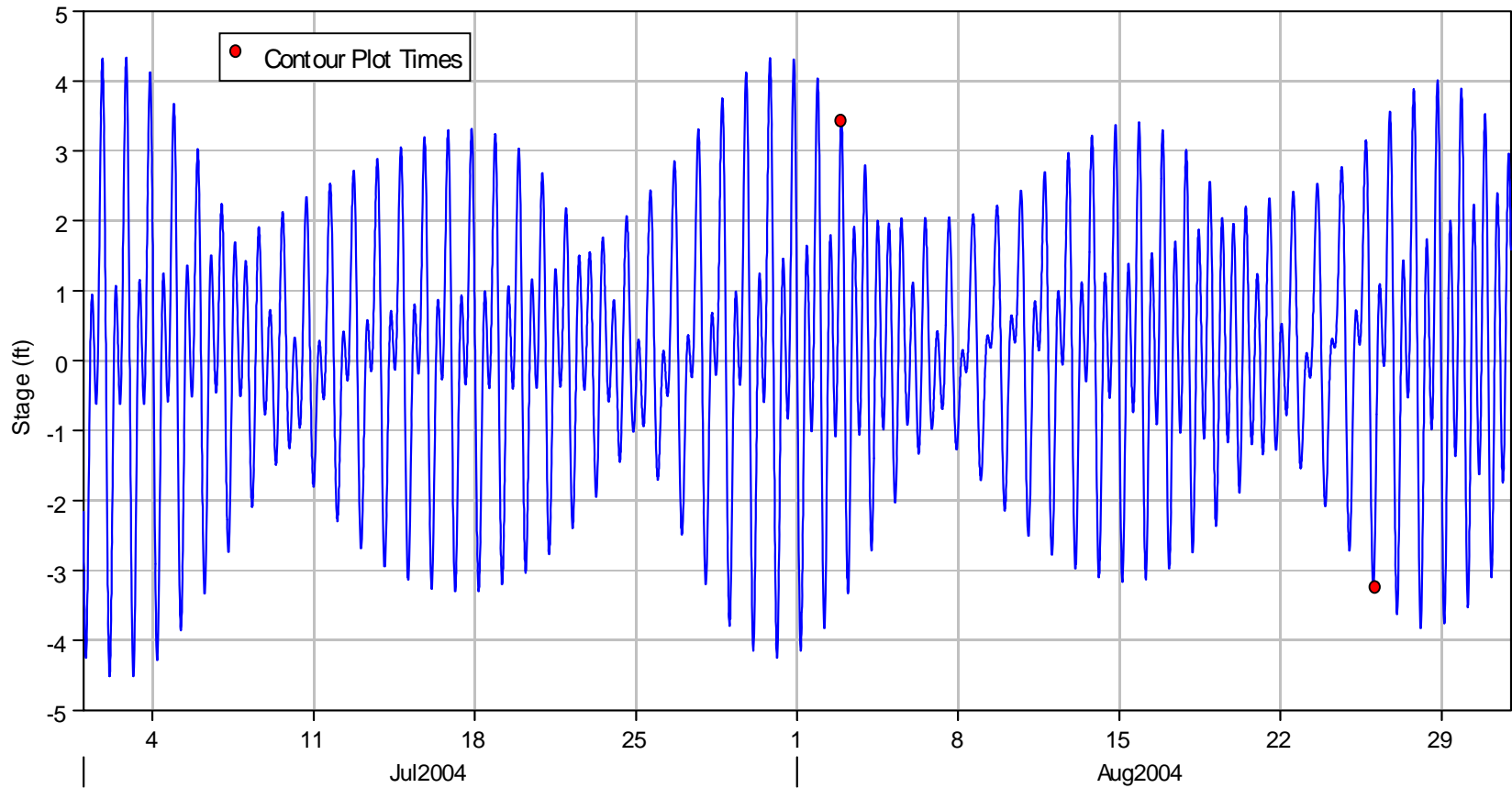


Figure 6-20 Time series of stage applied at the downstream model boundary for the 01 July – 31 August 2004 residence time simulation. Red dots indicate times of contour plots in Figure 6-19.

7. Reduced nutrient load simulations

To aid the Regional Board staff in selection of appropriate numeric water quality objectives for nutrients entering Newport Bay, the calibrated model has been used to simulate macroalgae blooms for reduced loading alternatives.

The approach was to limit total nitrogen entering the Bay based on concentration limits for the inflows. Different limits were set for storm flows versus low flow periods. A storm flow was considered to be any combined inflow (San Diego Creek plus Santa Ana Delhi Channel) greater than 50 cfs. Two different limits were set for storm flows (3 and 5 mg/L) and three for low flow periods (0.5, 1 and 2 mg/L), and each combination was simulated. For each alternative, concentrations of NH₃ and NO₃ of each inflow were allotted according to mass ratios of each constituent in the daily inflows. For example, if Santa Ana Delhi had an NH₃ concentration of 1 mg/L and flow rate of 1 m³/s, and San Diego creek had an NH₃ concentration of 5 mg/L and flow rate of 2 m³/s, the mass ratios of NH₃ of Santa Ana Delhi and San Diego Creek would be $1 \text{ mg/L} \times 1 \text{ m}^3/\text{s} / (1 \text{ mg/L} \times 1 \text{ m}^3/\text{s} + 5 \text{ mg/L} \times 2 \text{ m}^3/\text{s})$ and $5 \text{ mg/L} \times 2 \text{ m}^3/\text{s} / (1 \text{ mg/L} \times 1 \text{ m}^3/\text{s} + 5 \text{ mg/L} \times 2 \text{ m}^3/\text{s})$, respectively,. A reduction in the ratio of particulate nitrogen to suspended sediment corresponding to the storm flow limit was applied as well, assuming a reduction in the nitrogen content of sediment under reduced loading alternatives. The ratio of particulate nitrogen to suspended sediment used in the calibration/validation simulations was 0.001. For the simulations with storm flows limited to 3 mg/L total nitrogen, the particulate nitrogen to suspended sediment ratio was set to .0003 assuming a 70% reduction of particulate nitrogen in the suspended sediments coming from inflows. For the simulations with storm flows limited to 5 mg/L total nitrogen, the ratio was set to .0005, assuming a 50% reduction of particulate nitrogen in the suspended sediments coming from inflows. Concentration limits and particulate nitrogen to suspended sediment ratios are summarized for each alternative in

Table 7-1.

Simulations were performed for the 2004 through 2006 period and the model calibration/validation results are used as the Base case for comparison. Figure 7-1 through Figure 7-6 show time series of total nitrogen entering the Bay in the inflows (San Diego Creek and Santa Ana Delhi Channel) for each of the alternatives in comparison with the Base case. Annually averaged total nitrogen is plotted in Figure 7-7 and Figure 7-8 for each of the inflows and annual median total nitrogen is plotted in Figure 7-9 and Figure 7-10 for each of the inflows. Note that annual medians are nearly identical for the alternatives with the same low flow loading (e.g. Alternative 1 and Alternative 4) and thus they plot on top of each other.

Alternative simulation results are plotted with the Base case for 2004 in Figure 7-11 through Figure 7-19, 2005 in Figure 7-20 through Figure 7-28 and 2006 in Figure 7-29 through Figure 7-37. The first plot for each year shows time series total macroalgae mass in the Bay and the next plots show time series of macroalgae concentration at each of the algae sampling locations. Alternatives 1 – 3, those with the greatest reduction in storm flow nitrogen load, produce the lowest concentrations of macroalgae. Alternative 1, with the lowest total nitrogen limits for both storm and low flow periods, reduces the peak total macroalgae mass by just over 50% for each year. Alternative 6, with the highest total nitrogen limits, reduces the peak total macroalgae mass by approximately 30% for each year.

Table 7-1 Summary of concentration limits and particulate nitrogen to suspended sediment ratios for alternatives.

	Total Nitrogen Concentration limit (mg/L)		Particulate nitrogen to suspended sediment ratio
	Storm flow (>50 cfs)	Low flow (≤50 cfs)	
Base case	No limit	No limit	0.001
Alternative 1	3	0.5	0.0003
Alternative 2	3	1	0.0003
Alternative 3	3	2	0.0003
Alternative 4	5	0.5	0.0005
Alternative 5	5	1	0.0005
Alternative 6	5	2	0.0005

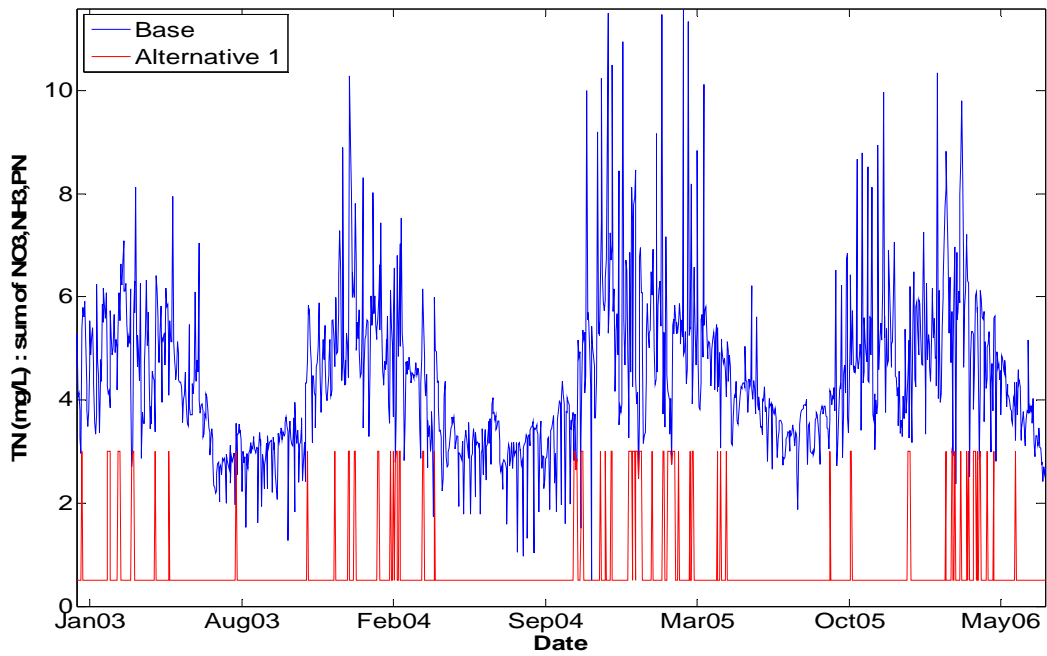


Figure 7-1 Time series of total nitrogen entering the Bay from Santa Ana Delhi and San Diego Creek for Base case and Alternative 1 (3.0 mg/L-0.5 mg/L).

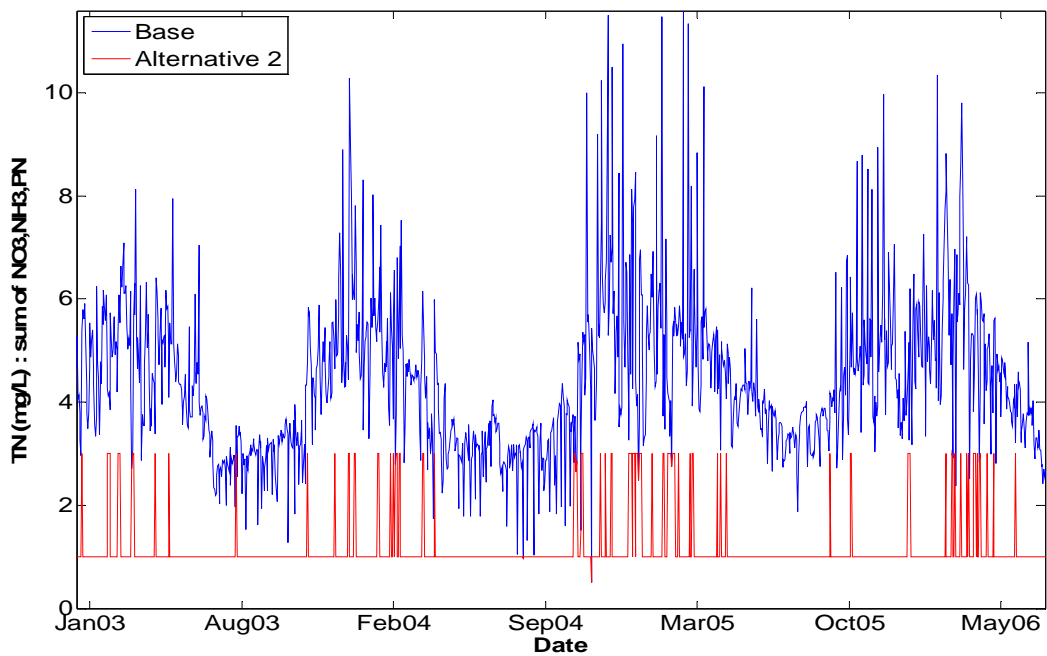


Figure 7-2 Time series of total nitrogen entering the Bay from Santa Ana Delhi and San Diego Creek for Base case and Alternative 2 (3.0 mg/L-1.0 mg/L).

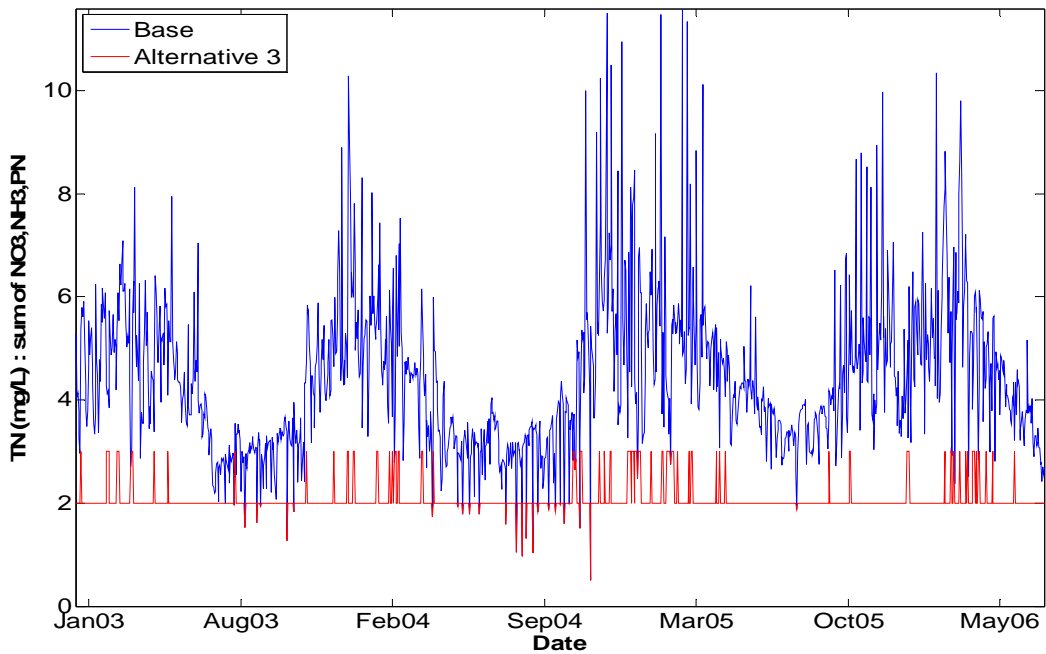


Figure 7-3 Time series of total nitrogen entering the Bay from Santa Ana Delhi and San Diego Creek for Base case and Alternative 3 (3.0 mg/L-2.0 mg/L).

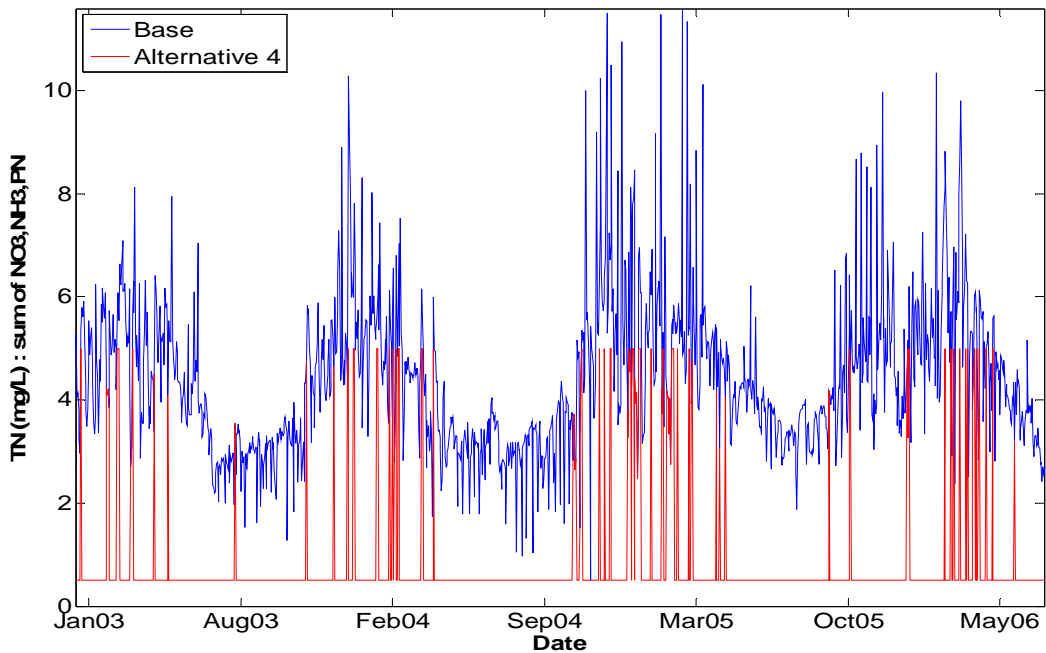


Figure 7-4 Time series of total nitrogen entering the Bay from Santa Ana Delhi and San Diego Creek for Base case and Alternative 4 (5.0 mg/L-0.5 mg/L).

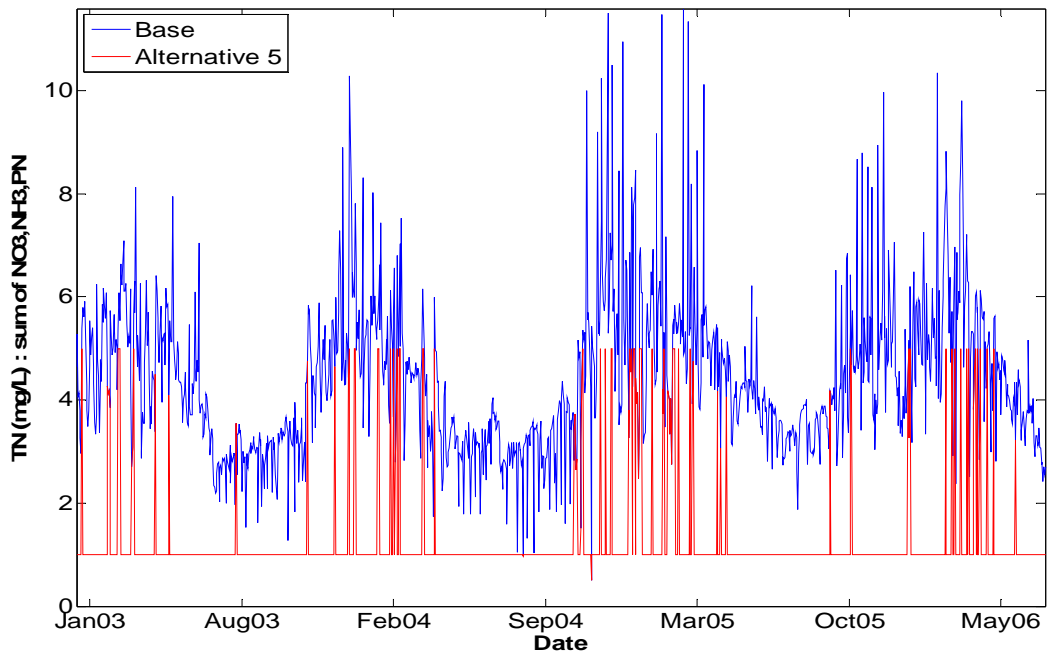


Figure 7-5 Time series of total nitrogen entering the Bay from Santa Ana Delhi and San Diego Creek for Base case and Alternative 5 (5.0 mg/L-1.0 mg/L).

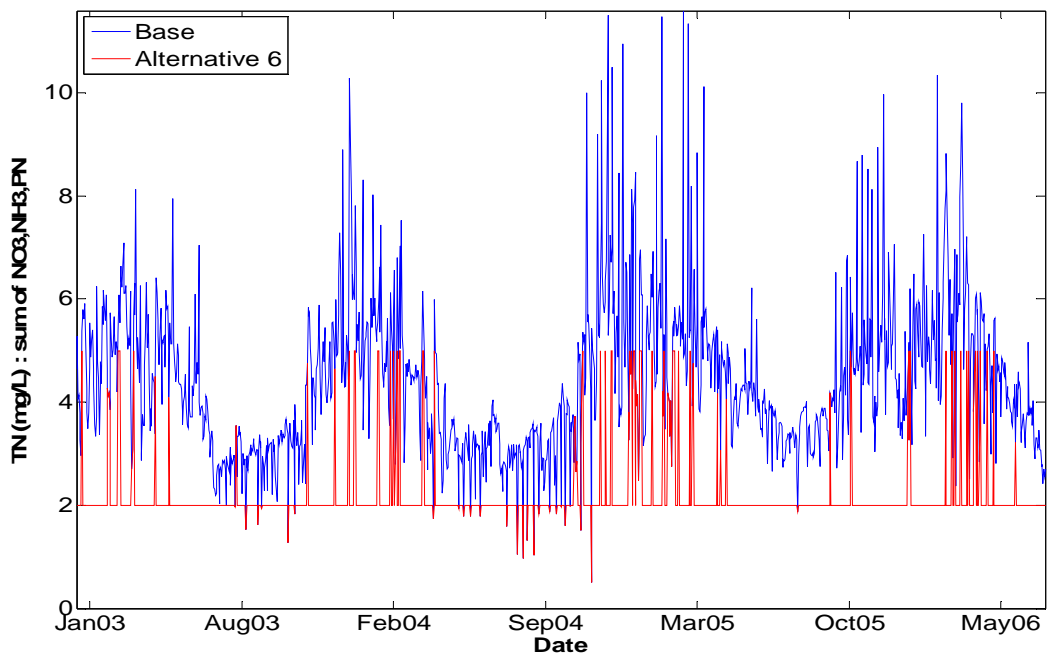


Figure 7-6 Time series of total nitrogen entering the Bay from Santa Ana Delhi and San Diego Creek for Base case and Alternative 6 (5.0 mg/L-2.0 mg/L).

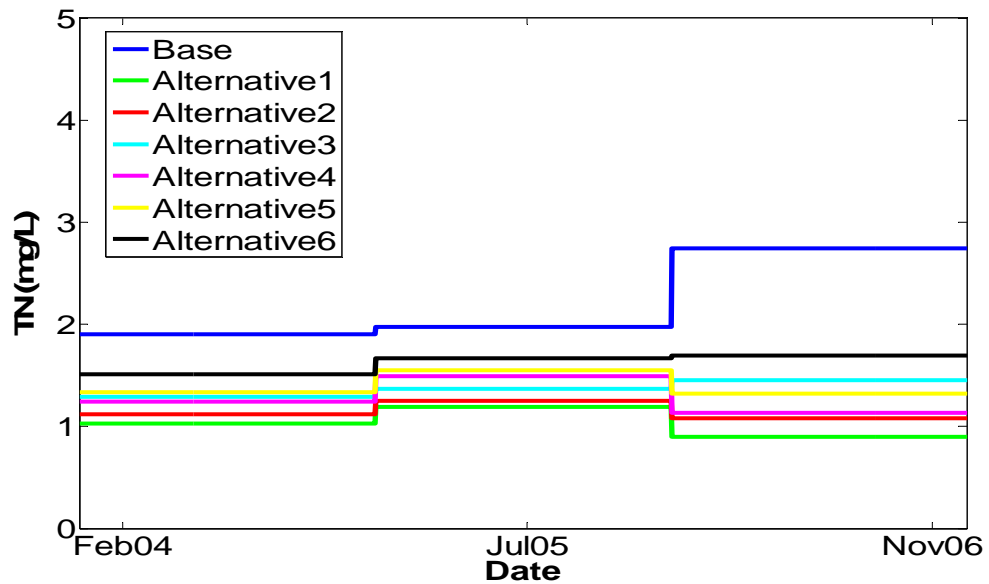


Figure 7-7 Annually averaged total nitrogen concentration of Santa Ana Delhi for Base case and alternatives.

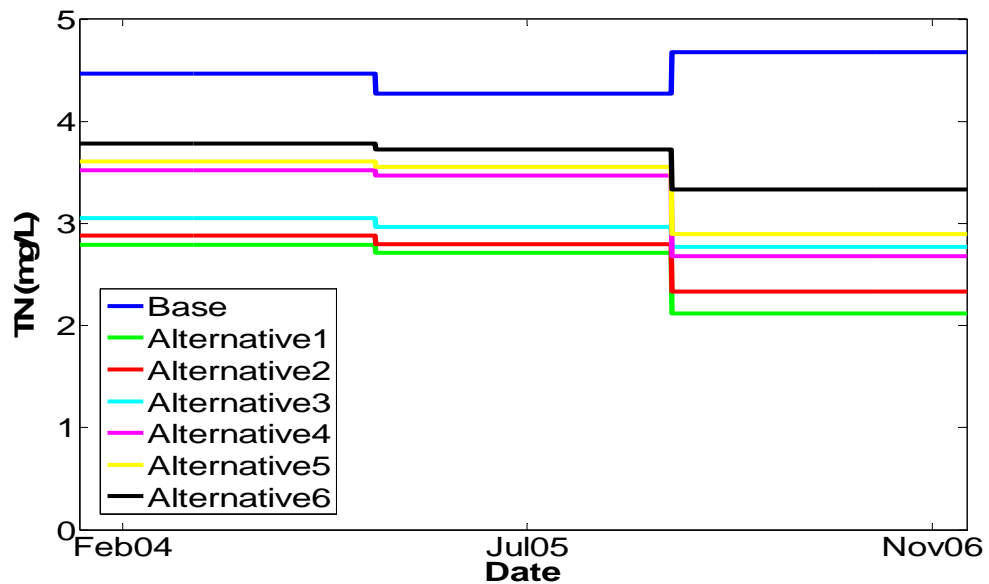


Figure 7-8 Annually averaged total nitrogen concentration of San Diego Creek for Base case and alternatives.

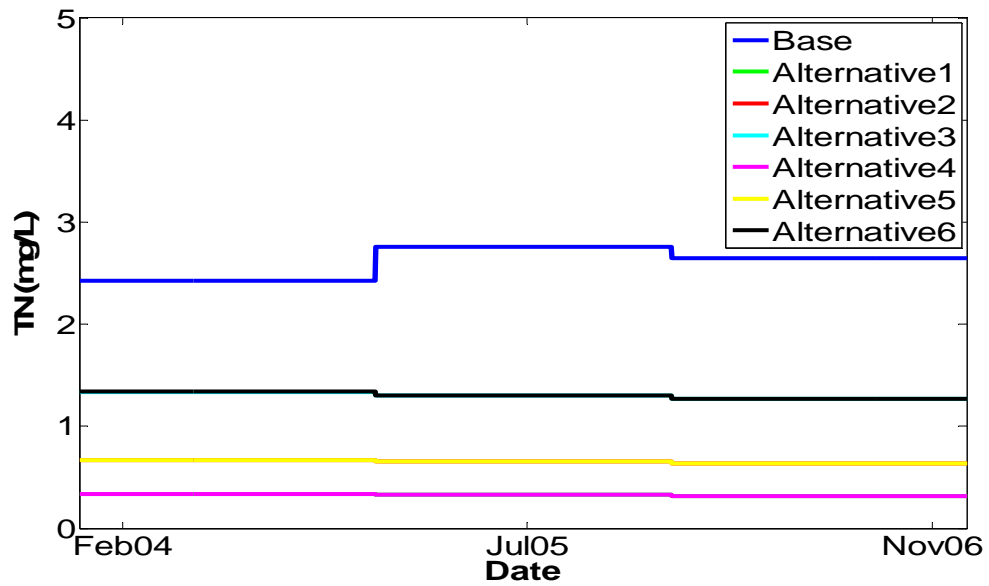


Figure 7-9 Annual median of total nitrogen concentration of Santa Ana Delhi for Base case and alternatives. Note that the alternatives with the same dry season loading (e.g. 1 and 4) have nearly identical annual medians and thus plot on top of one another.

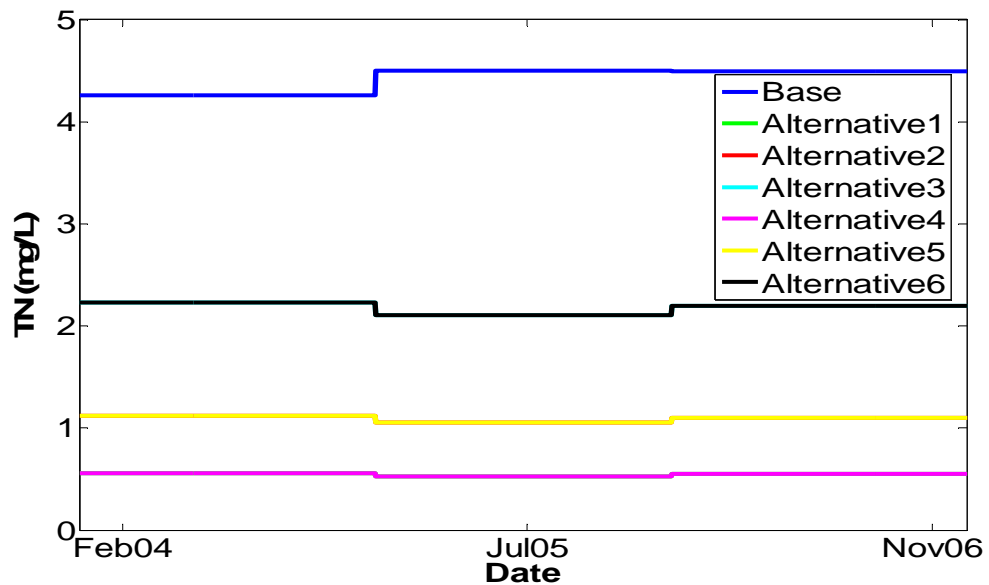


Figure 7-10 Annual median of total nitrogen concentration of San Diego Creek for Base case and alternatives. Note that the alternatives with the same dry season loading (e.g. 1 and 4) have nearly identical annual medians and thus plot on top of one another.

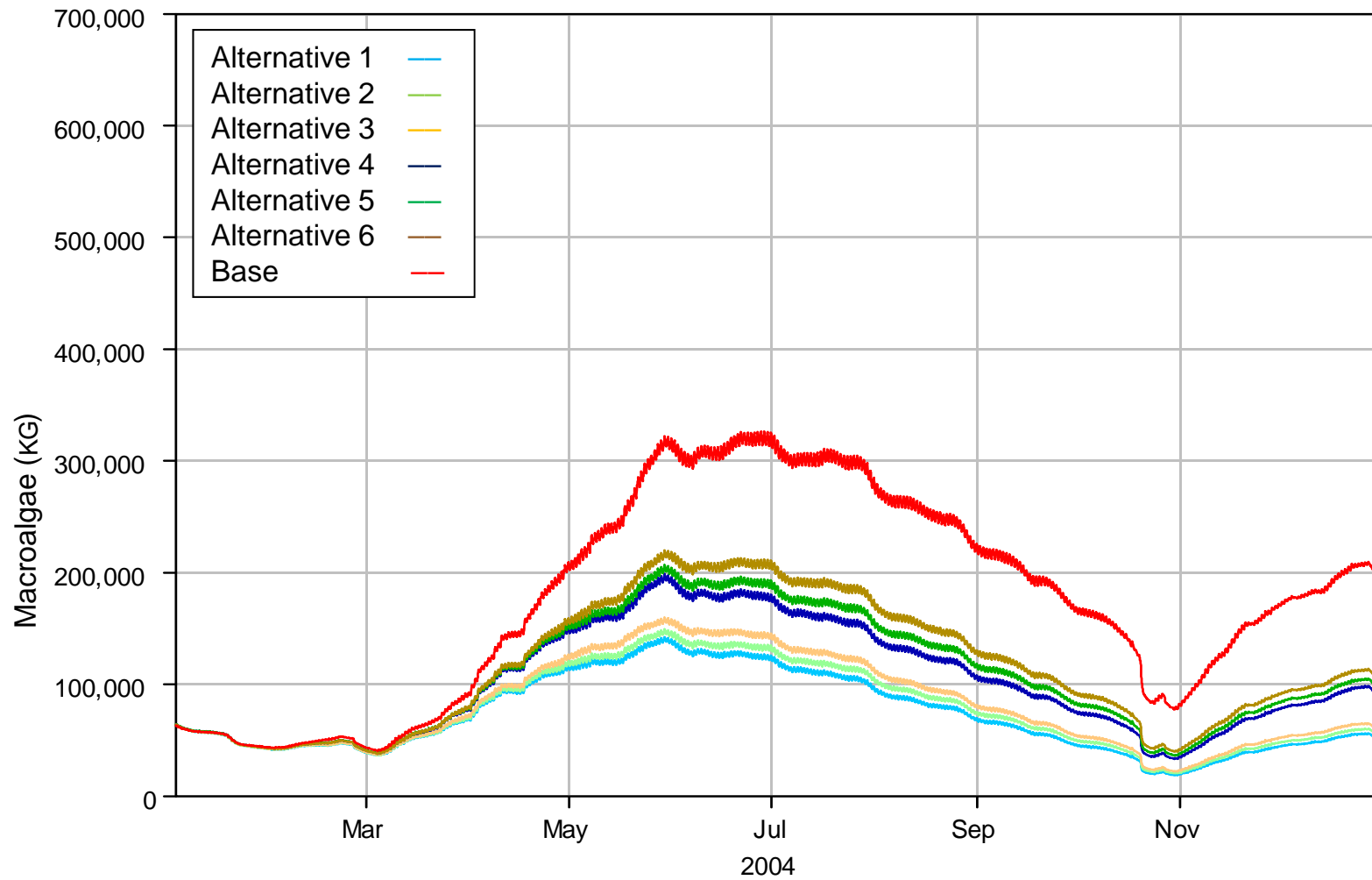


Figure 7-11 Comparison of total dry mass of macroalgae among alternatives with the Base case in 2004.

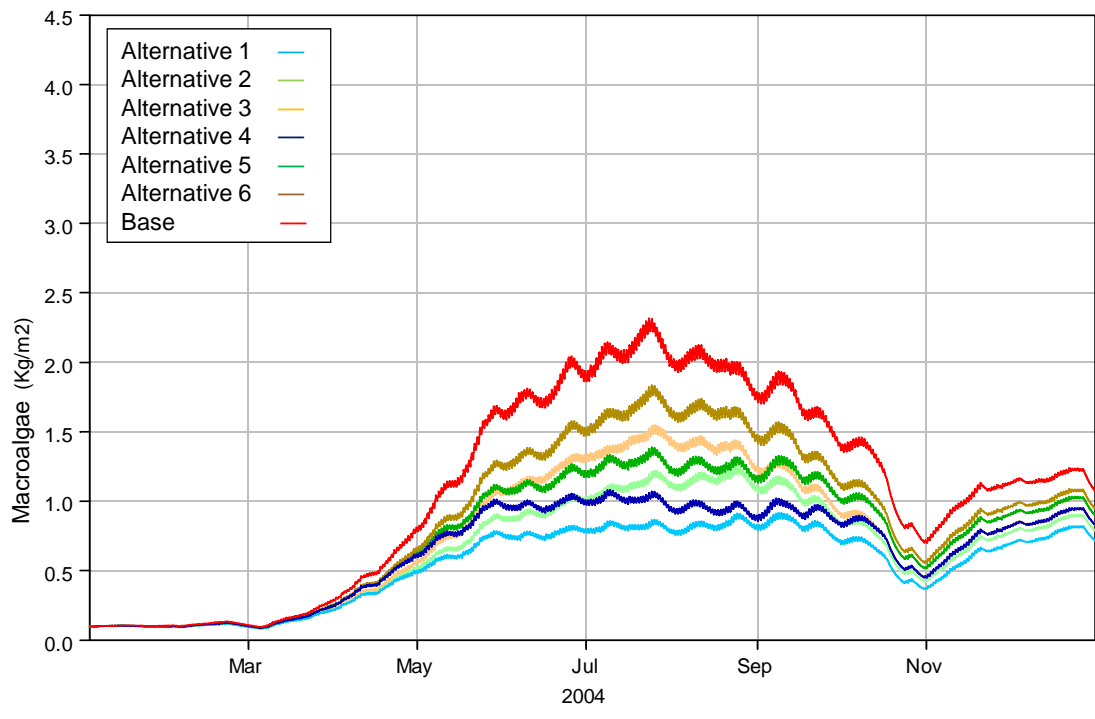


Figure 7-12 Comparison of macroalgae concentrations among alternatives with the Base case at station ALG24 in 2004.

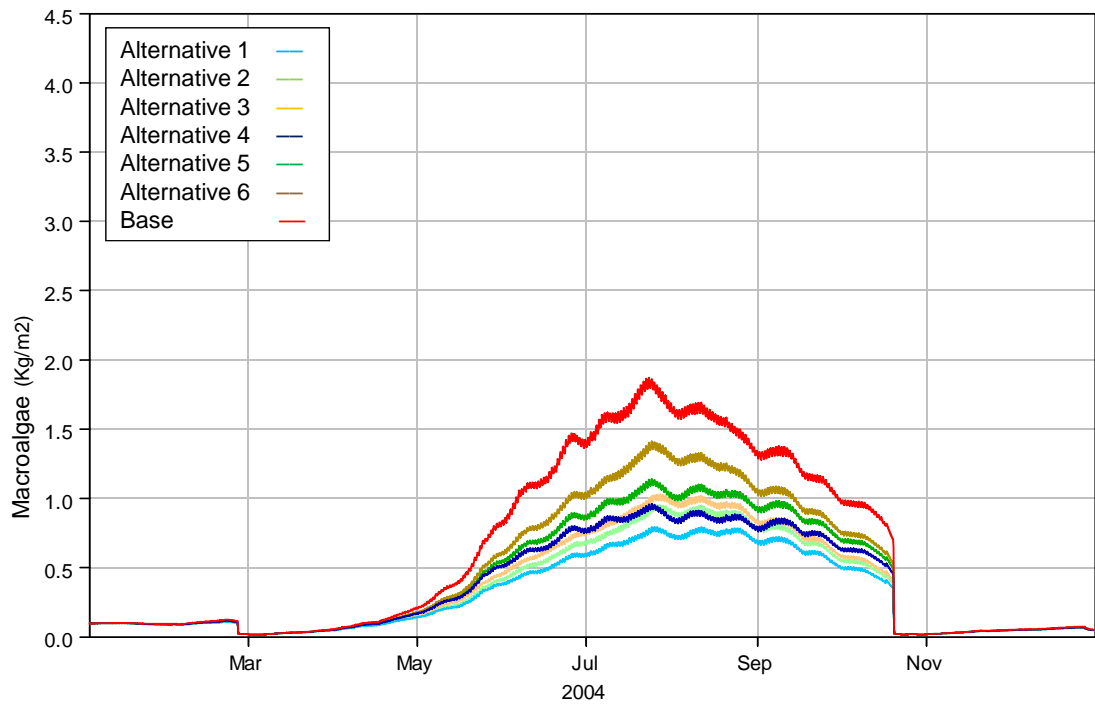


Figure 7-13 Comparison of macroalgae concentrations among alternatives with the Base case at station ALG19 in 2004.

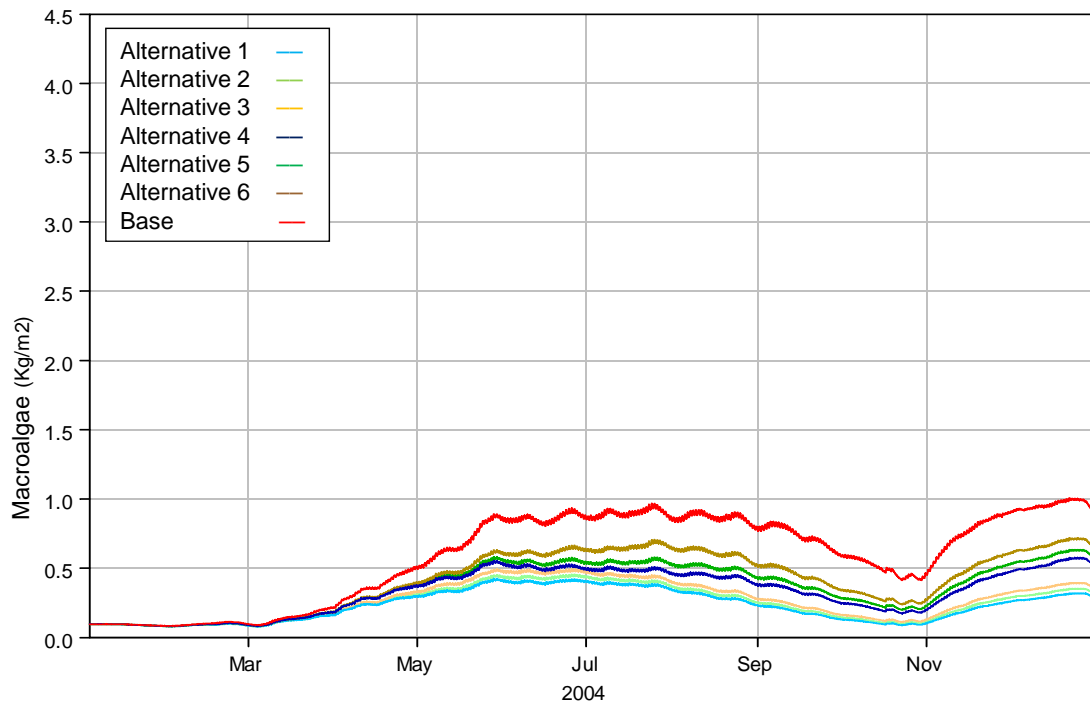


Figure 7-14 Comparison of macroalgae concentrations among alternatives with the Base case at station ALG16 in 2004.

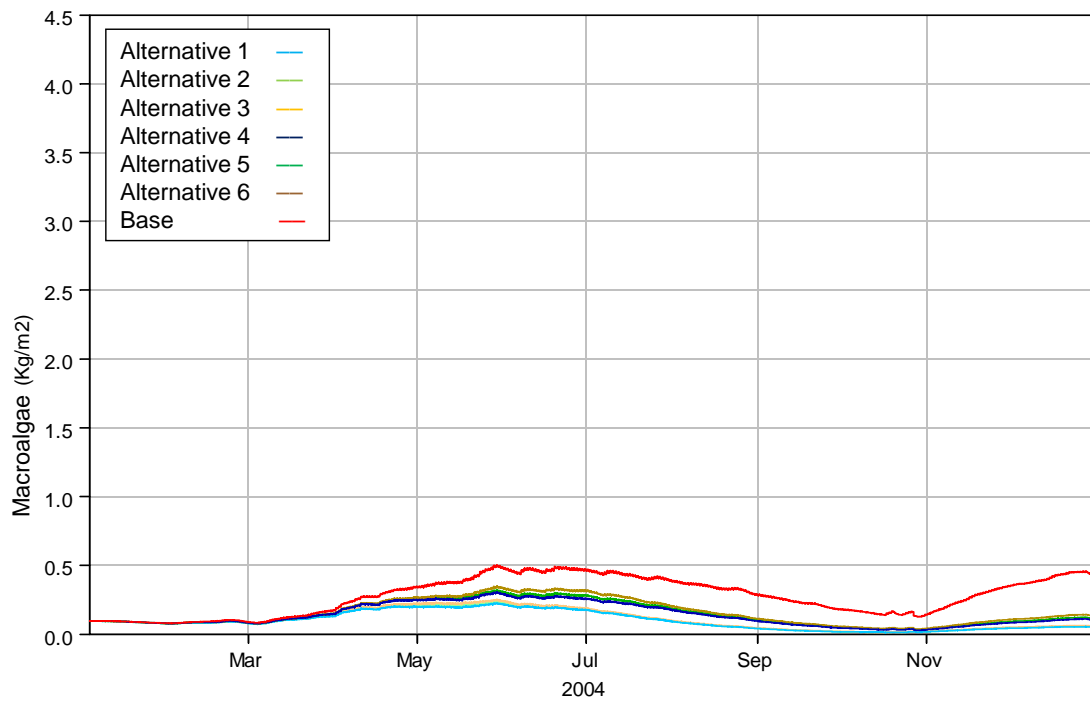


Figure 7-15 Comparison of macroalgae concentrations among alternatives with the Base case at station ALG13 in 2004.

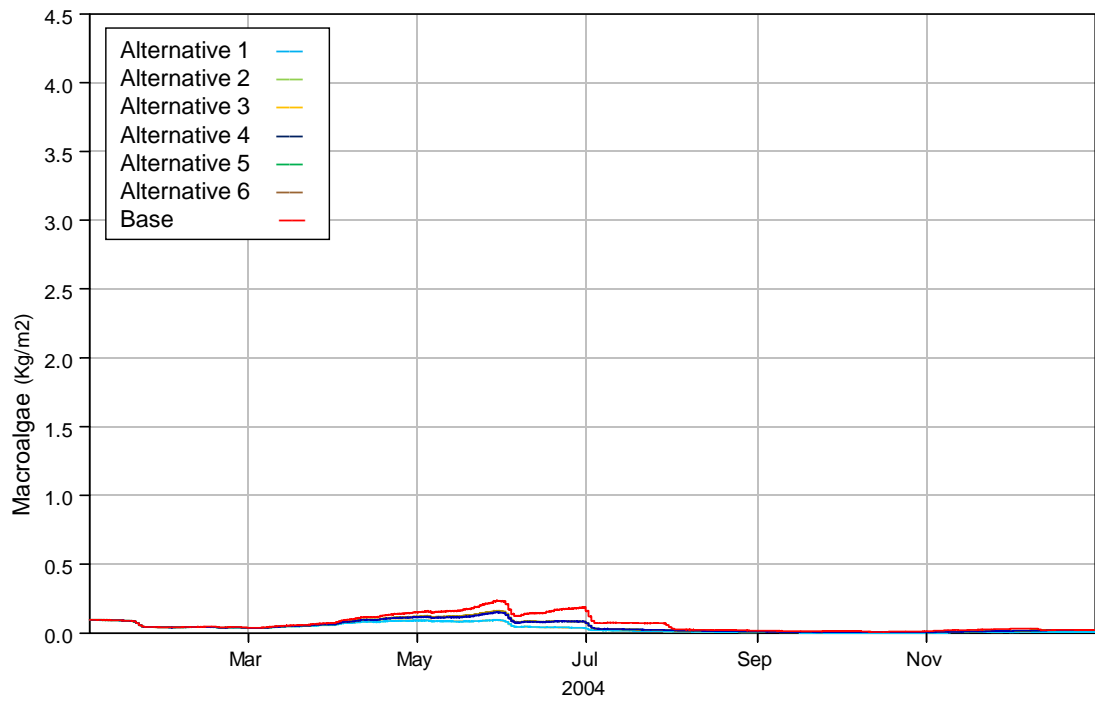


Figure 7-16 Comparison of macroalgae concentrations among alternatives with the Base case at station ALG9 in 2004.

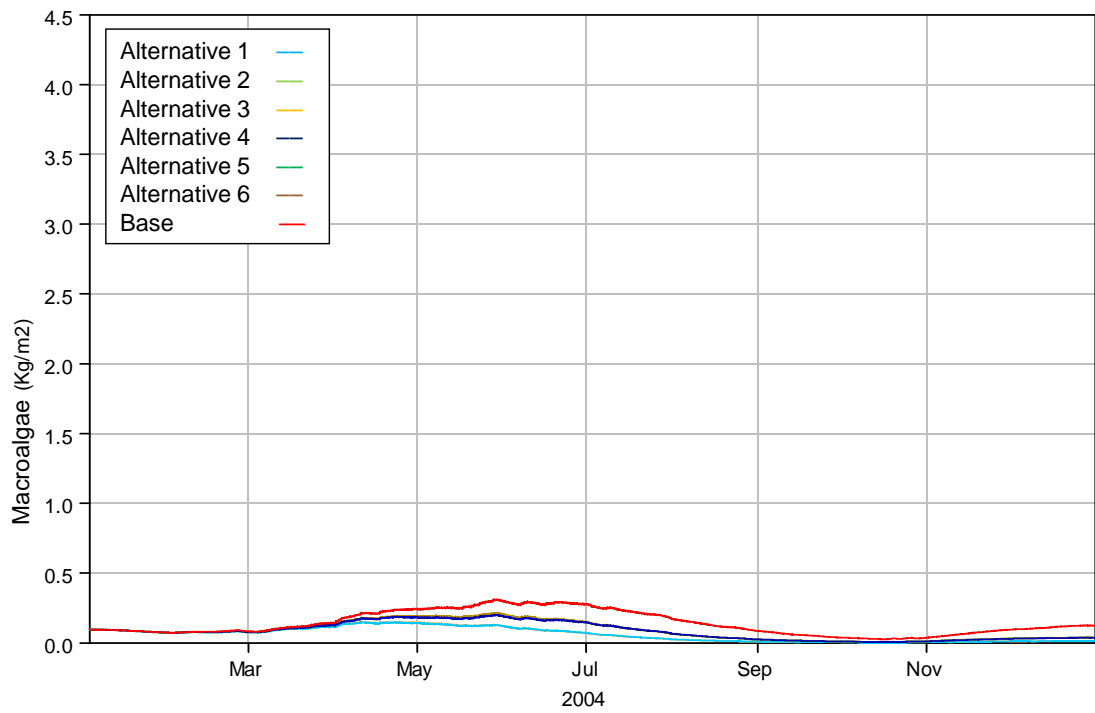


Figure 7-17 Comparison of macroalgae concentrations among alternatives with the Base case at station ALG7 in 2004.

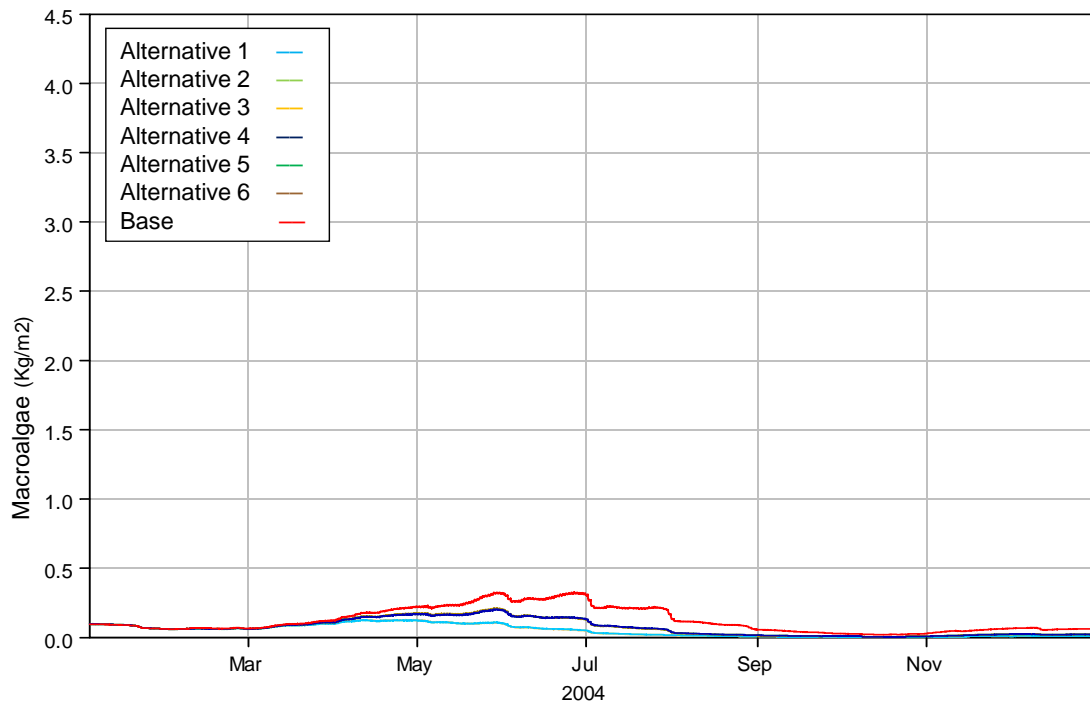


Figure 7-18 Comparison of macroalgae concentrations among alternatives with the Base case at station ALG4 in 2004.

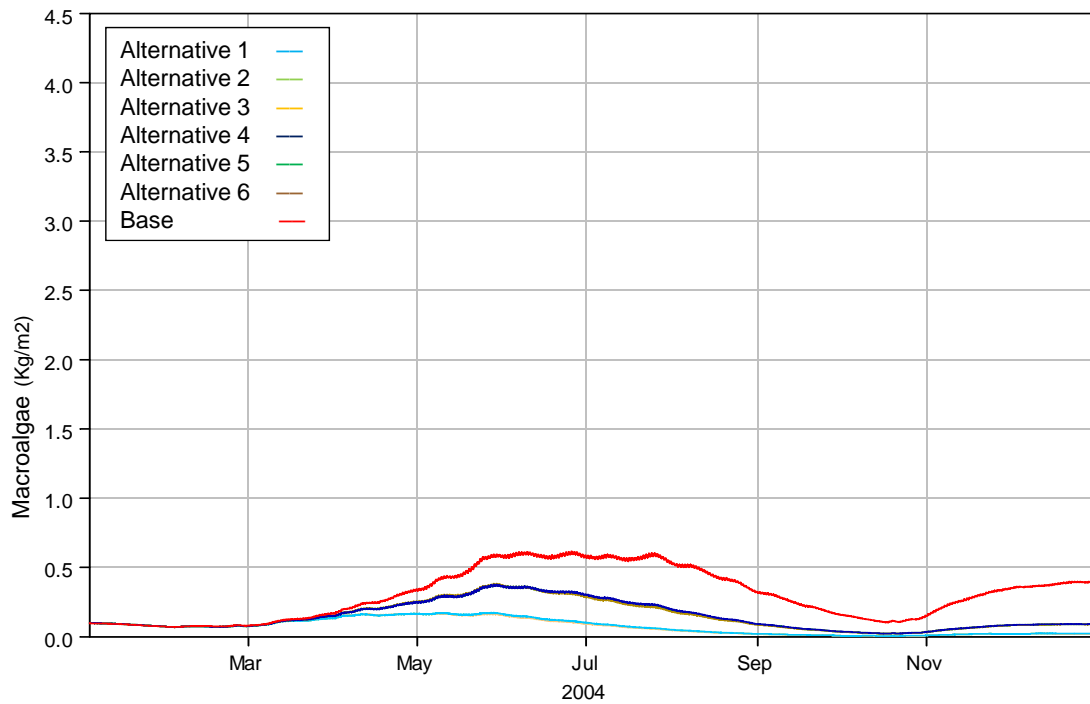


Figure 7-19 Comparison of macroalgae concentrations among alternatives with the Base case at station ALG2 in 2004.

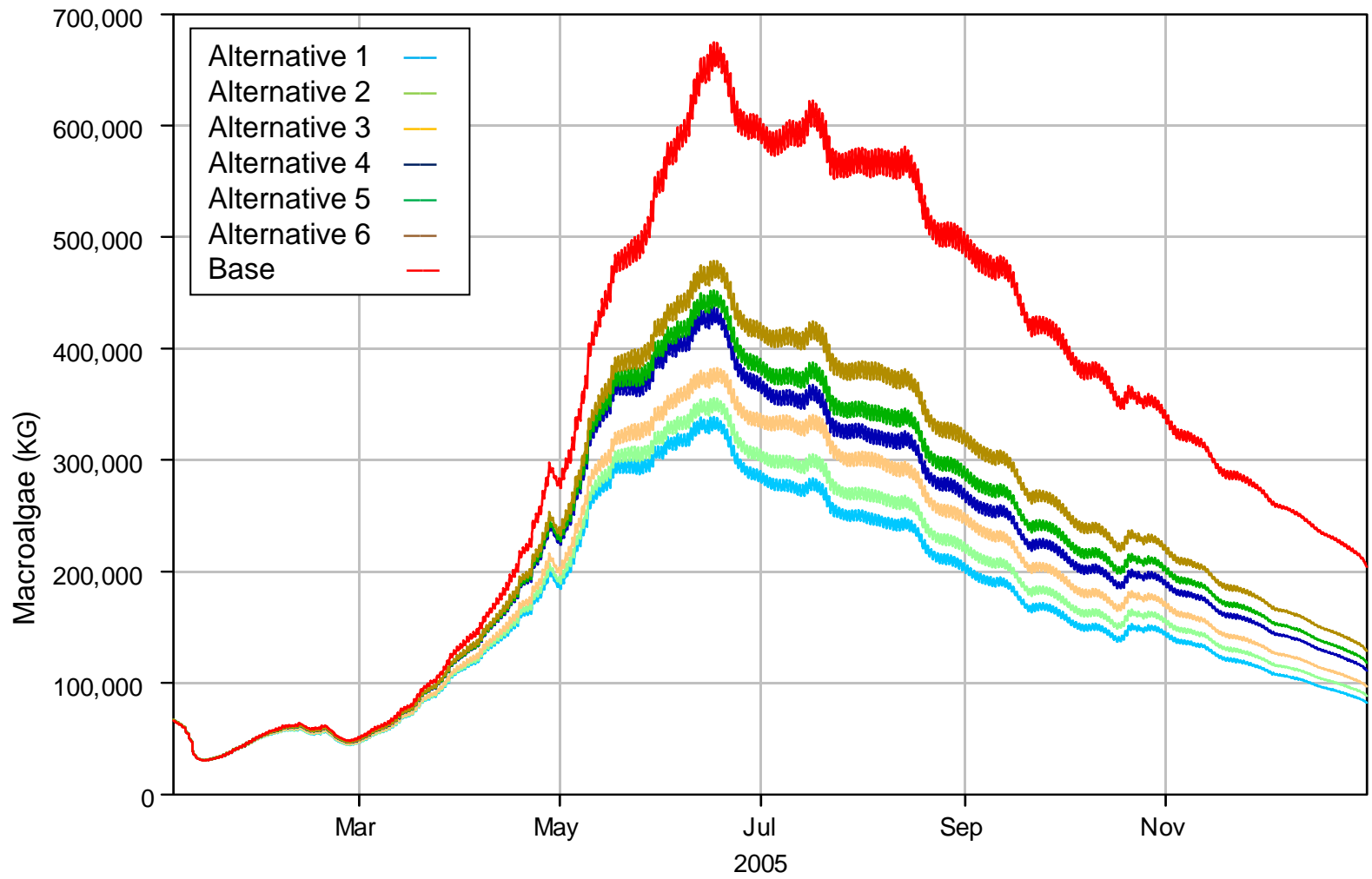


Figure 7-20 Comparison of total dry mass of macroalgae among alternatives with the Base case in 2005.

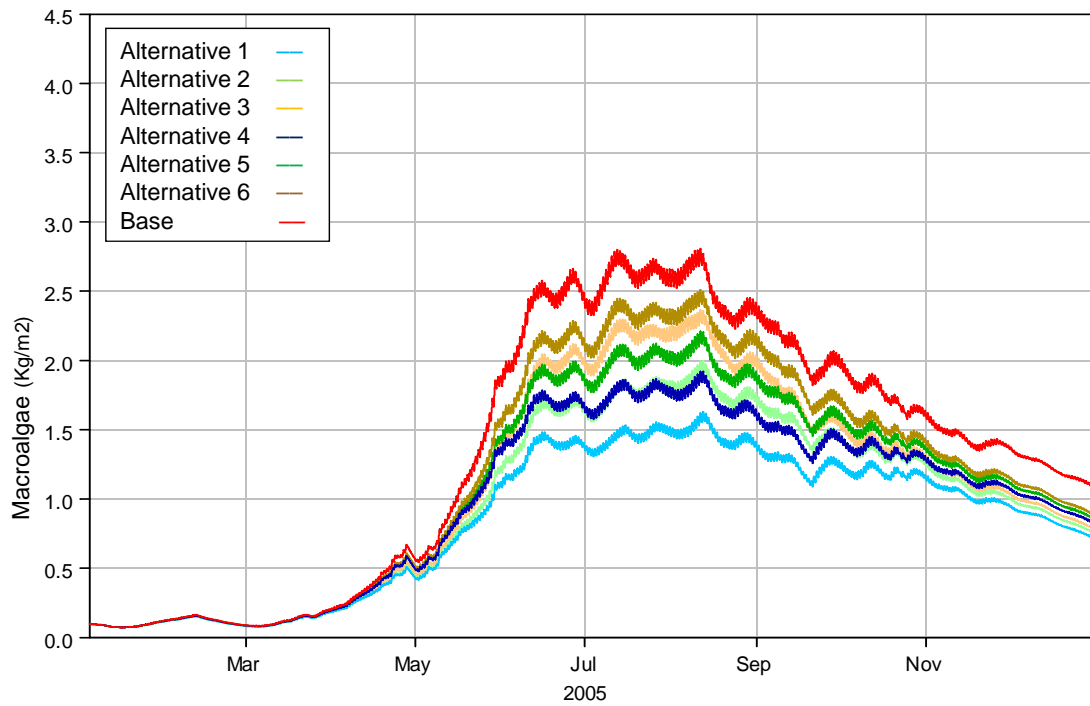


Figure 7-21 Comparison of macroalgae concentrations among alternatives with the Base case at station ALG24 in 2005.

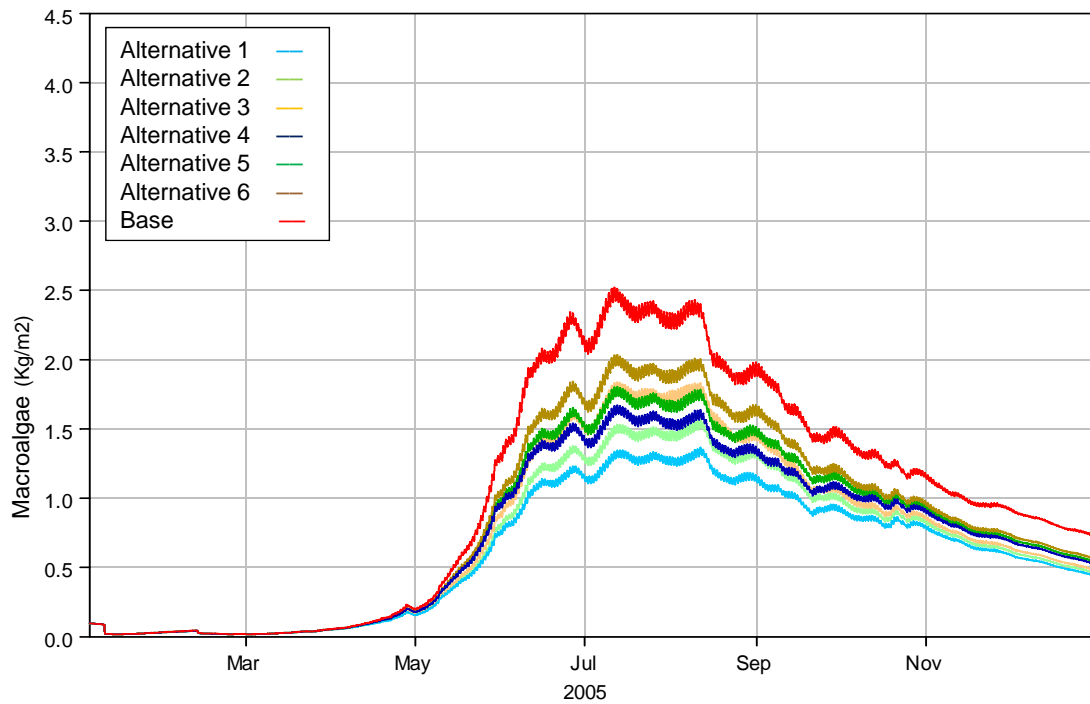


Figure 7-22 Comparison of macroalgae concentrations among alternatives with the Base case at station ALG19 in 2005.

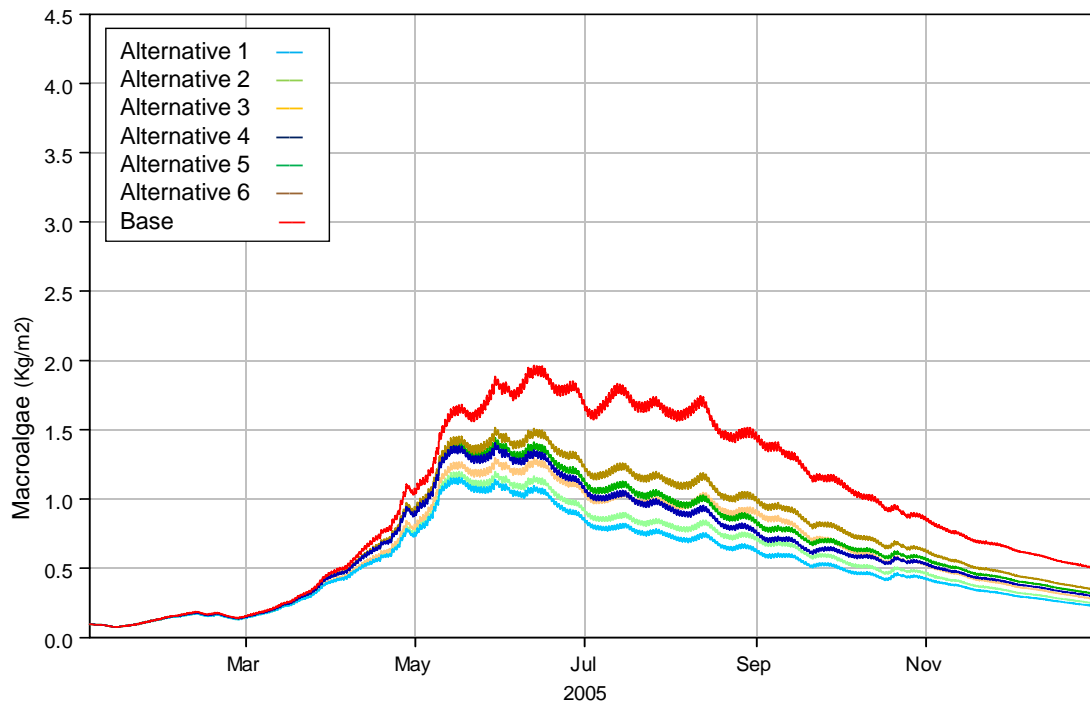


Figure 7-23 Comparison of macroalgae concentrations among alternatives with the Base case at station ALG16 in 2005.

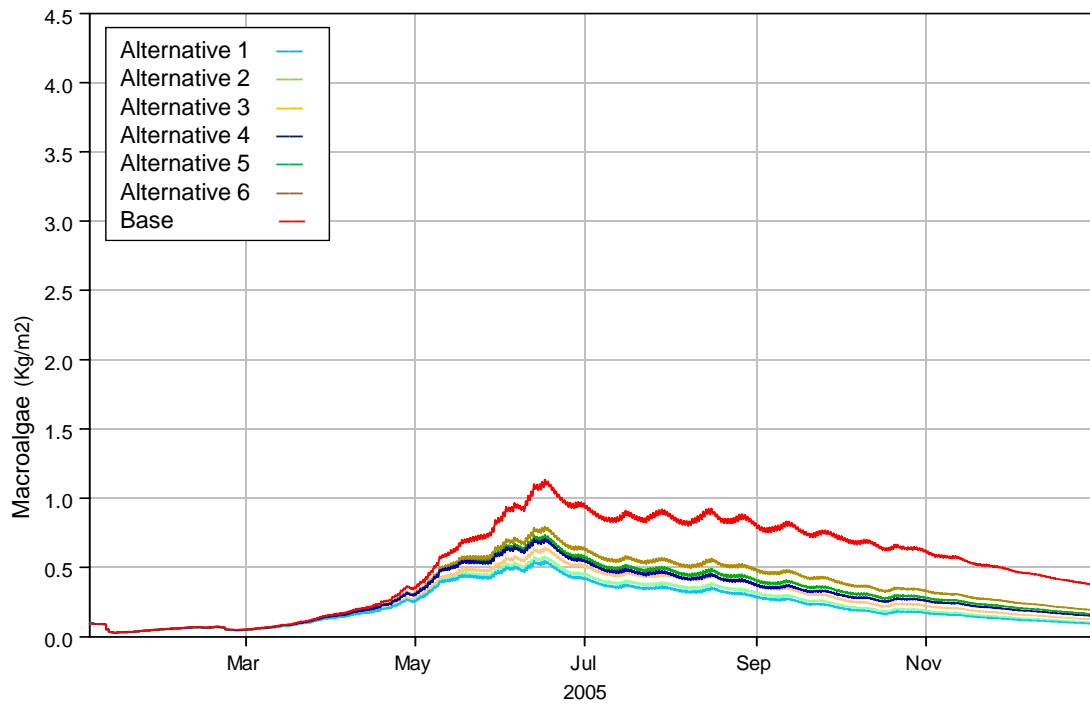


Figure 7-24 Comparison of macroalgae concentrations among alternatives with the Base case at station ALG13 in 2005.

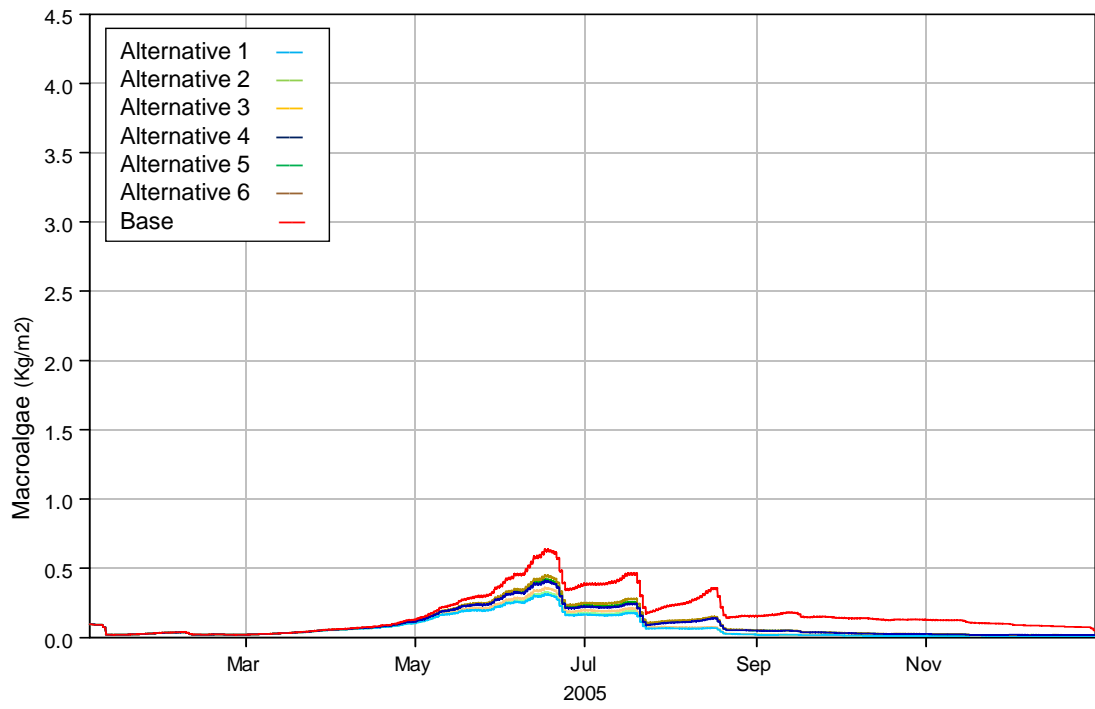


Figure 7-25 Comparison of macroalgae concentrations among alternatives with the Base case at station ALG9 in 2005.

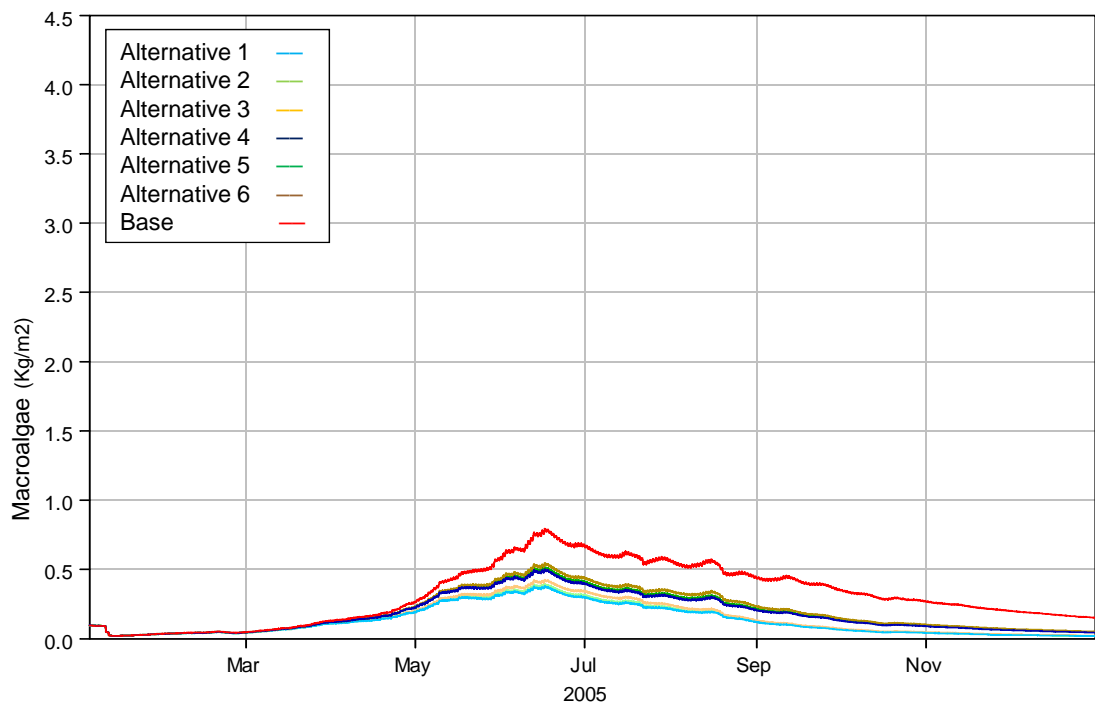


Figure 7-26 Comparison of macroalgae concentrations among alternatives with the Base case at station ALG7 in 2005.

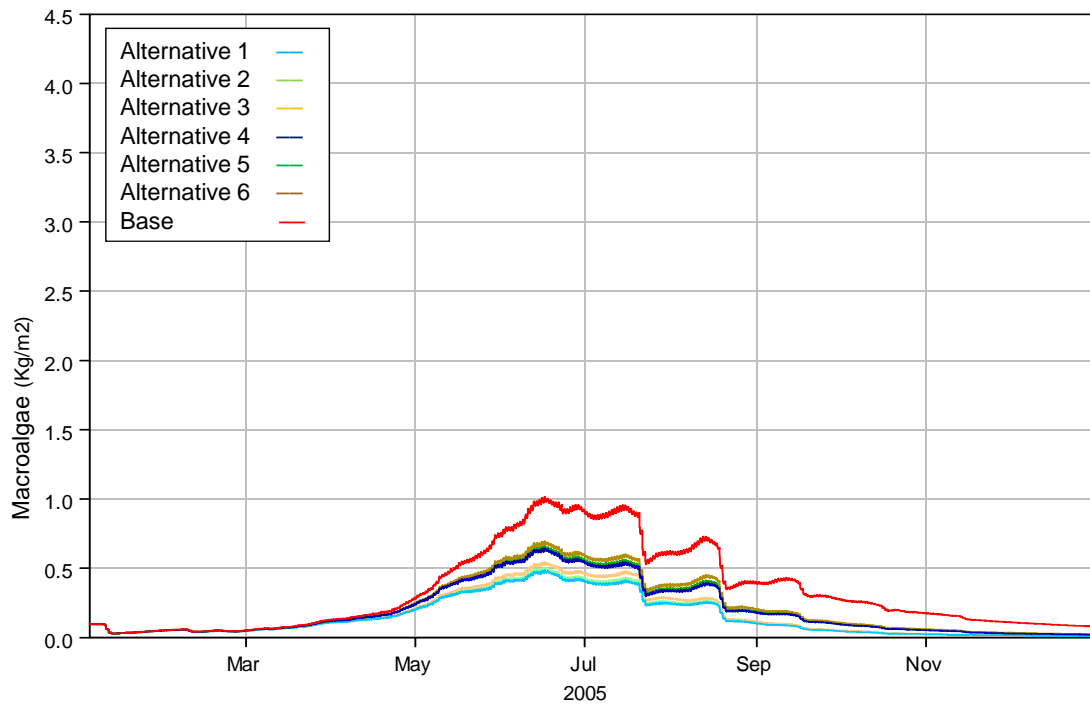


Figure 7-27 Comparison of macroalgae concentrations among alternatives with the Base case at station ALG4 in 2005.

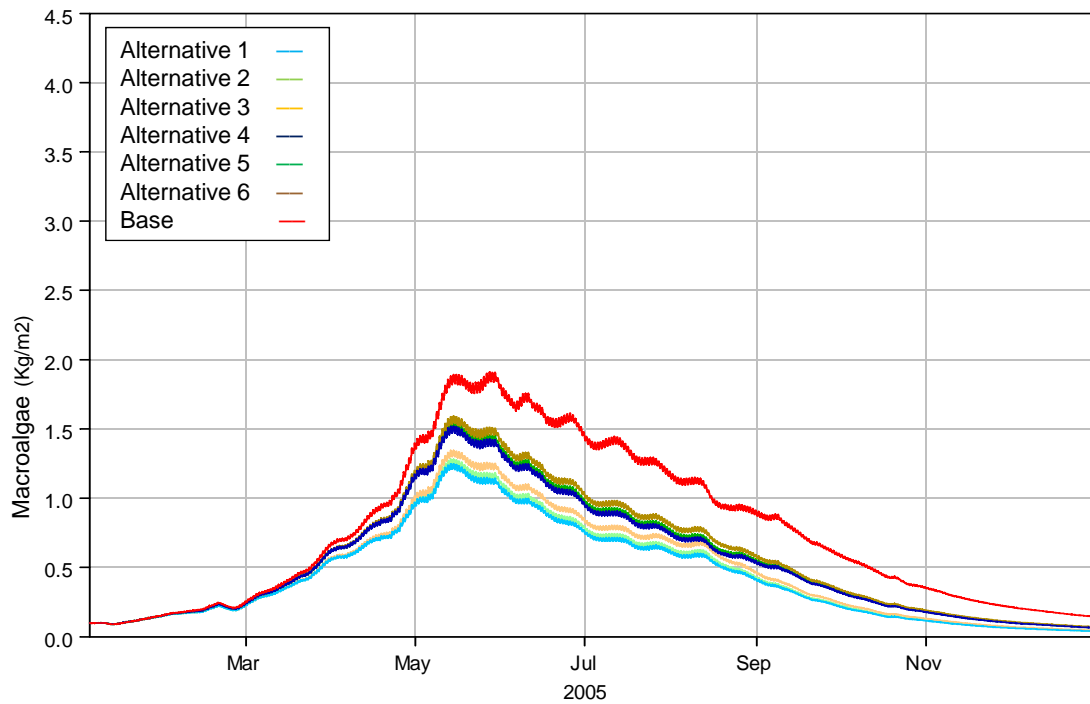


Figure 7-28 Comparison of macroalgae concentrations among alternatives with the Base case at station ALG2 in 2005.

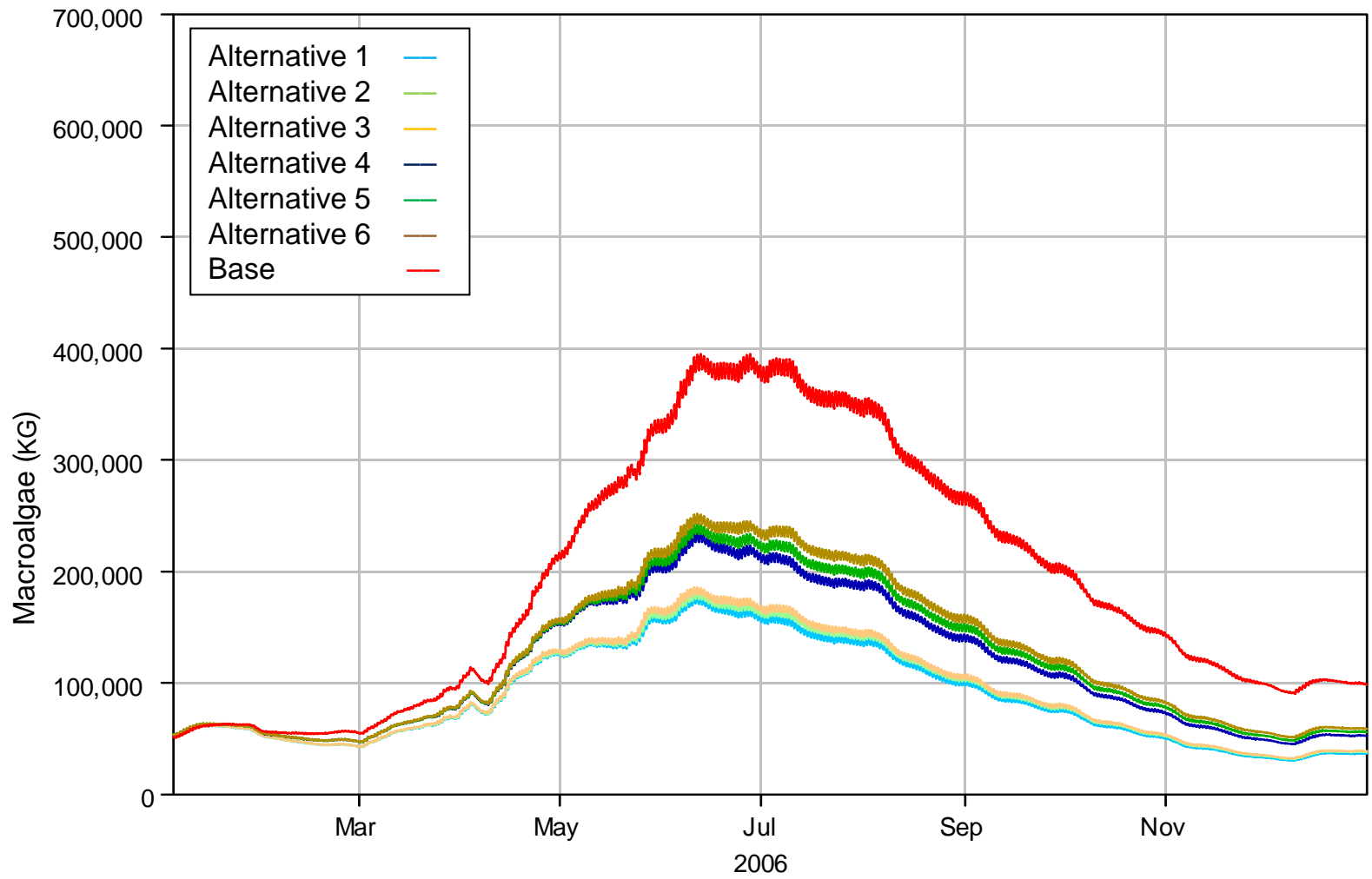


Figure 7-29 Comparison of total dry mass of macroalgae among alternatives with the Base case in 2006.

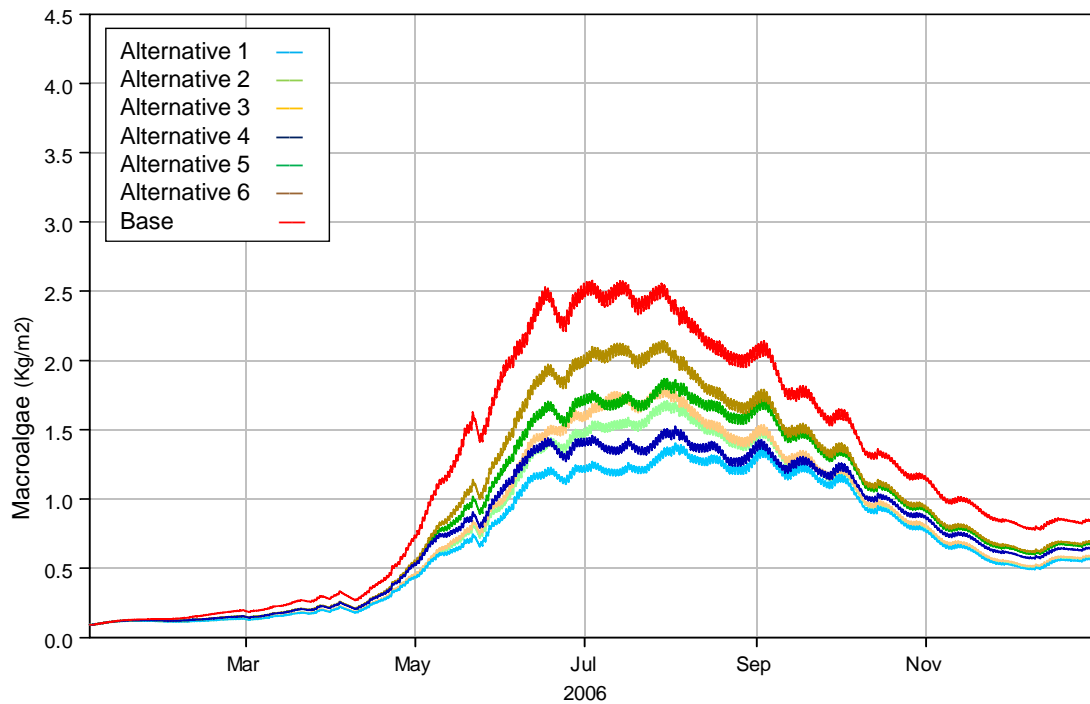


Figure 7-30 Comparison of macroalgae concentrations among alternatives with the Base case at station ALG24 in 2006.

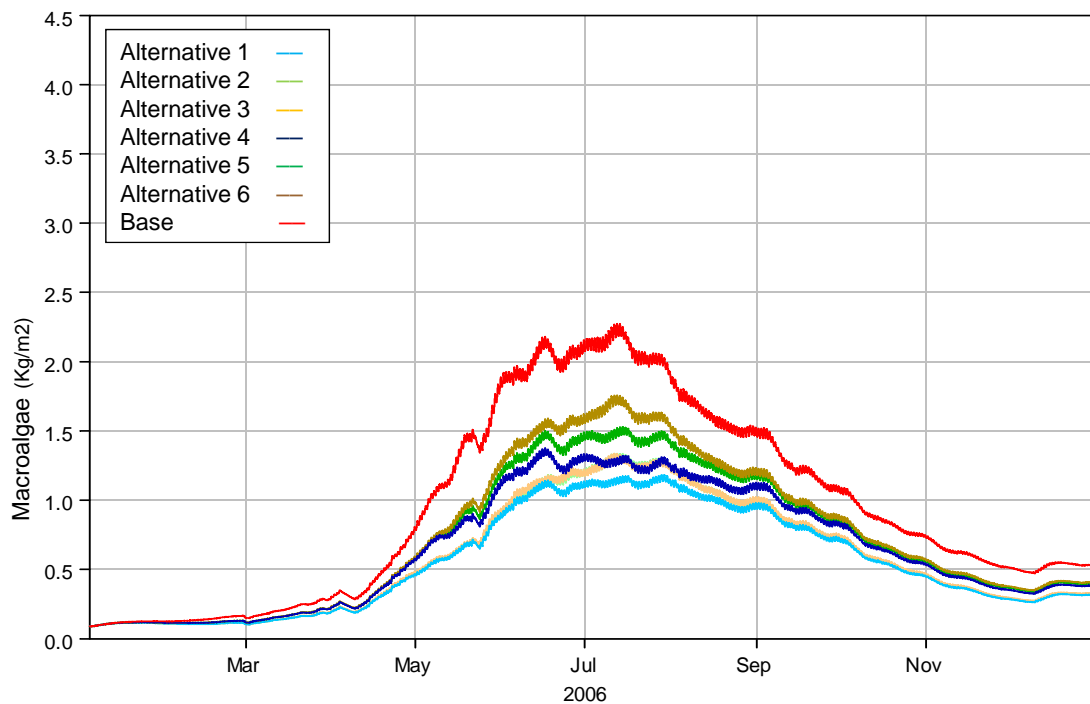


Figure 7-31 Comparison of macroalgae concentrations among alternatives with the Base case at station ALG19 in 2006.

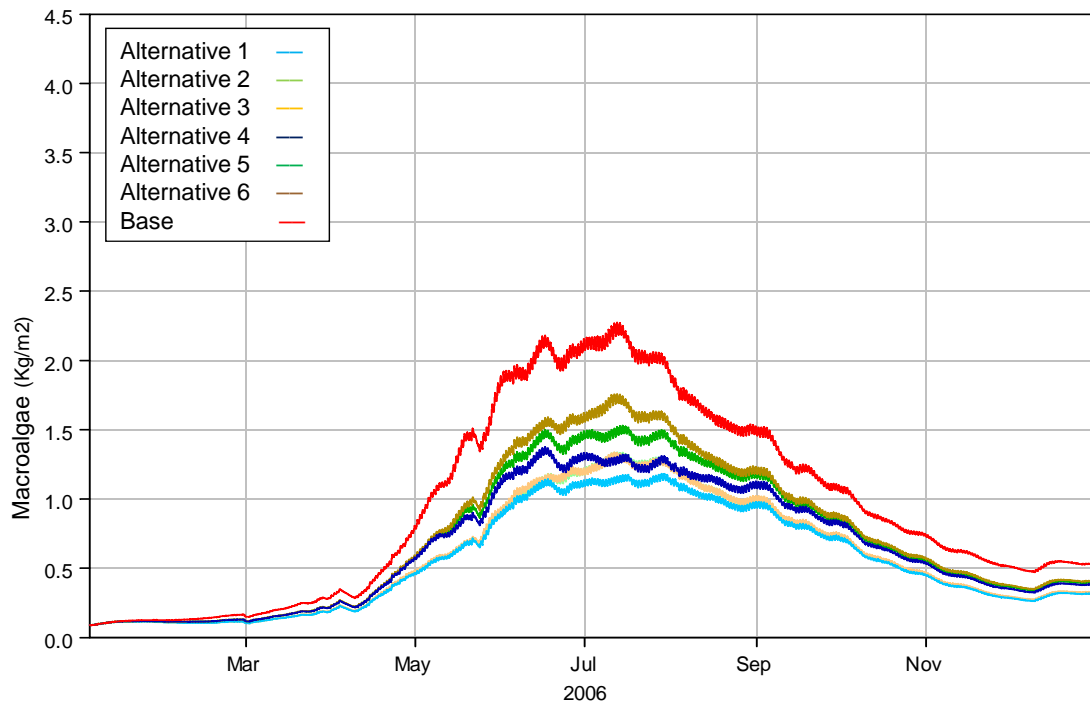


Figure 7-32 Comparison of macroalgae concentrations among alternatives with the Base case at station ALG16 in 2006.

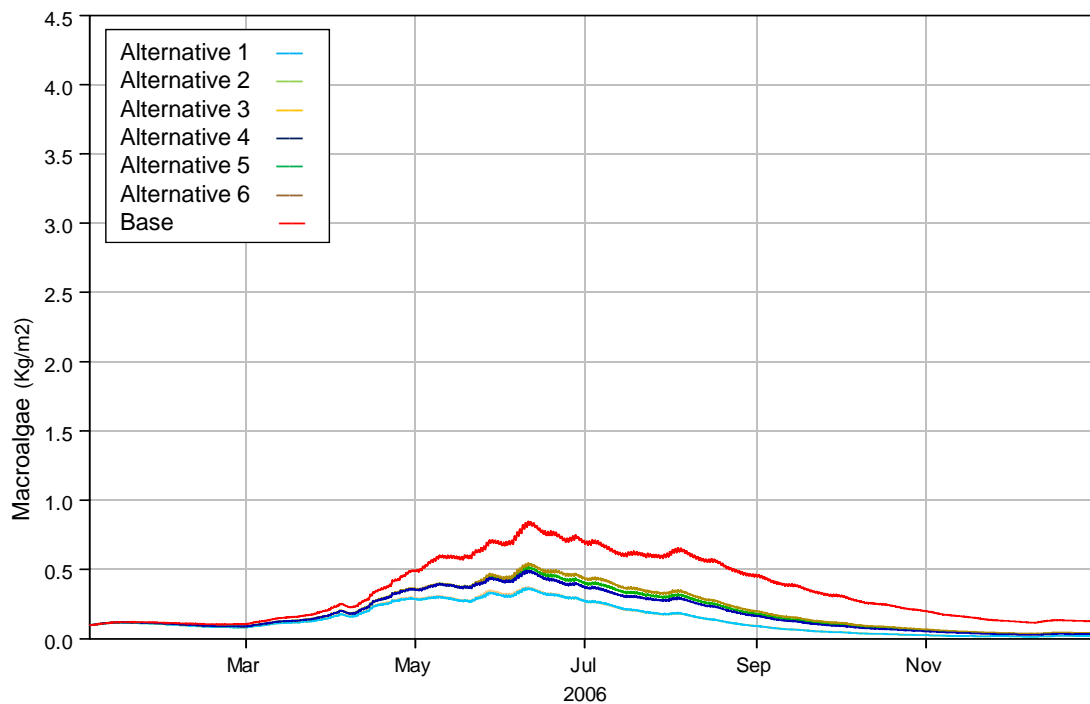


Figure 7-33 Comparison of macroalgae concentrations among alternatives with the Base case at station ALG13 in 2006.

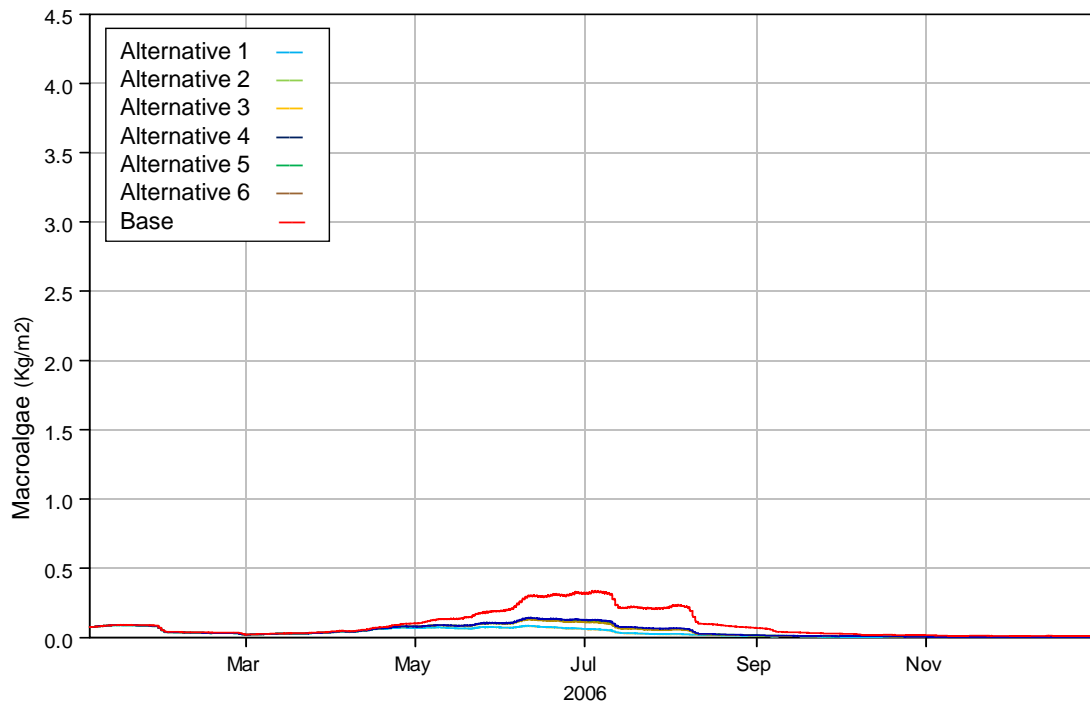


Figure 7-34 Comparison of macroalgae concentrations among alternatives with the Base case at station ALG9 in 2006.

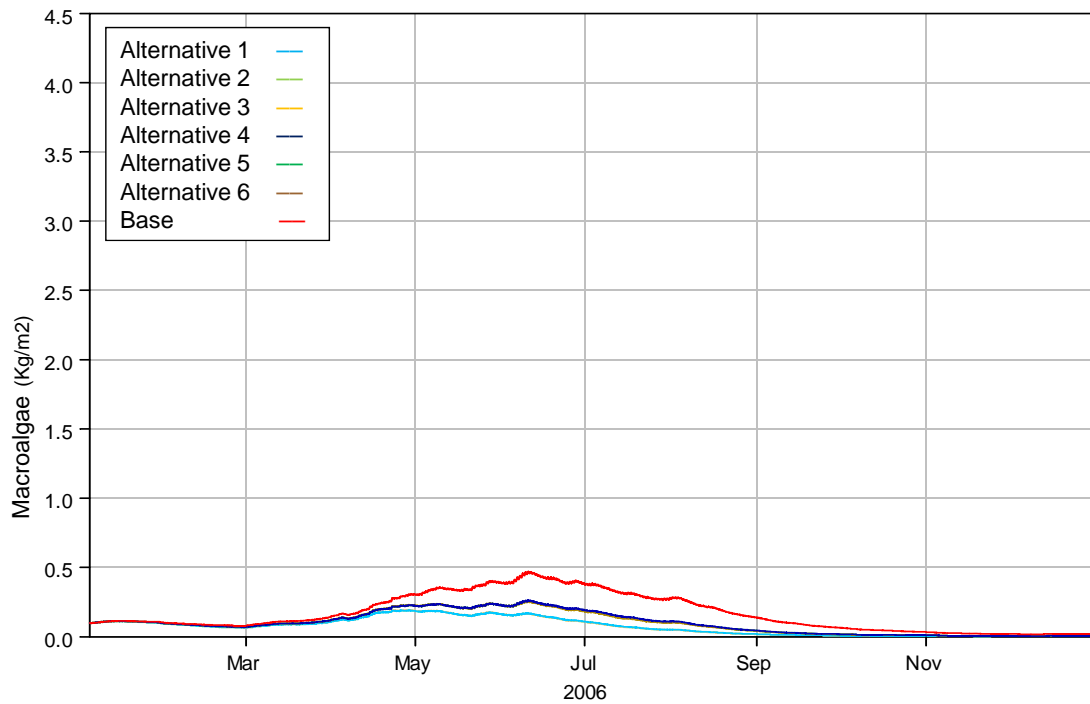


Figure 7-35 Comparison of macroalgae concentrations among alternatives with the Base case at station ALG7 in 2006.

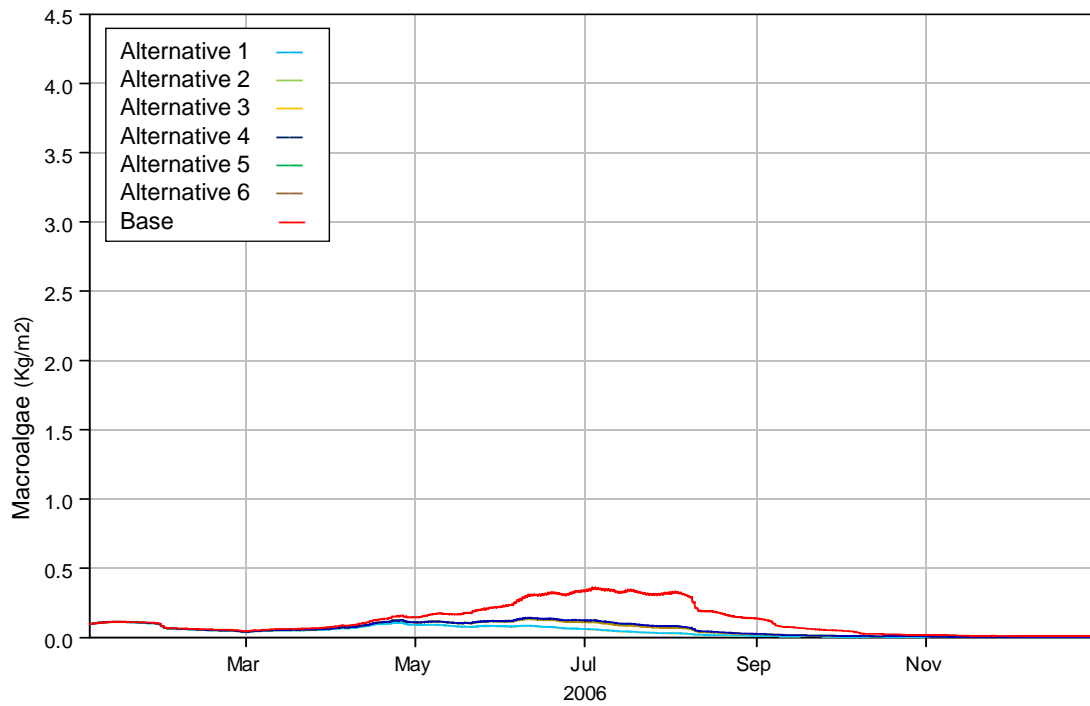


Figure 7-36 Comparison of macroalgae concentrations among alternatives with the Base case at station ALG4 in 2006.

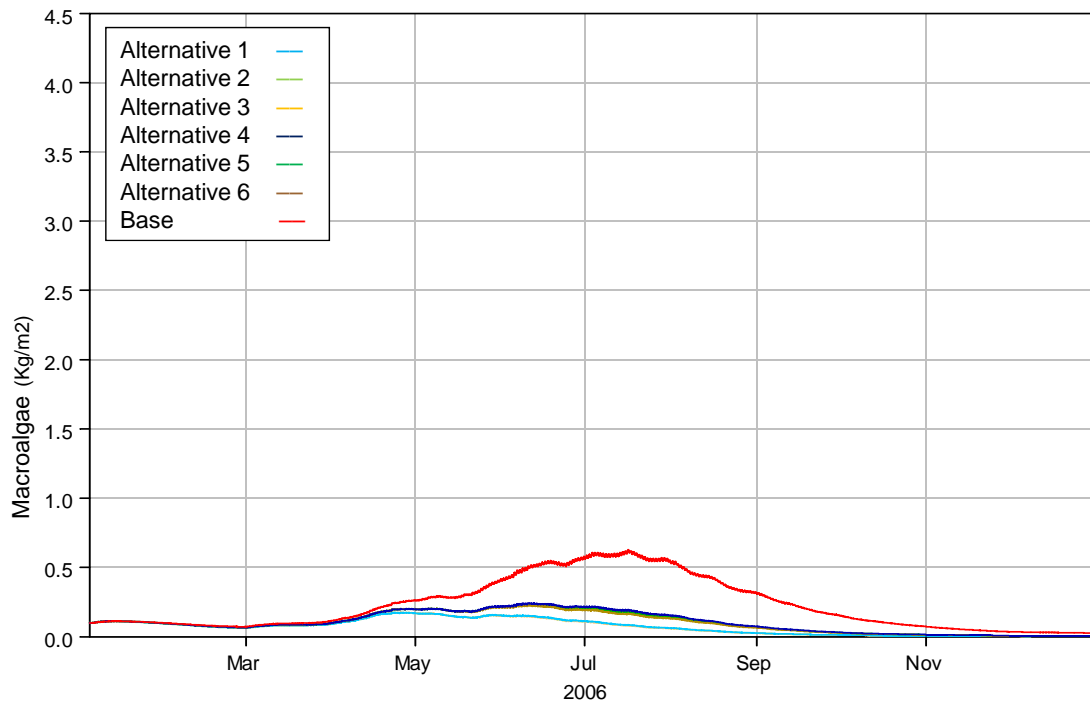


Figure 7-37 Comparison of macroalgae concentrations among alternatives with the Base case at station ALG2 in 2006.

8. Summary and conclusions

The Newport Bay water quality model has been updated and calibrated to support short term and long term management of Newport Bay and aid the Regional Board in determination of new numeric water quality objectives for the TMDL implementation plan.

Previous versions of the model have simulated the occurrence of macroalgal blooms, however, the model could not predict yearly variations in the magnitude of the blooms. In this study, the water quality model for Newport Bay has been updated with the sediment nutrient fluxes based on the SCCWRP sediment study, a review of relevant literature and available data. The model was calibrated and validated using new data sets for 2004 to 2006 from the annual monitoring program performed by the Regional Board.

The key improvement to the model is the addition of a sediment flux model. Sediment transport simulations were performed to provide appropriate sediment depth and distribution to the sediment flux model.

The model was successfully calibrated and validated over the three-year period of 2004 through 2006 to assure that variations in the magnitude of annual macroalgae blooms resulting from different year types was reproduced by the model. There was a particularly large sediment load entering the Bay in 2005, with corresponding large summer macroalgae blooms. The model was able to reproduce this larger bloom relative to years 2004 and 2006.

Overall, the model calibration and validation results were in reasonable agreement with macroalgae, nutrient, dissolved oxygen, temperature and porewater nutrient observations.

An examination of limitation factors from the model indicates that nitrogen and phosphorus are the most important factors controlling macroalgae blooms in Newport Bay.

The calibrated model was run in a predictive mode to evaluate the impacts of alternative total nitrogen load levels entering the Bay. Six alternative nitrogen loading levels were analyzed with different total nitrogen limits during storm and low flow periods. The fraction of particulate nitrogen in the suspended sediment was set to reduced levels corresponding to the storm flow nitrogen limits. Alternative simulation results indicate that reductions in total nitrogen in storm flows and fraction of particulate nitrogen in the sediment have a greater impact on reducing macroalgae blooms than reduction in total nitrogen inputs during low flow periods.

Simulations were performed to compare results from the calibrated model to results from simulations with no sediment interactions. Elimination of the sediment interactions reduced

macroalgae biomass to minimal amounts, thus confirming the importance of sediments as a nutrient source for macroalgae blooms.

For future study, development of a sediment flux model which better represents an anaerobic environment or a sediment model with resuspension induced by waves and currents in the bay may improve model results.

9. References

- Alex Horne Associates (AHA), 1997, Macroalgae (seaweed) and phytoplankton in Newport Bay-Estuary: Summer-Fall 1996, report to the Irvine Ranch Water District.
- Atkinson, M. J. and S. V. Smith, 1983, C:N:P ratios of benthic marine plants, *Limnology and Oceanography*, 28(3): 568-574.
- Bowie, G. L., W. B. Mills, D. B. Porcella, C. L. Campbell, J. R. Pagenkopf, G. L. Rupp, K. M. Johnson, P. W. H. Chan, S. A. Gheini, 1985, Rates, constants and kinetics formulations in surface water quality modelling, 2nd ed. U.S. Environmental Protection Agency, Report EPA/600/3-85/040, 454 pp.
- Brush, M. J. and S. W. Nixon, 2003, Biomass layering and metabolism in mats of the macroalga *Ulva Lactuca* L., *Limnology and Oceanography*, 26(4A): 916-926.
- California's Nearshore Waters and Open Ocean, California Coastal Resource Guide, <http://ceres.ca.gov/ceres/calweb/coastal/waters.html>.
- Chapra, S. C., 1997, Surface Water Quality Modeling, McGraw-Hill, Singapore.
- Chapra, S., G. Pelletier and H. Tao, QUAL2K: A modeling framework for simulating river and stream water quality (Version 2.07), <http://www.epa.gov/athens/wwqtsc/html/qual2k.html>
- Coffaro, G. and A. Sfriso, 1997, Simulation model of *Ulva rigida* growth in shallow water of the Lagoon of Venice, *Ecological Modelling*, 102:55-66.
- Cohen, R. A., P. Fong, 2004, Nitrogen uptake and assimilation in *Enteromorpha intestinalis* (L.) Link (Chlorophyta): using ¹⁵N to determine preference during simultaneous pulses of nitrate and ammonium), *Journal of Experimental Marine Biology and Ecology*, 309: 67-77.
- Cole, T. M., S. A. Wells, 2006, CE-QUAL-W2: A two-dimensional, laterally averaged, hydrodynamic and water quality model, version 3.5", Introduction report EL-06-1, US Army Engineering and Research Development Center, Vicksburg, MS.
- The County of Orange, The Cities of Irvine, Tustin, Newport Beach, Lake Forest, Santa Ana, Orange and Costa Mesa, and The Irvine Company, and Irvine Ranch Water District, 2004, Report of the regional monitoring program for the Newport Bay/San Diego creek watershed nutrient TMDL, (Source: http://www.ocwatersheds.com/watersheds/tmdls_nutrient_intro.asp).
- The County of Orange, The Cities of Irvine, Tustin, Newport Beach, Lake Forest, Santa Ana, Orange and Costa Mesa, and The Irvine Company, and Irvine Ranch Water District, 2005, Regional monitoring program for the Newport Bay/San Diego creek watershed nutrient TMDL, (Source: http://www.ocwatersheds.com/watersheds/tmdls_nutrient_intro.asp).
- The County of Orange, The Cities of Irvine, Tustin, Newport Beach, Lake Forest, Santa Ana, Orange and Costa Mesa, and The Irvine Company, and Irvine Ranch Water District, July-

- September 2005, Quarterly Data Report Newport Bay Watershed Nutrient TMDL. (Source: http://www.ocwatersheds.com/watersheds/tmdls_nutrient_intro.asp).
- The County of Orange, The Cities of Irvine, Tustin, Newport Beach, Lake Forest, Santa Ana, Orange and Costa Mesa, and The Irvine Company, and Irvine Ranch Water District, October-December 2005, Quarterly Data Report Newport Bay Watershed Nutrient TMDL. (Source: http://www.ocwatersheds.com/watersheds/tmdls_nutrient_intro.asp).
- The County of Orange, The Cities of Irvine, Tustin, Newport Beach, Lake Forest, Santa Ana, Orange and Costa Mesa, and The Irvine Company, and Irvine Ranch Water District, January-March 2006, Quarterly Data Report Newport Bay Watershed Nutrient TMDL. (Source: http://www.ocwatersheds.com/watersheds/tmdls_nutrient_intro.asp).
- The County of Orange, The Cities of Irvine, Tustin, Newport Beach, Lake Forest, Santa Ana, Orange and Costa Mesa, and The Irvine Company, and Irvine Ranch Water District, April-June 2006, Quarterly Data Report Newport Bay Watershed Nutrient TMDL. (Source: http://www.ocwatersheds.com/watersheds/tmdls_nutrient_intro.asp).
- The County of Orange, The Cities of Irvine, Tustin, Newport Beach, Lake Forest, Santa Ana, Orange and Costa Mesa, and The Irvine Company, and Irvine Ranch Water District, July-September 2006, Quarterly Data Report Newport Bay Watershed Nutrient TMDL. (Source: http://www.ocwatersheds.com/watersheds/tmdls_nutrient_intro.asp).
- The County of Orange, The Cities of Irvine, Tustin, Newport Beach, Lake Forest, Santa Ana, Orange and Costa Mesa, and The Irvine Company, and Irvine Ranch Water District, October-December 2006, Quarterly Data Report Newport Bay Watershed Nutrient TMDL. (Source: http://www.ocwatersheds.com/watersheds/tmdls_nutrient_intro.asp).
- The County of Orange, the Cities of Costa Mesa, Irvine, Lake Forest, Newport Beach, Orange, Santa Ana and Tustin, 2004, Upper Newport Bay/ San Diego Creek watershed sediment TMDL, 2003-2004 annual report, (Source: http://www.ocwatersheds.com/watersheds/tmdls_sediment_intro.asp).
- The County of Orange, the Cities of Costa Mesa, Irvine, Lake Forest, Newport Beach, Orange, Santa Ana and Tustin, 2005, Upper Newport Bay/ San Diego Creek watershed sediment TMDL, 2004-2005 annual report, (Source: http://www.ocwatersheds.com/watersheds/tmdls_sediment_intro.asp).
- The County of Orange, the Cities of Costa Mesa, Irvine, Lake Forest, Newport Beach, Orange, Santa Ana and Tustin, 2006, Upper Newport Bay/ San Diego Creek watershed sediment TMDL, 2005-2006 annual report, (Source: http://www.ocwatersheds.com/watersheds/tmdls_sediment_intro.asp).
- DiToro, D. M., 2001, Sediment flux modeling, John Wiley & Sons., Inc, New York.
- Flindt, M. R., C. B. Pedersen, C. L. Amos, A. Levy, A. Bergamasco, P. L. Friend, 2007, Transport, sloughing and settling rates of estuarine macrophytes: Mechanisms and ecological implications, *Continental Shelf Research*, 27: 1096-1103.
- Fujii, M., S. Murashige, Y. Ohnishi, A. Yuzawa, H. Miyasaka, Y. Suzuki, H. Komiyama, 2002, Decomposition of phytoplankton in seawater. Part I: Kinetic analysis of the effect of organic matter concentration, *Journal of Oceanography*, 58:433-438.

- Garber, J. H., 1984, ^{15}N Tracer study of the short-term fate of particulate organic nitrogen at the surface of coastal marine sediments, *Marine Ecology – Progress Series*, 16: 89-104.
- Giusti, E. and S. Marsili-Libelli, 2005, Modelling the interactions between nutrients and the submersed vegetation in the Orbetello Lagoon, *Ecological Modelling*, 184:141-161.
- Hattori, A., 1983, Denitrification and dissimilatory nitrate reduction, p 191-232, Nitrogen in the Marine Environment, Ed. Carpenter, E. J. and Capone, D. G., Academic Press, New York.
- Hauxwell, J. I. Valiela, 2004, Effects of nutrient loading on shallow seagrass-dominated coastal systems: patterns and progress, In S. L. Nielsen, G. T. Banta, and M. F. Pedersen, (Ed.), Estuarine nutrient cycling: The influence of primary producers, Kluwer Academic Publishers, Dordrecht.
- Hernandez, I., G. Peralta, J. Perez-Llorens, J. Vergara, and F. Niell, 1997, Biomass and dynamics of growth of *Ulva* species in Palmones River estuary, *Journal of Oceanography*, 33:764-772.
- Howarth, R. W. and R. Marino, 2006, Nitrogen as the limiting nutrient for eutrophication in coastal marine ecosystems: Evolving views over three decades, *Limnology and Oceanography*, 51(1): 364-376.
- Jellison, R., L. G. Miller, J. M. Melack, G. L. Dana, 1993, Meromixis in Hypersaline Mono Lake, California. 2. Nitrogen Fluxes, *Limnology and Oceanography*, 38(5): 1020-1039.
- Kamer, K., K. A. Boyle, P. Fong, 2001, Macroalgal bloom dynamics in a highly eutrophic southern California estuary, *Estuaries*, 24(4): 623-635.
- Kamer, K. K., K. C. Schiff, R. L. Kennison, P. Fong, 2002, Macroalgal nutrient dynamics in Upper Newport Bay, Technical report 365, Southern California Coastal Water Research Project.
- King, I. P., W. R. Norton and K. R. Iceman, 1975, A finite element solution for two-dimensional stratified flow problems', in R. H. Gallagher, J. T. Oden, C. Taylor and O. C. Zienkiewicz, Finite Elements in Fluids, J. Wiley, Chapter 7.
- Kremer, J. N., A. Reischauer, C. D'Avanzo, 2003, Estuary-specific variation in the air-water gas exchange coefficient for oxygen, *Estuaries*, 26(4A): 829-836.
- Martins, I., R. Lopes, A. Lillebo, J. Neto, M. Pardal, J. Ferreira and J. Marques, 2007, Significant variations in the productivity of green macroalgae in a mesotidal estuary: Implications to the nutrient loading of the system and the adjacent coastal area, *Marine Pollution Bulletin*, 54:678-690.
- Martins, I., J. C. Marques, 2002, A model for the growth of opportunistic macroalgae (*Enteromorpha* sp.) in Tidal Estuaries, *Estuarine, Coastal and Shelf Science*, 55:247-257.
- Martins, I., J. M. Oliveira, M. R. Flindt, J. C. Marques, 1999, The effect of salinity of the growth rate of the macroalgae *Enteromorpha intestinalis* (Chlorophyta) in the Mondego estuary (west Portugal), *Acta Oecologica*, 20(4): 259-265.
- Martins, I., M. A. Pardal, A. I. Lillebø, M. R. Flindt, J. C. Marques, 2001, Hydrodynamics as a major controlling the occurrence of green macroalgal blooms in a eutrophic estuary: A

- case study on the influence of precipitation and river management, *Estuarine, Coastal and Shelf Science*, 52:165-177.
- Naldi, M., P. Viaroli, 2002, nitrate uptake and storage in the seaweed *Ulva rigida* C. Agardh in relation to nitrate availability and thallus nitrate content in a eutrophic coastal lagoon (Sacca di Goro, Po River Delta, Italy), *Journal of Experimental Marine Biology and Ecology*, 269: 65-83.
- Ni, J., 1999, Mechanistic models of ammonia release from liquid manure: a review, *Journal of Agricultural Engineering Research*, 72: 1-17.
- Pedersen, M. F., S. L. Nielsen, and G. T. Banta, 2004, Interactions between vegetation and nutrient dynamics in coastal marine ecosystems: an introduction, In S. L. Nielsen, G. T. Banta, and M. F. Pedersen, (Ed.), *Estuarine nutrient cycling: The influence of primary producers*, Kluwer Academic Publishers, Dordrecht.
- Peng, J., K. Maruya, K. Schiff, D. Tsukada, D. Diehl, W. Lao, J. Gan, E. Zeng, 2007, Organochlorine pesticides and other trace organic contaminants in the upper Newport Bay watershed, Technical report #512, Southern California Coastal Water Research Project.
- Oberg, J., 2006, Primary production by macroalgae in Kattegat, estimated from monitoring data, seafloor properties, and model simulations, *Continental Shelf Research*, 26: 2415-2432.
- Resource Management Associates, Inc. (RMA), 1997 "Upper Newport Bay Final Model and GUI Development and Implementation Report", prepared for U.S. Army Corps of Engineers Los Angeles District, October 1997.
- Resource Management Associates, Inc. (RMA), 1999 "Upper Newport Bay Feasibility Report: Upper Newport Bay Alternative Analysis", prepared for U.S. Army Corps of Engineers Los Angeles District, November 1999.
- Resource Management Associates, Inc. (RMA), 1998a "Upper Newport Bay Feasibility Report: Upper Newport Bay Salinity Study", prepared for U.S. Army Corps of Engineers Los Angeles District, October 1998.
- Resource Management Associates, Inc. (RMA), 1998b "Upper Newport Bay Feasibility Report: Upper Newport Bay Numerical Model Development Baseline Conditions Analysis", prepared for U.S. Army Corps of Engineers Los Angeles District, July 1998.
- Resource Management Associates, Inc. (RMA), 2001 "Newport Bay Water Quality Model Development" 3-D Stratified Flow Analysis, prepared for California Regional Water Quality Control Board, Santa Ana Region, February 2001.
- Resource Management Associates, Inc. (RMA), 2003 "Newport Bay Water Quality Model Update", prepared for California Regional Water Quality Control Board, Santa Ana Region, November 2003.
- Sand-Jensen, K. and S. L. Nielsen, 2004, Estuarine primary producers, In S. L. Nielsen, G. T. Banta, and M. F. Pedersen, (Ed.), *Estuarine nutrient cycling: The influence of primary producers*, Kluwer Academic Publishers, Dordrecht.
- Sanford, L. P. and S. M. Crawford, 2000, Mass transfer versus kinetic control of uptake across solid-water boundaries, *Limnology and Oceanography*, 45(5): 1180-1186.

- Solidoro, C., C. Dejak, D. Franco, R. Pastres, G. Pecenic, 1995, A model for macroalgae and phytoplankton growth in the Venice lagoon, *Environment International*, 21:619-626.
- Solidoro, C., G. Pecenic, R. Pastres, D. Franco, C. Dejak, 1997, Modelling macroalgae (*Ulva Rigida*) in the Venice lagoon: Model structure identification and first parameters estimation, *Ecological Modelling*, 94:191-206.
- Sutula, M., K. Kamer, J. Cable, H. Collis, W. Berelson and J. Mendez, 2006, Sediments as an internal source of nutrients to upper Newport Bay, California, Technical report #482, Southern California Coastal Water Research Project.
- Trancoso, A. R. R., R. Neves, P. Pina, L. Fernandes, 2002, Modelling macroalgae in estuaries, report, Universidade Técnica de Lisboa Instituto Superior Técnico.
- Trancoso, A. R. , S. Saraiva, L. Fernandes, P. Pina, P. Leitão, R. Neves, 2005, Modelling macroalgae using a 3D hydrodynamic-ecological model in a shallow, temperate estuary, report, *Ecological Modelling*, 187:232-246.
- US Army Corps of Engineers, 1997,
- US Army Corps of Engineers, 1998, Valiela, I., J. McClelland, J. Hauxwell, P. J. Behr, D. Hersh, K. Foreman, 1997, Macroalgal blooms in shallow estuaries: Controls and ecophysiological and ecosystem consequences, *Limnology and Oceanography*, 42(5): 1105-1118.
- Wainright, S. and C. Hopkinson Jr., 1997, Effects of sediment resuspension on organic matter processing in coastal environments: a simulation model, *Journal of Marine System*, 11:353-368.
- Wheeler, P. and Bjornsater, B., 1992, Seasonal fluctuations in tissue nitrogen, phosphorus, and N:P for five macroalgal species common to the pacific northwest coast, *Journal of Phycology*, 28:1-6.